6.0 Test Results

The following sections document the results of tests performed on a total of 11 systems.

Field of View Plots

Much of the data presented in the following sections is referenced to the sensor detection zones (or field of view) measured during the static tests. Lane change tests results are overlaid onto the static pattern measured with the automobile target. This zone is typically denoted by a dashed line extending out from the host vehicle. Lane markers, represented by the parallel dashed lines, have been added to provide a sense of realism to the picture. The approximate sensor location is indicated by an x.

6.1 System "A"

6.1.1 System Description

This system is an ultrasonic ranging system designed for side obstacle detection. The system will warn the driver with both a visual and audio alarm if an obstacle is detected within the blind spot zone. The unit was mounted on the passenger side of the host vehicle 0.1 m from the rear corner of the car at a height of 1.1 m above the ground.

6.1.2 Overview of System Performance

This unit demonstrated extremely poor performance during the controlled static and dynamic tests. In fact, the system was returned to the vendor for system check out and the tests were repeated. Even after verification of normal system performance by the vendor, the spatial extent of the static patterns measured were limited. Perpendicular delay time measurements showed no system response above 24 KPH. Furthermore, the data was characterized by scatter that was so large that no conclusions could be drawn from the data. A similarly poor response was seen during the parallel delay time tests. Such poor system performance made the collection of meaningful data during the controlled track tests impossible.

Even though system performance was poor, an attempt to judge the system under realistic road conditions was made. During the road test which lasted 73.9 min, almost half of the legitimate targets went undetected by the system. In addition, most of the reactions that were triggered were false alarms with no apparent target in sight. All in all, the performance and utility of this system was very poor.

6.1.3 Test Results

<u>Static Tests</u>

Static patterns were measured for the following types of targets:

1) 0.3m x 0.3m foil covered Styrofoam
2) 0.6m x 0.6m foil covered Styrofoam
3) human
4) motorcycle
5) Ford Thunderbird

The small cross section targets were located at the vertical height of the sensor.

Figure 6.1-1 summarizes the results of the static tests for this sensor system. The static detection zones measured with the 0.3m x 0.3m and 0.6m x 0.6m aluminum foil covered targets are compared in figures (a) and (b). There is not much difference in the characteristics of the patterns measured. Both are small extending out only about 2m.

The results measured with a human target are shown in Figure 6.1-1 (c). The extent of this pattern is even smaller than that measured with the foil targets.

The static detection zone of both a motorcycle and car are shown in figures (d) and (e). The motorcycle target pattern is referenced to the front wheel. In the case of the T-Bird target, the outline of the target vehicle has been included for clarity. The position of reference post Pl is shown by the asterisk and indicates the point of reference for the measurement. The static detection zone is denoted by the dashed line. System reaction was recorded at 0.6m intervals along the longitudinal and lateral axes.

The motorcycle target is not much different than the foil targets despite the fact that it presents a larger cross section to the sensor system. The T-Bird pattern is characterized by a highly irregular shape. This is indicative of the fact that the system was not performing well.

Vertical Extent

The vertical extent of the static pattern was determined by placing a target at a distance, D, from the sensor and measuring the system response as a function of vertical position. Figure 6.1-2 summarizes the angular extent in elevation of this sensor system. The sensor pattern has a total vertical FOV of 37.4" and is aimed slightly upward, although it is not physically tilted.

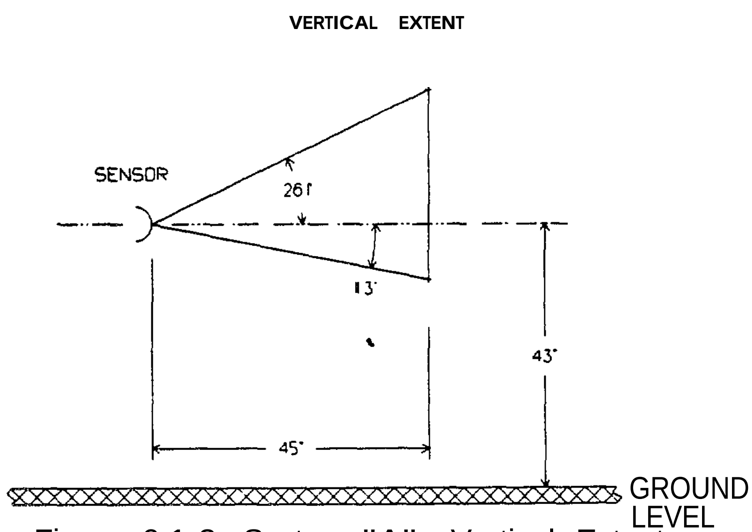

Figure 6.1-2: System "A" - Vertical Extent

Figure 6.1-1: System "A" Static Test Results

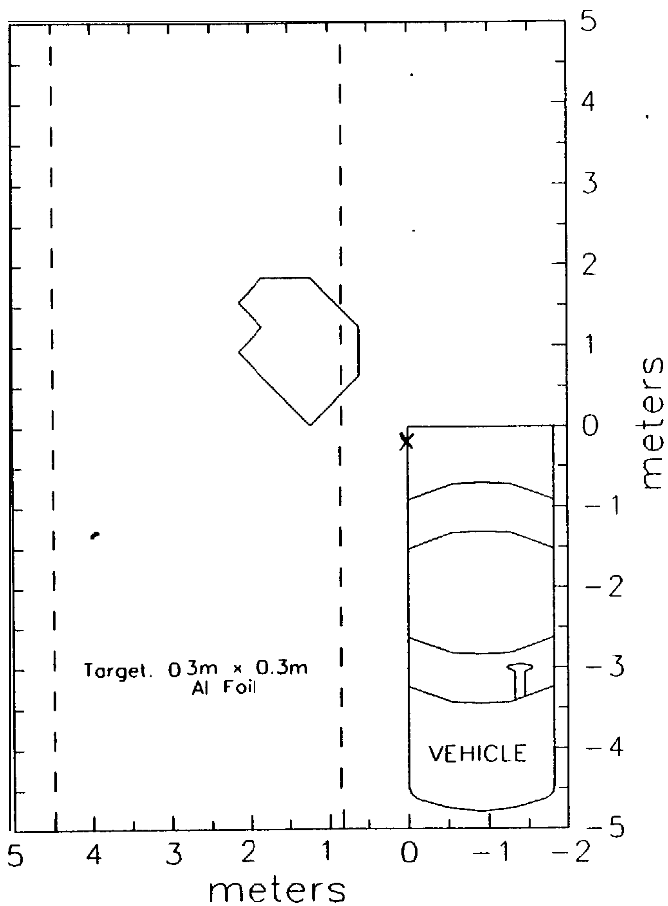

(a) 0.3m x 0.3m Aluminum Foil Target

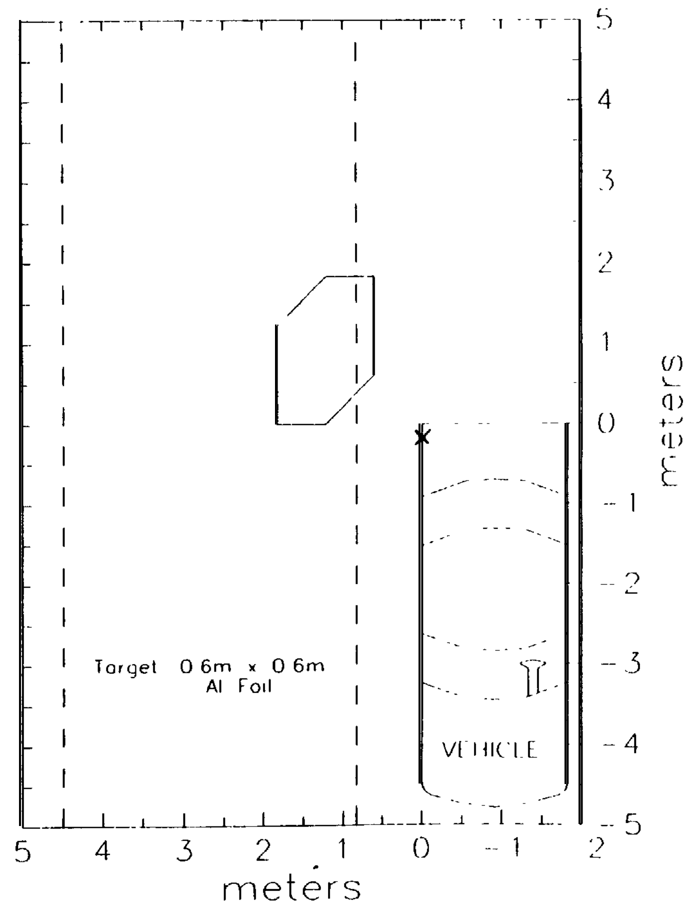

(b) 0.6m x 0.6m Aluminum Foil Target

Figure 6.1-1: System "A" Static Test Results (con'd)

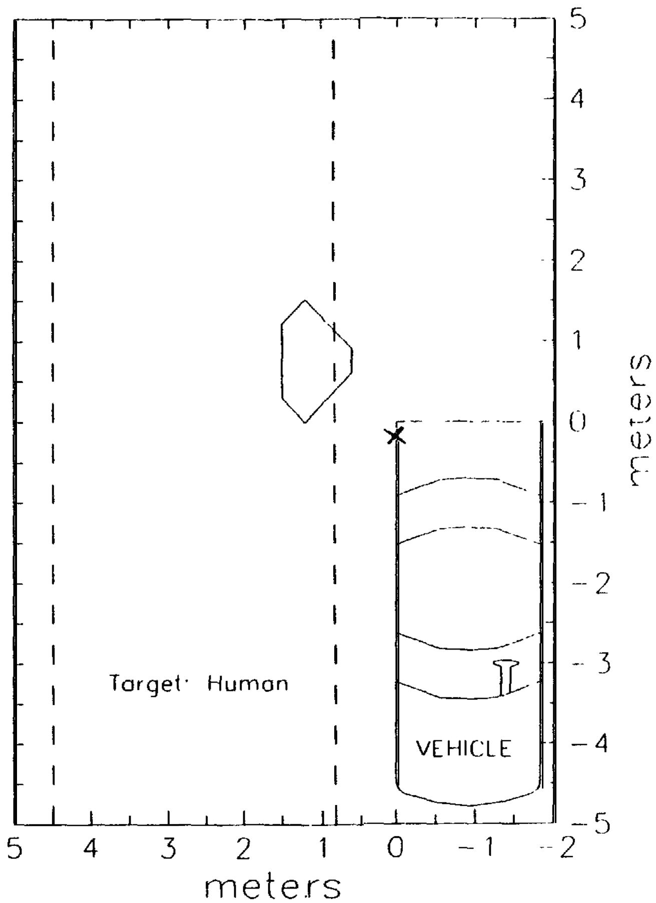

(c) Human Target

Figure 6.1-1: System "A" Static Test Results (con 'd)

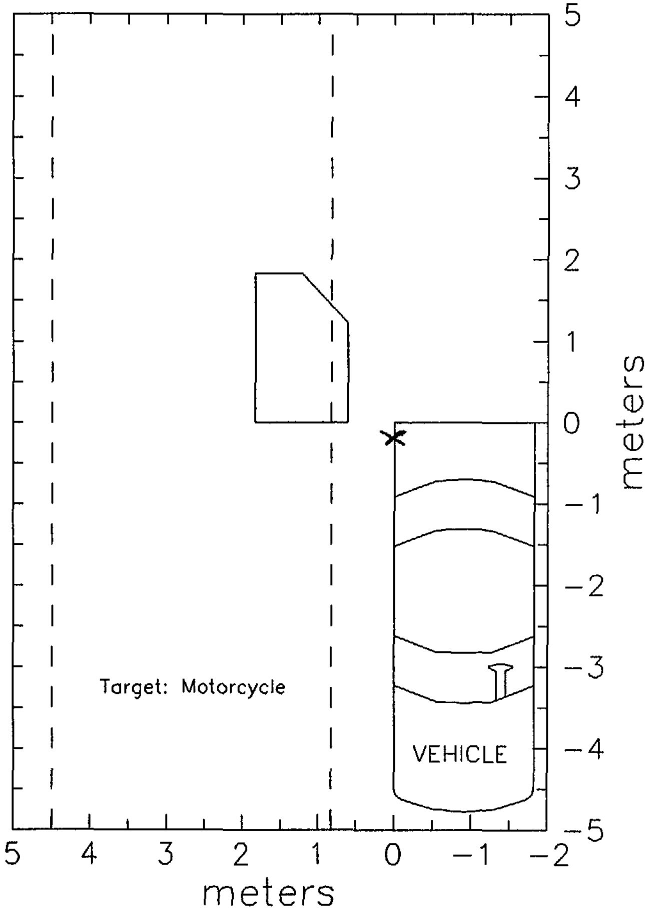

(d) Motorcycle Target

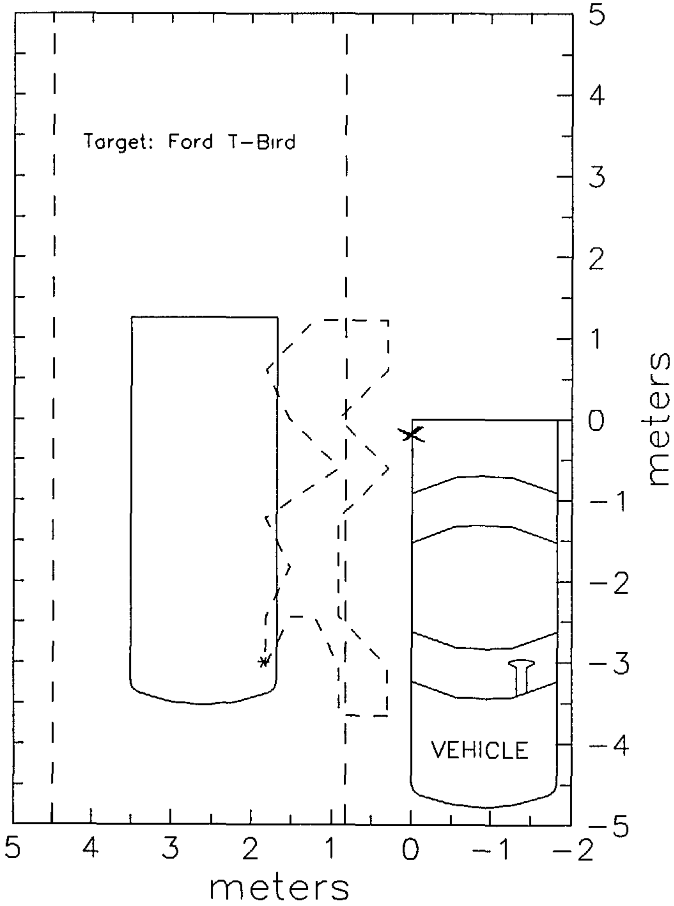

(e) Ford Thunderbird Target

Dynamic Tests

Perpendicular Delay Time

Figure 6.1-3 in which the target vehicle position has been plotted as a function of vehicle speed summarizes the results of the perpendicular delay time tests for this system. The target vehicle was driven past the sensor vehicle at speeds of 1.6, 8, 16.1, 24.1, 32.2, and 40.2 KPH. All data has been referenced to post P2 on the front passenger side of the target vehicle.

Figure 6.1-3: Perpendicular Latency Time

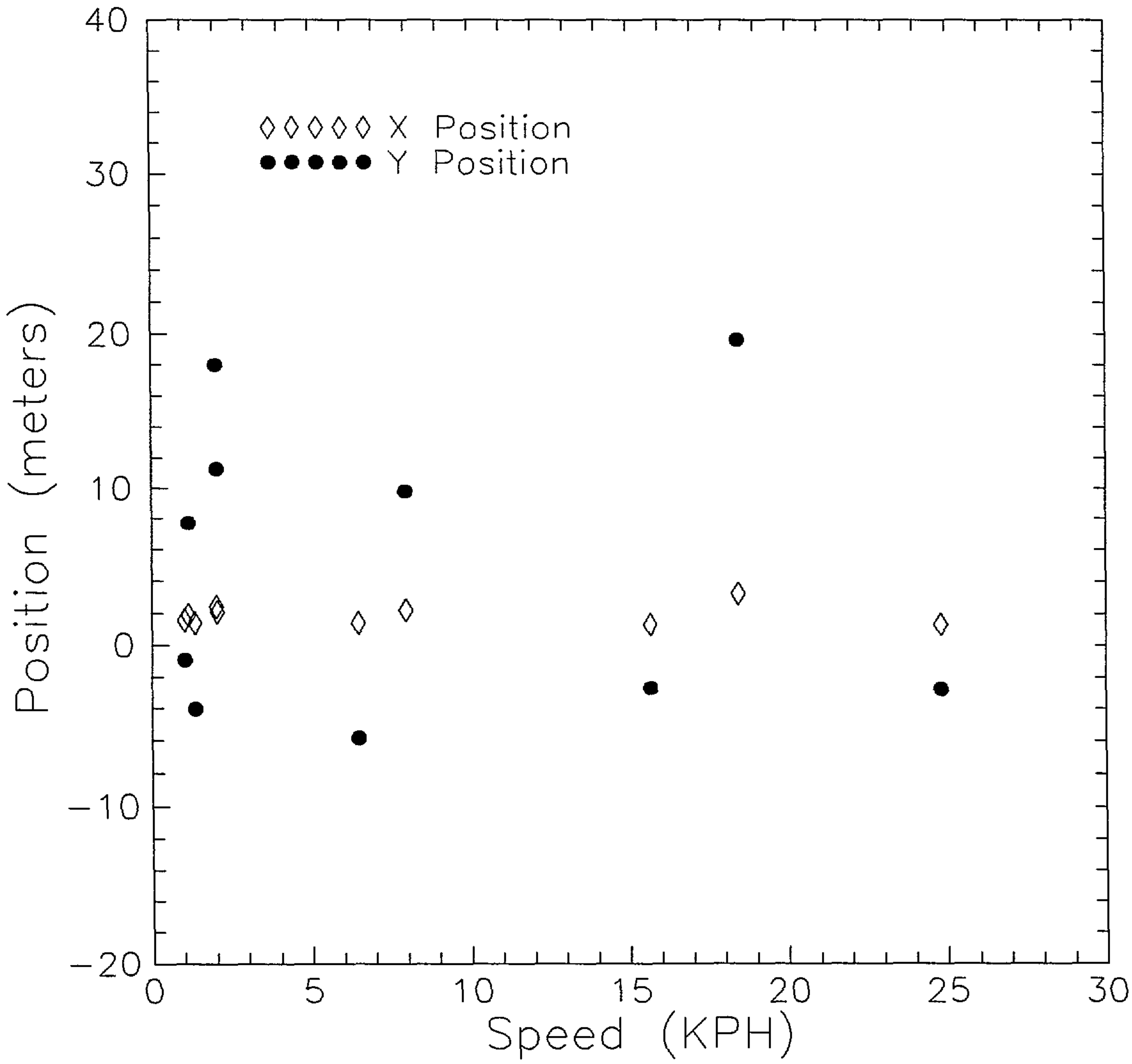

No system reactions were triggered at speeds above 24 KPH. At speeds below this, the number of system reactions was as follows:

2 KPH - 5 out of 5
8 KPH - 2 out of 5
16 KPH - 2 out of 5
24 KPH - 1 out of 5

Thus, only half of the passes made triggered a system response.

The Y position of the target vehicle at the instant of system reaction is shown by the filled circles. There is an inordinate amount of scatter in this data in some cases showing an-early system reaction at Y = 20m and in other cases a late reaction at Y = -6m. These results reflect the actual response of the system and raised our suspicions about the utility of this particular system. No information on the perpendicular latency can be derived from this data.

The lateral separation (X) between the two vehicles is denoted by the open triangles. Because there is so much variation in the Y position at which the system reacts, the variation in the lateral spacing shows more variation than is typical. This is understandable because the driver is not worried about maintaining a certain lateral position at a distance of 20m from the sensor vehicle.

Parallel Delay Time

The results of the parallel delay time tests are presented in Figure 6.1-4. The speed of the approaching target vehicle was varied between 1.6 and 40.2 KPH. No system reactions were triggered at speeds above 8 KPH. At speeds below this, the system reacted for every vehicle pass.

For these tests, the lateral separation shown by the open triangles was held fairly constant at about a meter. However, the X position at which the system reacts still shows a tremendous amount of variation. If the two stray points (on at X = 2.5m , Y = -4m and the other at X = 8m, Y = -1.5m) are ignored, the parallel delay time is computed to be 1.9 sec. Such a long system reaction time is the first clue that the performance of this system can be expected to be poor. A long system latency time combined with a small static detection zone means that many targets passing through the detection zone will slip through undetected.

Persistence Time

Because the scatter in the parallel delay time test data was so large, no computation of persistence was attempted.

Figure 6.1-4: Parallel Latency Time

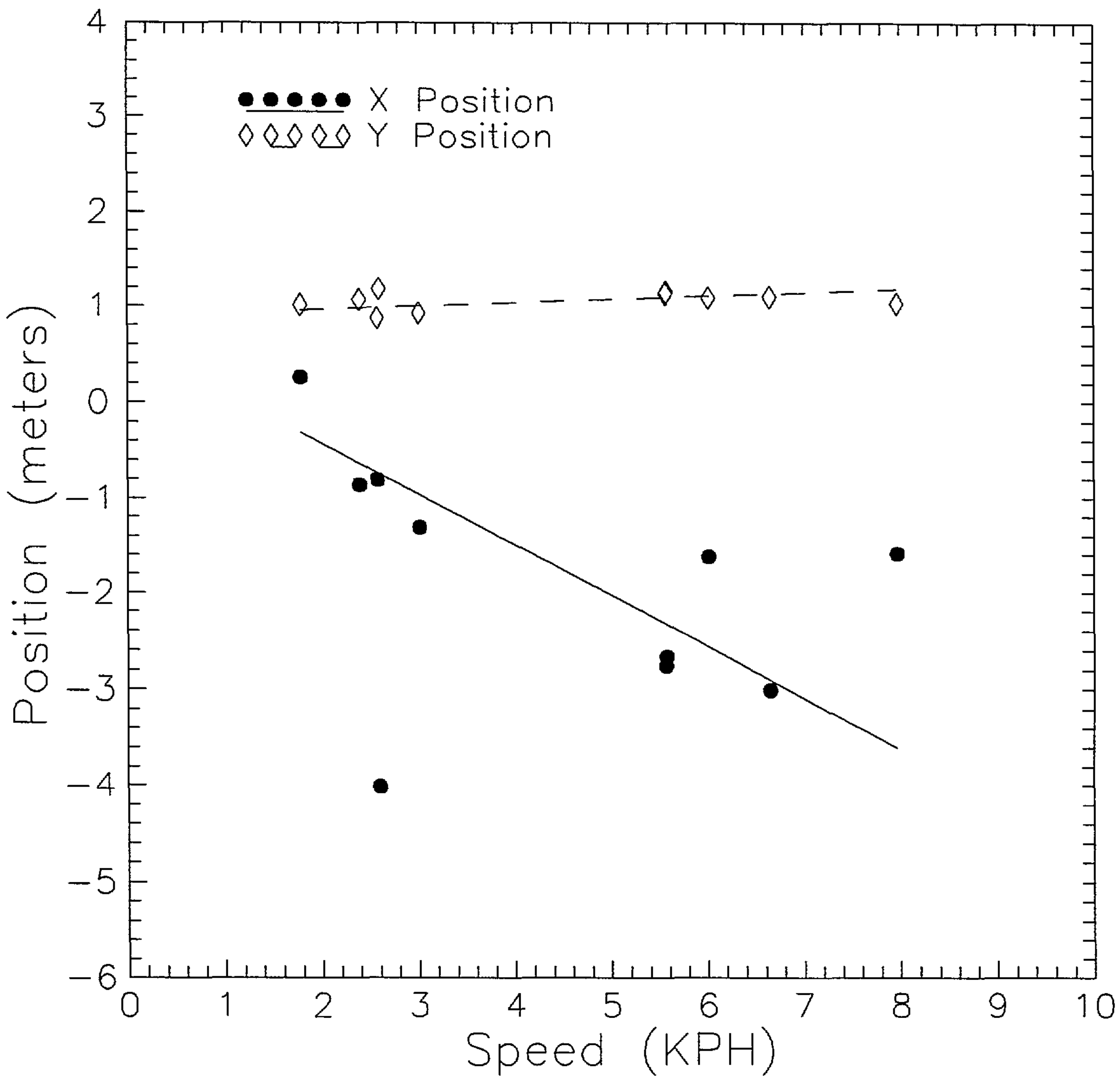

Road Test

Despite this sensor system's poor performance during the static and dynamic tests, it was evaluated under realistic road conditions involving freeway, city, two-lane highway, and parking lot driving. The total exposure time was 73.9 minutes.

Statistics were compiled on the number and types of **targets** detected. Figure 6.1-5 summarizes the results.

This sensor system performed poorly during the road tests. System performance was characterized by numerous false alarms. In addition, many targets which should have resulted in a system alarm failed to trigger any response from the system.

Figure 6.1-5: Summary of Road Test Statistics - System "A"

System: 'A"
Total number of detects: 84

Classification	Freeway	Two-lane	City	Parking Lot	TOTAL
TP	2	1	17	10	30
FP	19	17	16	2	54
TOTAL	21	18	33	12	84
FN	25	0	1	0	26
TN					95.3%

General Comments:

system warning indicator tended to remain lit for 10 sec (system persistence)

numerous false alarms were triggered

nearly half of the legitimate targets failed to trigger a **response**

6.2 System "B"

6.2.1 System Description

This system is a microwave (27GHz) pulse Doppler radar collision warning system that is designed for side object detection. The system advertises the capability to reject meaningless ground clutter such as fence posts, mailboxes, and guardrails and parked vehicles. The unit tested was mounted on the passenger side of the host vehicle, 0.25m forward of the rear corner of the car at a height of about lm above the ground level. The driver display consists of a bar that lights continuously as long as a target remains in the field of view of the sensor.

6.2.2 Overview of System Performance

The unit tested performed well as a proximity detector during both the controlled static and dynamic tests. Sensor system reaction to targets within its field of view was consistent and characterized by minimal scatter (+/-0.3m). Very few operational difficulties were encountered during the entire week of testing.

System performance in terms of its ability to reject ground clutter was far from ideal. During the road test, the percentage of inappropriate alarms was 48%. In other words, 48% of the system detections were caused by ground clutter. This number seems high for a system which claims to be able to filter out non-threatening targets within its field of view. Most of these alarms were generated when passing parked vehicles at low'relative velocities, especially if the vehicles presented a high cross section to the radar. Other non-threatening ground clutter such as road signs, trees, poles, etc. did not generate an inappropriate alarm. On the plus side, there were no instances in which the system failed to detect a target within its detection zone (i.e., FN). The importance of minimizing or eliminating the occurrence of false negatives has been emphasized in Section 5.4.

6.2.3 Test Results

<u>Static Tests</u>

Static patterns were measured for the following types of targets:

1) 0.3m x 0.3m foil covered styrpfoam
2) 0.6m x 0.6m foil covered Styrofoam
3) human
4) motorcycle
5) Ford Thunderbird

The small cross section targets were located at the vertical height of the sensor. Figure 6.2-1 (a) and (b) summarizes the results of the static tests for this sensor system. The static detection zones measured with the 0.3m x 0.3m and 0.6m x 0.6m aluminum foil covered targets are compared in figures (a) and (b). There is more structure detail in the edge pattern for the smaller target which emphasizes its greater similarity to a true "point source" target. Data was collected by moving the target on a 0.3m x 0.3m grid. The data from the larger target was collected on a coarser 0.6m x 0.6m grid. Both zones are characterized by a double lobe structure. The region separating the two lobes appears to be slightly larger for the 0.6m x 0.6m target. This is probably an artifact of the coarser grid spacing.

The results measured with a human target are shown in Figure 6.2-l (c). This pattern is also characterized by a double lobe structure having very little overlap between lobes. The extent of the pattern is slightly less than measured with the 0.3m x 0.3m target.

The static detection zone of both a motorcycle and car are shown in figures (d) and (e). Although there is a hint of a double lobe structure in the motorcycle pattern, both of these targets produce a distributed detection zone. The larger size of these targets makes it impossible for the target to "hide" in between the multiple lobe structure of the sensor's antenna pattern. For the purposes of collision avoidance during lane changes, it is important to note that the zone of detection for vehicles extends more than halfway into the adjacent lane and a couple of meters in front of and to the rear of the host vehicle.

Vertical Extent

The vertical extent of the static pattern was determined by placing a target at a distance, D, from the sensor and measuring the system response as a function of vertical position. Figure 6.2 -2 summarizes the angular extent of this sensor. The sensor has a total vertical FOV of 49^{o} which is symmetrical about the centerline of the sensor.

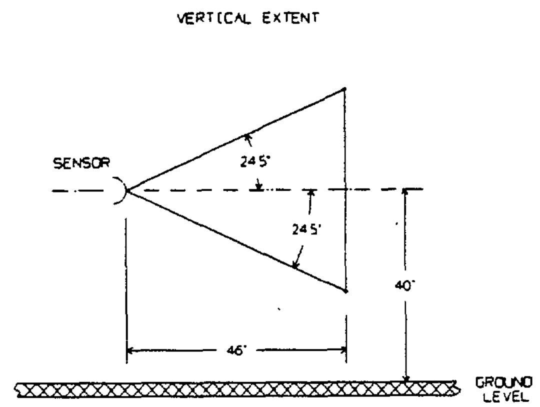

Figure 6.2-2: System 'B" - Vertical Extent

Figure 6.2-1: System "B" Static Test Results

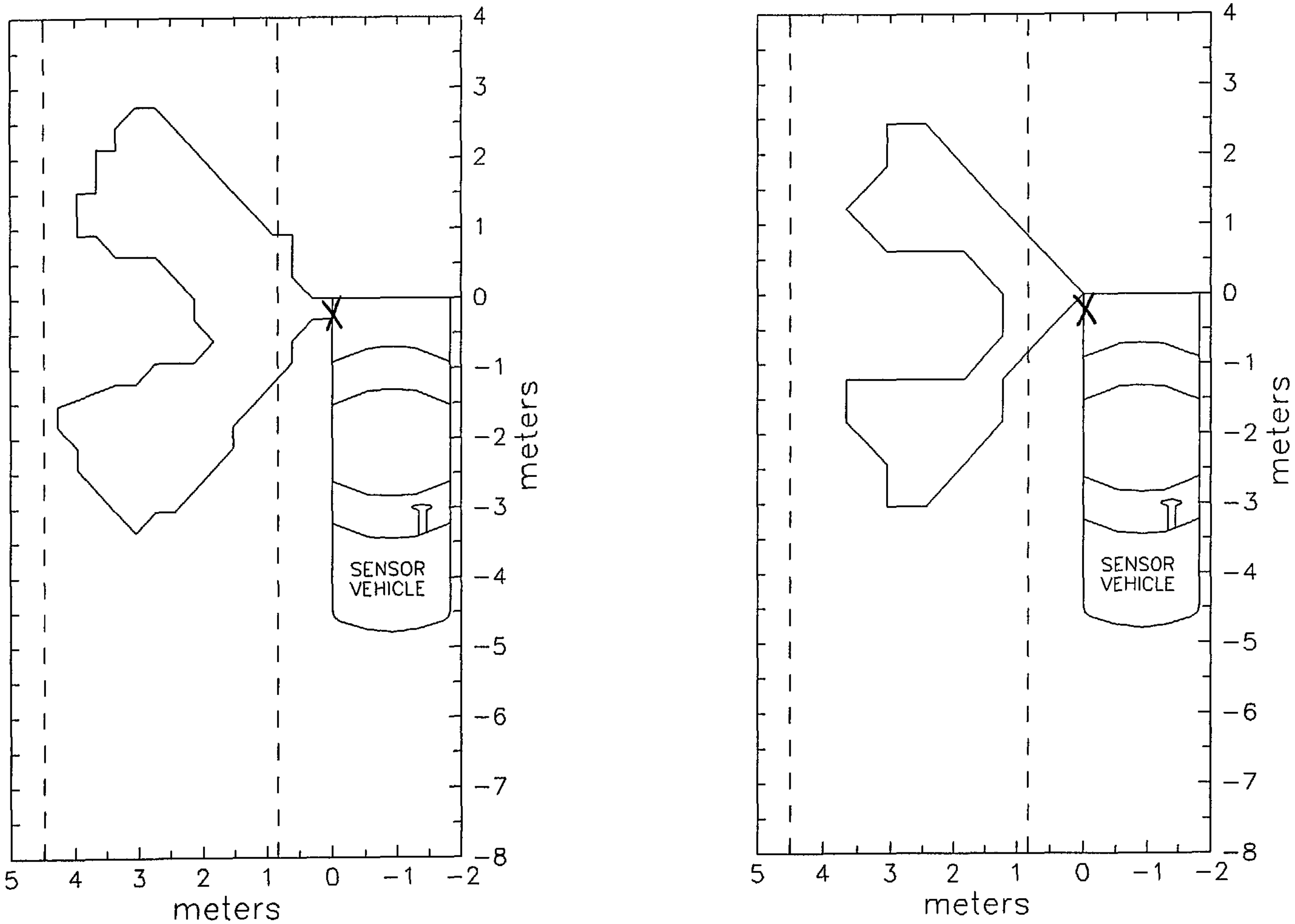

(a) 0.3m x 0.3m Aluminum Foil Target

(b) 0.6m x 0.6m Aluminum Foil Target

Figure 6.2-1: System "B" Static Test Results (con'd)

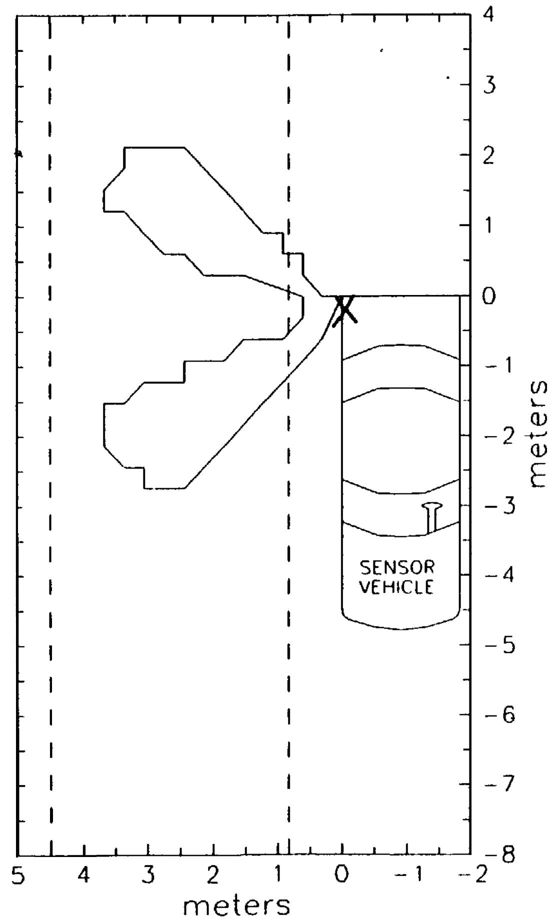

(c) Human Target

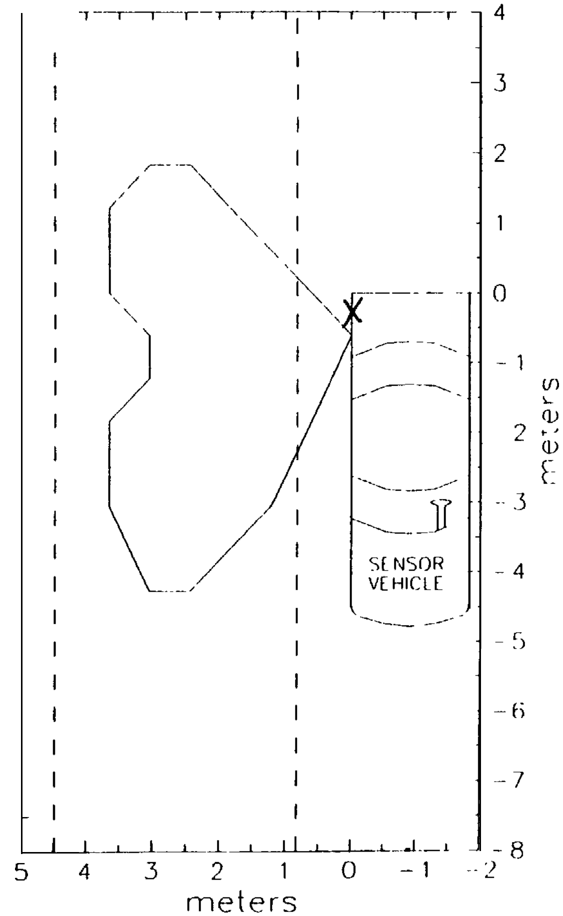

(d) Motorcycle Target

Figure 6.2-1: System "B" Static Test Results (con 'd)

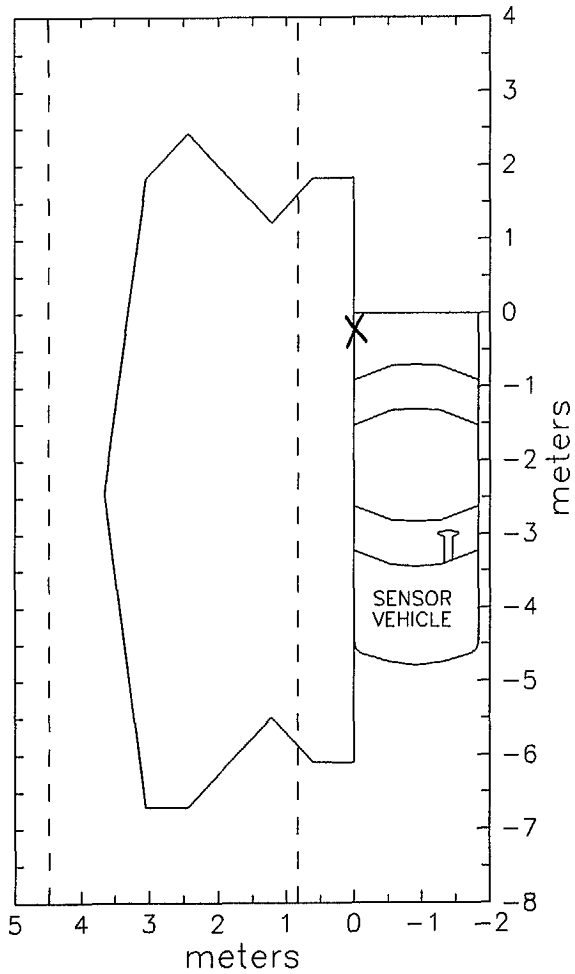

(e) Ford Thunderbird Target

Dynamic Tests

Perpendicular Delay Time

Figure 6.2-3 in which the target vehicle position has been plotted as a function of vehicle speed summarizes the results of the perpendicular delay time tests for this system. The target vehicle was driven past the sensor vehicle at speeds of 1.6, 8, 16.1, 24.1, 32.2, and 40.2 KPH. All data has been referenced to post P2 on the front passenger side of the target vehicle.

Figure 6.2-3: Perpendicular Latency Time

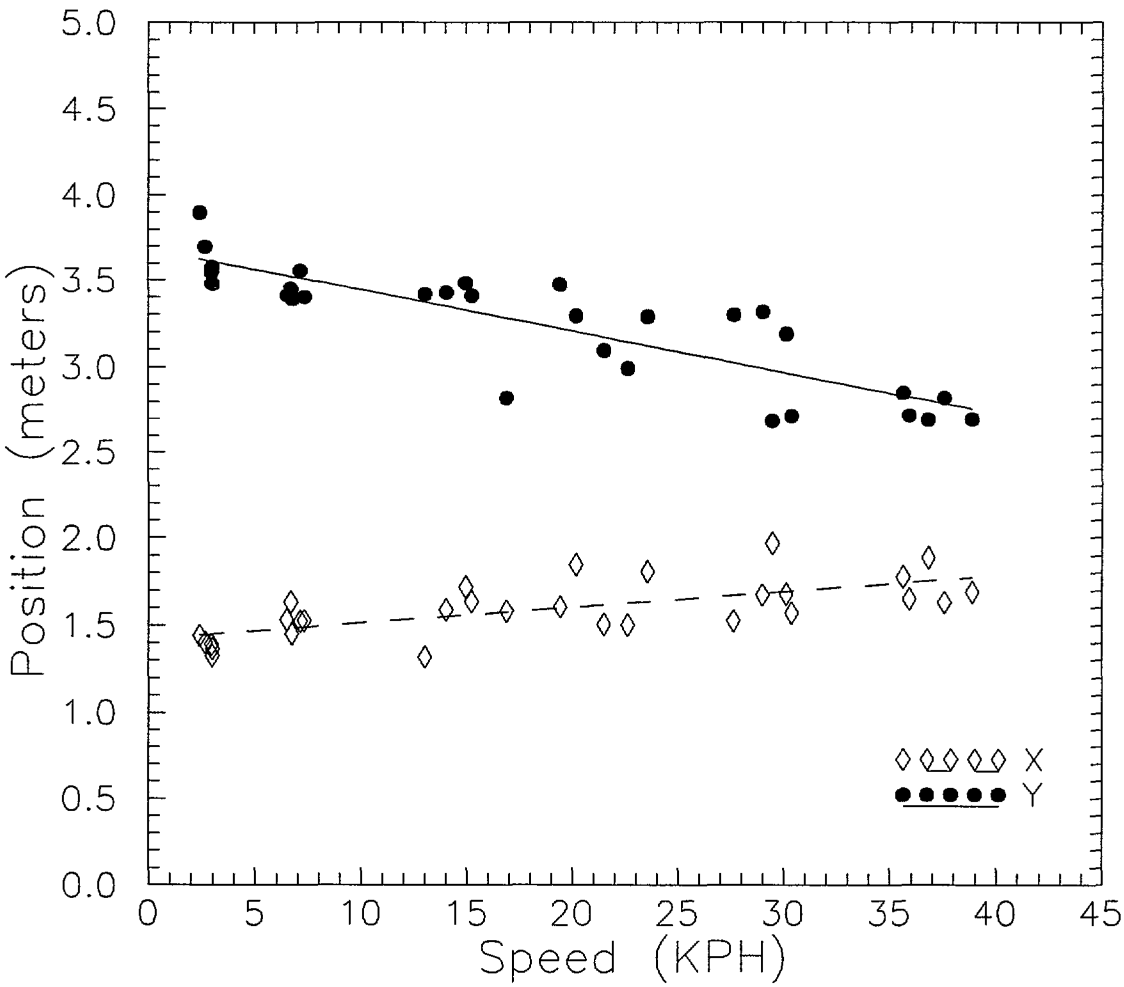

The lateral separation (X) between the two vehicles is denoted by the open triangles. This distance increases slightly at higher vehicle speeds reflecting the driver's natural tendency to increase the distance between his vehicle and a parked obstacle with increasing speed. The scatter about the mean is at most ±0.3m.

The Y position of the target vehicle at the instant of system reaction is shown by the filled circles. The slope of a linear best fit to the data yields the perpendicular latency time. With a characteristic scatter of roughly ±0.5m, the latency is calculated to be 85 msec ± 45 msec.

Parallel Delay Time

The results of the parallel delay time tests are presented in Figure 6.2-4. The speed of the approaching target vehicle was varied between 1.6 and 56.3 KPH.

Figure 6.2-4: Parallel Latency Time

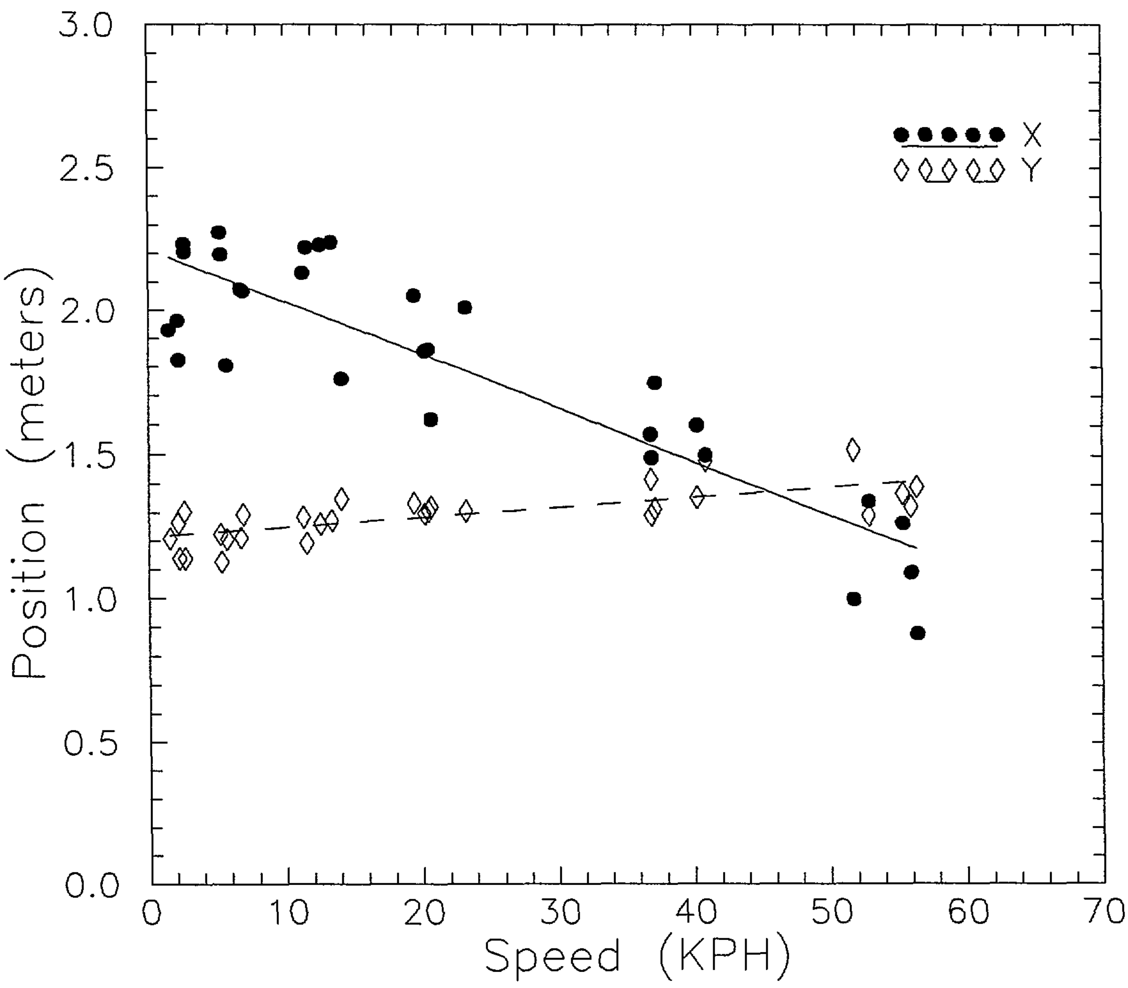

The lateral separation shown by the open triangles increases predictably with increasing closing velocity. The scatter in this parameter is less than 0.3m. The parallel coordinate of the approaching vehicle at the instant the system responds is shown by the filled circles. The scatter in this data represents real variation in the system response. The parallel latency time computed from this data is 66 +/- 22 msec.

Persistence Time

Information on the turn-off characteristics of the system has been extracted from the parallel delay time test results. The position of the target vehicle at the instant the system display turns off is plotted in Figure 6.2-5. This data has been computed from a projection of the car's position based on the trajectory and speed calculated from two earlier reference video frames. All data has been referenced to post P1 on the driver's side of the target vehicle. Because the static detection zone of this sensor system extends beyond the front of the host vehicle, the target vehicle position at the time the system turns off is far out of the field of view of the video cameras. Because the data has to be projected so far forward, any errors in this technique due to changing trajectories and speeds will be most evident at the faster speeds. Indeed, we observe that the scatter in the data is greatest at 40 and 50 KPH. Typical scatter in the parallel delay time data was +/-0.3m whereas the scatter in this data is as much as flm. This suggests that much of the scatter is probably due to inaccuracies in the projection which are, in turn, due to the large distances over which the projection must be made. The latency time associated with system turn-off is 0.51 sec +/- 0.12 sec.

Controlled Passing Tests - Target Vehicle Passing Sensor Vehicle

A series of controlled passing tests was performed on the High Speed Track in which the sensor vehicle was driven at a constant speed and passed on the right by the target vehicle. The vehicle speeds for this test were:

Sensor Vehicle Speed (KPH)	Target Vehicle Speed (KPH)	Closing Velocity (KPH)	Number of Passes
48.3	64.4	16.1	7
48.3	80.4	32.1	6
48.3	96.5	48.2	6
64.4	80.4	16.1	6
64.4	96.5	32.1	6
64.4	112.6	48.2	6
80.4	96.5	16.1	6
80.4	112.6	32.1	6

Figure 6.2-5: Persistence Time

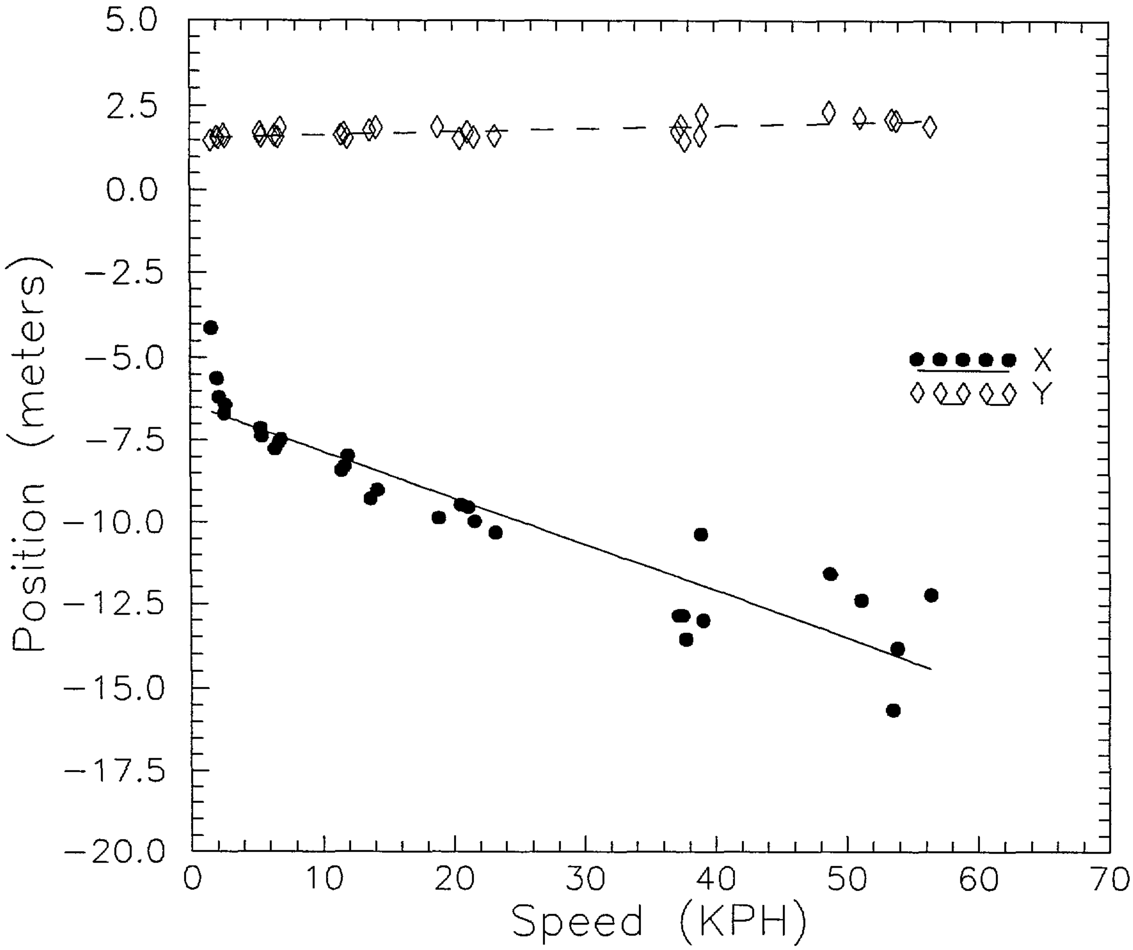

Roughly half of these tests were conducted on the curved portion of the High Speed Track. The intent of these tests was twofold: 1) to investigate the system performance as a function of relative speed and correlate the results with the measured system latency and 2) to investigate the effect on system performance when passing occurs on a curved path.

Figure 6.2-6(a) summarizes the target vehicle range at which the system first reacts to the passing vehicle. All results have been referenced to post P1 on the front driver side of the passing vehicle and have been segregated according to the closing velocity of the test. The static detection zone measured with the Ford Thunderbird target is denoted by the dashed line. Lane markers are identified by the vertical dashed lines. System latency can be as much as 0.4m at 16.1 KPH, 0.8m at 32.2 KPH and 1.2m at 48.3 KPH. With the exception of three data points at 48.3 KPH closing velocity, all results are clustered within 1m of the static

Figure 6.6-6: System "B" Controlled Passing Test Results
Target Vehicle Passing Sensor Vehicle

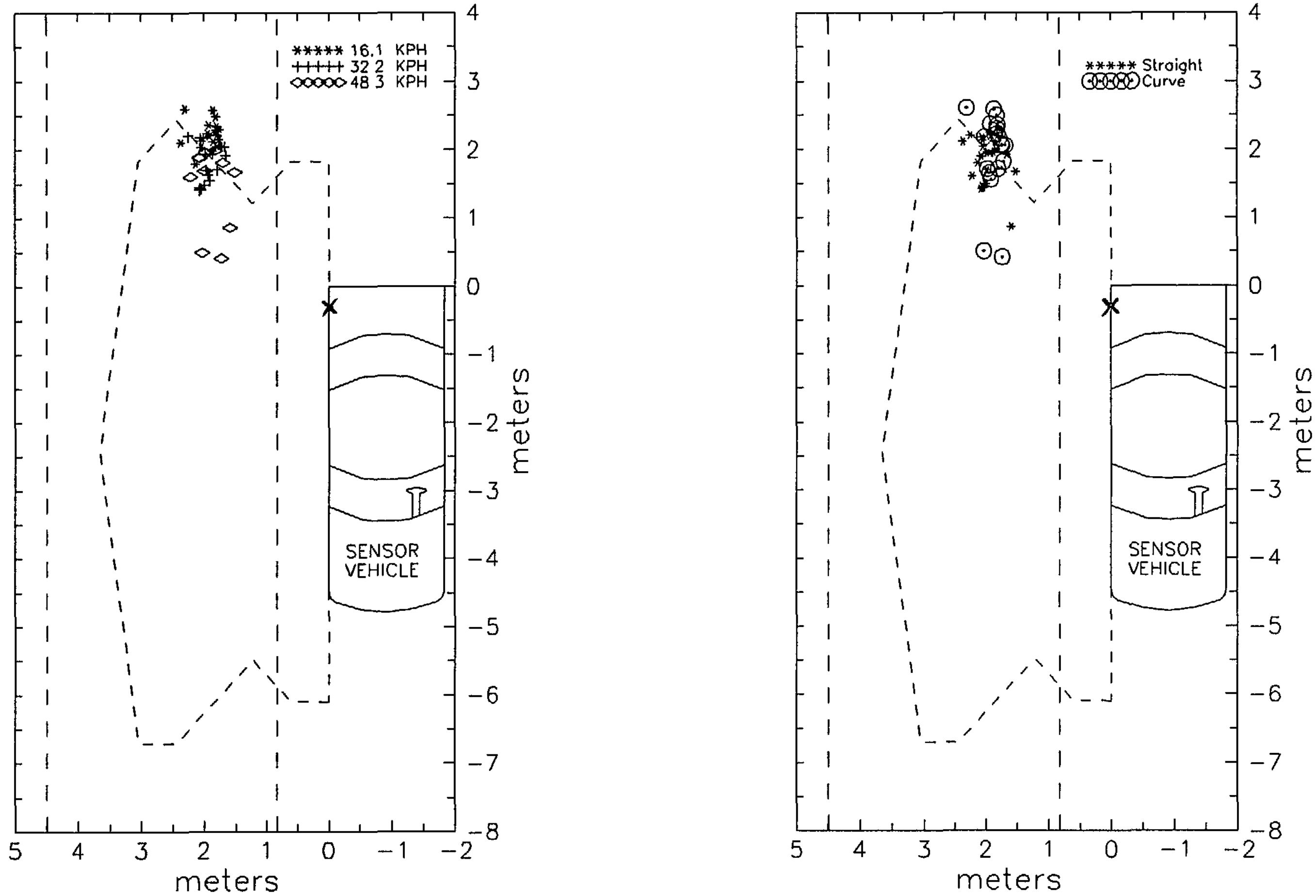

(a) System Performance vs. Relative Speed

(b) Curved vs. Straight Path

detection zone boundary and are thus consistent with the system latency. The three data points lying further towards the interior of the detection zone can be classified as “late” detects.

The effects of a curved path is shown in Figure 6.2-6(b). The data has now been plotted as a function of straight and curved path. In general, the results indicate that vehicles passing along a curve are no more difficult to detect than those vehicles passing on the straight-a-way. This is explainable in terms of the fact that this sensor system has a relatively short range. Such systems should be immune to degradations in system performance along gentle curves. It is interesting to note, however, that the two data points with the longest delay were acquired on a curved path. This suggests that these “late” detects at high closing velocity may show more dependence on the curvature of the passing trajectory.

These tests were repeated with a clutter vehicle located directly behind the sensor vehicle at separation distances of 4.6, 3.2, and 13.7m. The objective in these tests was to trigger a false alarm in the presence of typical highway traffic. Figure 6.2-7 summarizes the results of this test. The relative speed of the approaching vehicle varies between 16.1 and 32.2 KPH. Even with the clutter vehicle following only 4.6m behind the sensor vehicle (a distance that constitutes ‘tail-gating at highway speeds), no false alarms were triggered. The system performance is independent of clutter to the extent tested.

Controlled Passing Tests - Sensor Vehicle Passing Target Vehicle

A series of tests was performed in which the sensor vehicle passes the target vehicle in order to evaluate the system’s ability to distinguish between positive and negative closing speeds. A summary of the tests performed is as follows:

Sensor Vehicle Speed (KPH)	Target Vehicle Speed (KPH)	Closing Velocity (KPH)	Number of Passes
80.4	64.4	16.0	4
96.5	64.4	32.1	4

The results are presented in Figure 6.2-8. At these relative velocities, the longest delay that can be explained by the system latency is 0.8m[1] Most of the data collected shows delays of more than 1m. This suggests that this particular system has some difficulty detecting vehicles with a negative closing velocity.

1 **This number is derived by taking the maximum parallel latency** time, 0.088 set (see **p.** 60), **which includes measurement uncertainty, and calculating how far the target vehicle** travels in this time at the **highest relative speed of 32KPH.**

Figure 6.2-7: System "B" Controlled Passing With Clutter Vehicle
Target Vehicle Passing Sensor Vehicle

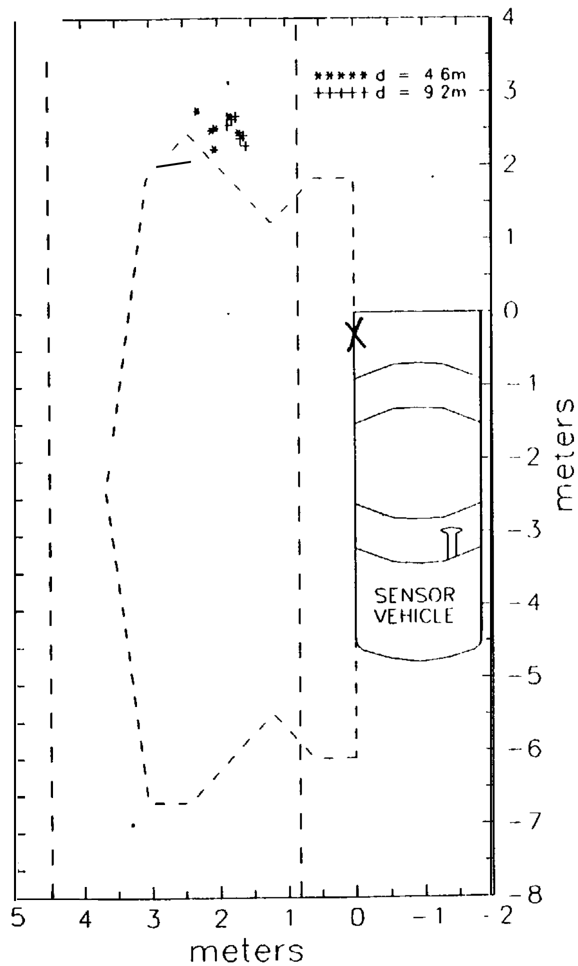

Figure 6.2-8: System "B" Controlled Passing Test Results
Sensor Vehicle Passing Target Vehicle

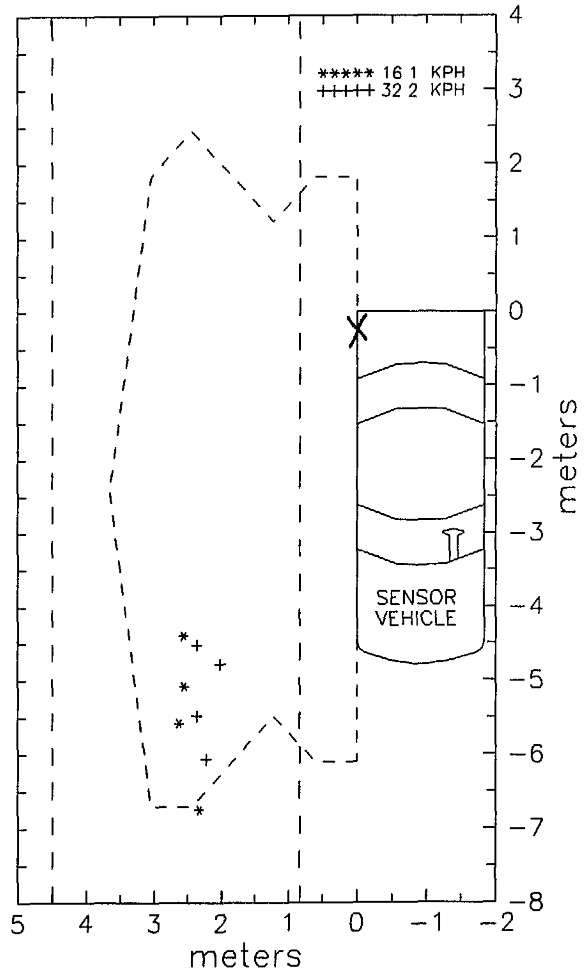

Approach and Pass Tests

A short series of tests was performed to investigate the system's utility in a typical highway passing scenario in which an approaching car in the same lane as the sensor vehicle swerves into an adjacent lane to pass. Six separate maneuvers were made with the sensor vehicle driving at a fixed speed of 64.4 KPH. The results are summarized in Figure 6.2-9. All data has been referenced to post P1 on the target vehicle. No attempt to maintain a fixed speed with the target vehicle was attempted because of the nature of the test. Note that the system does not detect the approaching vehicle until that vehicle has crossed over into the adjacent lane. Once again, the data collected is consistent with the static detection patterns measured.

Three Lane Tests

A series of 15 three lane maneuvers was performed to understand the potential for vehicles in a non-interfering lane to trigger a system response. These tests were done with the nose-to-nose (s) separation between vehicles varying from 0 to two car lengths. The number of passes that were made at the various separation distances are as follows:

Number of Passes	Separation Distance, s	System Reaction
2	0 (nose-to-nose)	YES
1	1/2 car length	YES
3	3/4 car length	YES
2	1-1/2 car length	YES
6	2 car lengths	NO
1	3 car lengths	NO

Notice that the system failed to react to a vehicle that was positioned at distances greater than 1-1/2 car lengths (i.e., about 2.25m behind the rear bumper of the sensor vehicle). This is consistent with the measured static pattern which extends at most, 2.5m behind the rear of the host vehicle. A total of eight passes caused a positive reaction. Three of these passes, however, one at s = 3/4 and both at s = 1-1/2 car lengths, had only two reference points visible in the video data. This is insufficient to get an accurate computation of the range. The only way to calculate range data from two reference points is to assume the target vehicle is oriented exactly parallel to the sensor vehicle. The resulting error in substantially exceeds 2m in the worst cases. Therefore, only the five cases in which three reference posts were visible with one camera have been analyzed. The results are summarized in Figure,6.2-10. In all cases, the system reacted to the target vehicle

Figure 6.2-9: System "B" Approach and Pass Test Results

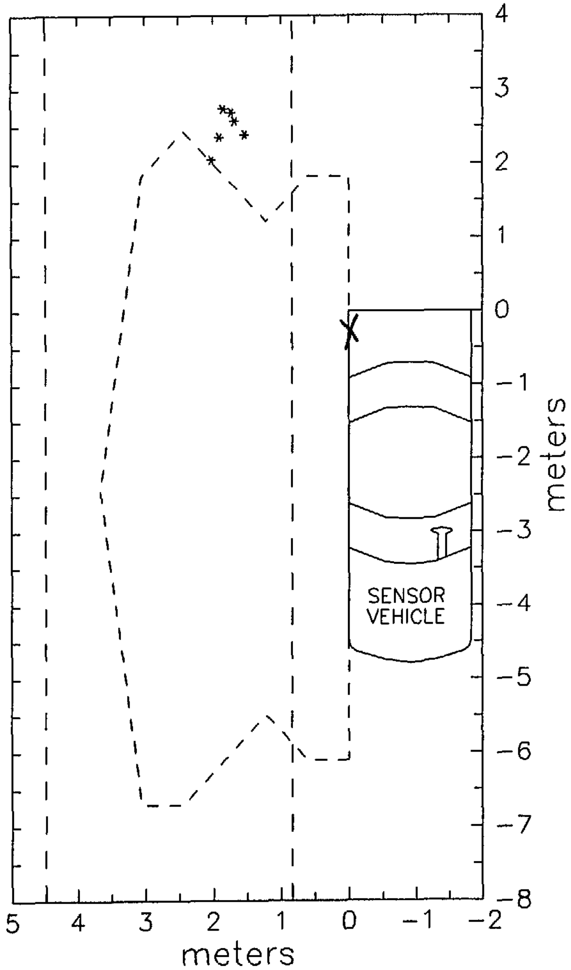

Figure 6.2-10: System "B" Three Lane Test Results

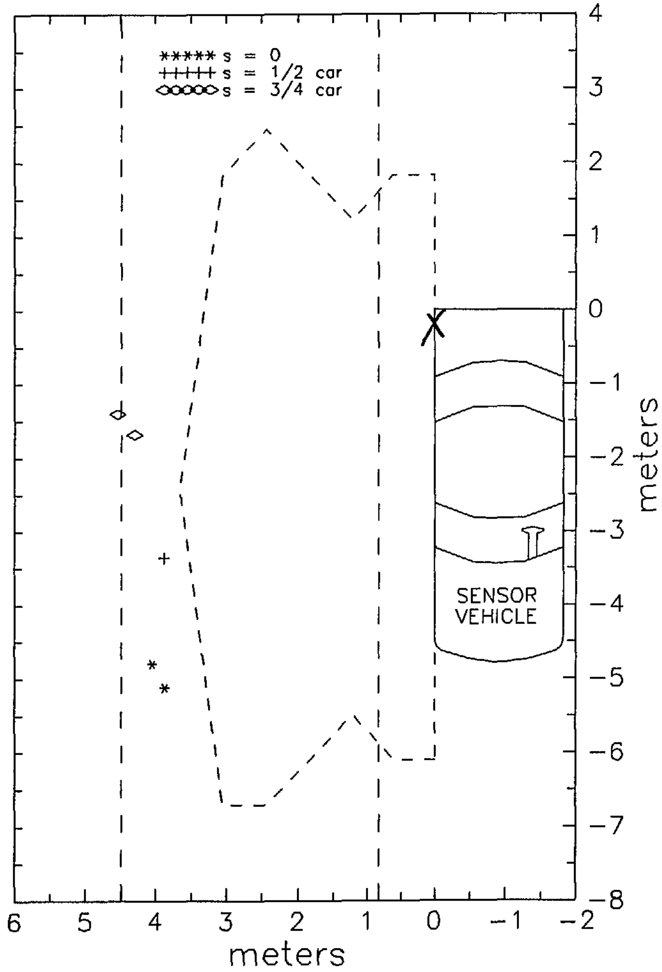

as it was in the process of making a lane change. The position of post P1 at the instant the system reacted was consistently on or inside the lane marker separating the middle and far lanes. Although the data lies outside the boundary of the measured static pattern, the error is within the day to day variation of the static measurement.

Merge Tests

In order to evaluate the system's utility during merging situations, the angle of approach of the target vehicle was varied from 0^o to 17^o to 27^o to 43^o The sensor vehicle was stationary and the target vehicle was driven past at speeds of 32.2, 48.3, and 64.4 KPH. The tests conducted with an angle of approach of 43^o failed to yield any response from the system despite the speed of the target vehicle.

Test results for the O^o, 17^o, and 27" merge tests are summarized in Figure 6.2-11 (a), (b), and (c) respectively. All data has been referenced to post P1 on the target vehicle and has been plotted as a function of target vehicle speed. A solid line indicating the angle of approach has been added to the off-axis tests to illustrate the path of the target vehicle's approach. System latency can be as much as 0.8m at 32.2 KPH, 1.2m at 48.3 KPH, and 1.6m at 64.4 KPH. Figure (a) demonstrates that all of the parallel approach data is consistent with the system latency. As the angle of approach is increased, however, it is apparent that roughly half of the data cannot be explained merely by the system latency. The data that falls far into the interior of the static detection zone can be classified as "late" detects. The degradation in system performance in these cases may be due to the fact that the approaching vehicle presents a smaller cross-section to the sensor as the angle of approach increases.

Road Test

This sensor system was evaluated under realistic road conditions involving freeway, city, two-lane highway, and parking lot driving. The total exposure time was 71.8 minutes. Statistics were compiled on the number and types of targets detected. Figure 6.2-l 2 summarizes the results.

This system performed very well as an obstacle detector during the road tests. There was not a single incidence in which the system failed to react to a target within its detection zone. Although this sensor system advertises the capability to discriminate between general ground clutter and valid traffic concerns, there were numerous cases in which general ground clutter triggered an inappropriate alarm. Most of the inappropriate alarms were triggered by parked vehicles especially ones of larger cross-section (such as vans and pick-up trucks). The average inappropriate alarm rate was computed to be 0.6 per minute.

Figure 6.2-11: System "B" Merge Test Results

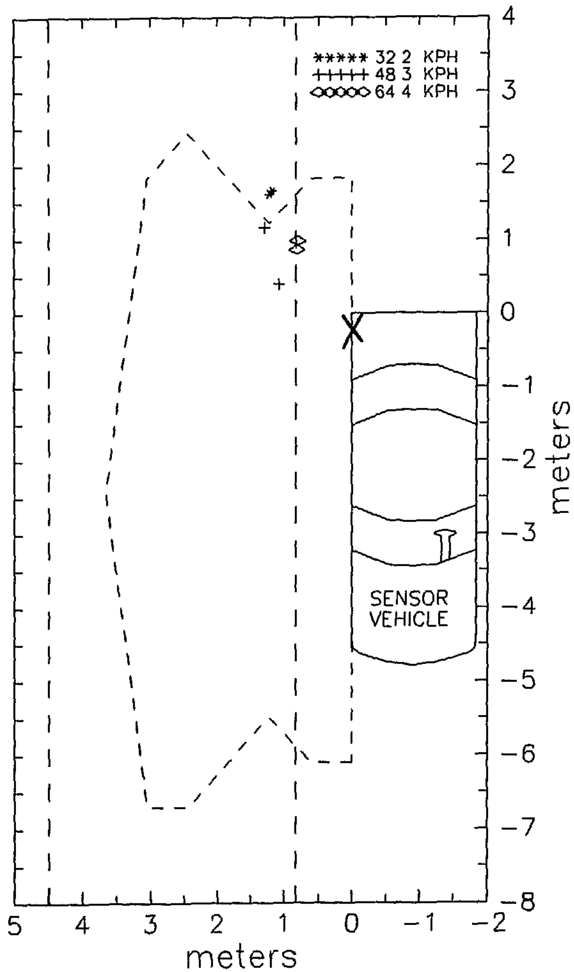

(a) 0º Angle of Approach

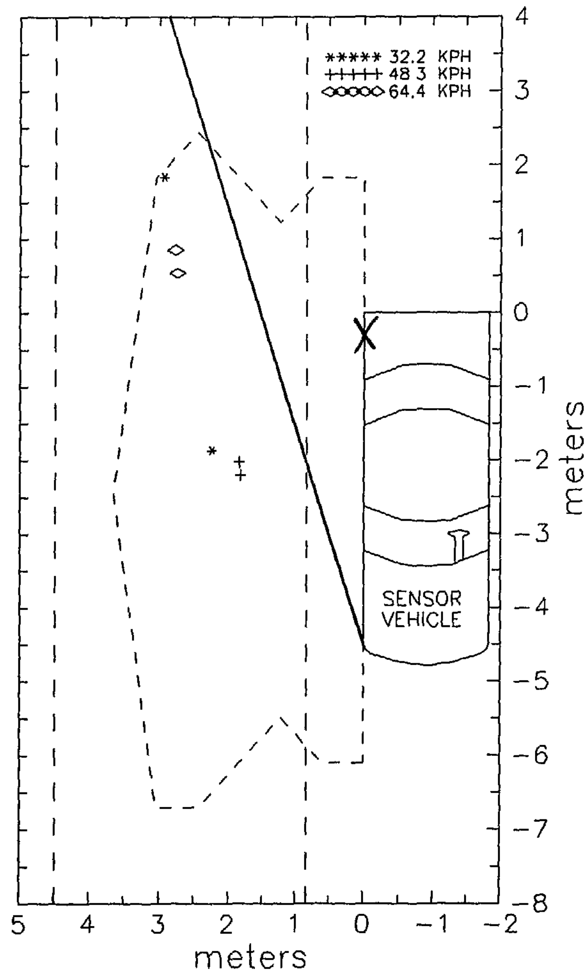

(a) 17º Angle of Approach

Figure 6.2-11: System "B" Merge Test Results (con'd)

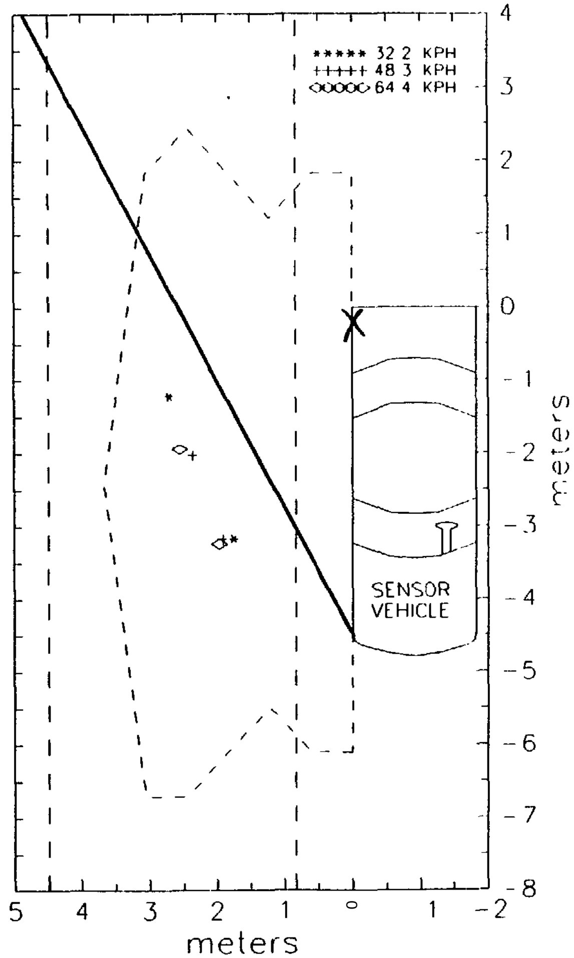

(c) 27° Angle of Approach

Figure 6.2-12: Summary of Road Test Statistics - System "B"

System: 'B"
Total number of detects: 76

Classification	Freeway	Two-lane	City	Parking Lot	TOTAL
TP	32	0	0	0	32
I	0	5	36	3.	44
FP	0	0	0	0	0
TOTAL	32	5	36	3	76
FN	0	0	0	0	0
TN					99.9 %

General Comments:

No unexplained misses (FN)

Road signs, trees, pole, concrete pillars did not cause inappropriate alarms

44 inappropriate alarms (I) - most of these were parked vehicles, especially high profile vehicles such as vans and pick-up trucks. Most of these alarms occurred at low relative speeds

6.4 System 'D"

6.4.1 System Description

This sensor system is a microwave radar collision warning system that is designed for side object detection. The center frequency was not known exactly but it is in the vicinity of 30GHz. The system has a velocity indicator which displays the speed of nearby targets relative to the host vehicle. The unit tested was mounted on the passenger side of the host vehicle near the side view mirror at a height of about lm above the ground level. The driver display consists of an indicator light that denotes the presence of a target. A light located above the main indicator represents a closing target and a light below represents a receding target.

6.4.2 Overview of System Performance

The unit tested performed fairly well as a proximity detector during both the controlled static and dynamic tests. Because this sensor system demonstrated a long range (20 - 25m) system response showed a definite dependence on the curvature of the path'taken by the host vehicle. In general, the dynamic response of the system was consistent with the measured static detection zone and exhibited typical scatter of a couple of meters. During all tests, the lights representing an approaching or receding target functioned properly.

During the initial road test, the system's clutter rejection performance was poor. This was due to the fact that the speed input to the system from the car's transmission was faulty. The road test was repeated, therefore, on a subsequent test trip. Before that trip the vendor visited VRTC during which the orientation and aim of the sensor was adjusted and the faulty velocity input corrected. The reorientation of the sensor had the effect of greatly increasing the field of view in the horizontal direction. In fact, the field of view encompassed the adjacent three lanes. Although this was not deemed optimal by the test conductors, it was so tested because it was configured by a vendor representative. During the second road test, the number of inappropriate alarms generated by normal ground clutter was greatly reduced. There were still, however, a significant number of alarms triggered when passing parked vehicles, especially if the relative speed was small. No false negatives (FN) were recorded.

6.4.3 Test Results

<u>Static Tests</u>

Static patterns were measured for the following types of targets:

1) 0.6m x 0.6m foil covered Styrofoam

2) human
3) Ford Thunderbird

The foil target was located at the vertical height of the sensor. Additional static measurements were made after the sensor was realigned. These results are applicable only to the road test data and will be discussed there.

Figure 6.4-1 summarizes the results of the static measurements made using the 0.6m x 0.6m aluminum foil covered target. It was immediately obvious with this sensor system that the detection zone was very long range. This pattern extends beyond the back of the host vehicle more than 21m. The lateral extent of the pattern covers most of the adjacent lane.

The results measured with a human target are shown in Figure 6.4-2. The extent of the pattern is significantly less than that measured with the 0.6m x 0.6m foil target. The longitudinal extent has been reduced to about 13m and the pattern extends laterally about a third of the way into the adjacent lane.

The static detection zone measured with a Ford Thunderbird target is shown in Figure 6.4-3. Similar to the foil target, this pattern is characterized by a 23m longitudinal range. The lateral extent is somewhat less extending only half way into the adjacent lane.

Vertical Extent

Vertical extent data for this sensor was not available. However, the half power beam width (HPBW) of the radiating antenna can easily be computed from the measured dimensions of the horn. For a pyramidal horn, the gain is determined from the following equation:

$$G = \frac{4\pi A_e}{\lambda^2}$$

where A_e is the effective aperture area (0.5ab) and λ is the wavelength. Substituting the length and width of the antenna aperture into the above equation yields a gain of 20.4 dB. The HPBW of the E-plane dimension (in this case, the vertical extent of the sensor), is given by:

$$\text{E-plane HPBW} = \frac{56\ \lambda}{b}$$

Using the short dimension of the antenna aperture, the calculated vertical extent is 19° centered at the midpoint of the sensor.

Figure 6.4-1 System "D" - Static Test Results
0.6m x 0.6m Foil Target

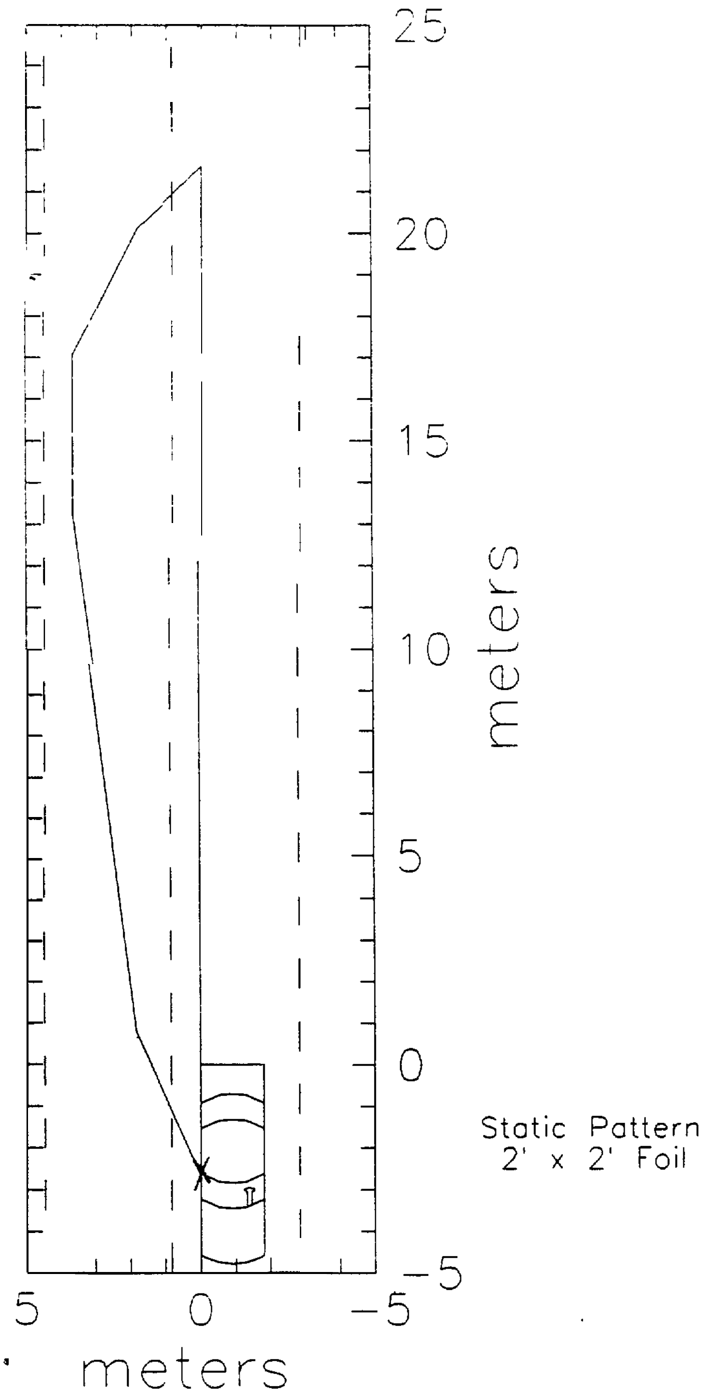

Figure 6.4-2: System "D" - Static Test Results
Human Target

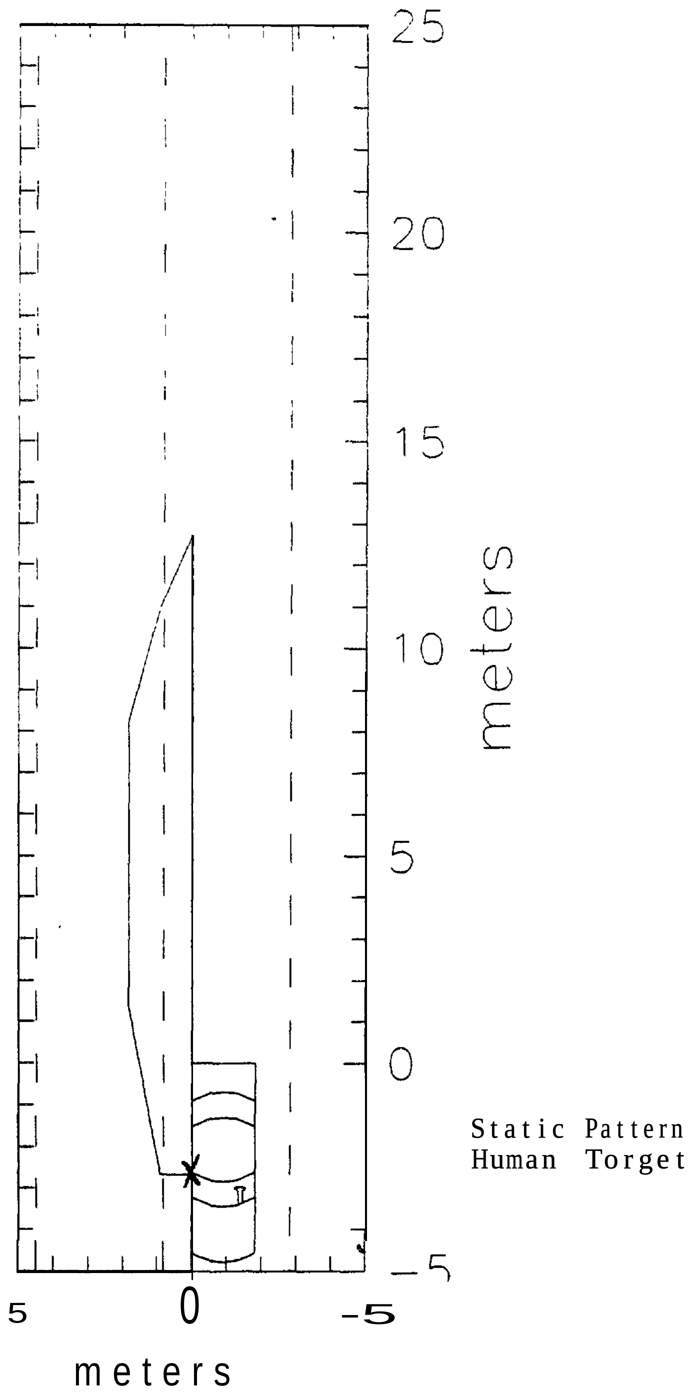

Figure 6.4-3: System "D" - Static Test Results
T-Bird Target

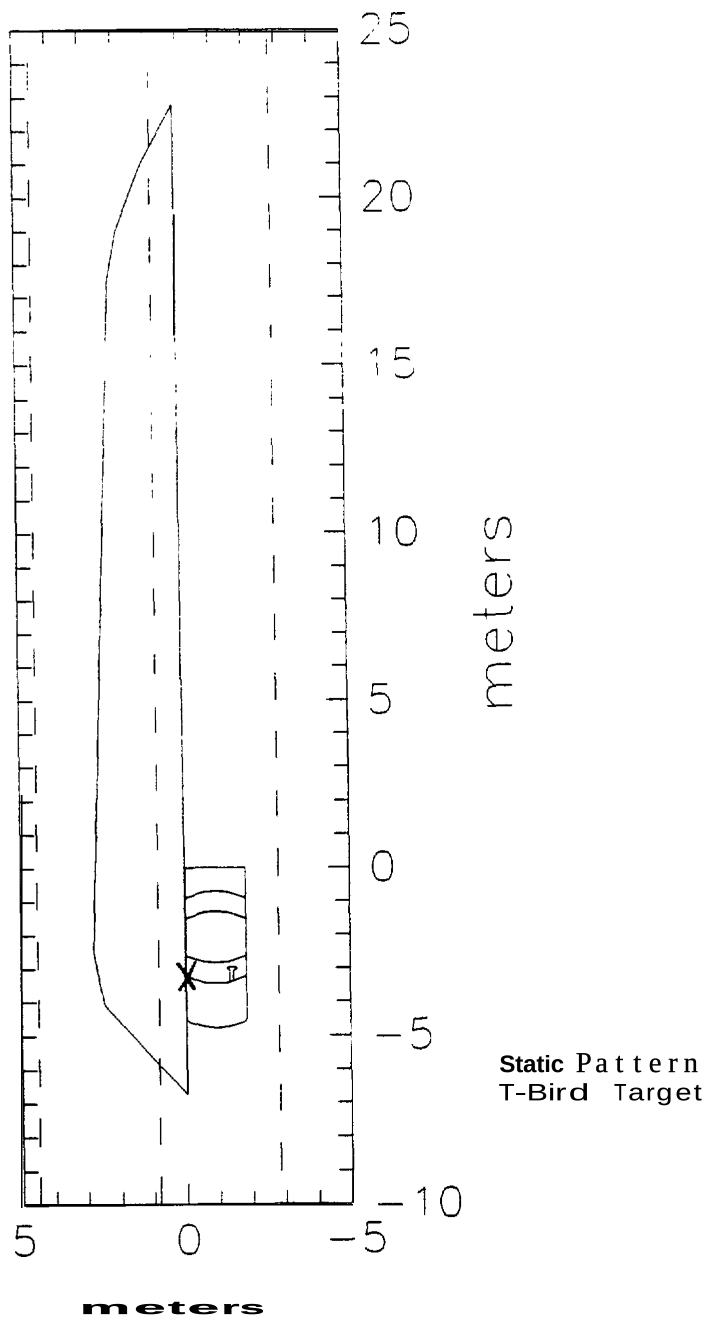

Dynamic Tests

Perpendicular Delay Time

Figure 6.4-4 summarizes the results of the perpendicular delay time tests for this system. The target vehicle was driven past the sensor vehicle at speeds of 1.6, 8, 16.1, 24.1, 32.2, and 40.2 KPH. All data has been referenced to post P2 on the front passenger side of the target vehicle.

Figure 6.4-4: Perpendicular Latency Time
System "D"

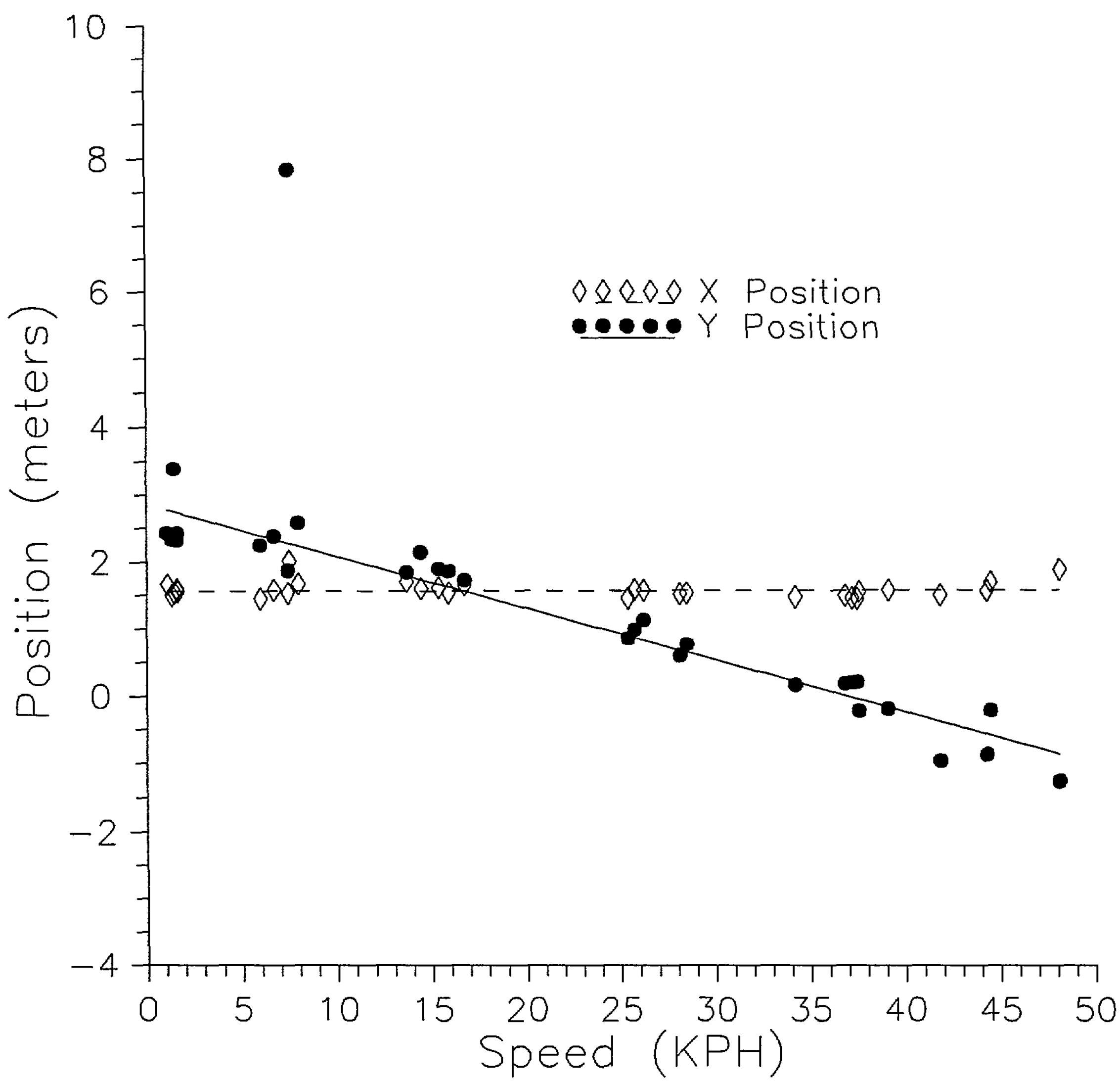

The lateral separation (X) between the two vehicles is denoted by the open diamonds. This distance increases slightly at higher vehicle speeds reflecting the driver's natural tendency to increase the distance between his vehicle and a parked obstacle with increasing speed. The scatter about the mean is less than +/-0.5m.

The Y position of the target vehicle at the instant of system reaction is shown by the filled circles. Notice that a single data point taken with a vehicle speed of 8 KPH is far outside the typical scatter. The system did indeed react very early on this particular pass. However, most likely, this represents a false alarm and was not included in the linear regression analysis of the data. The perpendicular latency computed from this data is 0.27 set +/- 30 msec.

Parallel Delay Time

The results of the parallel delay time tests are presented in Figure 6.4-5. During the controlled parallel delay time tests, the system was not functioning properly. This was not discovered until the data was analyzed. The indication of malfunction turned out to be that the velocity indicator displayed a fixed speed regardless of the speed of the approaching target. Therefore, the parallel latency time was determined from the 0^o merge tests during which the system was functioning properly. One slight disadvantage of using the merge data is that no system reaction information is obtained with vehicle speeds of less than 32.2 KPH. This data was collected with vehicle speeds of 32.2, 48.3, and 64.4 KPH.

The lateral separation shown by the open diamonds and is held fairly constant to about 1.5m. The scatter in this parameter is about a meter due to the high relative speeds of the test. The parallel coordinate of the approaching vehicle at the instant the system responds is shown by the filled circles. The scatter in this data represents real variation in the system response and can be as large as 3m. This represents a variation about the mean of about 25%. The parallel latency time computed from this data is 0.52 sec +/- 0.36 sec.

Persistence Time

For this system, information on the turn-off characteristics have been extracted from the 0^o merge test results. The position of the target vehicle at the instant the system display turns off is plotted in Figure 6.4-6. This data has been computed from a projection of the car's position based on the trajectory and speed calculated from two earlier reference video frames. All data has been referenced to post P1 on the driver's side of the target vehicle. The characteristic scatter in this data is about a meter which is much small than that observed during system turn-on. The latency time associated with system persistence is 0.118 sec +/- 50 msec.

Figure 6.4-5: Parallel Latency Time
System "D"

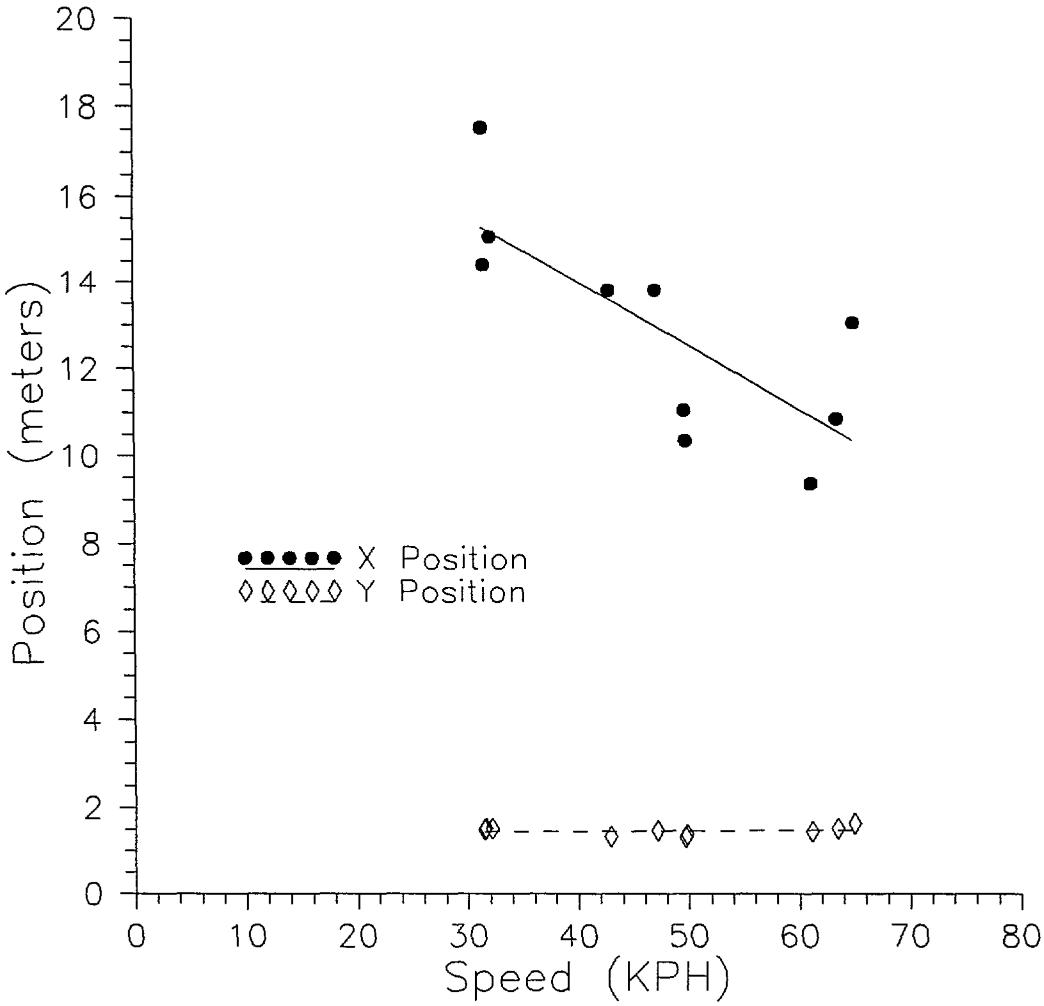

Controlled Passing Tests - Target Vehicle Passing Sensor Vehicle

A total of 42 controlled passing tests were performed on the High Speed Track in which the sensor vehicle was passed on the right by the target vehicle. The vehicle closing speeds for this test were:

Closing Velocity (KPH)	Number of Passes
8	3
16.1	16
24.1	14
32.2	9

Figure 6.4-6: System Persistence Time
System "D"

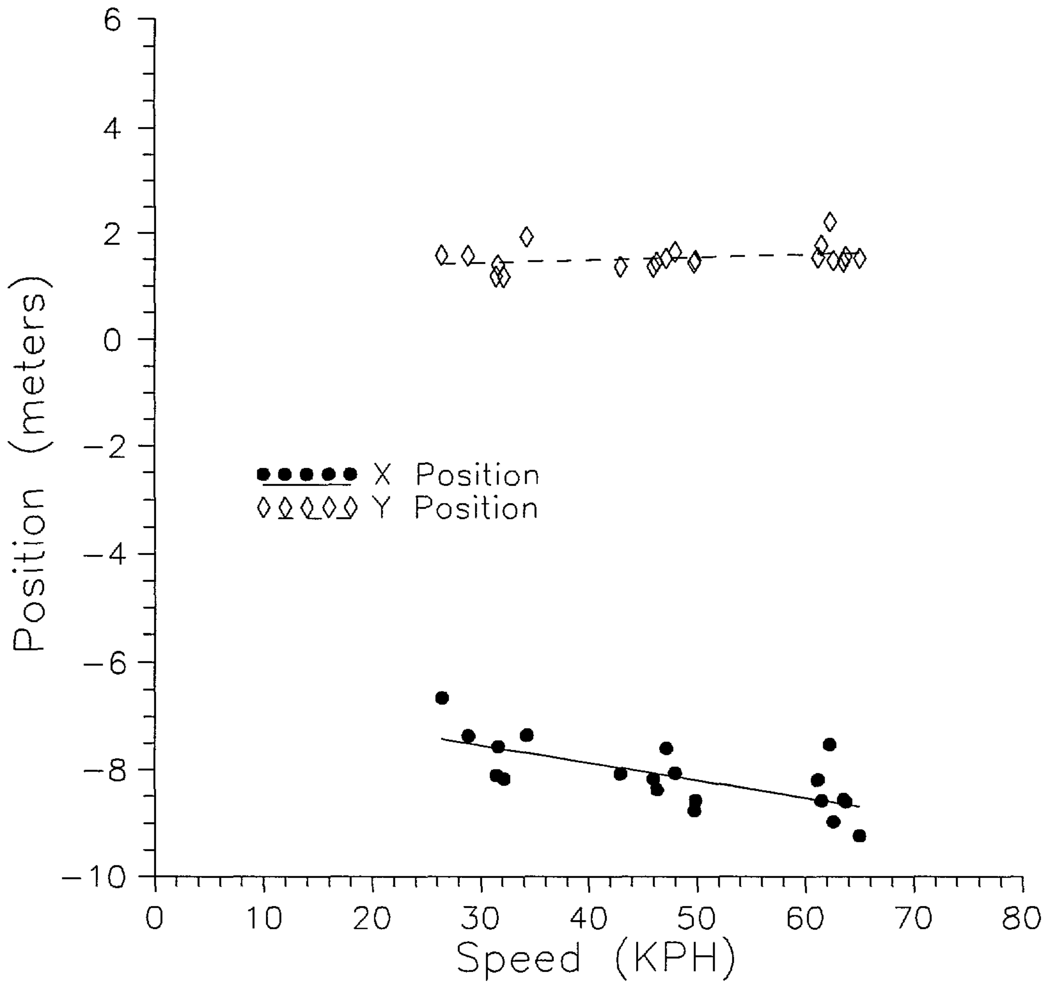

Roughly 19% of these tests were conducted on the curved portion of the High Speed Track. The intent of these tests was twofold: 1) to investigate the system performance as a function of relative speed and correlate the results with the measured system latency and 2) to investigate the effect on system performance when passing occurs on a curved path.

Figure 6.4-7 summarizes the target vehicle range at which the system first reacts to the passing vehicle. All results have been referenced to post P1 on the front driver side of the passing vehicle and have been segregated according to the closing velocity of the test. The static detection zone measured with the Ford Thunderbird target is denoted by the dashed line. Lane markers are identified by the vertical dashed lines.

Figure 6.4-7: System "D" Controlled Passing Tests
Target Vehicle Passing Sensor Vehicle

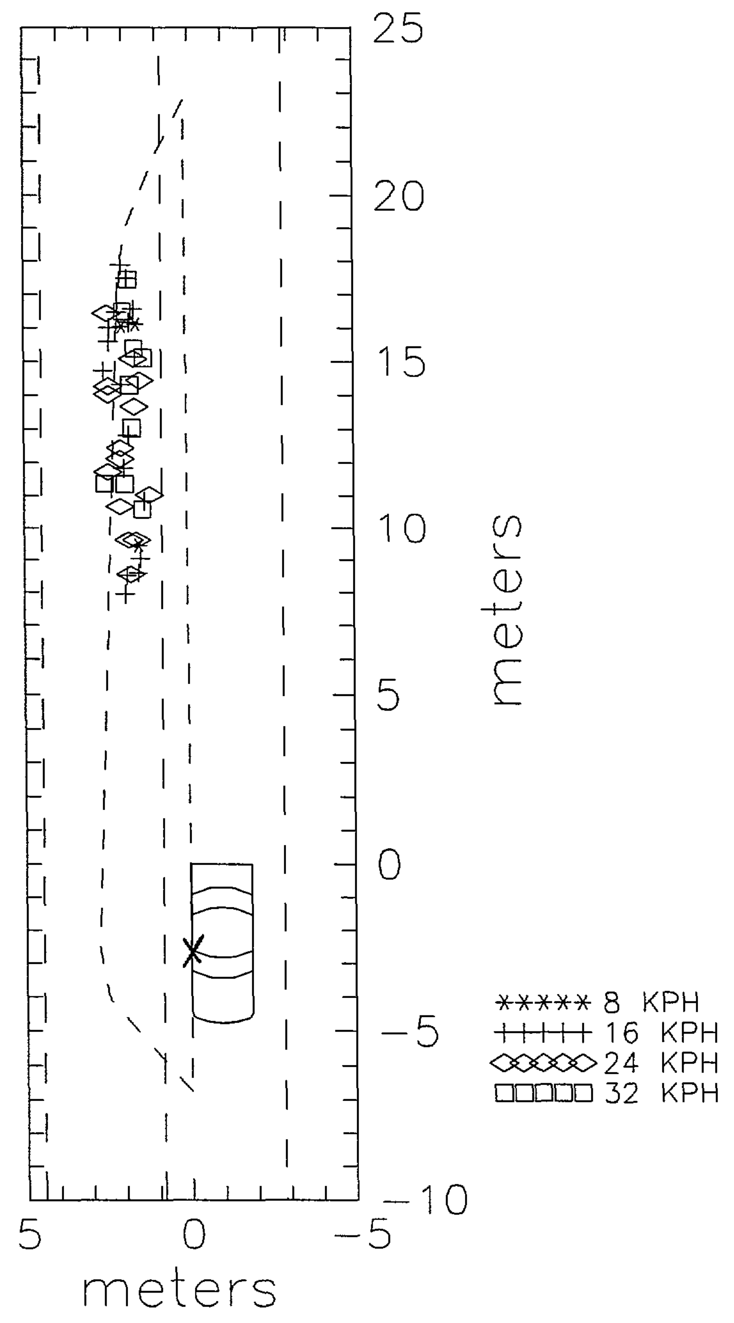

At first glance, it appears difficult to draw any definitive conclusions from the data. Ranges vary between 8 and 17m and do not show any correlation to vehicle speed. The main factor in the apparent lack of correlation in the data is that the approaching vehicle enters the detection zone along its edge. Thus, it is difficult to determine the exact position that the-target first enters the zone. This may vary significantly from pass to pass depending on the lateral separation between the vehicles. The bottom line is that the data presented represents real variations in system performance.

The effects of a curved path is shown in Figure 6.4-8. The data has now been plotted as a function of straight and curved path. Unlike the short range sensor systems, this system begins to exhibit a correlation between the performance and the trajectories of the vehicles in question. Generally speaking, those data points collected along a curve are detected later than those acquired along a straight path. This result can be explained by referring to the picture below.

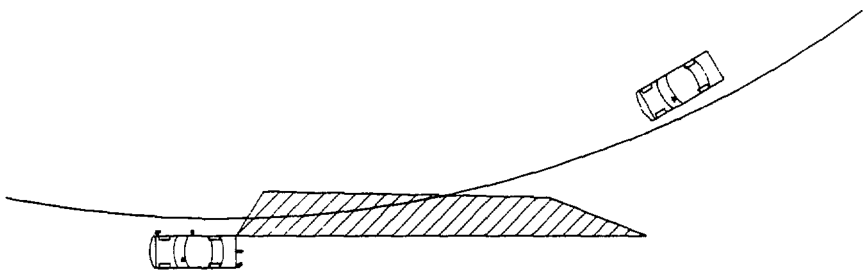

A vehicle equipped with a long range sensor system is being approached by another vehicle along a curved trajectory. The static detection zone is denoted by the hatched area. A car approaching along a curved path will enter the detection zone more towards the middle resulting in a closer range for the initial detect.

These tests were repeated with a clutter vehicle located directly behind the sensor vehicle at separation distances of 10.7, 29.3, and 55.5m. The objective in these tests was to trigger a false alarm in the presence of typical highway traffic. Figure 6.4-9 summarizes the results of this test. The relative speed of the approaching vehicle was held to approximately 16 KPH. At first glance, it appears that the data collected in the presence of a clutter vehicle is within the general scatter of the data collected in the absence of clutter. It should be noted here that data collected with the clutter vehicle positioned more than 25m behind the host vehicle really represents a clutter-free environment since the static detection zone only extends to about 23m. It is useful to examine this data as a function of the

Figure 6.4-8: System "D" Controlled Passing Tests
Target Vehicle Passing Sensor Vehicle
Curved vs. Straight Path Performance

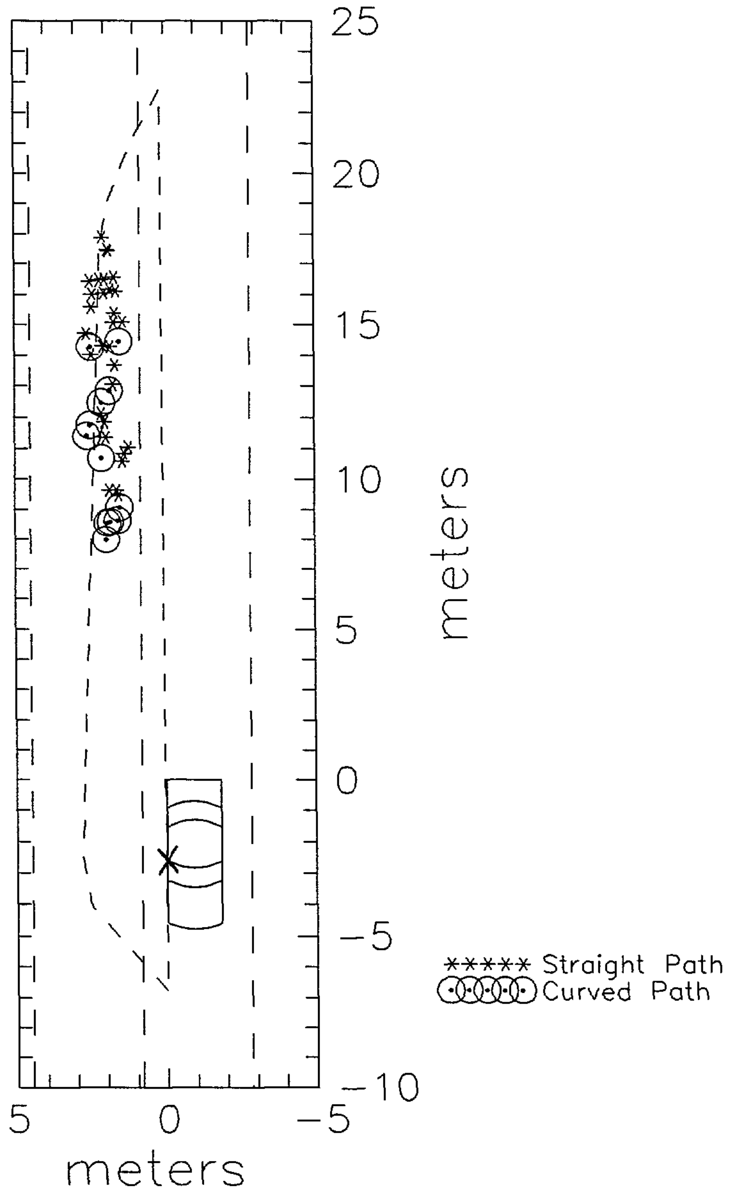

Figure 6.4-9: System "D" Controlled Passing Tests With Clutter Vehicle
Target Vehicle Passing Sensor Vehicle

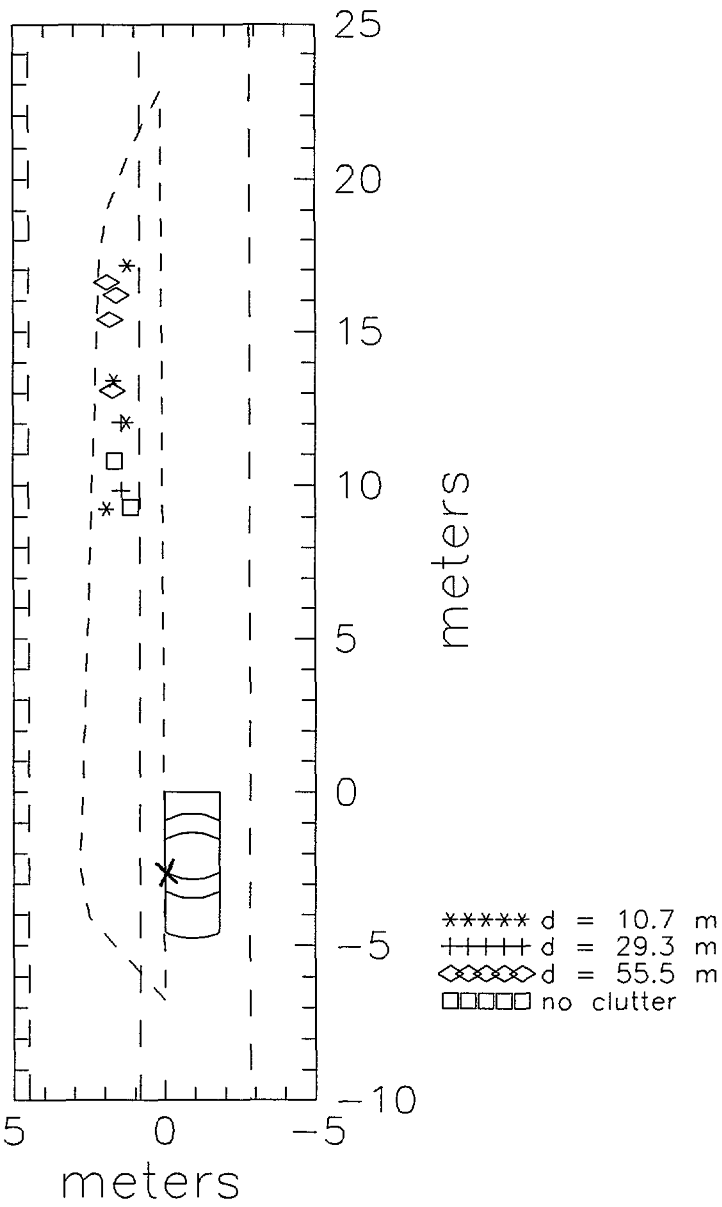

curvature of the path of approach. The data has been replotted to compare a straight to a curved trajectory in Figure 6.4-10. Notice once again that the data collected along a curved path tends to fall more towards the middle of the detection zone. This suggests a stronger correlation to the trajectory of the approaching vehicle than to the presence of a clutter vehicle. No false alarms were triggered even with the clutter vehicle position at 10.7m.

Controlled Passing Tests - Sensor Vehicle Passing Target Vehicle

Ten passes were made in which the sensor vehicle passed the target vehicle. The purpose was to evaluate the system's ability to distinguish between positive and negative closing speeds. A summary of the tests performed is as follows:

Closing Velocity (KPH)	Number of Passes
8	5
16.1	5

The results are presented in Figure 6.4-11. The system latency can be as much as 2m at 8 KPH and 4m at 16 KPH. The data reflects a delay of 2 to 3m at 8 KPH and 2.5 to 6m at 16 KPH. A single data point taken at 16 KPH shows a delay of 6m which is longer than the system latency can explain. Otherwise, the data is consistent with the measured static detection zone and the system latency.

Approach and Pass Tests

A short series of three passes were made to investigate the system's utility in a typical highway passing scenario in which an approaching car in the same lane as the sensor vehicle swerves into an adjacent lane to pass. The results are summarized in Figure 6.4-12. All data has been referenced to post P1 on the target vehicle. The passing vehicle is detected as it begins to move to the adjacent lane. As referenced to post P1, the data collected lies about one meter outside the measured zone. This inconsistency with the measured pattern is most probably due to an extended response of the static pattern behind the sensor vehicle, which unfortunately was not measured with the target car during the static portion of these tests.

Three Lane Tests

A series of ten three lane maneuvers was performed to understand the potential for vehicles in a non-interfering lane to trigger a false alarm. These tests were done with the nose-to-nose (s) separation between vehicles varying from 0 to two

Figure 6.4-10: System "D" Controlled Passing Tests With Clutter Vehicle
Target Vehicle Passing Sensor Vehicle
Curved vs. Straight Path

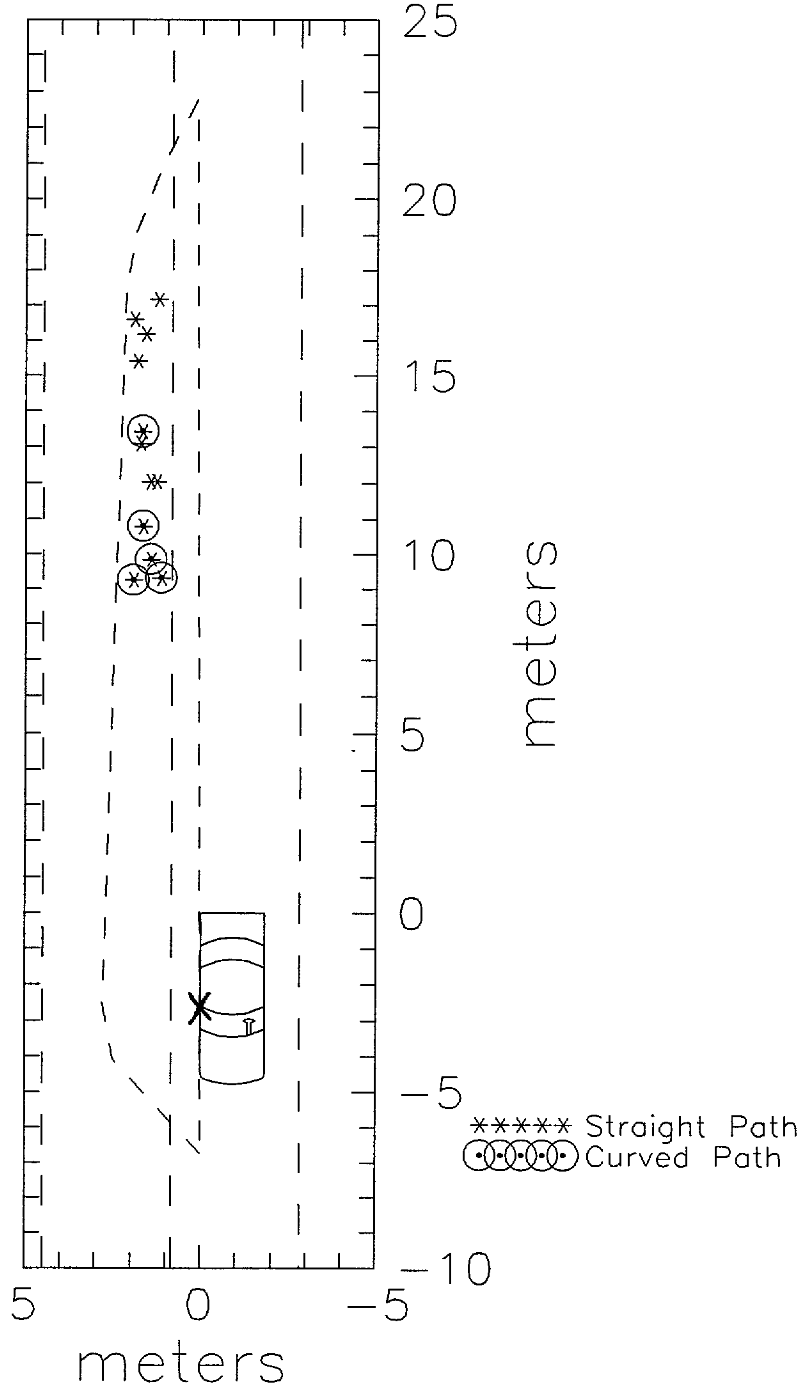

Figure 6.4-11: System "D" Controlled Passing Tests
Sensor Vehicle Passing Target Vehicle

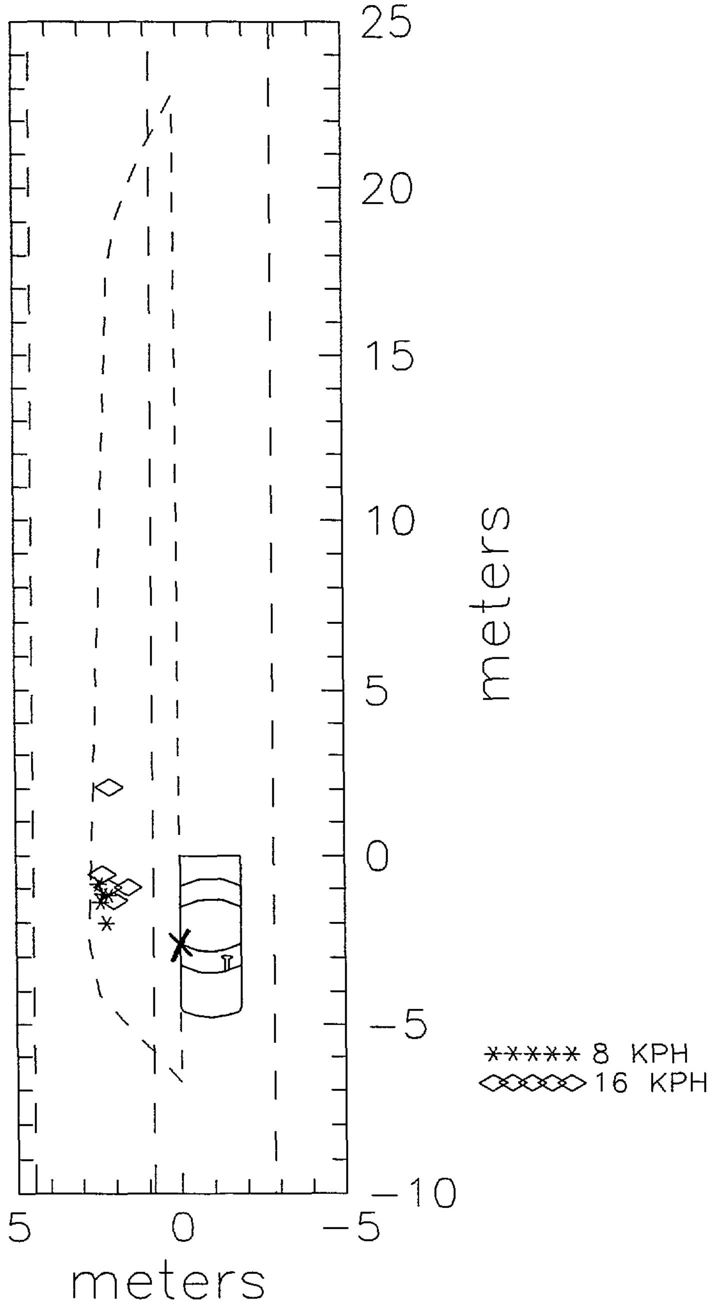

Figure 6.4-12: System "D" Approach and Pass Tests

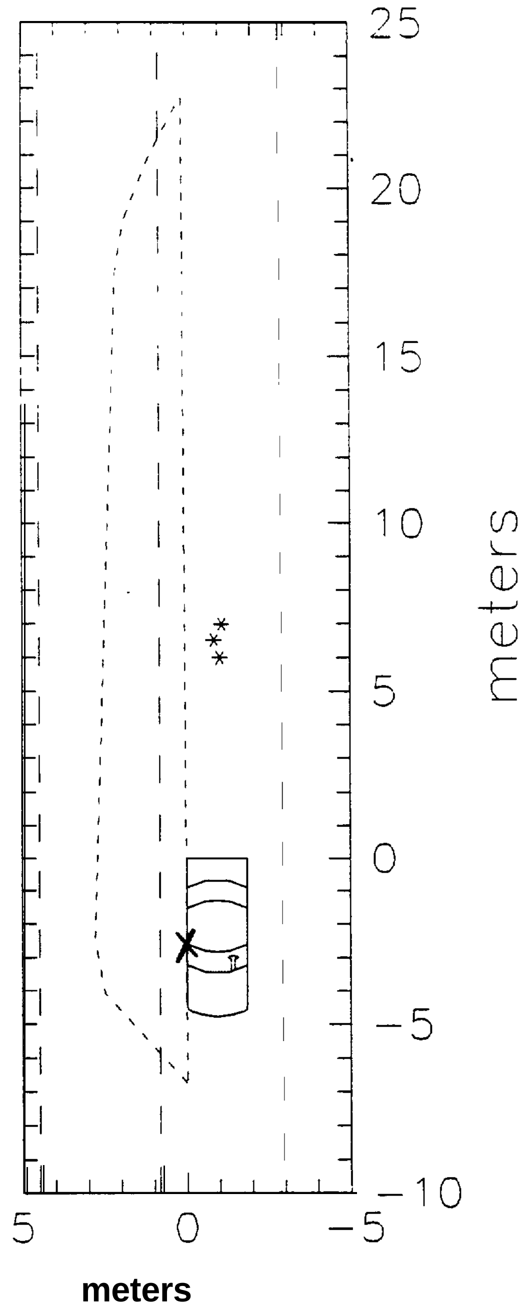

car lengths. The number of passes that were made at the various separation distances are as follows

Number of Passes	Separation Distance, s	System Reaction
4	0 (nose-to-nose)	YES (2 out of 4)
3	1/2 car length	YES (1 out of 3)
1	1 car length	YES
2	2 car lengths	YES (1 out of 2)

The target was detected at nose-to-nose separations up to 2 car lengths. However, only five out of the ten passes triggered a system response as shown in Figure 6.4-13. The data collected, however, is consistent with the static detection pattern measured indicating that no false alarms are generated by vehicles in a non-interfering lane.

Merge Tests

In order to evaluate the system's utility during merging situations, the angle of approach of the target vehicle was varied from 0" to 9" to 24°. The sensor vehicle was stationary and the target vehicle was driven past at speeds of 32.2, 48.3, and 64.4 KPH. The tests conducted with an angle of approach of 24° failed to yield any response from the system despite the speed of the target vehicle.

Test results for the 0° and 9° merge tests are summarized in Figure 6.4-14 and 6.4-l 5, respectively. All data has been referenced to post P1 on the target vehicle and has been plotted as a function of target vehicle speed. A solid line indicating the angle of approach has been added to the off-axis tests to illustrate the path of the target vehicle's approach. System latency can be as much as 8m at 32.2 KPH, 12m at 48.3 KPH, and 16m at 64.4 KPH. The data collected during the 0° merge tests show a delay of 2 to 5.5 m at 32 KPH, 6 to 10 m at 48 KPH and 7 to 11 m at 64 KPH. Thus, the measured response is consistent with both the static detection zone and the system latency.

As the angle of approach is increased to 9°, however, it is apparent that all of the detections occur on or outside the measured static detection zone. The most plausible explanation for the data is that the approaching vehicle presents a larger cross-section to the system as the angle of approach increases. This may trigger an earlier response than that measured during the static tests in which the angle of approach was fixed at 0°.

Figure 6.4-13: System "D" Three Lane Tests

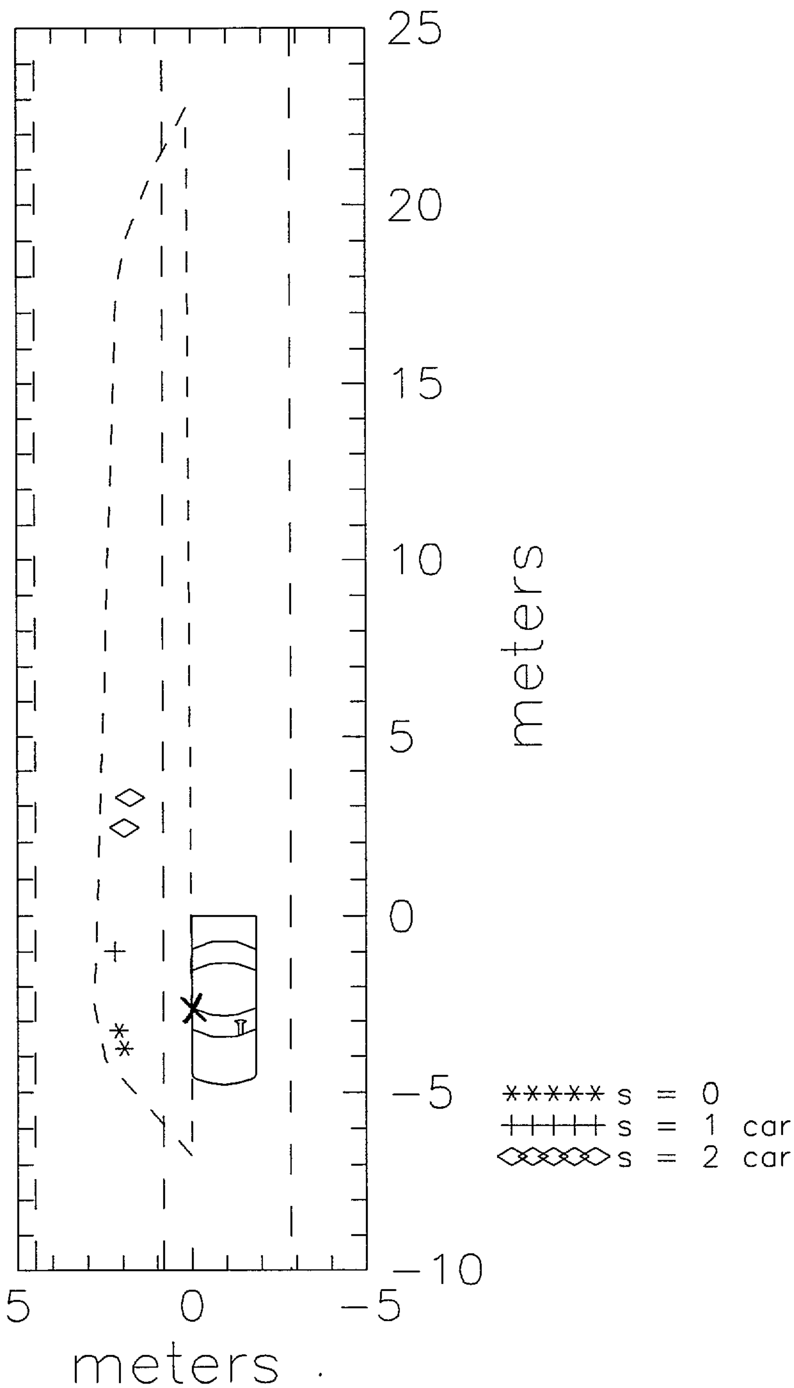

Figure 6.4-14: System "D" 0 Degree Merge Tests

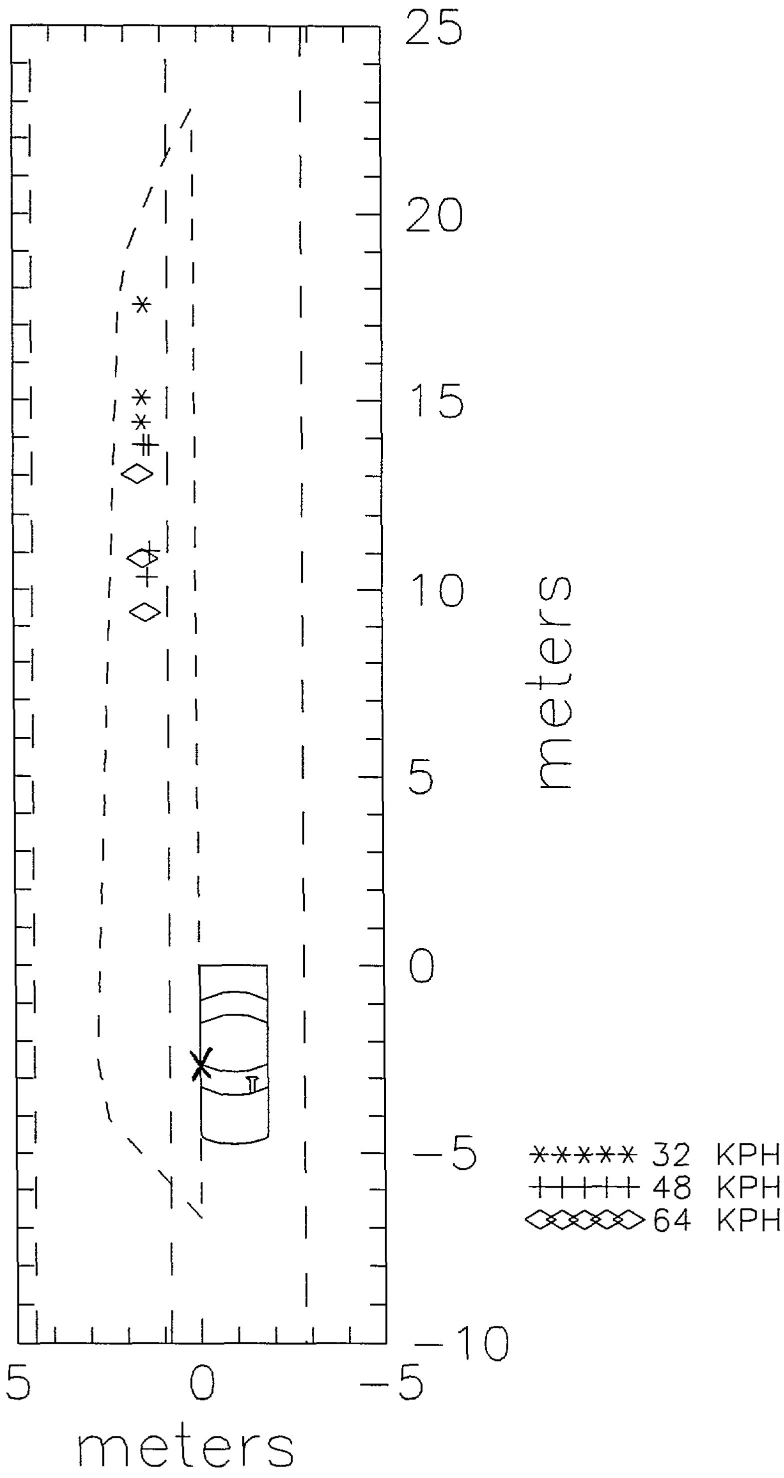

Figure 6.4-15: System "D" 9 Degree Merge Tests

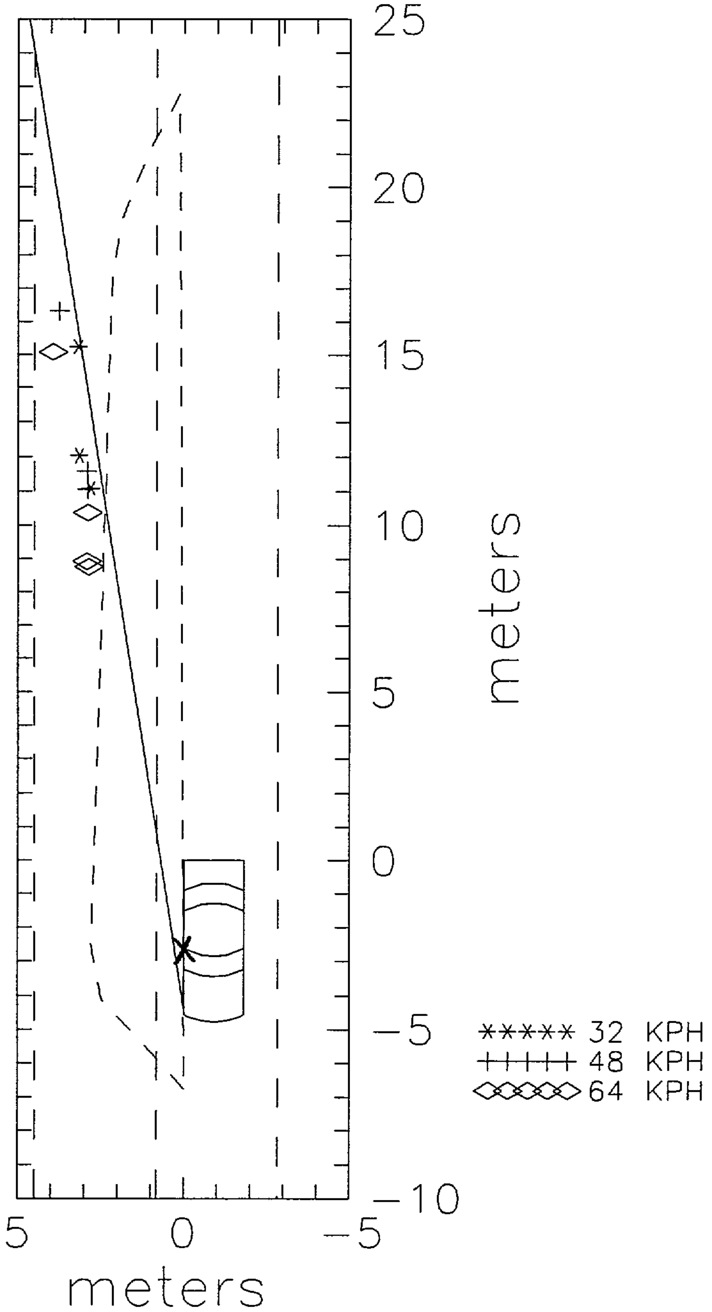

Road Test

As mentioned during the overview of the system's performance, during the **initial** road test, the system's clutter rejection performance was poor. This was due to the fact that the speed input to the system from the car's transmission was faulty. The road test was repeated, therefore, on a subsequent test trip. After a visit from the vendor during which the orientation and aim of the sensor was adjusted and the faulty velocity input corrected, the road test was repeated. At that time, new static detection patterns of the 0.6m x 0.6m foil target, a motorcycle, and the Ford Taurus were measured. These are shown in Figures 6.4-l 6 through 18, respectively. Notice that the extent of the pattern has shifted markedly over the earlier plots. Now the system has visibility at least three lanes over from the host vehicle lane. Thus, the system will react to non-interfering vehicles traveling more than one lane over from the host vehicle. This will result in an increased number of nuisance responses on freeways having three or more lanes. For tests in the Marysville area which included only two-lane freeway driving, the additional number of these responses was expected to be small.

After realignment and repair of the faulty speed input, this system was reevaluated under realistic road conditions involving freeway, city, two-lane highway, and parking lot driving. The total exposure time was 58 minutes. Statistics were compiled on the number and types of targets detected. Figure 6.4-19 summarizes the results.

As a proximity detector, this system performed well during the road tests. There was not a single incidence in which the system failed to react to a target within its detection zone (FN). However, the system's ability to discriminate between general ground clutter and valid traffic concerns was marginal. There were numerous cases in which general ground clutter triggered a inappropriate alarm. Most of the inappropriate alarms were triggered by parked vehicles which were passed with small relative velocities. The percentage of inappropriate alarms due to general ground clutter was found to be approximately 56% of the total number of system alarms. In addition, there were eight instances in which the system responded when there were no apparent targets within its field of view. There was one instance when the system detected a semi truck located three lanes over from the sensor vehicle as it merged off of the freeway. This instance was classified as a true positive because of the extended lateral range of this sensor after its reorientation by the vendor.

Figure 6.4-16: System "D" Remeasured Static Pattern
0.6m x 0.6m Foil Target

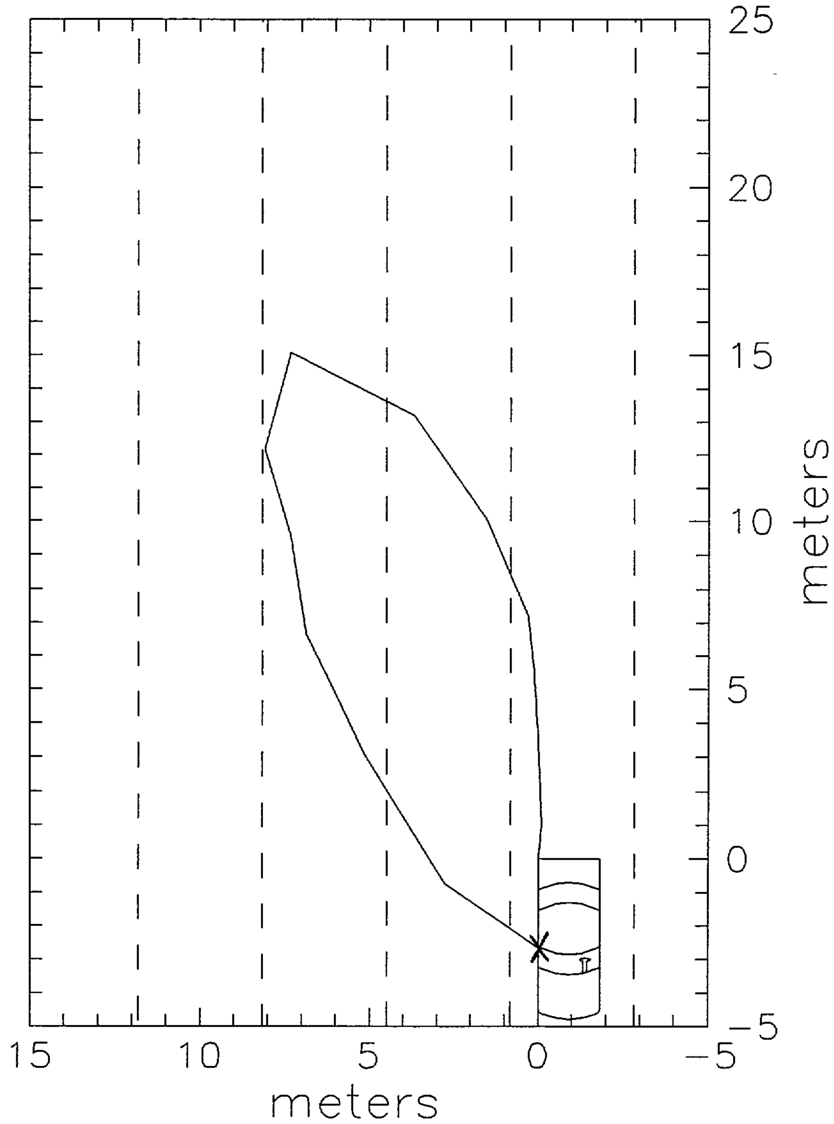

Figure 6.4-17: System "D" Remeasured Static Pattern
Motorcycle Target

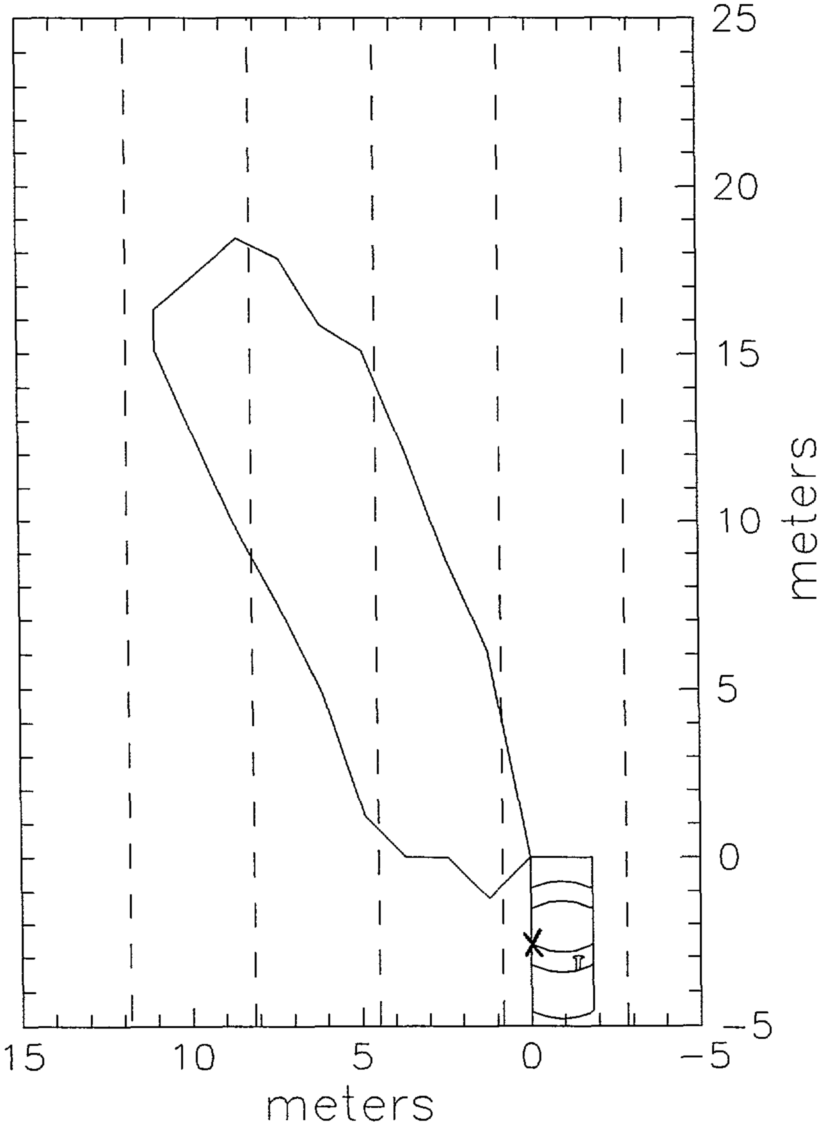

Figure 6.4-18: System "D" Remeasured Static Pattern
Ford Taurus Target

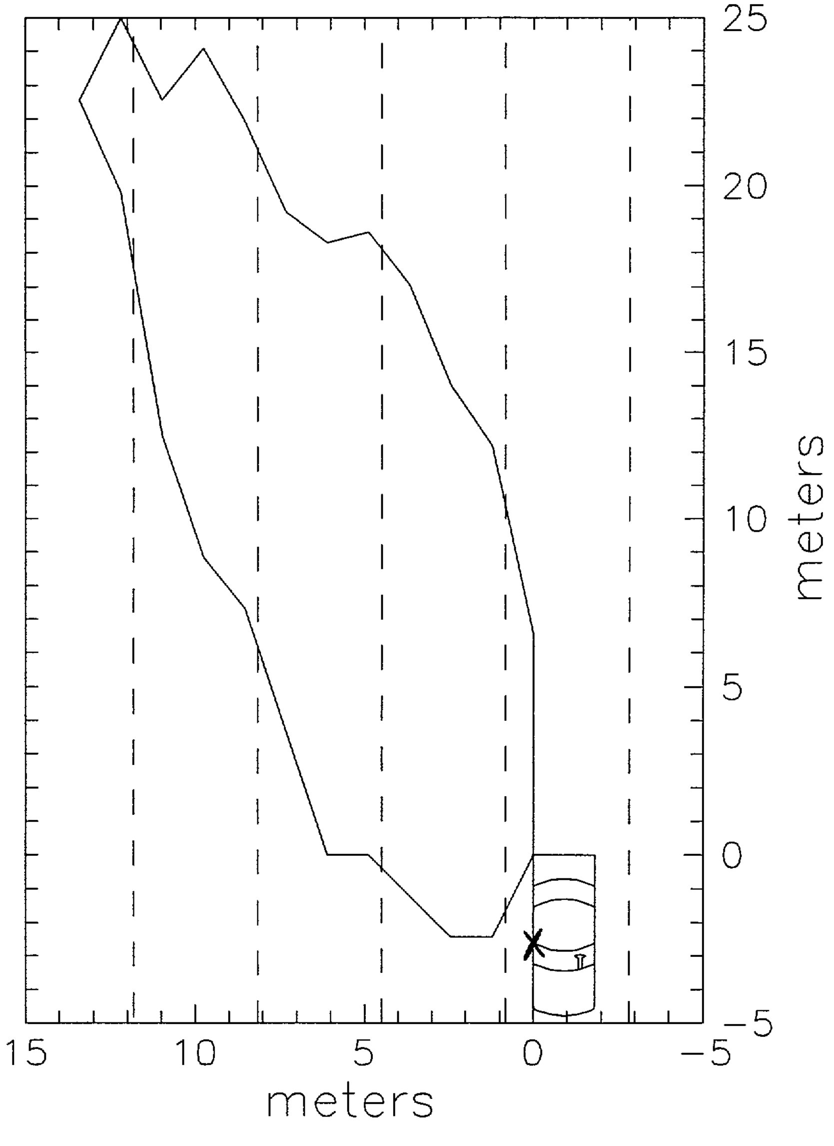

Figure 6.4-19: Summary of Road Test Statistics - System "D"

System: 'D"
Total number of detects: 93

Classification	Freeway	Two-lane	City	Parking Lot	TOTAL
TP	28	1	4	0	33
I	0	6	27	19	52
FP	0	5	1	2	8
TOTAL	28	12	32	21	93
FN	0	0	0	0	0
TN					98.6 %

General Comments:

No unexplained misses (FN)

Eight false alarms were triggered

52 inappropriate alarms - most of these were parked vehicles which were being passed at low relative speeds

One instance was cataloged in which the system detected a semi truck three lanes over -- it did not detect a van at that range

6.5 System 'E"

6.5.1 System Description

This sensor system is a microwave radar that is designed for side obstacle detection. Although no frequency information was provided, its use of coaxial cables to route the microwave signals suggests that the frequency is below 10GHr. The unit tested was designed for tractor trailers although it's performance was evaluated on an automobile. No attempt to discriminate between ground clutter and valid targets of concern is made so that the system functions as a proximity detector. The system was mounted on the side of the host vehicle near the rear bumper with the antenna height fixed at lm off of the ground pointing towards the adjacent lane.

6.5.2 Overview of System Performance

The major drawback in the performance of this system was that it was characterized by an extremely long system latency, greater than 0.6 sec. As a result, during the controlled passing tests, the system failed to respond to vehicles with closing velocities exceeding 32.2 KPH. Occasionally, the system did not respond to targets approaching with a velocity as low as 21 KPH.

Several "late" detects were noted during the parallel delay time measurements. These late responses were real, but were not factored into the calculation of the system latency.

Even with the unusually long system latency, there was only one False Negative encountered during the road test. This can be attributed to the fact that most 'real world" passing scenarios involve relative speeds of less than 32.2 KPH.

6.5.3 Test Results

<u>Static Tests</u>

The results of the static tests are shown in Figure 6.5-l (a) - (f). The response of the system to a 0.3m x 0.3m foil target is contrasted to that of a foam target in figures (a) and (b). Clearly, the extent of the detection zone is much larger for the reflective foil target. Another difference is that the edge profile of the foil target shows more irregularity than the foam target. Measurements made a couple of months later by a different individual (see Section 7.0) seem to show a more regular boundary. Much of the difference in the measured static zones lies in the test conductor's interpretation of a positive or negative response. The data

Figure 6.5-1: System "E" Static Test Results

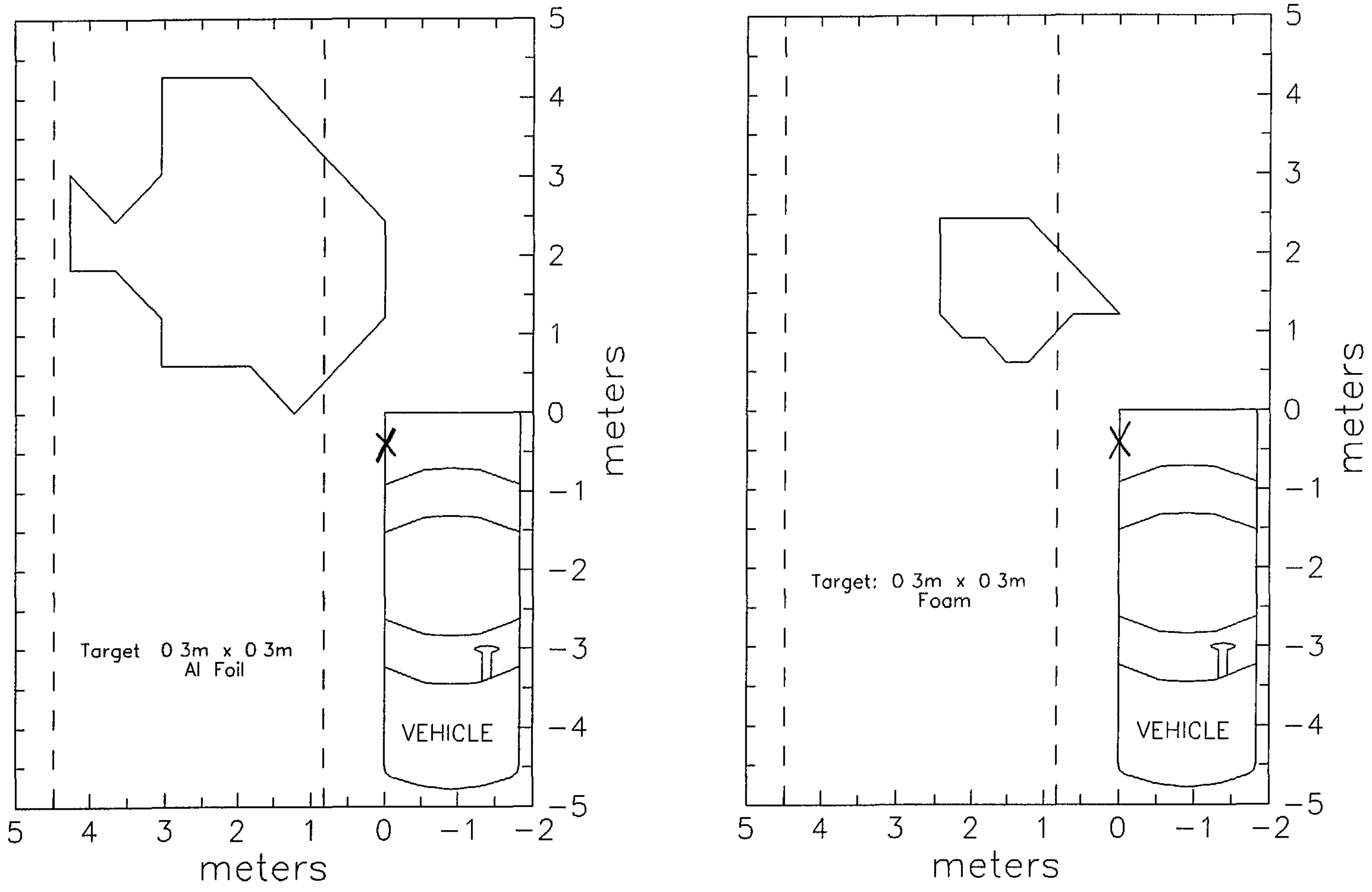

(a) 0.3m x 0.3m Aluminum Foil Target **(b) 0.3m x 0.3m White Foam Target**

Figure 6.5-1: System "E" Static Test Results (con'd)

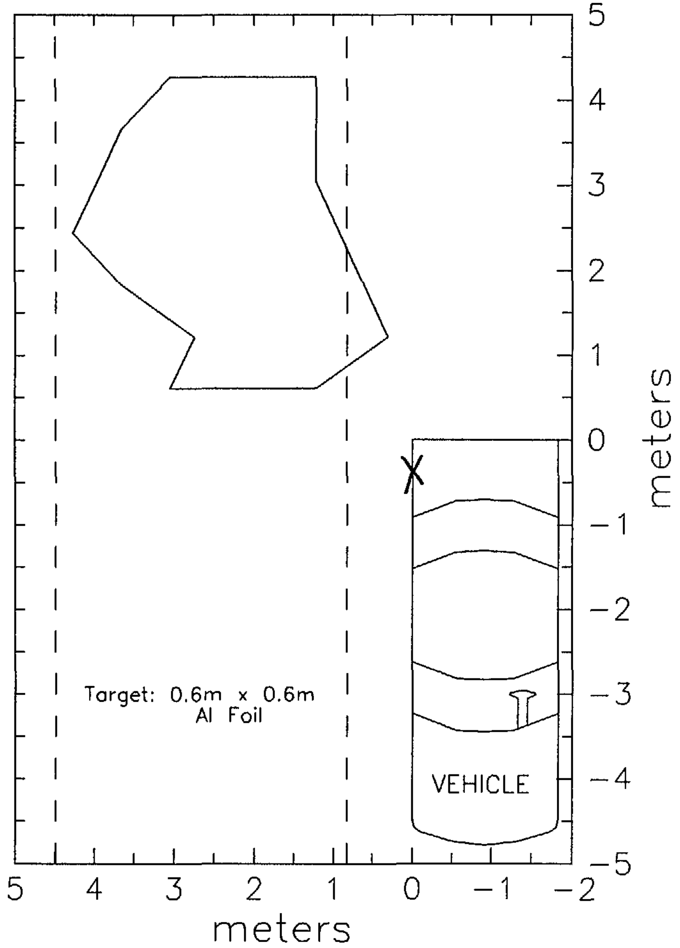

(c) 0.6m x 0.6m Aluminum Foil Target

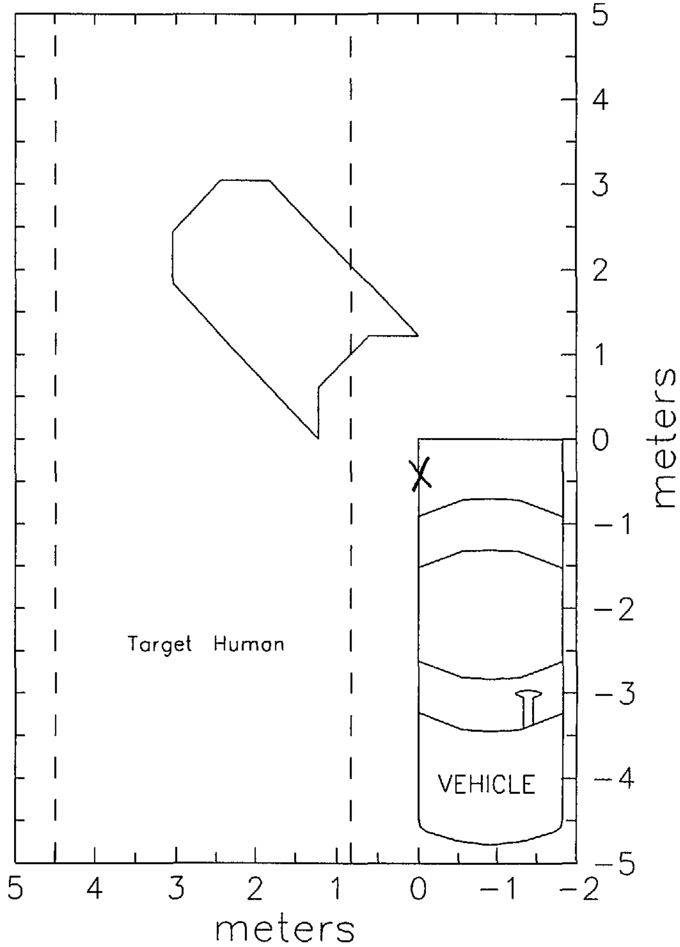

(d) Human Target

Figure 6.5-1: System "E" Static Test Results (con'd)

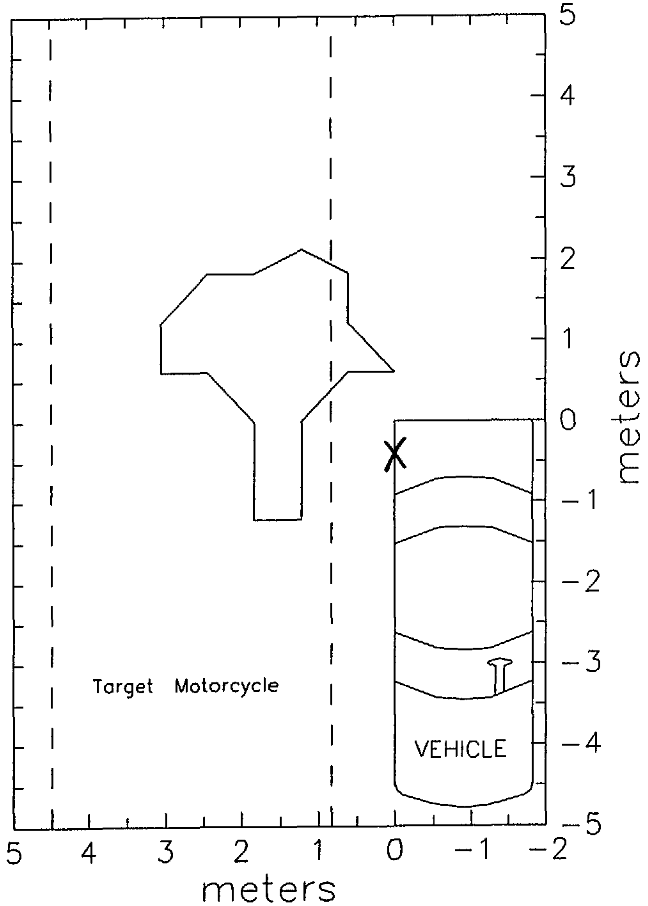

(e) Motorcycle Target

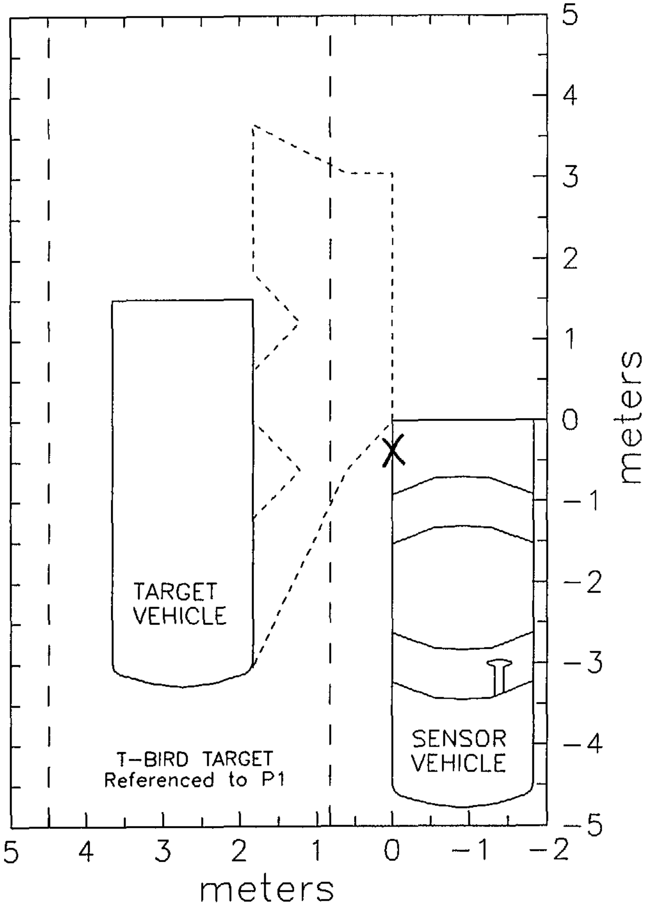

(f) Ford Thunderbird Target

presented here was considered to have a positive response if the system LED remained lit with no pausing intervals greater than two seconds.

The system's response to a 0.6m x 0.6m foil covered target is presented in figure (c). This data shows much similarity to the 0.3m x 0.3m foil target data. The extent of the coverage zone is about the same and some irregularity in the pattern boundary is evident.

Figures 6.5-1(d) shows the system response to a human target. The extent of the pattern is reduced compared to the foil targets. Figures 6.5-1(e) and (f) summarize the results for more realistic targets, a motorcycle and a Ford Thunderbird, respectively. The motorcycle pattern was generated by referencing the data to the leading edge of the front tire. The pattern is somewhat unusual showing a narrow detection zone extending towards the front of the sensor vehicle. Figure (e) indicates that this system will detect an approaching vehicle that is traveling in the center of the adjacent lane. The measured pattern suggests that the system will have difficulty detecting vehicles that have drifted to the outside of their lane.

Vertical Extent

The vertical extent of the static pattern was determined by placing a target at a distance, D, from the sensor and measuring the system response as a function of vertical position. Figure 6.5-2 summarizes the angular extent of the vertical FOV for this system. The total vertical extent is 47.8° and is angled upward.

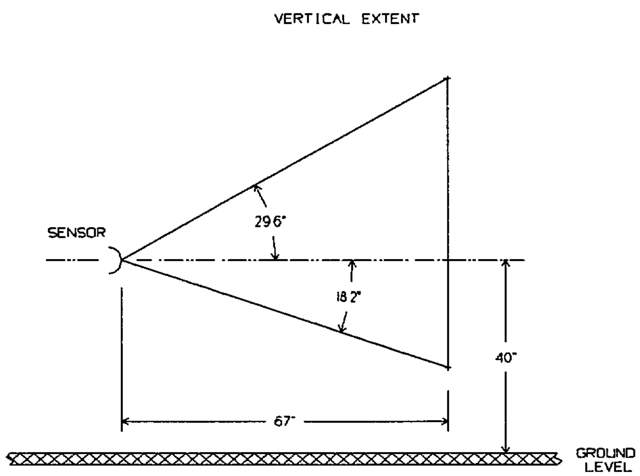

Figure 6.5-2: System "E" - Vertical Extent

Dynamic Tests

Perpendicular Delay Time

The perpendicular latency of the system was determined by driving the target vehicle past the sensor vehicle in a direction that is orthogonal to the longitudinal axis of the host vehicle. Closing speeds of 1.6, 8, 16.1, 24.1, 32.2, and 40.2 KPH. Figure 6.5-3 summarizes the results of these measurements. Both the X and Y positions at which the system first reacted to the approaching target have been plotted as a function of target vehicle speed. The vehicle speed has been calculated directly from two reference frames in the video data. All data has been referenced to post P2 on the front passenger side of the target vehicle.

The closest point of approach (X) between the two vehicles is denoted by the open triangles. This parameter was held very consistently to 1.7m +/-.25m. A single data point taken at the highest closing speed of 48 KPH is slightly outside the typical scatter probably due to the fact that the driver was increasing his collisional safety zone at the highest speeds.

The Y position of the target vehicle at the instant of system reaction is shown by the filled circles. It should be noted that one pass made at 40.2 KPH failed to yield a positive system response. The increased scatter in this data reflects the real variability of the system performance. The slope of a linear best fit to the data yields the perpendicular latency time. With a characteristic scatter of roughly +/- m, the latency is calculated to be 0.52 sec +/- 0.11 sec.

Parallel Delay Time

The results of the parallel delay time tests are shown in Figure 6.5-4. The target vehicle was driven past the sensor vehicle at speeds of 1.6, 8, 16.1, 24.1, 32.2, and 40.2 KPH. As before, the speed data points have been calculated directly from two reference frames in the video data. In this case, all data has been referenced to post Pl on the front driver side of the target vehicle.

The lateral separation between the two vehicles is shown by the open triangles. For these tests, this parameter has been held quite consistently to 1.2m +/- 0.25m. One data point taken at 26 KPH falls outside the typical scatter of the data. This data point is also characterized by a Y value that reflects a very late system reaction. However, the fact that there are several data points collected at three vastly different vehicle speeds that are indicative of a “late” detect, means that no significant conclusions should be drawn by the fact that a single correlation can be made between an increased lateral separation and a slow system response. Then

Figure 6.5-3: Perpendicular Latency Time
System "E"

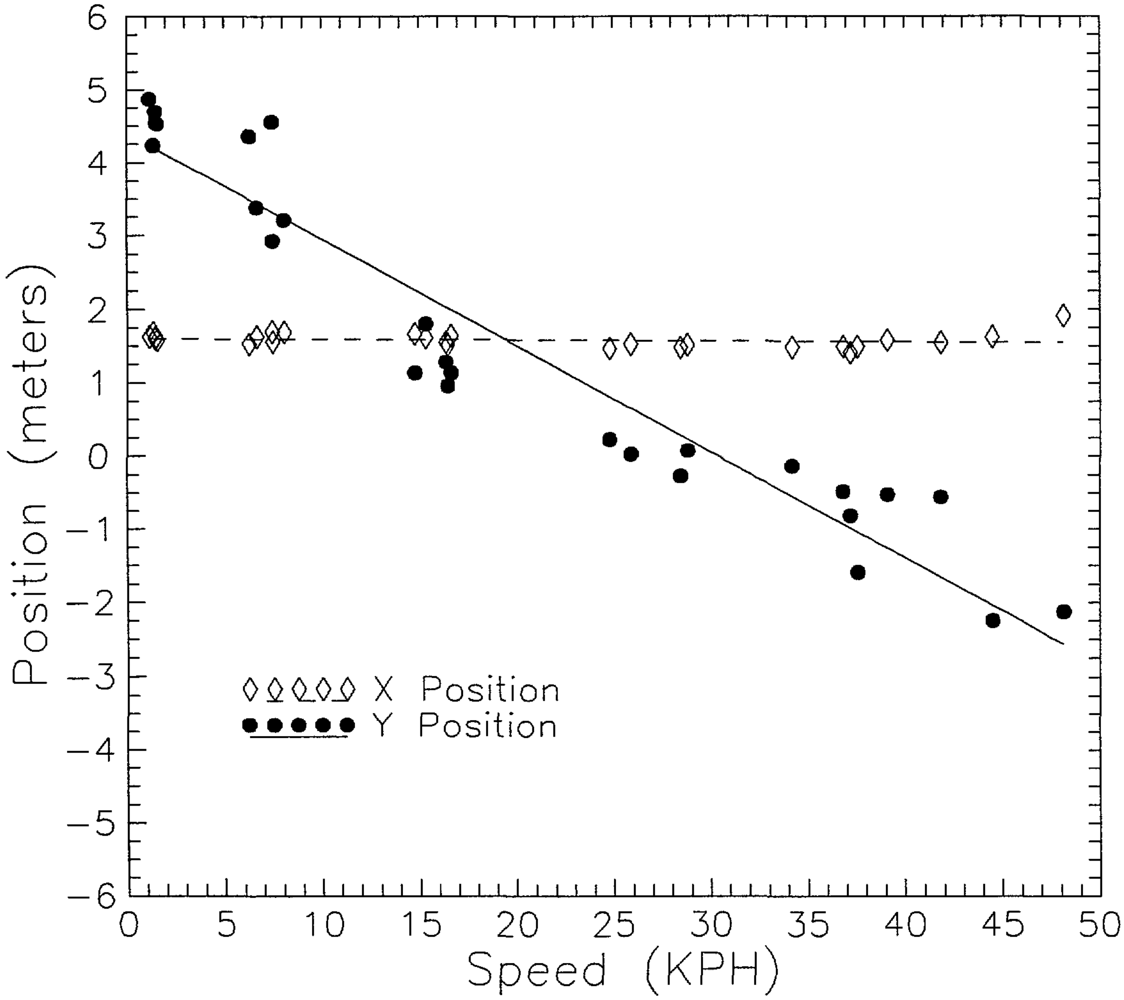

parallel system latency computed from a best fit to the Y-range data is 0.62 sec ± 0.17 sec.

Persistence Time

The position of the target vehicle at the time the system indicator turns off can be determined by projecting the car's position based upon the trajectory and speed calculated from two earlier reference frames. The latency time associated with system turn-off has been plotted in Figure 6.5-5.

This data was computed from the parallel delay time test results. The solid points represent the position of the target vehicle at the instant the system display ceases

Figure 6.5-4: Parallel Latency Time
System "E"

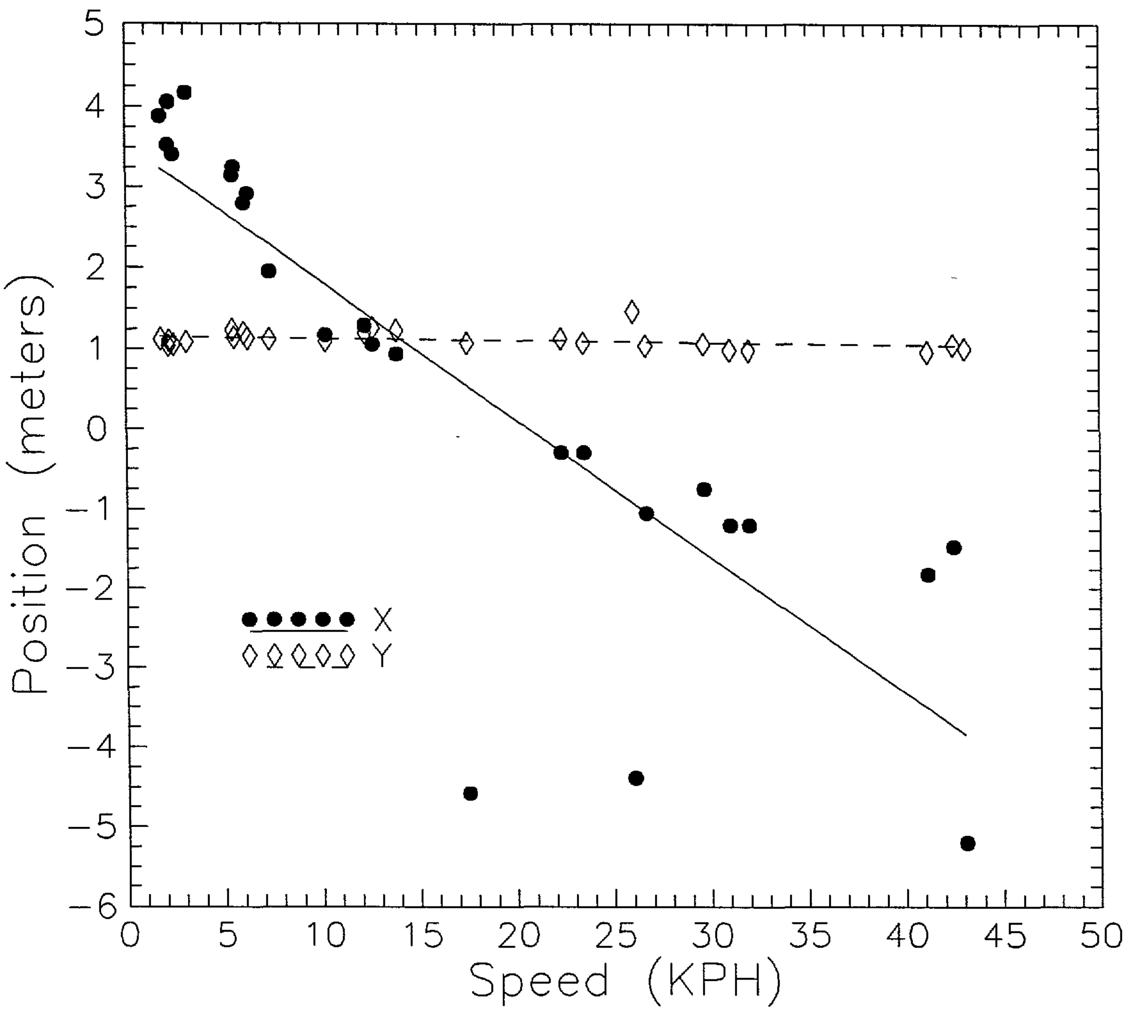

to flash. The slope of this line reflects a system turn-off persistence time of 1.23 sec ± 0.31 sec. Note that this data is well behaved in the sense that there are no "stray" data points that indicate atypical system performance.

Controlled Passing Tests - Target Vehicle Passing Sensor Vehicle

A total of 42 controlled passing tests were performed on the High Speed Track in which the sensor vehicle was passed on the right by the target vehicle. The vehicle closing speeds for this test were:

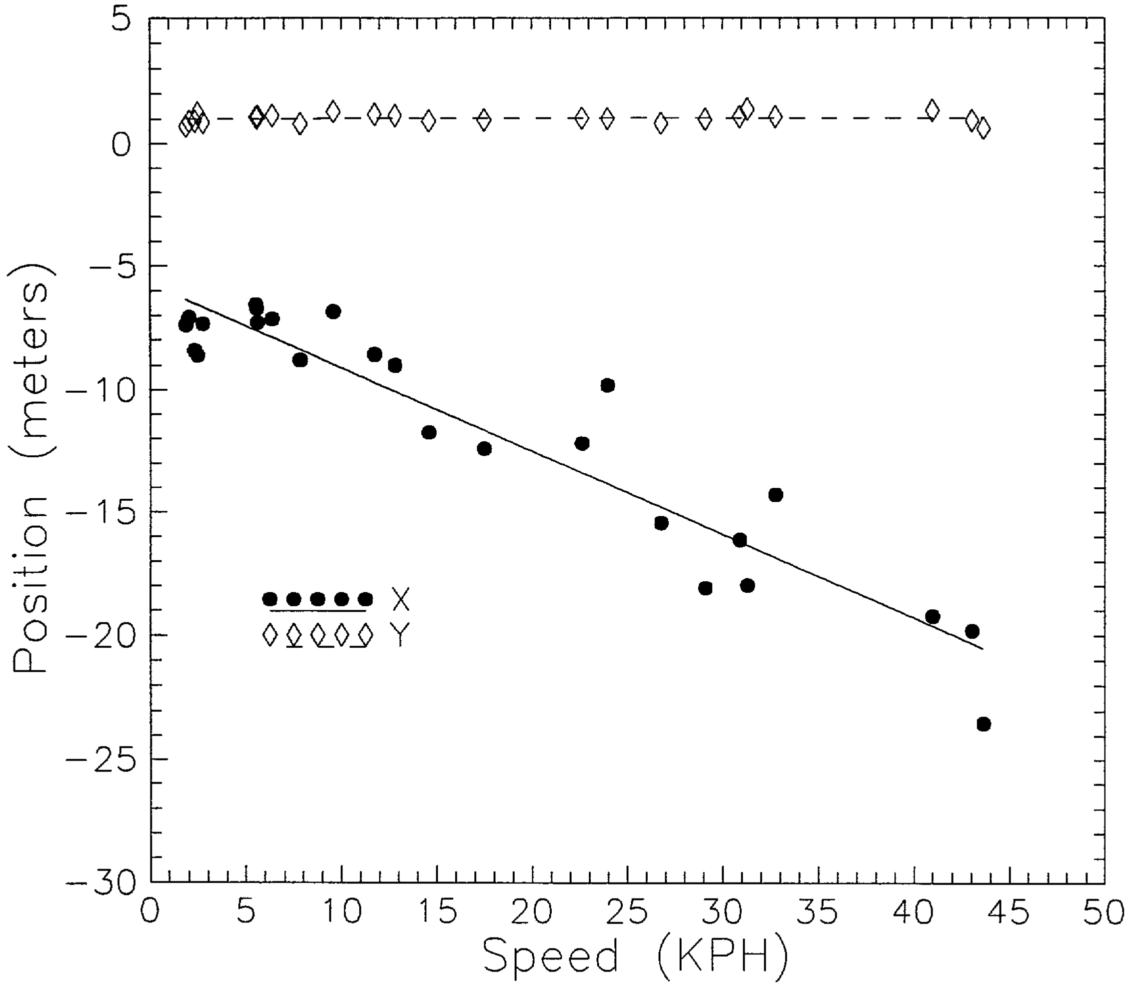

Figure 6.5-5: System Persistence Time
System "E"

Closing Velocity (KPH)	Number of Passes	Number of Missed Detects
8	6	0
16.1	15	0
24.1	13	7
32.2	8	6

Note that a total of 13 passes (7 at 24.1 KPH and 6 at 32.2 KPH) resulted in a missed detect. Roughly 19% of these tests were conducted on the curved portion of the High Speed Track. The intent of these tests was twofold: 1) to investigate the system performance as a function of relative speed and correlate the results with the measured system latency and 2) to investigate the effect on system performance when passing occurs on a curved path.

Figure 6.5-6(a) summarizes the position of the target vehicle at which the system first reacts to the approaching target. All results have been referenced to post P1 on the front driver side of the passing vehicle and have been segregated according to the closing velocity of the test. The static detection zone measured with the Ford Thunderbird target is denoted by the dashed line. Lane markers are identified by the parallel dashed lines. Before interpreting the results, it is useful to remember two facts about this system. First of all, the system is characterized by a very long system latency. It is easier, therefore, for a target to slip through the detection zone either without being detected at all or being detected at the last minute. Secondly, the static detection zone does not extend very far into the adjacent lane. Thus, vehicles passing along the right side will tend to brush the edge of the detection zone and target detection will depend more critically on the velocity and trajectory of the passing vehicle. Examination of the test results reveals a large scatter in the range of target detection. System latency can explain a delay of up to 1.8m at 8 KPH, 3.6m at 16.1 KPH, 5.4m at 24.1 KPH, and 7.1 m at 48.3 KPH. The long latency time demonstrated by this system increases the probability of missed detections, especially at high closing speeds. In other words; the system takes so long to respond to a target, that a vehicle passing through the detection zone at a higher speed will be past the zone before the system has time to react. In fact, 7 out of 13 passes were missed at 24.1 KPH and 6 out of 8 passes were missed at 32.2 KPH.

The effects of a curved path is shown in Figure 6.5-6(b). The data has now been plotted as a function of straight and curved path. The data points collected along a curved path are generally clustered within the balance of data taken along a straight path. Thus, there seems to be no degradation in system performance that can be directly attributable to the curvature of the path.

These tests were repeated with a clutter vehicle located directly behind the sensor vehicle at separation distances of 10.5, 29.3, and 55.5m. The objective in these tests was to trigger a false alarm in the presence of typical highway traffic. Figure 6.5-7 summarizes the results of this test. The relative speed of the approaching vehicle was about 16.1 KPH. At no time did the clutter vehicle trigger a false alarm. This result is not unexpected since the system under test was of short range.

Figure 6.5-6: System "E" Controlled Passing Test Results
Target Vehicle Passing Sensor Vehicle

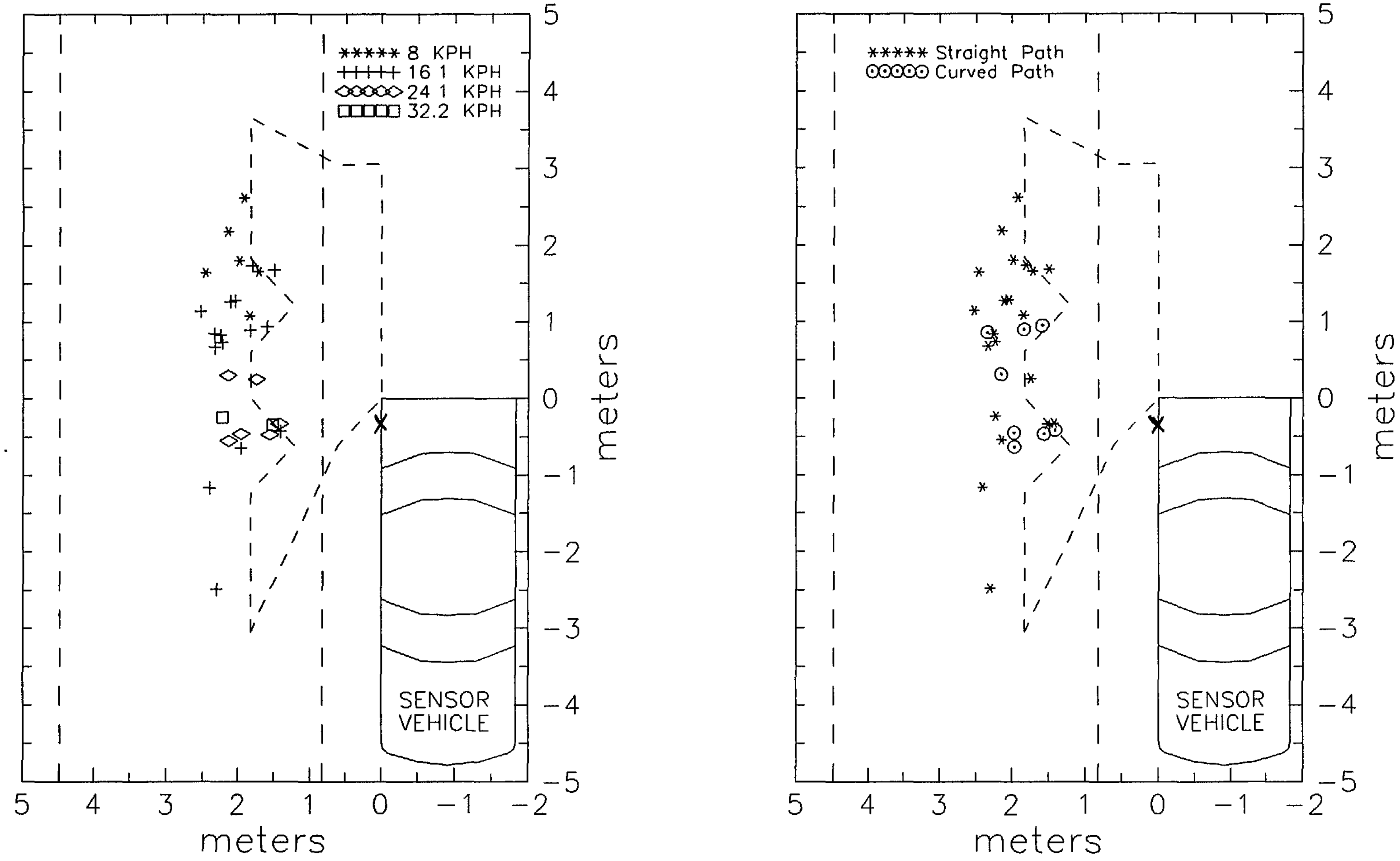

(a) System Performance vs. Relative Speed

(b) Curved vs. Straight Path

Figure 6.5-7: System "E" Controlled Passing With Clutter Vehicle

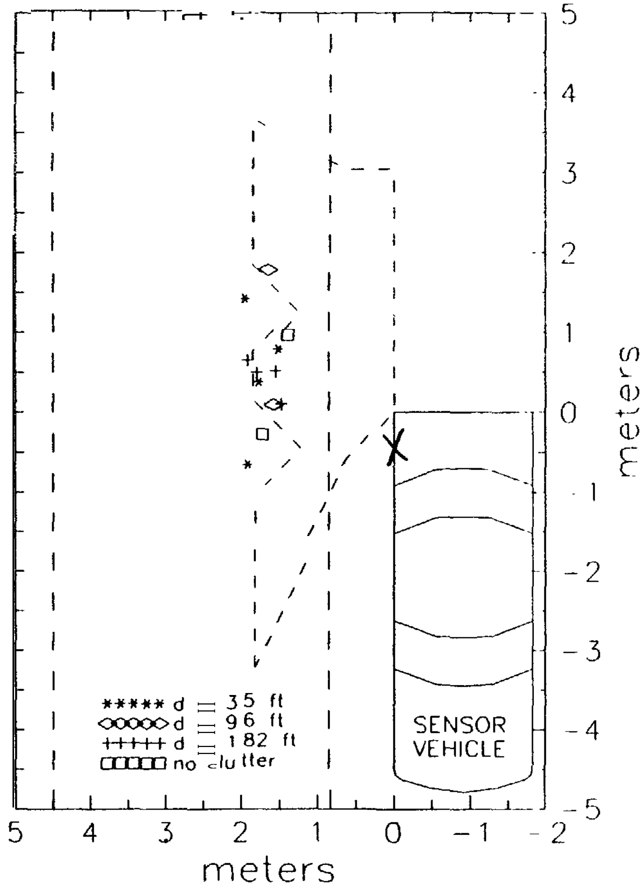

Controlled Passing Tests - Sensor Vehicle Passing Target Vehicie

Ten passes were made in which the sensor vehicle passed the target vehicle. The purpose was to evaluate the system's ability to distinguish between positive and negative closing speeds. A summary of the tests performed is as follows:

Closing Velocity (KPH)	Number of Passes
8	5
16.1	5

The results are presented in Figure 6.5-8. Note from the results that two out of the five passes made with a closing speed of 8 KPH failed to trigger a response from the system. Generally speaking, the faster relative speeds result in a longer delay in the system reaction time. At these relative velocities, the longest delay that can be explained by the system latency is 3.6m. The single data point towards the rear of the sensor vehicle shows a latency of 3.5 to 4m. However, the data point also lies at the boundary of the detection zone where the uncertainty in the system response is greatest. It is difficult to conclude whether system latency or boundary effects resulted in this late detect. Another noticeable feature of the data is that the system reacts earlier than expected based on the static pattern. This is contrary to the results obtained with a positive closing speed. The data suggests that this system may pick up targets with a negative closing speed quicker than those with a positive closing speed.

Approach and Pass Tests

A short series of tests was performed to investigate the system's utility in a typical highway passing scenario in which an approaching car in the same lane as the sensor vehicle swerves into an adjacent lane to pass. Seven separate maneuvers were made with the sensor vehicle driving at a fixed speed of 64.4 KPH. The results are summarized in Figure 6.5-9. All data has been referenced to post P1 on the target vehicle. No attempt to maintain a fixed speed with the target vehicle was attempted because of the nature of the test. Since this system has a short FOV, most of the detects occurred after the lane change had been completed. A single pass resulted in a detection on the lane marker. In this instance, the approaching vehicle clipped the back of the detection zone as it was completing the passing maneuver.

Figure 6.5-8: System "E" Controlled Passing Test Results
Sensor Vehicle Passing Target Vehicle

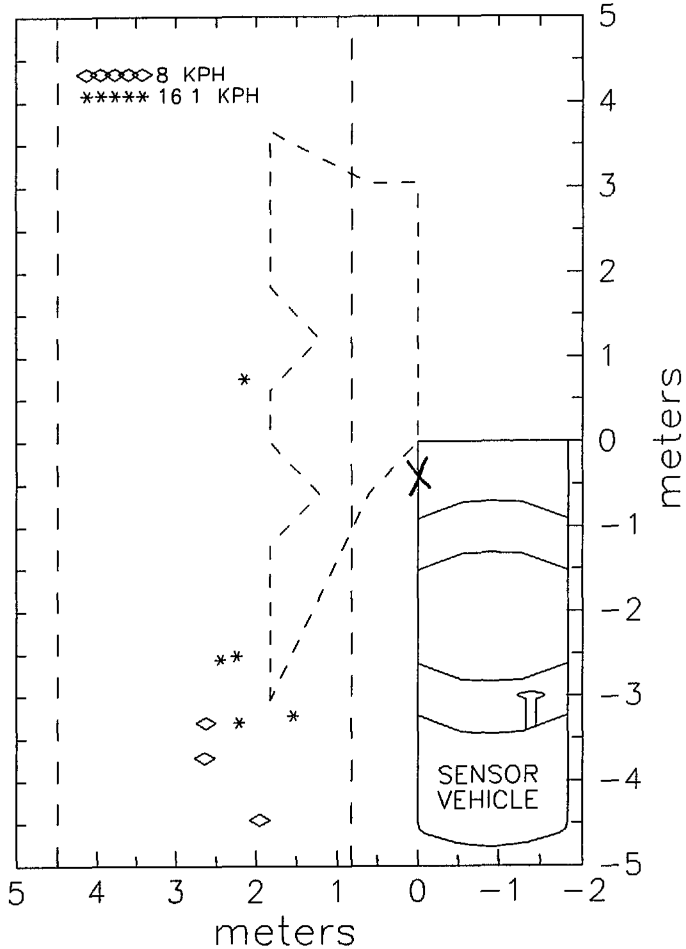

Figure 6.5-9: System "E" Approach and Pass Test Results

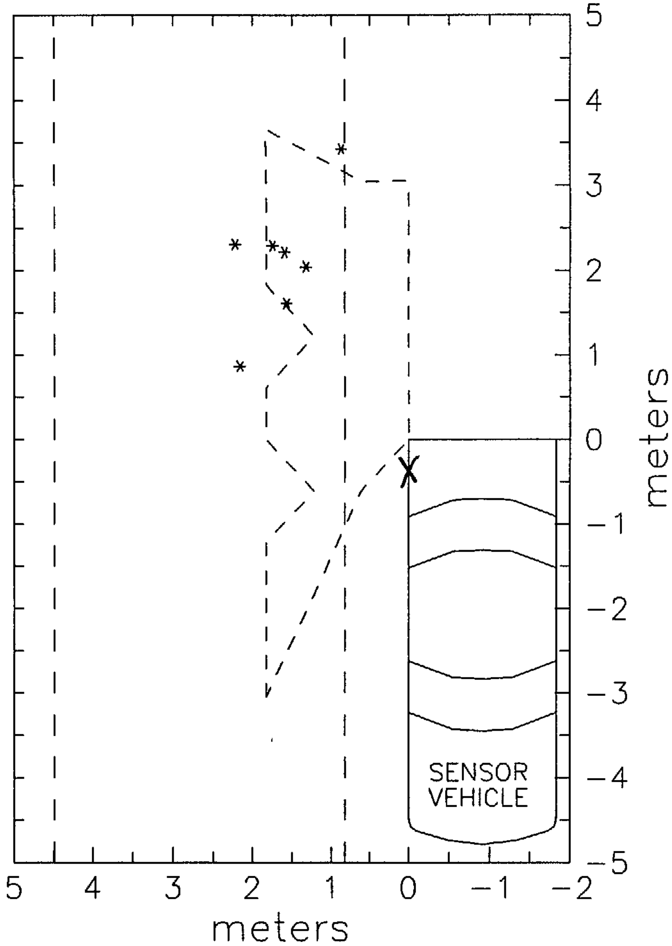

Figure 6.5-10: System "E" Three Lane Test Results

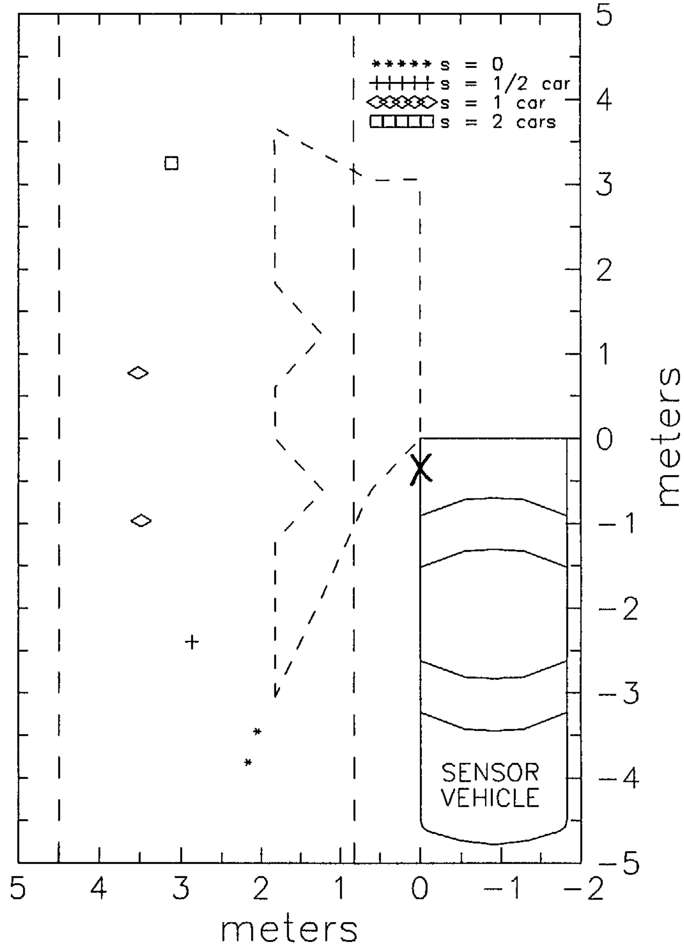

Three Lane Tests

Three lane maneuvers were performed to investigate the probability of a false alarm being triggered by a vehicle in a non-interfering lane. In these tests, the vehicles are initially separated by an entire lane. The target vehicle then maneuvers into the adjacent lane at nose-to-nose separation distances that vary between 0 and 3 car lengths. The following table describes the passes made.

Number of Passes	Separation Distance, s	System Reaction
4	0 (nose-to-nose)	YES (3 out of 4)
3	1/2 car length	YES
1	1 car length	YES
2	2 car lengths	NO

The target was detected at nose-to-nose separations up to 2 car lengths. One of the passes at s = 0 failed to trigger a system response. In addition, one of the passes at s =0 and one at s = 1/2 car length did not have enough reference points in the FOV of the video cameras for an accurate analysis. Therefore, as shown in Figure 6.510, a total of seven passes were analyzed. Another obvious observation is that the target is detected as it is initiating its lane change. In fact, the lateral detection range appears to be 1 to 2m outside of the measured static pattern. This difference is larger than the typical 0.3 to 0.6m uncertainty in the edge of the detection zone and suggests that this type of lane change maneuver will trigger an early response from this system.

Merge Tests

In order to evaluate the system's utility during merging situations, the angle of approach of the target vehicle was varied from 0^o to 9" to 24^o. The sensor vehicle was stationary and the target vehicle was driven past at speeds of 32.2, 48.3, and 64.4 KPH. The tests conducted with an angle of approach of 9^o and 24^o failed to yield any response from the system independent of the speed of the target vehicle.

Two sets of data was taken with a 0^o angle of approach. Because this system has such a long latency, positive reactions were only observed with a closing speed of 32.2 KPH. Even at this speed, the system failed to detect two out of six approaches. This 0^o merge data, which is analogous to the parallel delay time tests, is summarized in Figure 6.5-l 1. All data has been referenced to post P1 on the target vehicle. System latency can be as much as 7.1m at 32.2 KPH. With so little data, it is difficult to draw any definitive conclusions except to

Figure 6.5-11: System"E" Merge Test Results

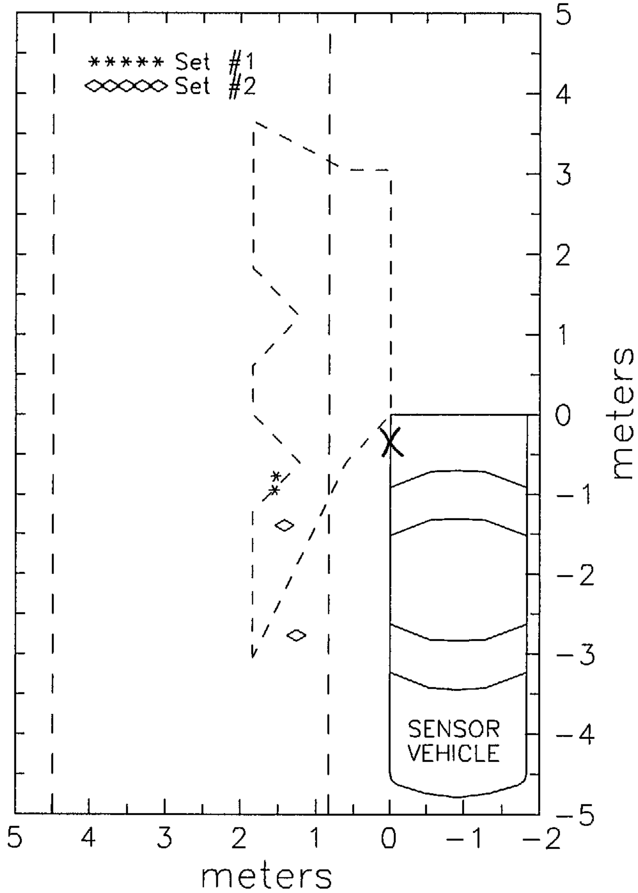

(b) 0° Angle of Approach

say that the data appears to lie within the expected uncertainty of a system that is characterized by a long latency time.

Road Test

This system was evaluated under realistic road conditions involving freeway, city, two-lane highway, and parking lot driving. The total exposure time was 73.9 minutes. Statistics were compiled on the number and types of targets detected. Figure 6.512 summarizes the results.

Figure 6.5-12: Summary of Road Test Statistics - System "E"

System: 'E"
Total number of detects: 129

Classification	Freeway	Two-lane	City	Parking Lot	TOTAL
TP	28	9	49	37	123
FP	0	1	5	0	6
TOTAL	29	10	54	37	129
FN	1	0	0	0	1
TN					98.2 %

General Comments: One obvious missed detect on freeway - target was a passing van

Six false alarms

In general all road signs, trees, poles, concrete pillars, etc. within the sensor's field of view generated a positive **response**

This system performed adequately during the road tests as a proximity detector demonstrating only 6 false alarms (FP) out of 129 warnings. There was, however, a single incidence in which the system failed to react to a target within its detection zone (FN). Further analysis revealed that the passing van was separated by about 2.6m laterally from the sensor car. At this distance, the passing vehicle lies about 0.5m outside the static detection zone. Because the static detection zone boundaries of these systems typically vary 0.3 to 0.6m, the fact that the vehicle lies slightly outside the measured boundary does not necessarily imply that the vehicle is completely out of the field of view of the sensor. However, the fact that the vehicle lies on the outer edge of the detection zone, in combination with the long system latency, may have allowed the vehicle to slip through the edge of the detection zone without triggering a positive system response. There were a total of six incidences in which the system triggered without any obvious target within its FOV. Most of these occurred during the city driving in which there is an abundance of general ground clutter.

6.6 System 'F"

6.6.1 System Description

This system is an infrared sensor that is designed to detect vehicles within the blind spot of the host vehicle. Based upon a discussion with the vendor's representatives, it was learned that each sensor contains six beams. Adjacent beams are pointed parallel to the ground and slightly downward to a point approximating tire height (0.6m - 0.8m) at a lateral distance of 3m. it is a proximity detector that is activated with the turn signal and is designed as a lane change aid. Two sensors mounted in the driver's side and one sensor mounted in the passenger side tail lights monitor the blind spots on both sides of the host vehicle. The passenger side sensor coverage zone is designed to look more forward than the driver's side sensor due to reduced visibility on the right side of the vehicle, The driver is notified of a target located within the sensor zone with a flashing LED indicator.

6.6.2 Overview of System Performance

Overall, this system performed well as a proximity detector during both the controlled static and dynamic tests. Because this sensor uses a multiple beam technology, certain dynamic tests (particularly the perpendicular delay time tests) were characterized by a significant variance in system reaction times. This is not unexpected since the system was not optimized for detecting vehicles approaching orthogonally from the side of the vehicle. As the speed of the approaching vehicle increases, the probability that certain sensor beams will "miss" the target increase. In general, the dynamic tests were consistent with the measured static patterns and the system latency time.

During the road tests, the system failed to detect two passing vehicles that were clearly within the sensor's detection zone. Because the consequences of these misses can be severe, the utility of this particular prototype system as a lane change aid is limited.

6.6.3 Test Results

<u>Static Tests</u>

Static patterns of both the driver side and passenger side sensors were measured. The types of targets used included

1) 0.3m x 0.3m foil covered Styrofoam
2) 0.3m x 0.3m white Styrofoam
3) 0.3m x 0.3m black cloth covered Styrofoam

4) human
5) Ford Thunderbird

The small cross section targets were located at the vertical height of the tail light sensor.

During the static tests, the effect of glint was evaluated by reflecting the sunlight from a flat piece of aluminum foil directly into the sensor. At no point during these tests did the system inadvertently trigger. Thus, it was concluded that this system was not susceptible to false alarms triggered by stray sunlight reflecting back into the sensor.

Driver Side Sensor

The static detection zones measured with the driver side sensor are shown in Figure 6.6-l. A comparison was made between black and white targets to understand the response of the system to targets of varying reflectivity. A painted black cloth was placed over the 0.3m x 0.3m Styrofoam to simulate a dark target. The measured response shown on the left of Figure 6.6-1 can be compared directly to the system response to a highly reflective target shown on the right side of the figure. The extent of the detection zone extends more than a meter further in both the backward and lateral directions when viewing the white foam target. Also evident in these plots, particularly for the white target, is the characteristic of a double lobe in the detection pattern. This is to be expected in a multiple beam sensor designed for large cross section targets. Smaller targets can "hide" between beams and remain virtually undetected.

The response to a human target is shown in Figure 6.6-1 (c). A human presents a larger cross section to the sensor and is therefore characterized by a slightly broader detection pattern. Multiple lobe effects can still be seen but the separation between lobes is not as pronounced as with the smaller targets.

Figure 6.6-1 (d) shows the response of the system to a motorcycle target. Notice with the larger, more distributed target, the double lobe structure seen in the earlier data is much less apparent. The extent of the detection zone has also increased.

The system's response to a Ford Thunderbird is shown in Figure 6.6.-1(e). For clarity, the outline of the target vehicle has been included. The position of reference post P2 is shown by the asterisk and indicates the point of reference for the measurement. The static detection zone is denoted by the dashed line. System reaction was recorded at 0.6m intervals along the longitudinal and lateral axes. Unlike the previous patterns discussed, there are no multiple lobe effects with this target due to its significantly larger cross section.

Figure 6.6-1: System "F" Static Test Results - Driver Side Sensor

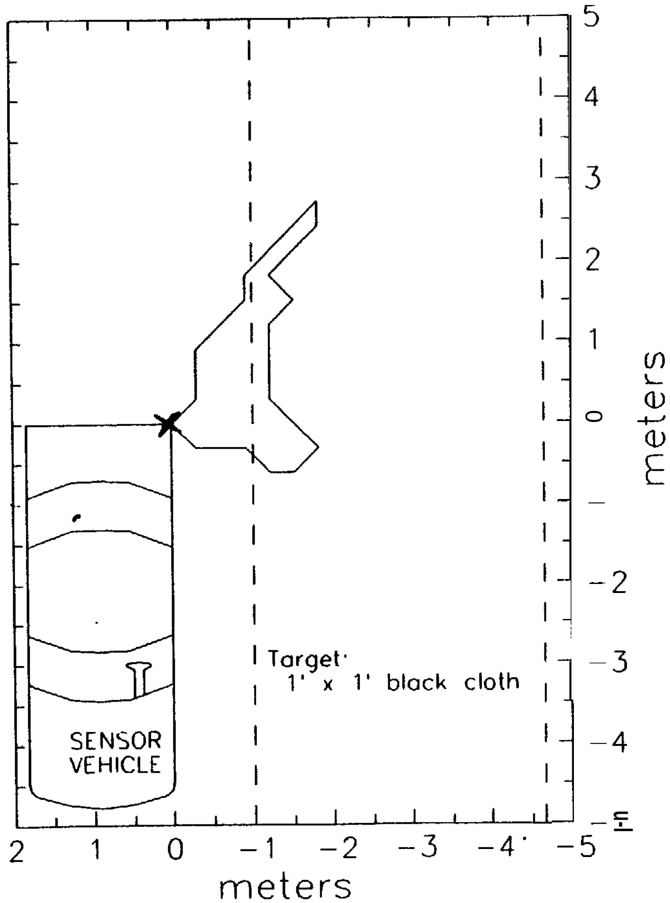

(a) 0.3m x 0.3m Black Cloth Target

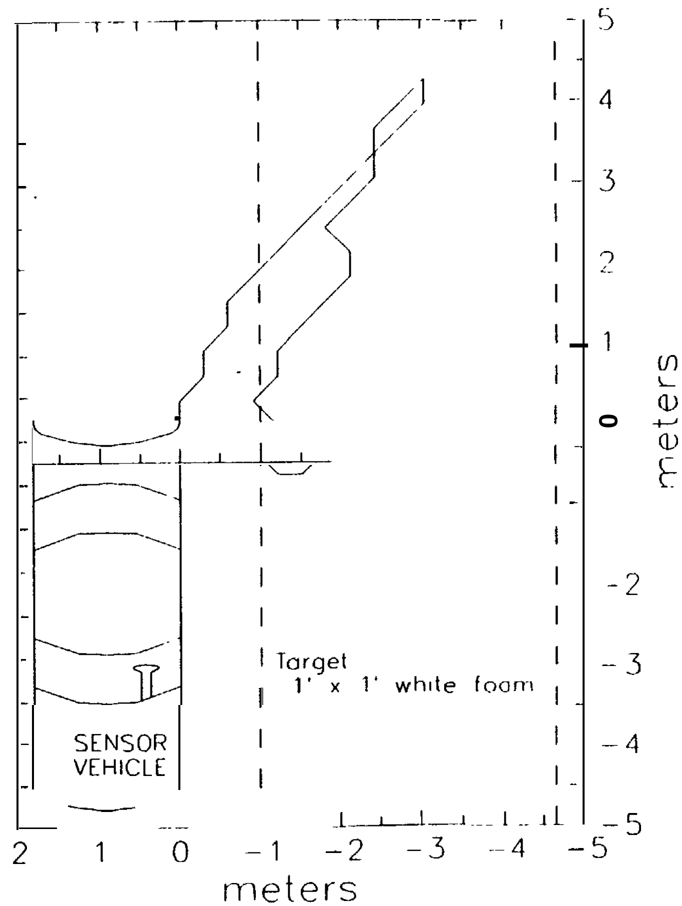

b) 0.3m x 0.3m White Foam Target

Figure 6.6-1: System "F" Static Test Results - Driver Side Sensor (con'd)

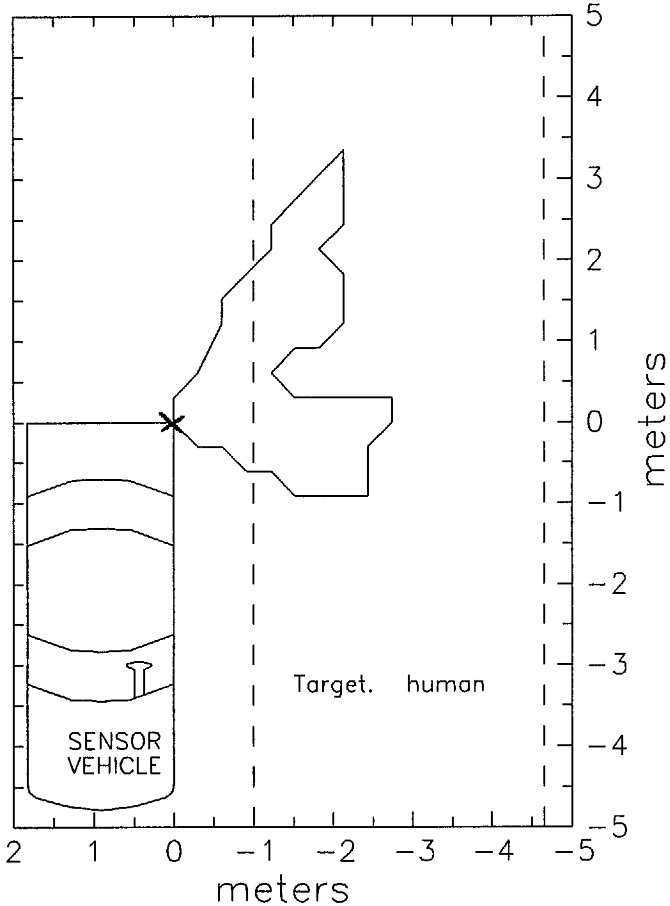

(c) Human Target

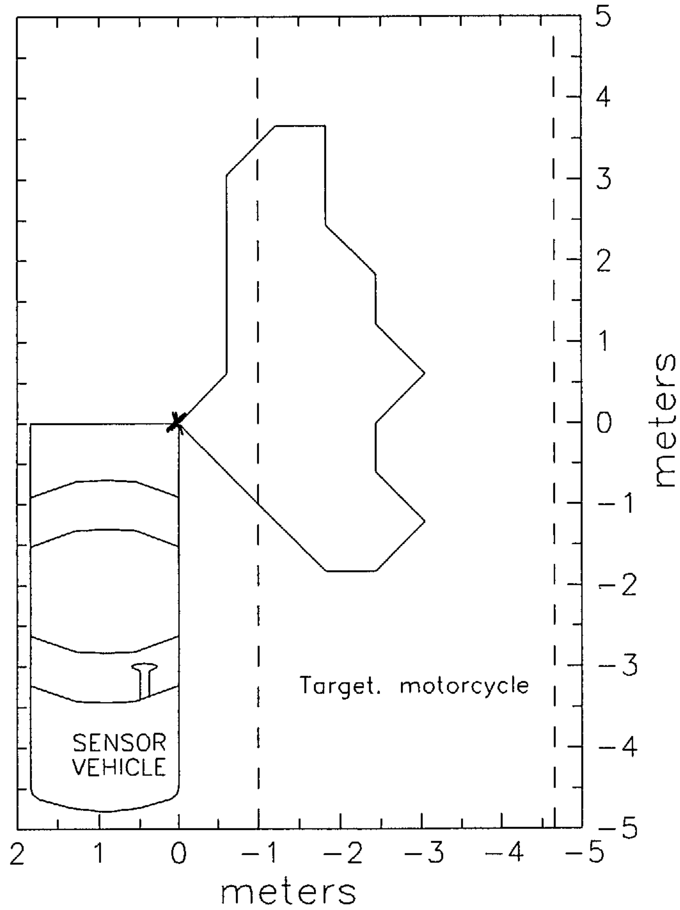

(d) Motorcycle Target

Figure 6.6-1: System "F" Static Test Results - Driver Side Sensor (con'd)

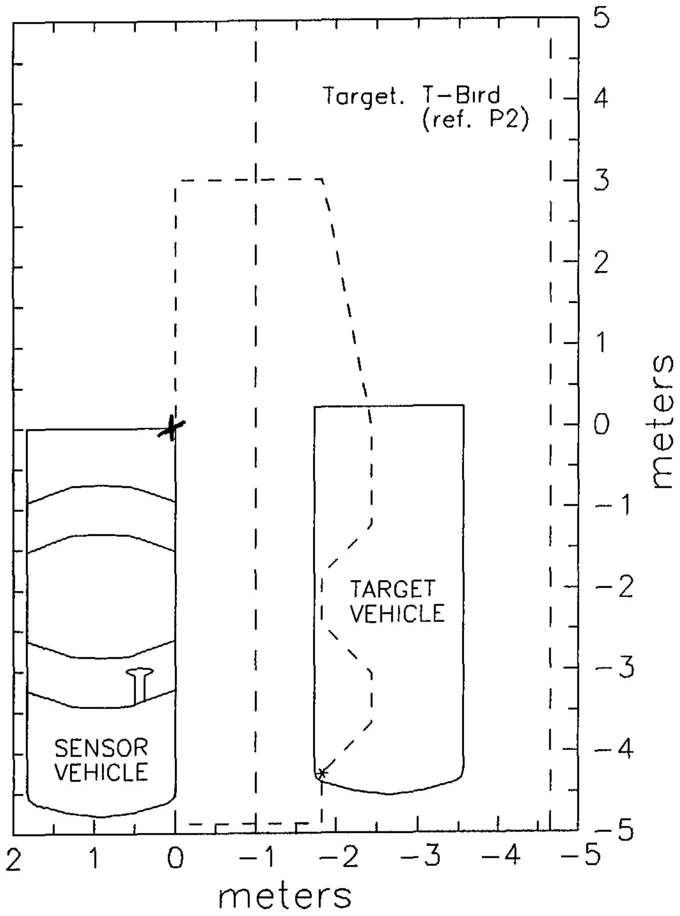

(e) Ford Thunderbird Target

Vertical Extent - Driver Side Sensor

The vertical extent of the static pattern was determined by placing a target at a distance, D, from the sensor and measuring the system response as a function of

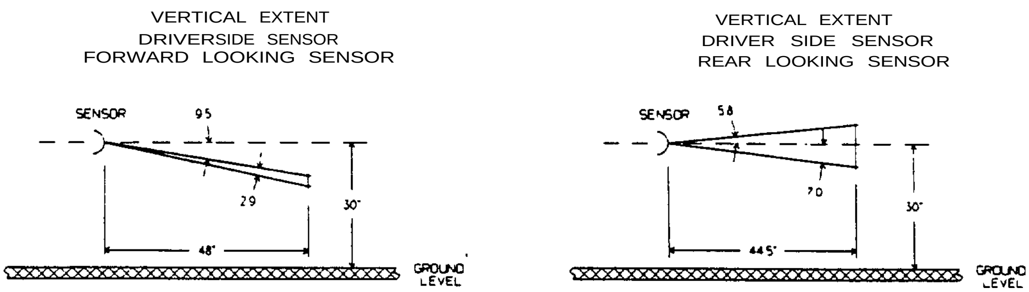

(a) Forward Looking Sensor (b) Rear Looking Sensor

Figure 6.6-2 System “F” - Vertical Extent, Driver Side Sensor

vertical position. The driver side sensor contains both a forward looking and rear looking set of beams. Figure 6.6-2(a) and (b) summarizes the angular extent of both sets of sensors. The forward looking sensor has a total vertical extent of 2.9” and is directed towards the ground. The forward looking sensor, on the other hand, has a total FOV of 12.8” and looks more or less straight out. Because of the limited spatial extent of the target used for this test, the results indicate that only one of the six beams in each sensor was intercepted. Discussions with vendor representatives pointed out that the beams are alternately pointed straight out or down.

Passenger Side Sensor

Static detection zones measured with the passenger side sensor are shown in Figure 6.6-3. The system response to the 0.3m x 0.3m.black cloth target (a) is compared to both a white Styrofoam target (b) and an aluminum foil covered Styrofoam target (c) The detection zones on the passenger side are characterized by a single lobe and cover a significantly smaller extent than the driver side sensor. Similar trends are observed, however, in that highly reflective targets have larger detection zones. Aluminum foil has the smallest detection zone. Figure 6.6.3(d) shows the response of the driver side sensor to a human target. The total extent of the static pattern extends approximately 2.5m laterally and 1.5m backwards.

Figure 6.6-3: System "F" Static Test Results - Passenger Side Sensor

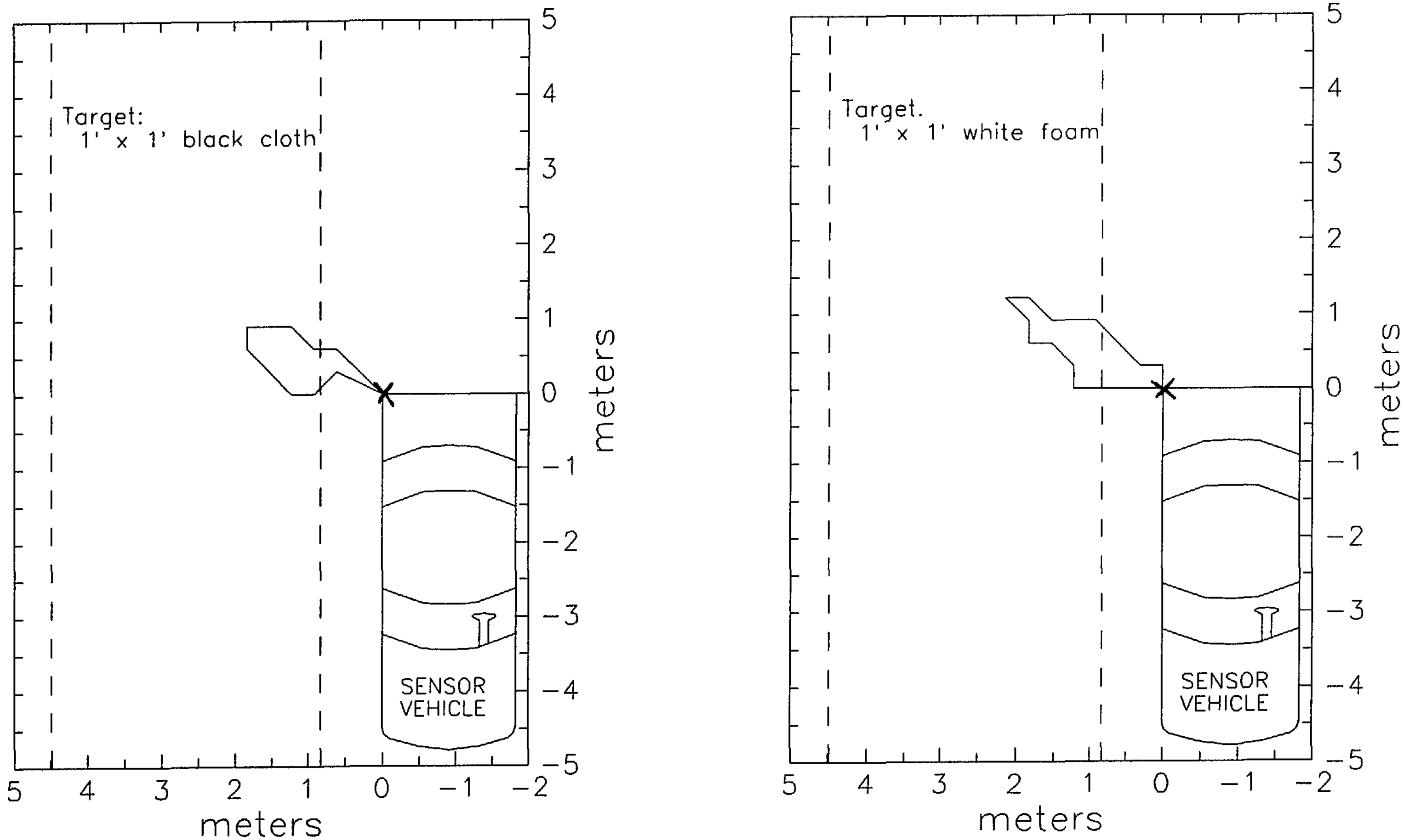

(a) 0.3m x 0.3m Black Cloth Target

(b) 0.3m x 0.3m White Foam Target

Figure 6.6-3: System "F" Static Test Results - Passenger Side Sensor (con 'd)

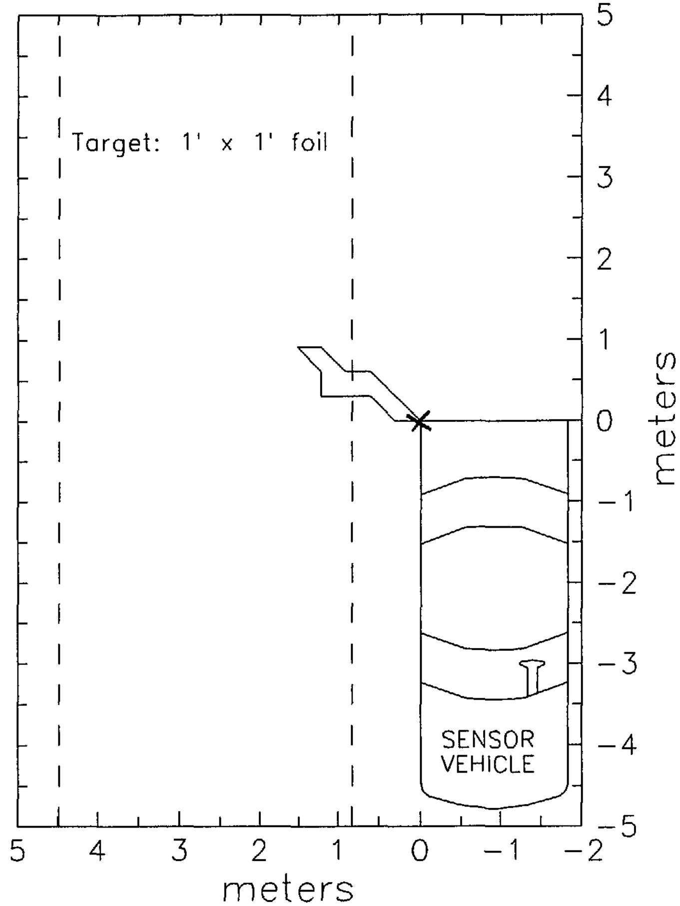

(c) 0.3m x 0.3m Aluminum Foil Target

Figure 6.6-3: System "F" Static Test Results - Passenger Side Sensor (con 'd)

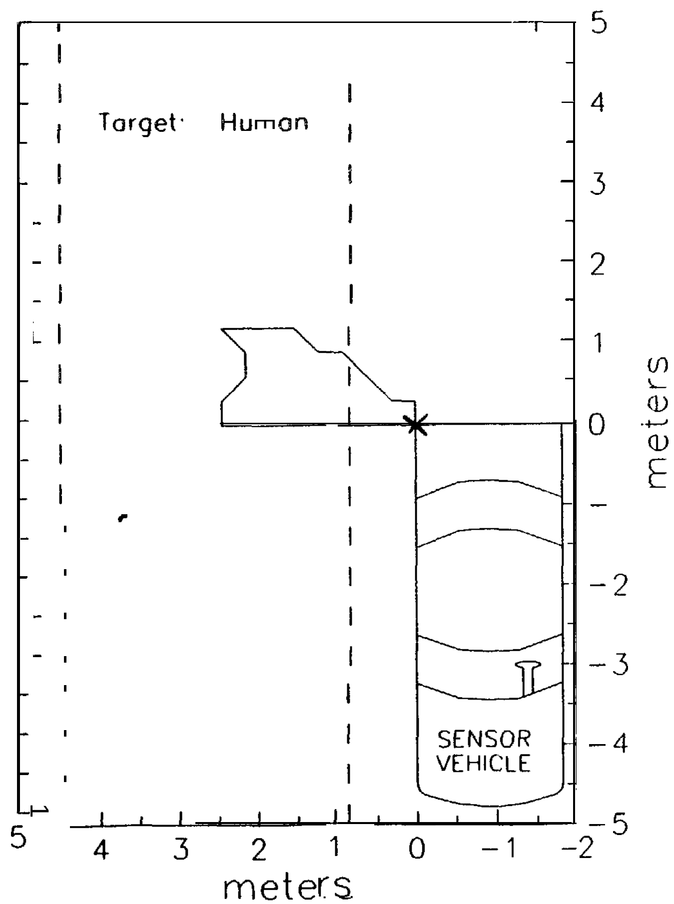

(d) Human Target

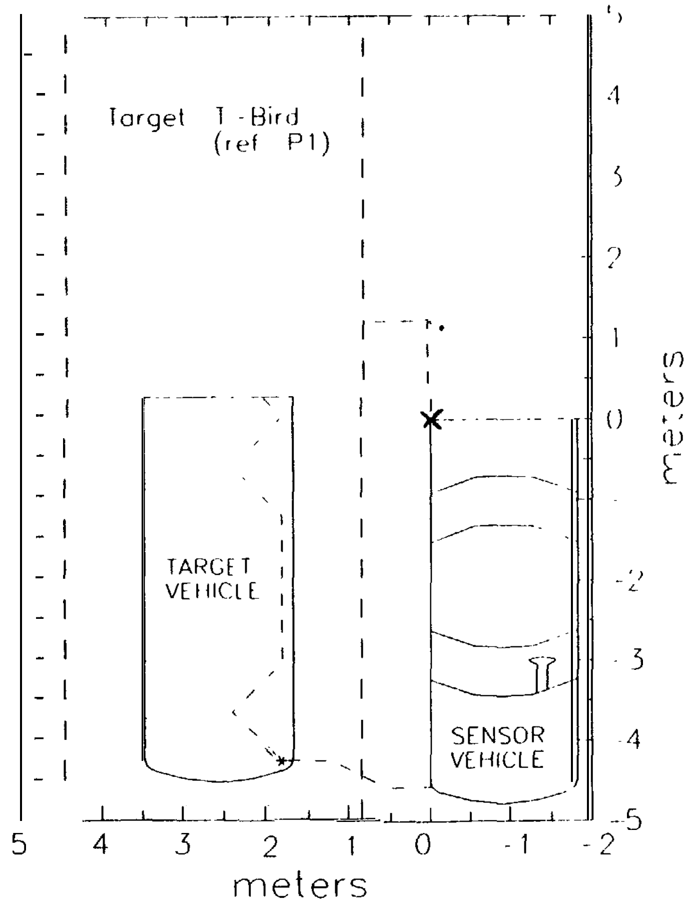

(e) Ford Thunderbird Target

Unlike the smaller targets, the detection zone measured with the vehicle target (e) looks very much the same as the earlier measurement with the driver's side sensor. The system detects the presence of vehicles approximately half way into the next lane.

Due to the fact that this sensor employs multiple narrow width beams, the small targets cannot give an accurate representation of the detection pattern. Only motor vehicles should be viewed as representative targets.

Vertical Extent - Passenger Side Sensor

Figure 6.6-4 depicts the vertical extent of the static pattern measured with the passenger side sensor. This sensor contains a single set of six beams. Because a small (0.3m x 0.3m) target was used, only one of the beams was intercepted. This sensor has a total vertical FOV of 6.9° and is directed towards the ground.

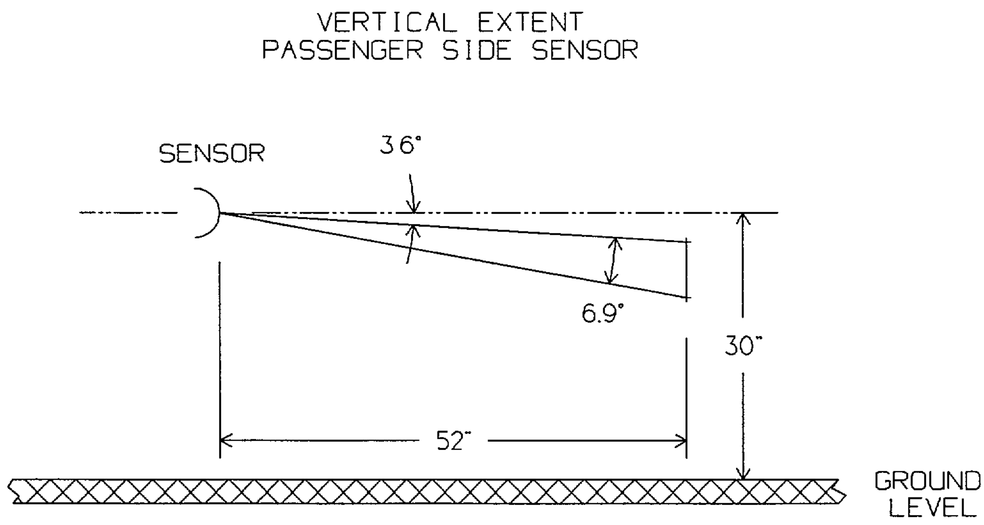

Figure 6.6-4: System "F" - Vertical Extent, Passenger Side Sensor

Dynamic Tests

Perpendicular Delay Time

The results of the perpendicular delay time measurements are presented in Figure 6.6-5. Both the X and Y positions at which the system reacted have been plotted as a function of target vehicle speed. The target vehicle was driven past the sensor vehicle at speeds of 1.6, 8, 16.1, 24.1, 32, and 48.3 KPH. The speed

Figure 6.6-5: Perpendicular Latency Time
Passenger Side Sensor

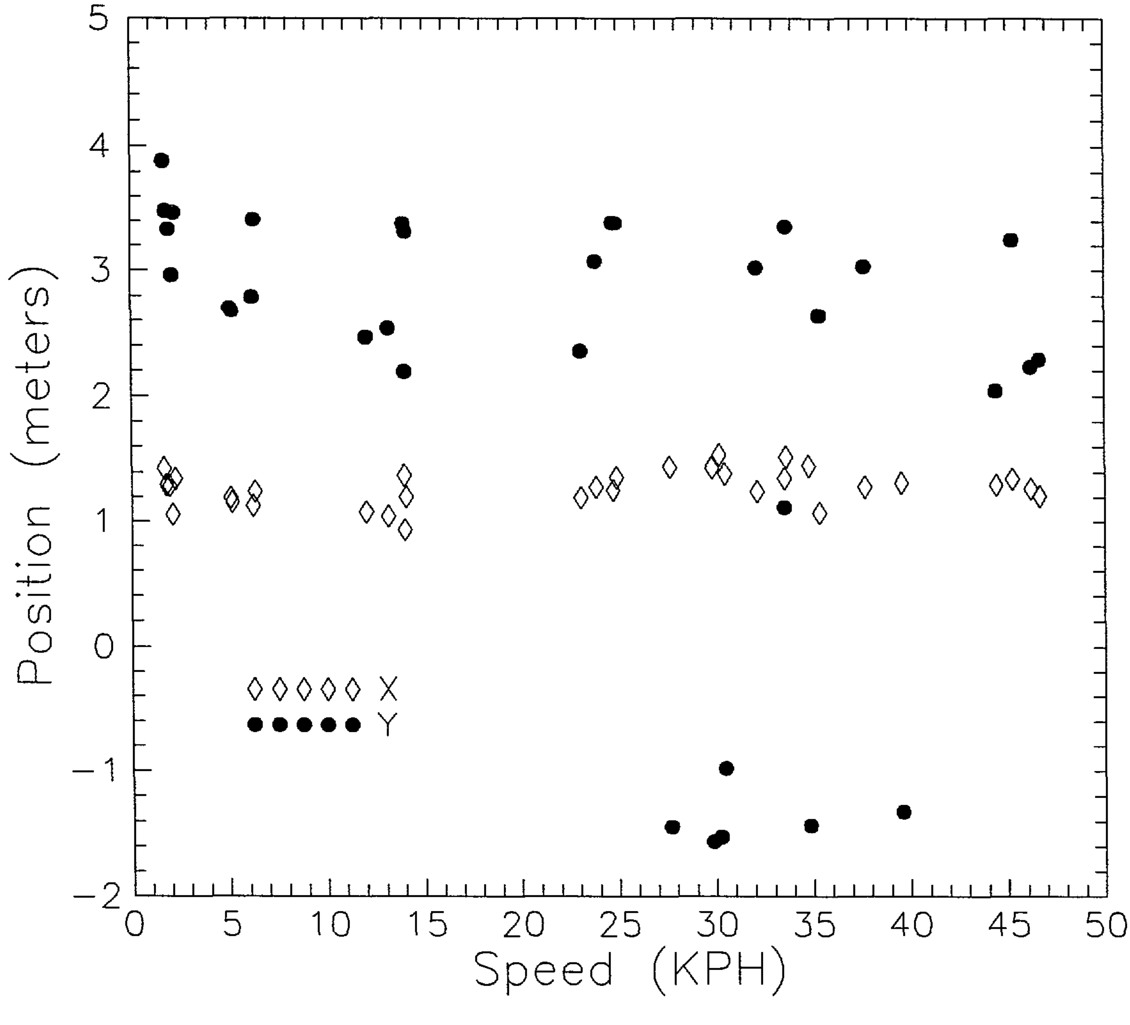

data points have been calculated directly from two reference frames in the video data. All data is referenced to post P2 on the front passenger side of the target vehicle.

The lateral separation (X) between the target and sensor vehicles varied between 1 and 1.5m over the duration of the tests. There are significant variations, however, in the Y position at which the system first detects the presence of the target vehicle. These variations are most dramatic at the higher target vehicle speeds. At speeds exceeding 25 KPH, there is as much as a 0.6s (4.5m at 27KPH) variation in the system reaction time. The data is suggestive of at least two different characteristic latency times. This bifurcation in the system performance may be explained by the multiple beam design of this particular sensor. Targets crossing orthogonal to the beams may indeed miss one or two or three beams before being detected. Since the system most likely requires a positive response for all beams to detect a target, the detection time will depend on precisely when the target enters the field of beams. This behavior should not be of great concern since the sensor was designed to look at targets approaching along a parallel path,

In summary, the system latency when subjected to targets approaching from an orthogonal direction can be bounded between 72 msec in the best case to 0.51 sec in the worst case.

Parallel Delay Time

The results of the parallel delay time tests are shown in Figure 6.6-6. The target vehicle was driven past the sensor vehicle at speeds of 1.6, 8, 16.1, 24.1, 40.2, 56.3, and 72.4 KPH. As before, the speed data points have been calculated directly from two reference frames in the video data. All data is referenced to post P1 on the front driver side of the target vehicle.

The lateral separation between the two vehicles is shown by the open triangles. This separation increases predictably at higher target vehicle speeds. This trend reflects the driver's natural tendency to put more space between his vehicle and an obstacle at higher vehicle speeds.

The parallel coordinate (X) at which the system reacts to the approaching vehicle is shown by the solid points. The absolute scatter in this data is much less than that seen in the orthogonal data (0.8m compared to 4.5m) with the greatest variation seen at higher target vehicle speeds. The parallel latency time computed from these measurements is 42 +/- 20 msec.

Persistence Time

The position of the target vehicle at the time the system indicator turns off can be determined by projecting'the car's position based upon the trajectory and speed calculated from two earlier reference frames. The latency time associated with system turn-off has been plotted in Figure 6.6-7 for the passenger side sensor.

This data was computed from the parallel delay time test results. The solid points represent the position of the target vehicle at the instant the system display ceases to flash. The slope of this line reflects a system turn-off persistence time of 0.92 sec +/- 80 msec. It should also be noted that the relative scatter of the data is much less for turn-off than for the turn-on data.

Figure 6.6-6: Parallel Latency Time
Passenger Side Sensor

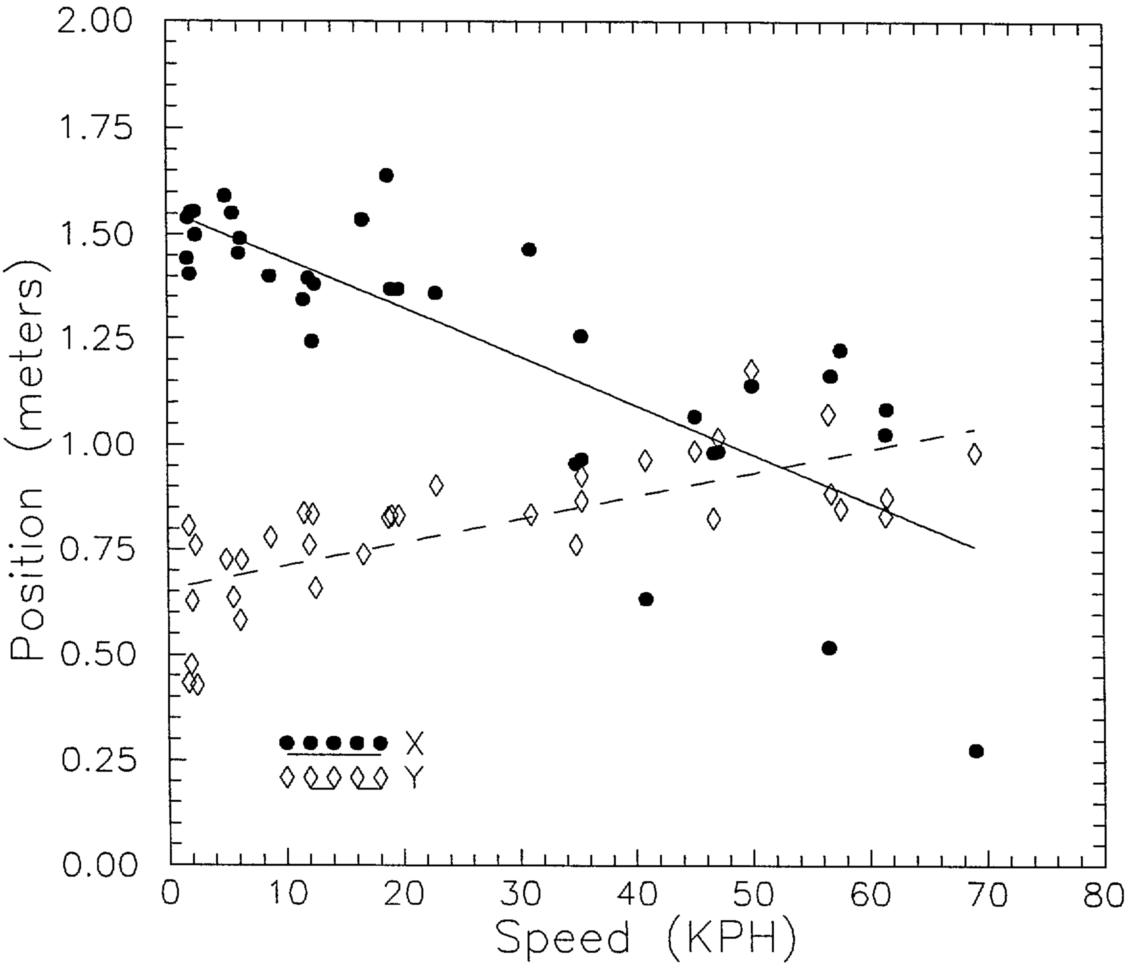

Controlled Passing Tests - Target Vehicle Passing Sensor Vehicle

A series of controlled passing tests were performed on the High Speed Track in which the sensor vehicle was driven at a constant speed and passed by the target vehicle at varying relative speeds of 16.1, 32.2, and 48.3 KPH. The intent of these tests was to examine the system latency as a function of relative speed and to investigate system performance on a curved road. All results have been referenced to post P1 on the front driver side of the target vehicle. Comparisons to the static detection zones measured earlier have been made and any inconsistencies noted.

Figure 6.6-8(a) depicts the x,y position at which the system first reacts to the passing vehicle. The data points have been identified according to the relative speed of the test. The static detection zone measured with the Ford Thunderbird target is denoted by the dashed line. Lane markers are identified by the parallel dashed lines. In general, the data collected is consistent with the measured static detection zone. With a delay time that can be a much as .062 sec, a delay of 0.8m can be expected in the system reaction at relative speeds of 48.3 KPH. Typical scatter about the static zone edge is within about 0.8m. In some cases the system reacts to the approaching target earlier than expected. A couple of

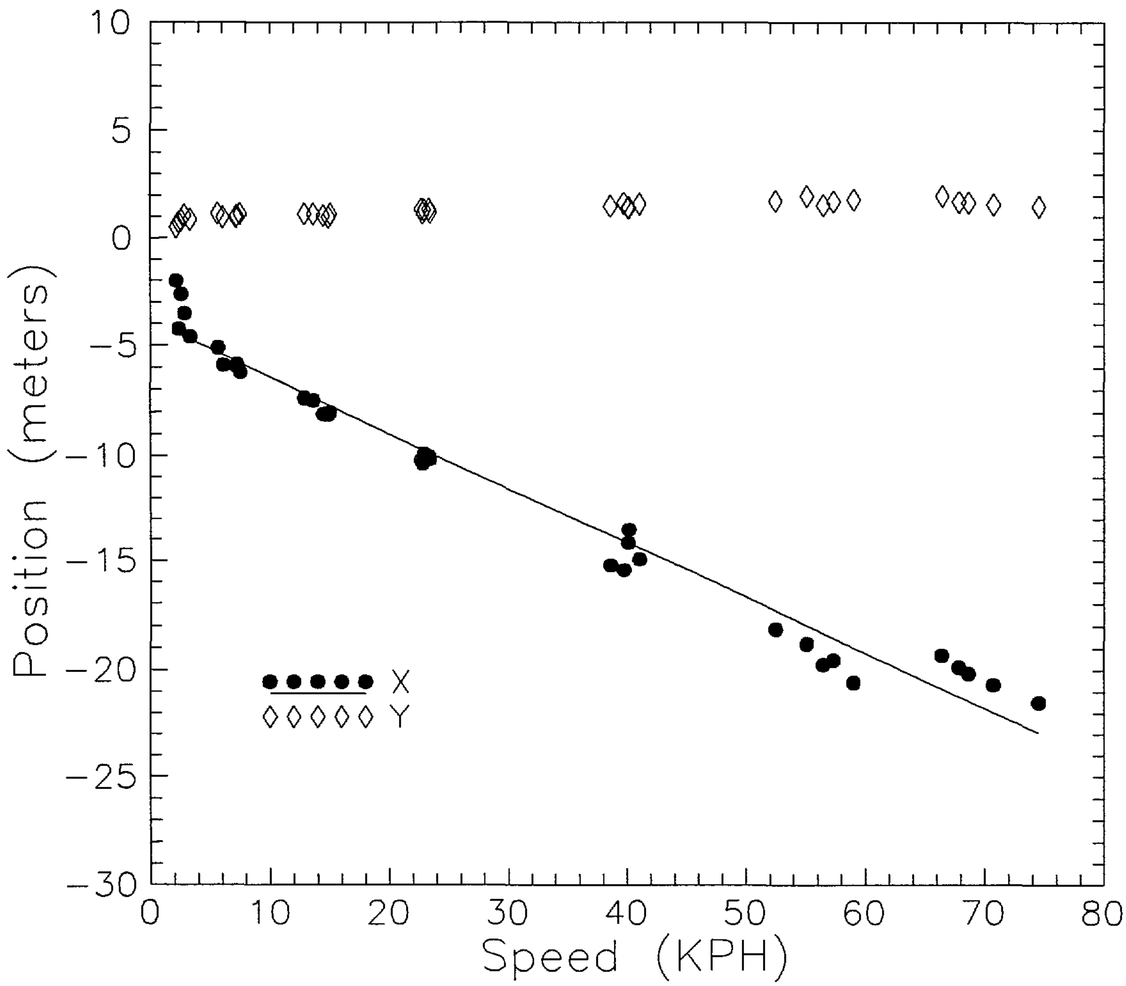

6.6-7: System Persistence Time
Passenger Side Sensor

Figure 6.6-8: Sy em "F" Controlled Passing Test Results - Passenger Side Sensor
Target Vehicle Passing Sensor Vehicle

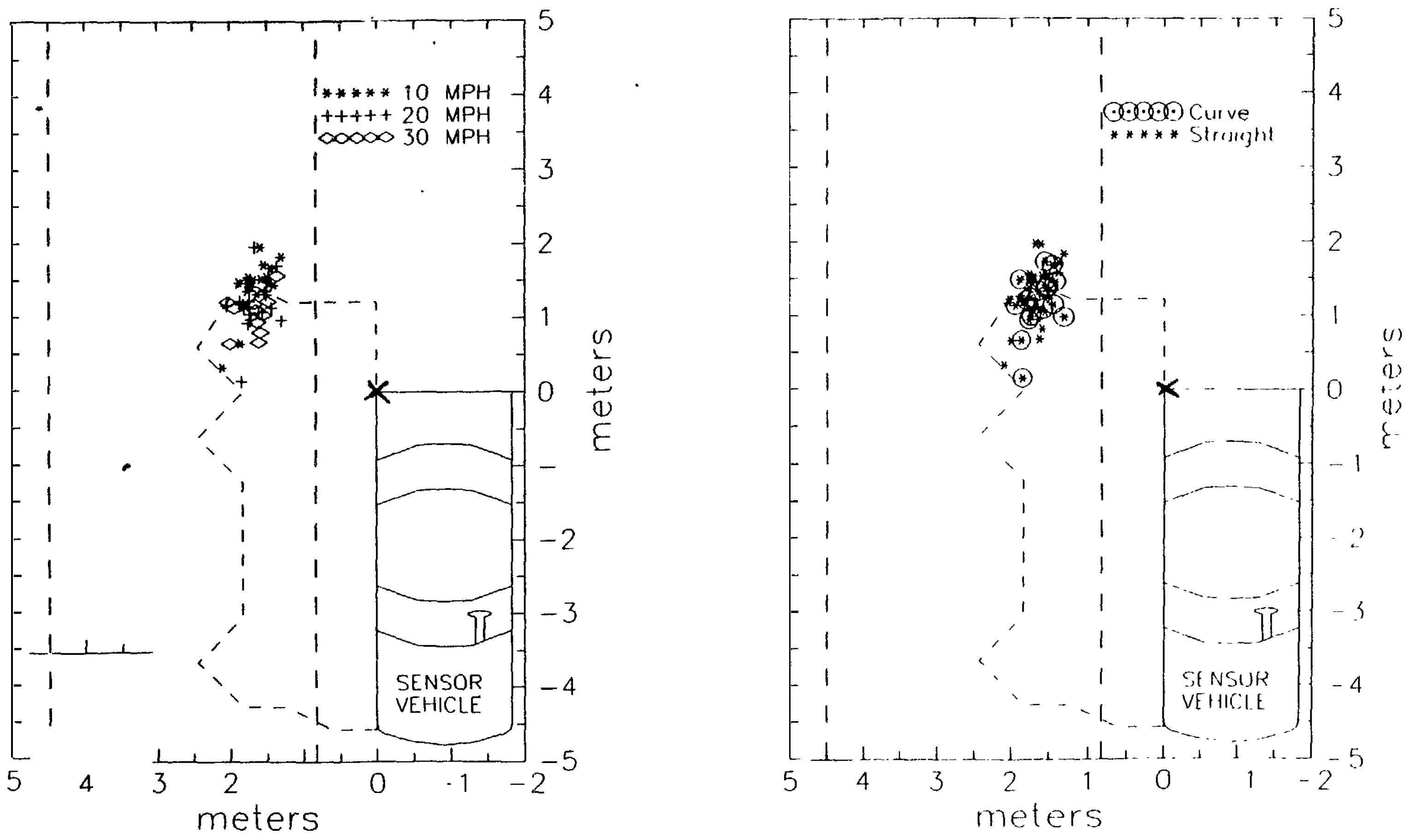

(a) System Performance vs. Relative Speed

(b) Curved vs. Straight Path

data points (one at 16.1 KPH and one at 32.2 KPH) exhibit delays that are slightly more than would be expected from the system latency time.

The effects of a curved path is shown in Figure 6.6-8(b). The data has now been plotted as a function of straight and curved path. The results indicate that vehicles passing along a curve are no more difficult to detect than those vehicles passing on the straight-a-way.

These tests were repeated with a clutter vehicle located directly behind the sensor vehicle at separation distances of 4.6, 9.2, and 13.7m. The objective in these tests was to trigger a false alarm in the presence of typical highway traffic. Figure 6.6-9 summarizes the results of this test. The relative speed of the approaching vehicle varies between 16.1 and 32.2 KPH. Even with the clutter vehicle foilowing only 4.6m behind the sensor vehicle (a distance that constitutes "tail-gating at highway speeds), no false alarms were triggered. The system performance is independent of clutter simply because the pattern does not extend behind the sensor vehicle.

Controlled Passing Tests - Sensor Vehicle Passing Target Vehicle

A series of tests was performed in which the sensor vehicle passed the target vehicle whose speed is held constant. The intent was to evaluate the system's ability to distinguish between positive and negative closing speeds. The sensor vehicle was driven past the target vehicle at relative speeds of 16.1 and 32.2 KPH. Figure 6.6-10 summarizes the target vehicle position at which the system first reacts to the presence of a target within its zone of detection. All data has been referenced to post P1 on the target vehicle and plotted as a function of relative speed. System latency time can explain up to a 0.55m delay in system reaction time. For the most part, the data is consistent with this delay. A few of points in which the lateral separation between the vehicles is larger seem to be catching the outer edge of the static detection zone.

Approach and Pass Tests

A short series of tests was performed to investigate the system's utility in a typical highway passing scenario in which an approaching car in the same lane as the sensor vehicle swerves into an adjacent lane to pass. Six separate maneuvers were made with the sensor vehicle driving at a fixed speed of 64.4 KPH. The results are summarized in Figure 6.6-11. All data has been referenced to post P1 on the target vehicle. No attempt to maintain a fixed speed with the target vehicle was attempted because of the nature of the test. Note that the system does not detect the approaching vehicle until that vehicle has crossed over into the adjacent lane. Once again, the data collected is consistent with the static detection patterns measured.

Figure 6.6-9: System "F" Controlled Passing With Clutter Vehicle
Passenger Side Sensor

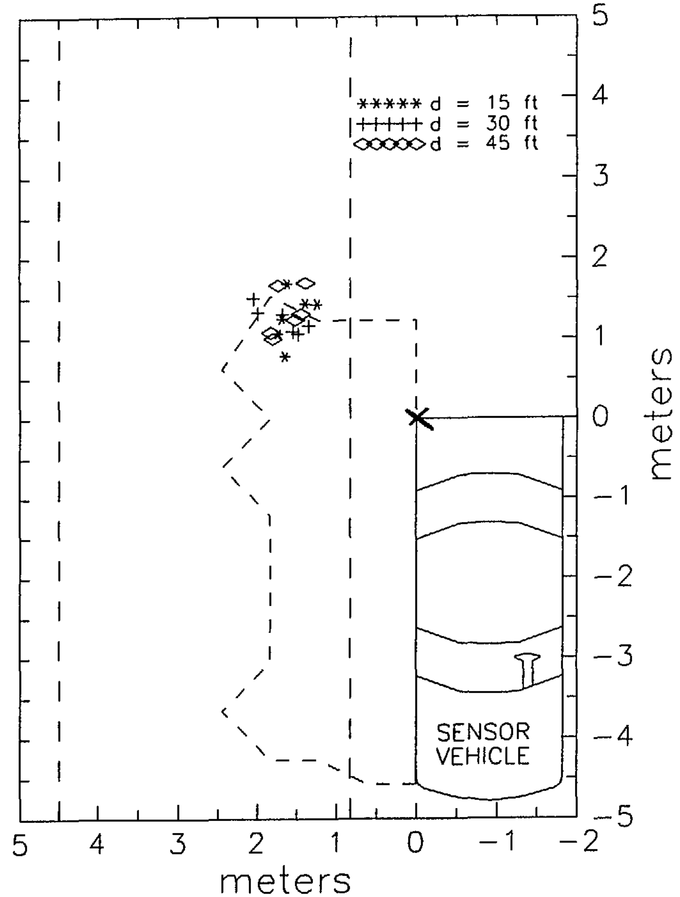

**Figure 6.6-10: System "F" Controlled Passing Test Results - Passenger Side Sensor
Sensor Vehicle Passing Target Vehicle**

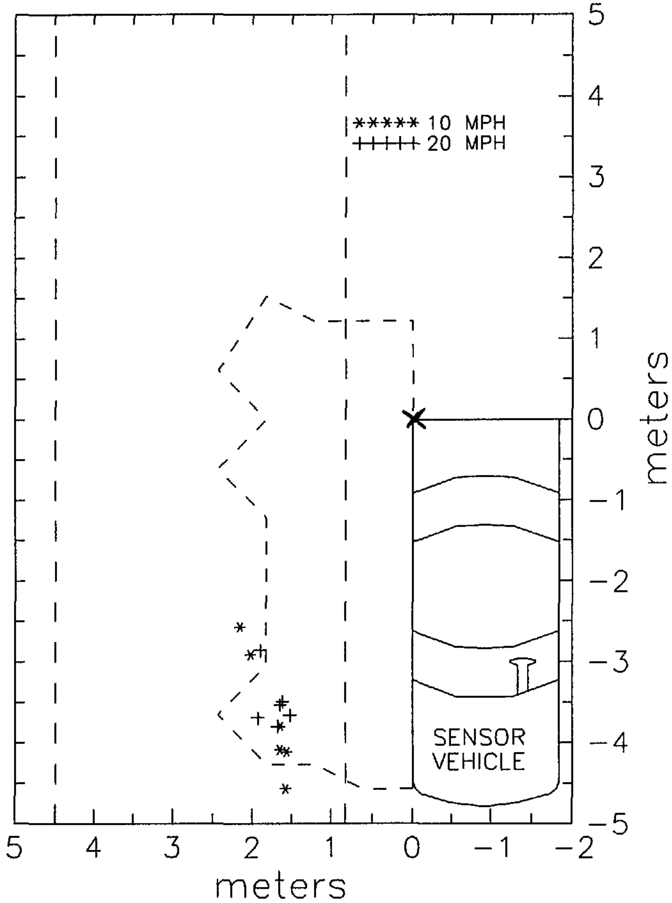

Figure 6.6-11: System "F" Approach and Pass Test Results
Passenger Side Sensor

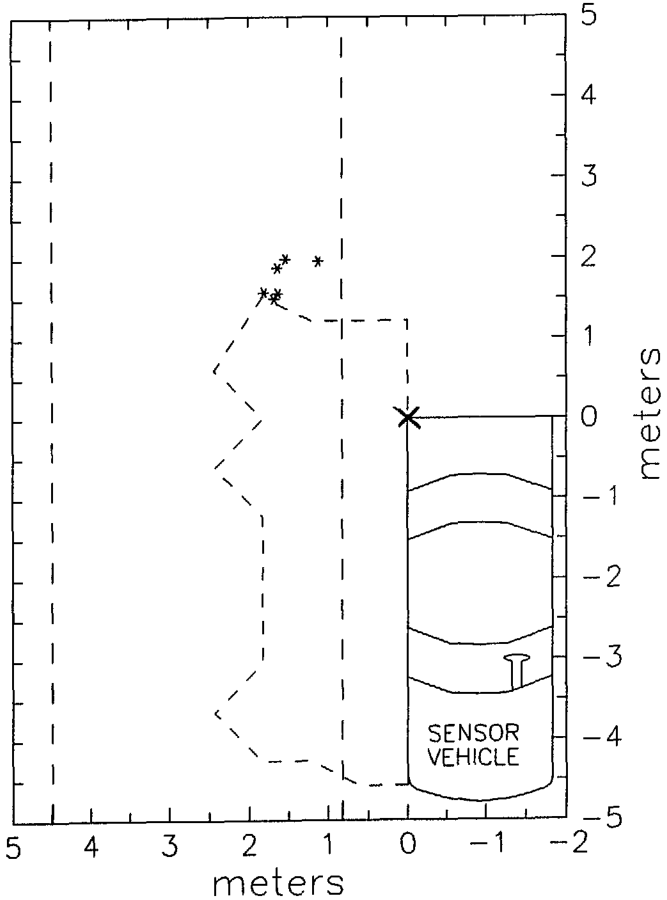

Figure 6.6-12: System "F" Three Lane Test Results
Passenger Side Sensor

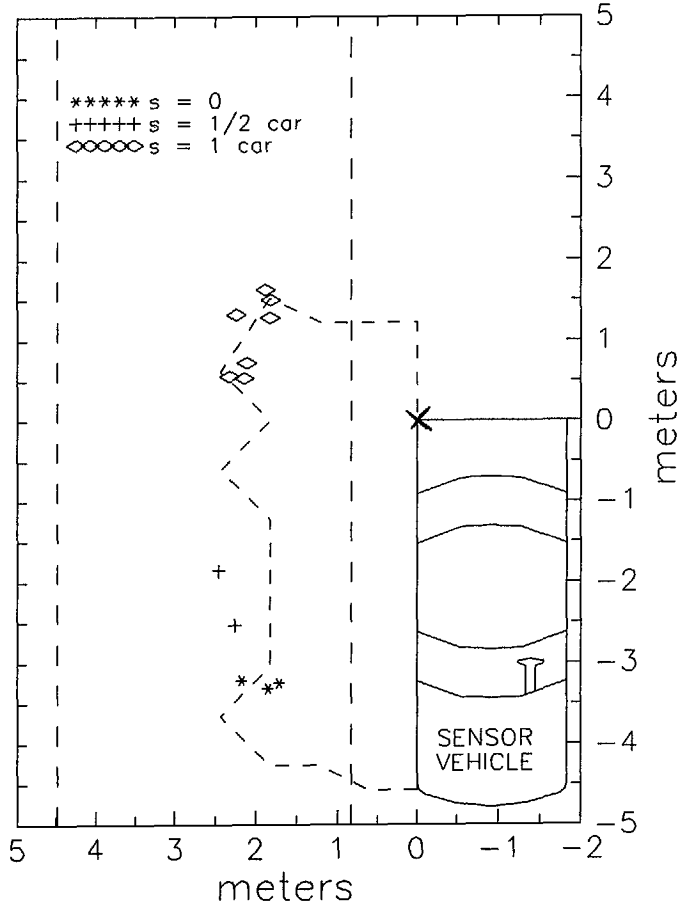

Three Lane Tests

Three lane maneuvers were performed to investigate the probability of a false alarm being triggered by a vehicle in a non-interfering lane. In these tests, the vehicles are initially separated by an entire lane. The target vehicle then maneuvers into the adjacent lane at nose-to-nose separation distances of 0, 1/2 car, 1 car, and 2 car lengths. The sensor vehicle speed was maintained at 64.4 KPH. Figure 6.6-l 2 summarizes the results. The target was detected at nose-to-nose separations up to 1 car length. At separation distances of greater than a car length, the target vehicle was located too far behind the static detection zone of the sensor to be detected. Otherwise, the target was detected along the outer lateral boundary of the detection zone.

Merge Tests

System applicability in a merging scenario was tested by approaching the sensor vehicle at various angles. The sensor vehicle was parked and the target vehicle driven past at speeds of 32.2, 64.4 and 64.4 KPH. The angle of approach varied from 0^o (parallel) to 14^o A series of tests was performed at an incident angle of 25^o but no detections were observed regardless of the speed of the approaching vehicle.

Test results from the 0^o and 14” merge tests are given in Figure 6.6-13(a) and (b), respectively. All data has been referenced to post P1 on the target vehicle and has been plotted as a function of target vehicle speed. With the exception of two data points, the 0^o data is characterized by relatively small scatter even at the higher vehicle speeds. The two exceptions have an apparent delay that is significantly greater than the system latency. This data is reminiscent of the bifurcated behavior that was observed during the perpendicular delay time tests. Certain passes were characterized by a very “late” detection time presumably due to the target sneaking through a couple of beams before being seen.

System latency effects are more pronounced in the 14^o data. Because the vehicle is approaching from an angle, the first opportunity for detection tends to occur at the outmost lateral edge of the detection zone. At the higher target vehicle speeds at which the tendency to increase the separation distance between vehicles is greater, the path tends to “cut the corner” of the detection zone. This is evidenced by the fact that only one out of ten passes at 64.4 KPH was detected by the system.

Figure 6.6-13: System "F" Merge Test Results
Passenger Side Sensor

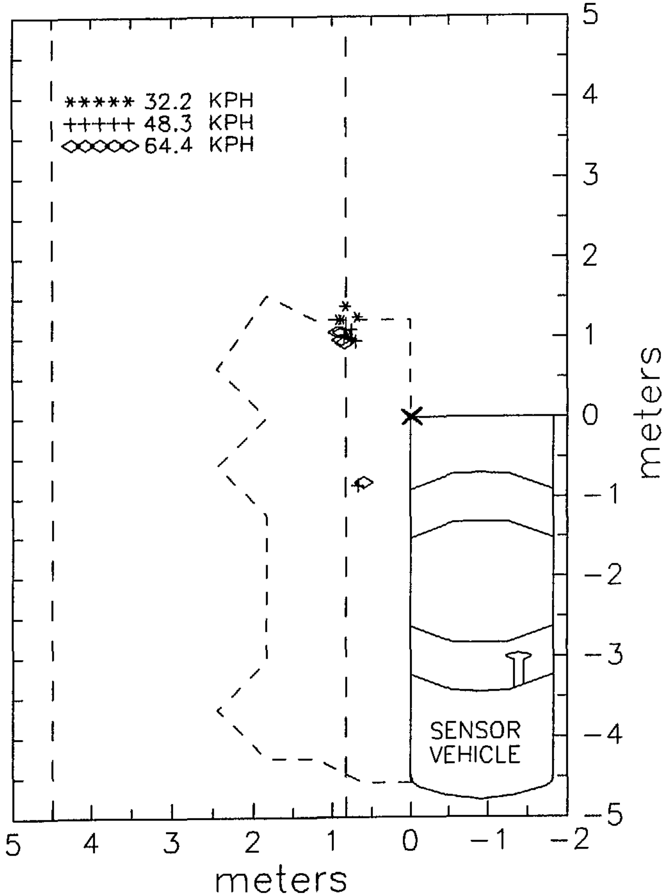

(b) 0° Angle of Approach

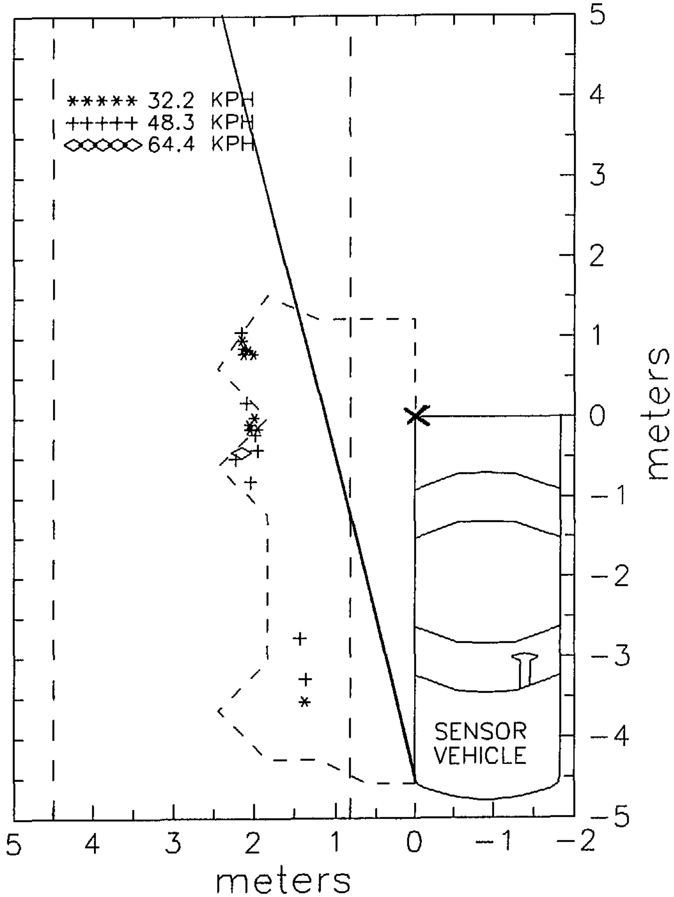

(a) 14° Angle of Approach

Road Test

This system was evaluated under realistic road conditions involving freeway, city, two-lane highway, and parking lot driving. The total exposure time was 58.3 minutes. Statistics were compiled on the number and types of targets detected, Figure 6.6-14 summarizes the results.

In general, this system did a good job of detecting all proximity targets. There were two cases on the freeway, however, in which the system failed to react to a passing vehicle (pick-up trucks). These two cases were studied in more detail to determine if there was a good reason that the system failed to react. A range analysis revealed that the lateral separation between the sensor vehicle and the passing vehicle was within 2.4m in both cases. This should have been within the static detection zone of the sensor. The closing speed of the approaching vehicles was less than 32.2 KPH. It was demonstrated in the controlled dynamic tests that this system is capable of detecting vehicles with closing speeds of up to

Figure 6.6-14: Summary of Road Test Statistics - System 'F"

System: 'F"
Total number of detects: 163

Classification	Freeway	Two-lane	City	Parking Lot	TOTAL
TP	61	7	38	55	161
FP	0	0	1	1	2
TOTAL	61	7	39	56	163
FN	2	0	0	0	2
TN					99.8 %

General Comments:

Two misses (FN)

Two unexplained detections

In general all road signs, trees, poles, concrete pillars, etc. within the sensor's field of view generated a positive response

System "loses" concrete barrier between metal guardrails

System "loses" semi trailer section between front and back wheels

64.4 KPH. The most probable explanation for the misses has to do with the fact that at a lateral distance of 2.4m, the vehicle is on the edge of the static detection zone. It has been repeatedly observed that the edges of these static patterns are characterized by the most uncertainty.

Another observation made was that the system lost sight of the trailer section of a semi-truck. Because the beams of the sensor point either parallel to the ground or are tilted down, it is understandable that the system turned off when being passed by a semi-truck. If the truck passes slowly enough there is enough time for the system to turn off when it is between the axles of the trailer. This could be mitigated by the addition of an uptilted beam to register the body of the trailer.

6.7 System 'G"

6.7.1 System Description

This system is a microwave radar collision warning system operates with a frequency in the vicinity of 35 GHz. It is designed as a presence detector with the capability of rejecting targets moving away from the sensor vehicle (e.g., meaningless ground clutter). The unit tested was mounted on the passenger side of the host vehicle near the side view mirror at a height of about lm above the ground level. The driver display consists of an indicator light that denotes the presence of a target.

6.7.2 Overview of System Performance

The static patterns measured with this system were characterized by a hysteresis that made it difficult to accurately determine the boundary of the detection zone, Furthermore, the system failed to detect both a human target and a motorcycle target during the static portion of the test cycle. The unit tested performed adequately during dynamic tests. However, since the system's reaction is dependent on the closing velocity of the target, it was sometimes difficult to correlate the dynamic test results with the measured static pattern.

In general, this system performed fairly well during the road test. The number of inappropriate aiarms was high (84%). Although currently available systems that claim to provide the added benefit of clutter rejection typically have a high number of inappropriate alarms, the number generated by this system is higher than the average. There were no cases in which the system failed to detect a target within its detection zone (FN).

6.7.3 Test Results

<u>Static Tests</u>

Static **patterns** were measured for the following types of targets:

1) 0.3m x 0.3m foil covered Styrofoam
2) 0.6m x 0.6m foil covered Styrofoam
3) human
4) motorcycle
5) Ford Taurus

The foil targets were located at the vertical height of the sensor. Before embarking on a discussion of the data collected, a few comments should be .made, Firstly, the static patterns measured with this sensor were characterized by some hysteresis. In other words, the apparent boundary of the pattern showed some dependence on the direction of approach resulting in some uncertainty in the accuracy of the boundaries displayed in the following plots. In addition, the static pattern measured with the automobile target was characterized by areas of no detection surrounded by areas of solid detects giving the appearance of "holes" in the static detection zone. For purposes of plotting, it was assumed that these holes were artifacts of the experimental test procedure and do not represent real blind spots. Thus, in the case of the automobile target, the boundary of the measured detection zone has been plotted.

Figure 6.7-1 (a) summarizes the results of the static measurements made using the 0.3m x 0.3m aluminum foil covered target. The resulting static detection zone is characterized by ah irregular boundary which tends to be long and narrow. The total extent is roughly 4m to the rear of the vehicle and 2.5m to the side, A comparison to the static pattern measured with the 0.6m x 0.6m foil target is given in figure (b). This pattern is much more regular in shape perhaps because of the increased cross-section of the target. However, the system failed to detect this target at distances within about lm of the host vehicle.

The static detection patterns associated with both a human and a motorcycle target were measured but no solid system detects were observed.

The static detection zone measured with a Ford Taurus target is shown in Figure 6.7-1 (c) The data has been referenced to post Pl on the front driver's side of the target vehicle. Similar to the pattern measured with the 0.3m x 0.3m foil target, the boundary is irregular. In addition, several 'holes" in the pattern were observed. For clarity, only the outer boundary of the pattern is displayed.

Vertical Extent

The vertical extent of the static pattern was determined by placing a target at a distance, D, from the sensor and measuring the system response as a function of vertical position. Figure 6.7-2 summarizes the angular extent of this sensor. The sensor has a total vertical FOV of 25.6" and is angled slightly downward.

Dynamic Tests

Perpendicular Delay Time

Figure 6.7-3 summarizes the results of the perpendicular delay time tests for this system. The target vehicle was driven past the sensor vehicle at speeds of approximately 1.6, 8,16.1, 24.1, and 32.2 KPH. For this series of tests, it was generally the case that the actual vehicle speed was somewhat greater than the

Figure 6.7-1: System "G" Sta   Test Results

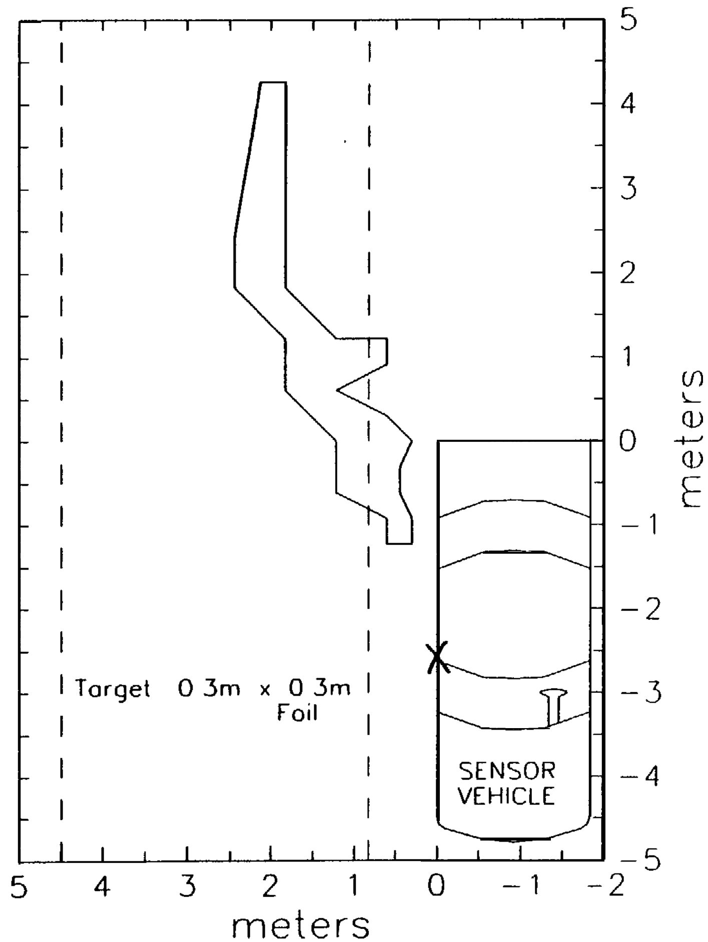

(a) 0.3m x 0.3m Aluminum Foil Target

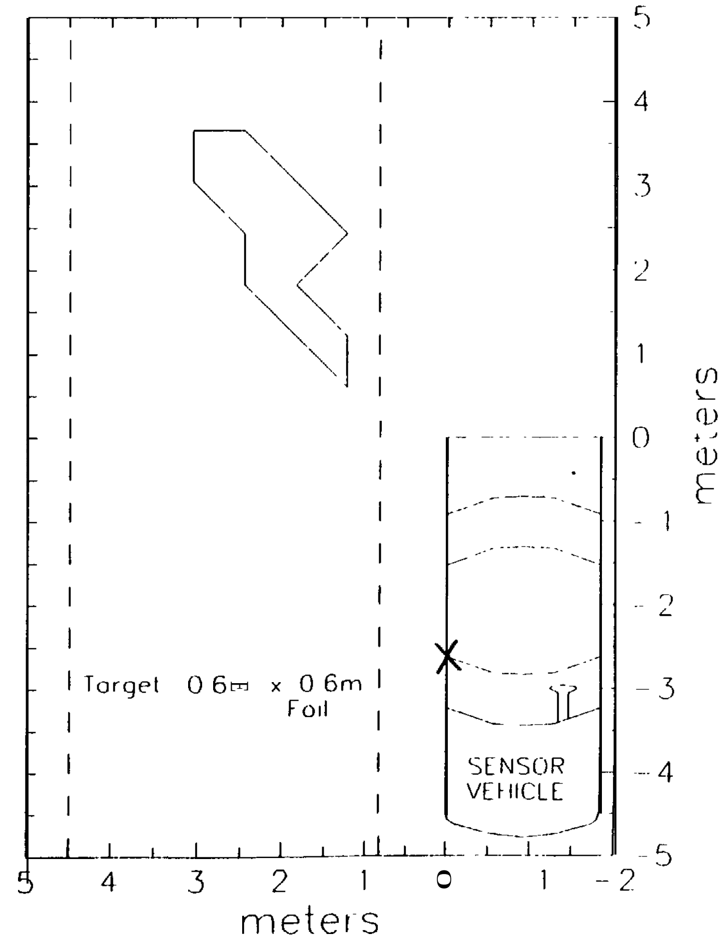

(b) 0.6m x 0.6m Aluminum Foil Target

Figure 6.7-1: System "G" Static Test Results (con 'd)

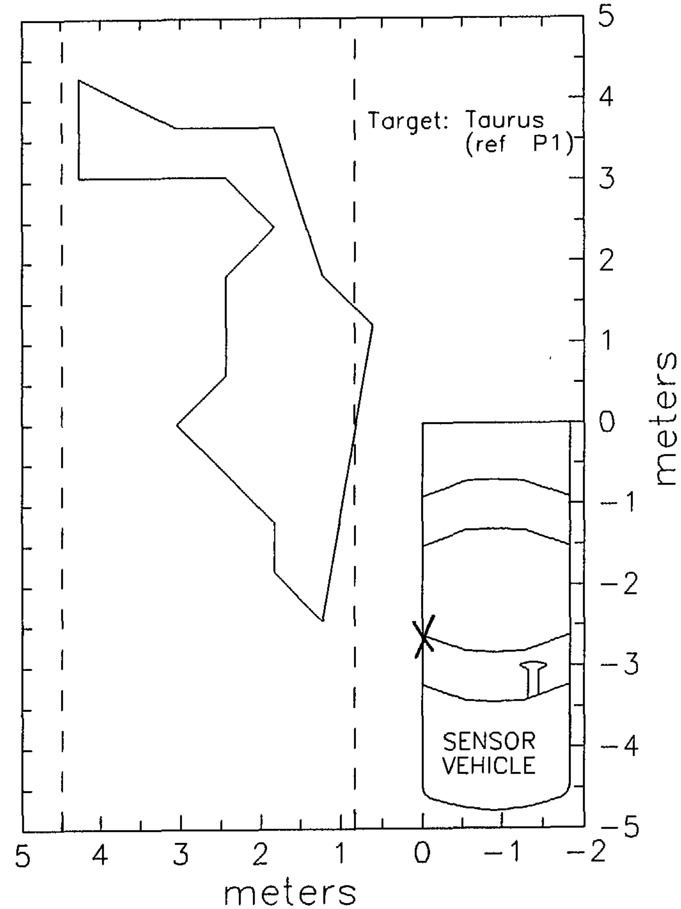

(c) Ford Taurus Target

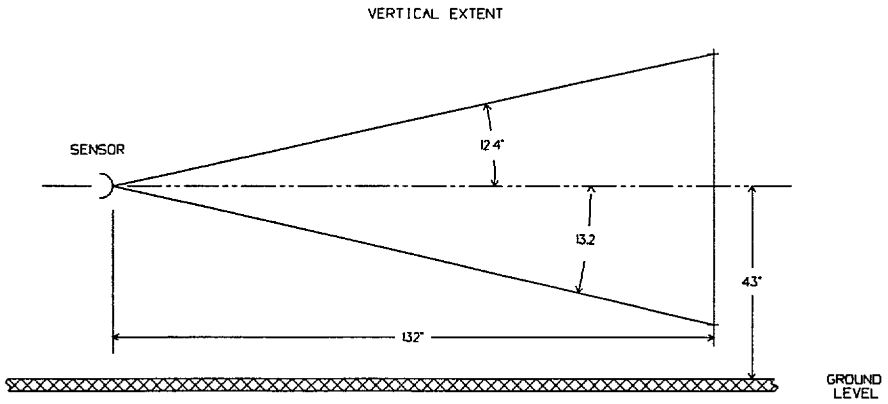

Figure 6.7-2: System "G" - Vertical Extent

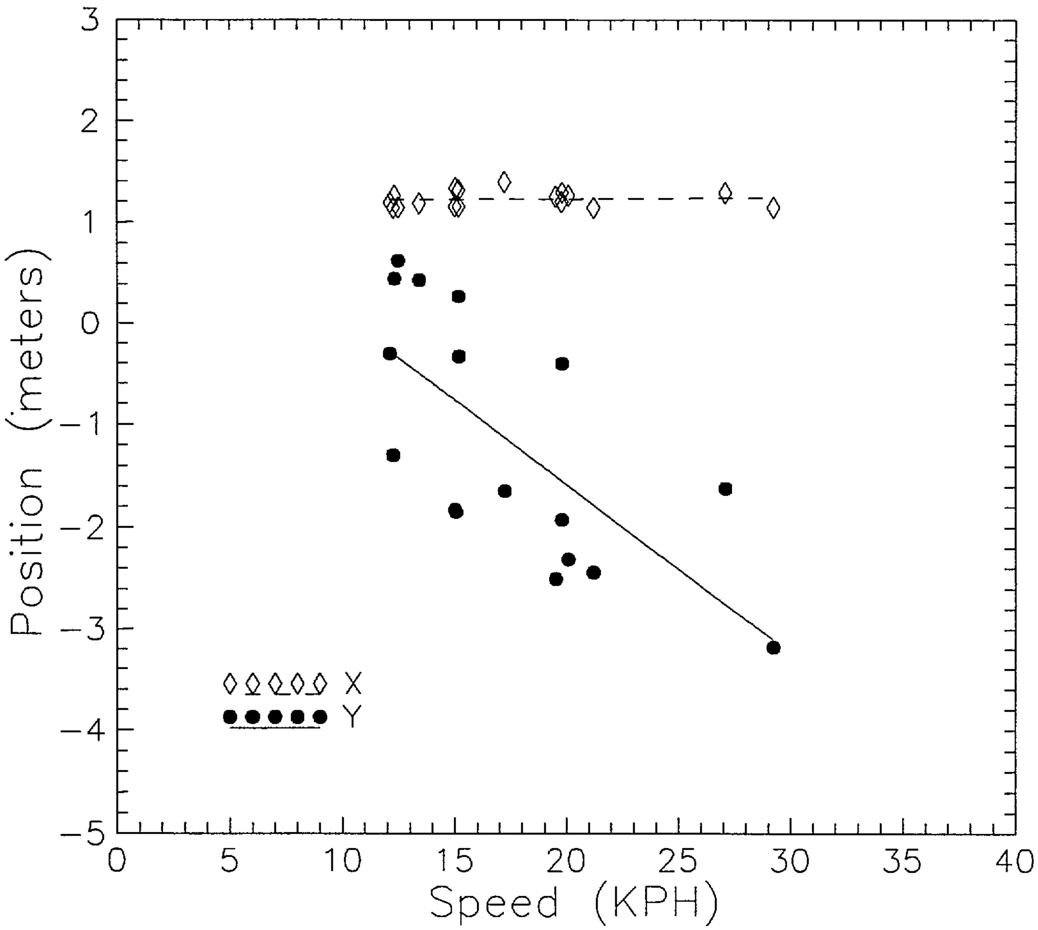

Figure 6.7-3: Perpendicular Latency Time
System "G"

targeted speed. No system detects were observed at a target vehicle speed of 32.2 KPH. However, it can be seen from the data that system reactions were observed at vehicle speeds of up to 30 KPH. All data has been referenced to post P2 on the front passenger side of the target vehicle.

The lateral separation (X) between the two vehicles is denoted by the open triangles. The scatter about the mean is less than +/- 0.2m.

The Y position of the target vehicle at the instant of system reaction is shown by the filled circles. Five passes were made at each vehicle speed. At a speed of 24 KPH, only two out the five passes resulted in a positive system reaction. The point at which the system reacts is characterized by scatter on the order of +/- In which in turn results in a larger uncertainty in the latency time. The perpendicular latency computed from a linear best fit to this data is 0.59 sec +/- .28 msec.

Parallel Delay Time

The results of the parallel delay time tests are presented in Figure 6.7-4. This data was collected with vehicle speeds of 1.6, 8, 16.1, 24.1, 32.2, 40.2, 48.3, and 64.4 KPH.

The lateral separation, (Y), denoted by the open triangles increases slightly at higher vehicle speeds reflecting the driver's natural tendency to increase the distance between his vehicle and a parked object at higher vehicle speeds. The scatter in this parameter is less than 0.2m. The parallel coordinate, (X), of the approaching vehicle at the instant the system responds is shown by the filled circles. The scatter in this data represents real variation in the system response and can be as large as 3m. The parallel latency time computed from this data is 0.46 sec +/- 0.19 sec.

Persistence Time

For this system, information on the turn-off characteristics of the system has been extracted from the perpendicular delay time test results. The position of the target vehicle at the instant the system display turns off is plotted in Figure 6.7-5. This data has been computed from a projection of the car's position based on the trajectory and speed calculated from two earlier reference video frames. All data has been referenced to post P2 on the passenger side of the target vehicle. The characteristic scatter in this data is about a meter which is much smaller than that observed during system turn-on. The latency time associated with system persistence is 0.54 sec +/- 0.27 sec.

Figure 6.7-4: Parallel Latency Time
System "G"

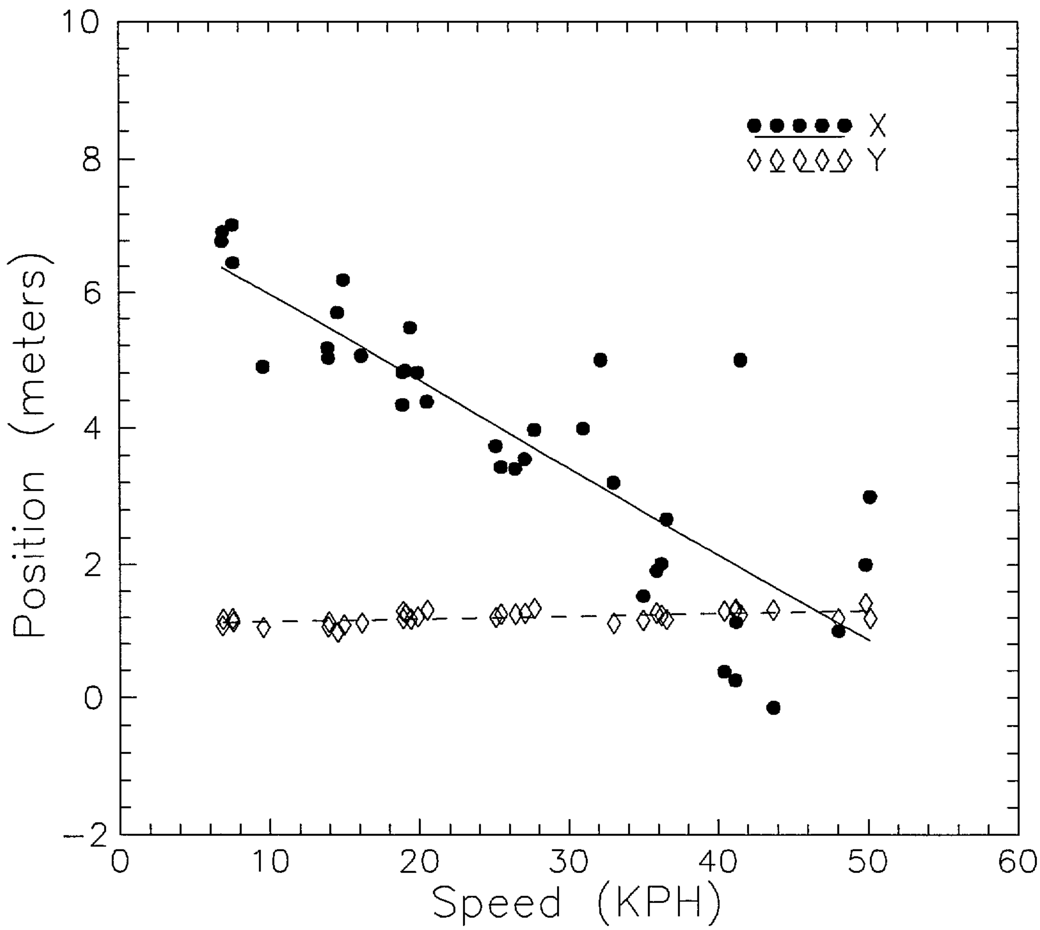

Controlled Passing Tests - Target Vehicle Passing Sensor Vehicle

A series of controlled passing tests was performed on the High Speed Track in which the sensor vehicle was driven at a constant speed and passed on the right by the target vehicle. The vehicle speeds for this test were:

Sensor Vehicle Speed (KPH)	Target Vehicle Speed (KPH)	Closing Velocity (KPH)	Number of Passes
64.4	80.4	16	6
64.4	96.5	32.1	6
64.4	112.6	48.2	2(4)
80.4	96.5	16	6
80.4	112.6	32.1	6
96.5	112.6	16	6

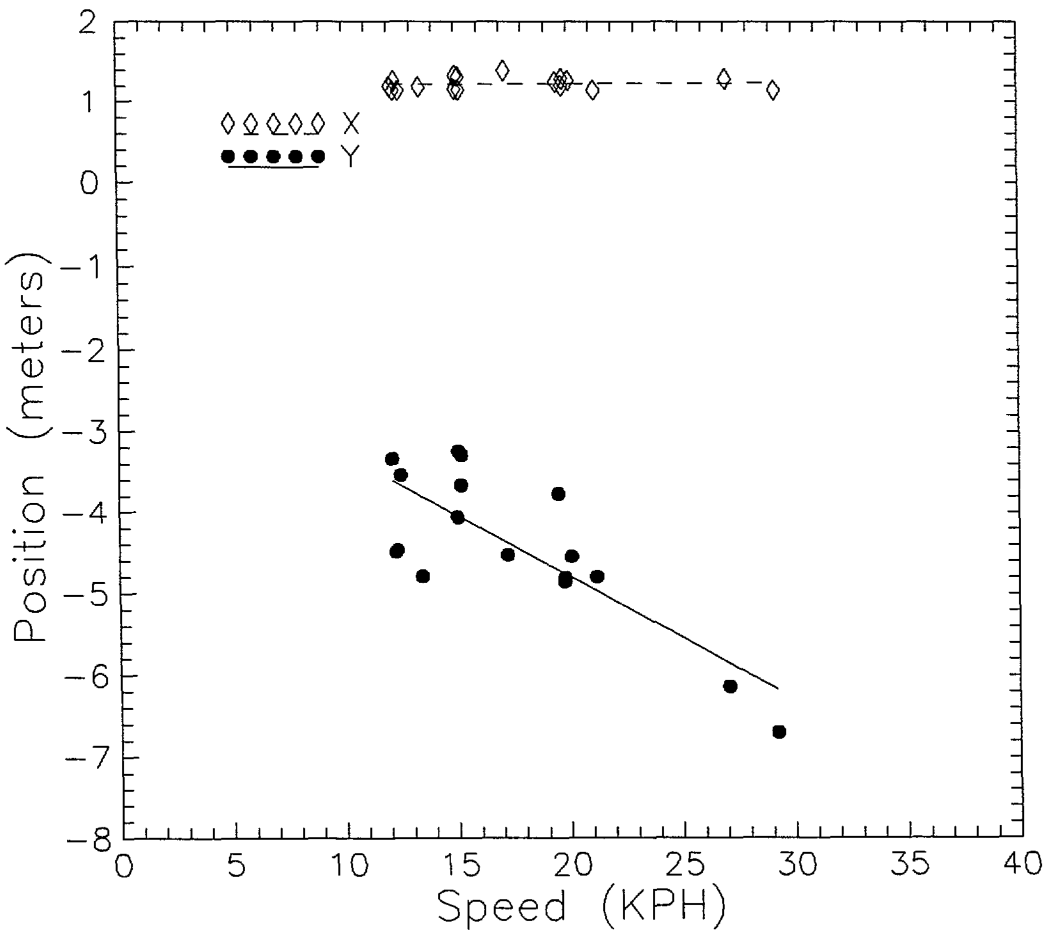

Figure 6.7-5: Persistence Time - System "G"

The numbers in parenthesis indicate the total number of passes made. For instance, the notation 5(6) means that five out of six passes resulted in a detection. Otherwise, a detection was observed for each pass.

Roughly 35% of these tests were conducted on the curved portion of the High Speed Track. The intent of these tests was twofold: 1) to investigate the sensor performance as a function of relative speed and correlate the results with the measured system latency and 2) to investigate the effect on sensor performance when passing occurs on a curved path.

Figure 6.7-6(a) summarizes the target vehicle range at which the sensor first reacts to the passing vehicle. All results have been referenced to post P1 on the front driver side of the passing vehicle and have been segregated according to the closing velocity of the test. The static detection zone measured with the Ford Taurus target is denoted by the dashed line. Lane markers are identified by the parallel dashed lines.

The data shows a clear dependence on the closing velocity of the approaching vehicle. Measurements made at similar (within 1.6 KPH) closing velocities are clustered together. The groups are separated by 2.5 to 3m which is consistent with the system latency (0.46 +/- 0.19 sec) and the speed differential (16 KPH).

Another observation is that the system apparently reacts to the approaching target much more quickly than suggested by the static pattern. This particular system is designed to react sooner to targets approaching with higher velocities. Obviously, during static testing, the relative velocity between the target and sensor vehicle is quite small compared to an actual passing scenario. Therefore, the boundary of the static detection zone actually extends further for these tests than is indicated by the static pattern displayed.

The effects of a curved path is shown in Figure 6.7-6(b). The data has now been plotted as a function of straight and curved path. Since this system is relatively short range, system performance is not a function of the curvature of the passing trajectory. The data clearly indicates that those passes made along the curved portion of the test track are scattered within the total range of system detects. If the trajectory curvature influenced system performance, the data would show a segregation between those data points measured along a straight path and those measured along a curved path.

These tests were repeated with a clutter vehicle located directly behind the sensor vehicle at separation distances of 3, 6, and 9m. The objective in these tests was to trigger a false alarm in the presence of typical highway traffic. Figure 6.7-7 summarizes the results of this test. The relative speed of the approaching vehicle was varied between 16 and 32 KPH. Once again, there is a clear relative speed

Figure 6.7-6: System "G" Controlled Passing Test Results
Target Vehicle Passing Sensor Vehicle

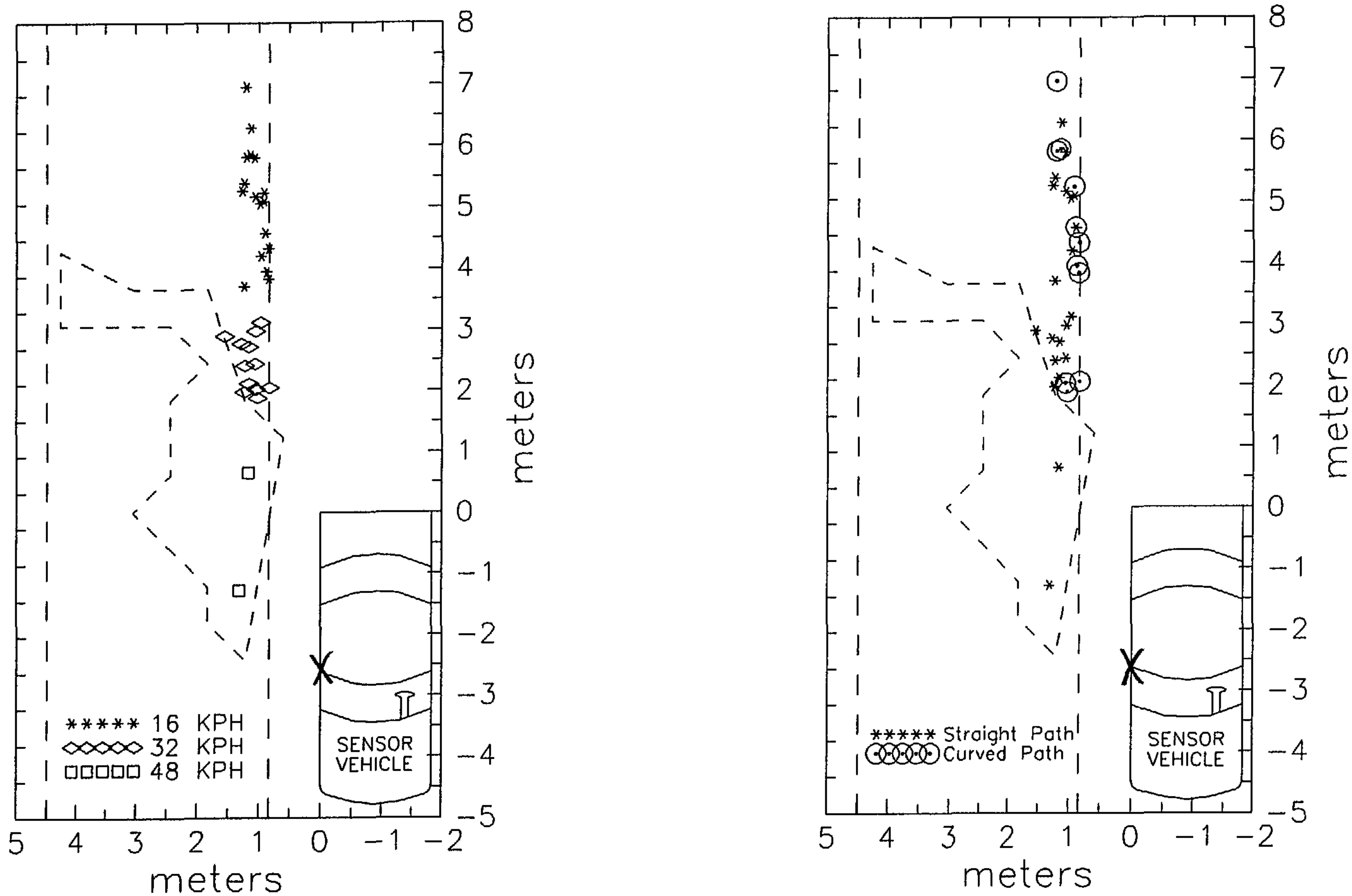

(a) System Performance vs. Relative Speed

(b) Curved vs. Straight Path

Figure 6.2-7: System "G" Controlled Passing With Clutter Vehicle
Target Vehicle Passing Sensor Vehicle

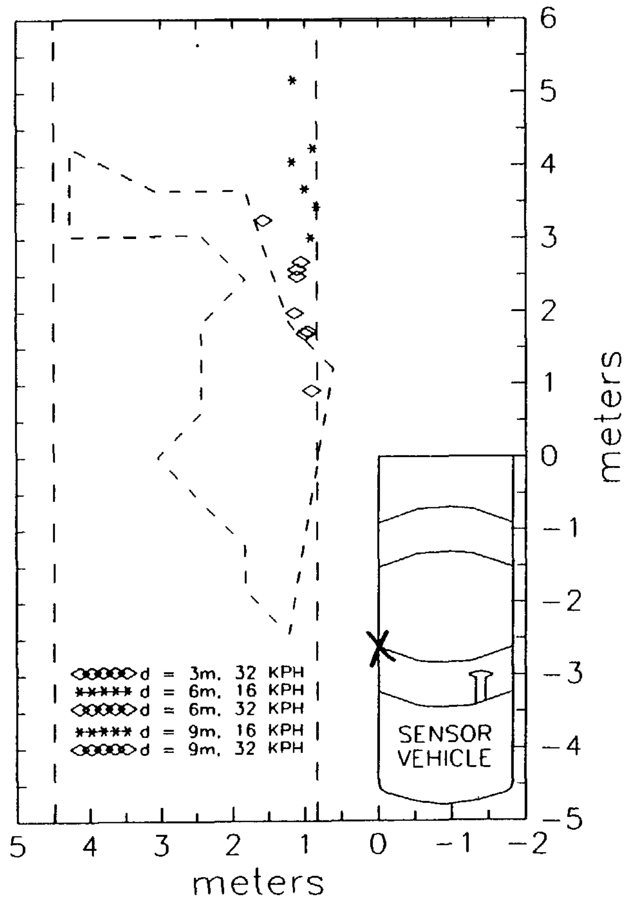

dependence in the measured data. However, this data is consistent with the earlier controlled passing tests without clutter and shows no evidence of early detections caused by the presence of the clutter vehicle. This is due to the fact that the sensor looks to the side of the sensor vehicle and has little or no visibility behind the vehicle.

Controlled Passing Tests - Sensor Vehicle Passing Target Vehicle

A series of tests was performed in which the sensor vehicle passes the target vehicle in order to evaluate the system's ability to distinguish between positive and negative closing speeds. A summary of the tests performed is as follows:

Sensor Vehicle Speed (KPH)	Target Vehicle Speed (KPH)	Closing Velocity (KPH)	Number of Passes
80.4	64.4	-16	6
96.5	64.4	-32.1	4(6)
112.6	64.4	-48.2	0(3)

Once again, the number in parenthesis indicates the total number of passes made. No system reactions were observed with a closing velocity of -48.2 KPH. The results are presented in Figure 6.7-8. Consistently, the data collected at the higher closing speed was characterized by a longer delay. System latency can explain delays of up to 2.8m. A couple of data points taken at a relative speed of -32.1 KPH show'a delay of 5 to 6m. These data represent real variation in the system performance and can be classified as "late" detects.

Approach and Pass Tests

A short series of passes were made to investigate the system's utility in a typical highway passing scenario in which an approaching car in the same lane as the sensor vehicle swerves into an adjacent lane to pass. Five separate maneuvers were made with the sensor vehicle driving at a fixed speed of 88.5 KPH. The results are summarized in Figure 6.7-9 in which all data has been referenced to post P1 on the target vehicle. No attempt to maintain a fixed speed with the target vehicle was attempted because of the nature of the test. The system detects the passing vehicle as it is making its lane change. Recalling that the point of reference is on the driver's side of the target vehicle, the system reacts as the target vehicle has approximately 3/4 to a full width into the adjacent lane. This is consistent with the extent of the static pattern.

Figure 6.7-8: System "G" Controlled Passing Test Results
Sensor Vehicle Passing Target Vehicle

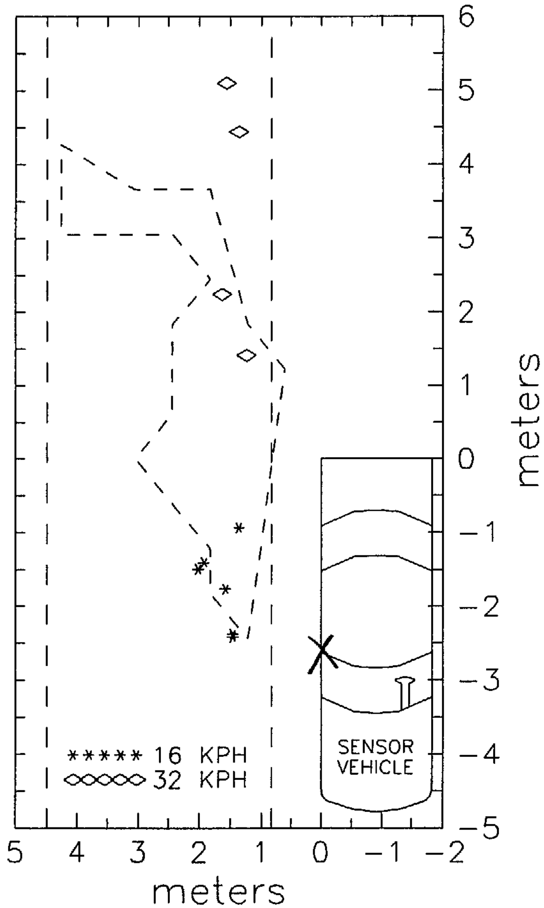

Figure 6.7-9: System "G" Approach and Pass Test Results

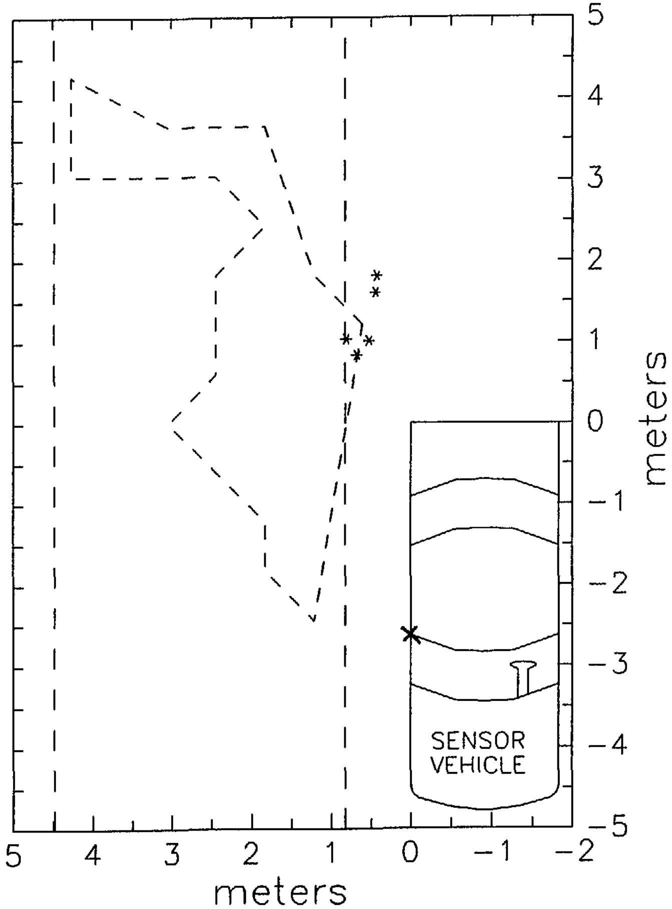

Figure 6.7-10: System "G" Three Lane Test Results

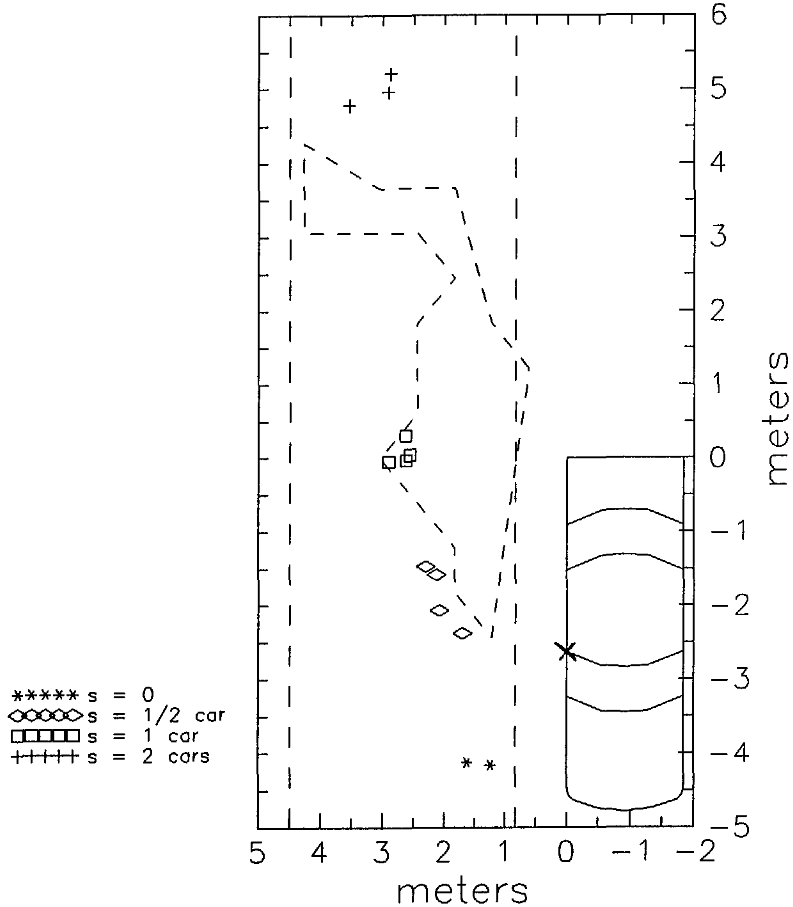

Three Lane Tests

A series of seventeen three lane maneuvers was performed to understand the potential for vehicles in a non-interfering lane to trigger a false alarm. In these tests, the vehicles are initially separated by an entire lane. The target vehicle then maneuvers into the adjacent lane at nose-to-nose separation distances of 0, 1/2 1, 2, and 3 car lengths. The sensor vehicle speed was maintained at 64.4 KPH. The number of passes that were made at the various separation distances are as follows:

Number of Passes	Separation Distance, s	System Reaction
3	0 (nose-to-nose)	YES (2 out of 3)
4	1/2 car length	YES
4	1 car length	YES
3	2 car lengths	YES
3	3 car lengths	NO

Note that the system did not react to a vehicle maneuver occurring 3 car lengths behind the host vehicle.

Figure 6.7-10 summarizes the results of this test. The data collected indicates that detections were observed farther forward than suggested by the static pattern and slightly further back. Otherwise the data is consistent with the measured static pattern.

Merge Tests

In order to evaluate the system's utility during merging situations, the angle of approach of the target vehicle was varied from 0^0 to 15^0 to 32^0. The sensor vehicle was stationary and the target vehicle was driven past at speeds of 32.2, 48.3, and 64.4 KPH. The tests conducted with an angle of approach of 32^0 failed to yield any response from the system despite the speed of the target vehicle. Test results for the 0^0 merge tests are summarized in Figure 6.7-11 (a). All data has been referenced to post P1 on the target vehicle and has been plotted as a function of target vehicle speed. No system detects were observed at a target vehicle speed of 64.4 KPH. The data shows a clear dependence on vehicle speed. Measured system latency suggests that there should be between 1.2 and 2.9 m between a cluster of data collected at 32 KPH and one collected at 48 KPH (a relative difference of 16 KPH). With the exception of two data points take an 48 KPH which appear towards the front of the sensor vehicle, the average difference between the two sets of data is roughly 2m. The two data points that appear outside this range represent "late" detects.

Figure 6.7-11: System "G" Merge Test Results

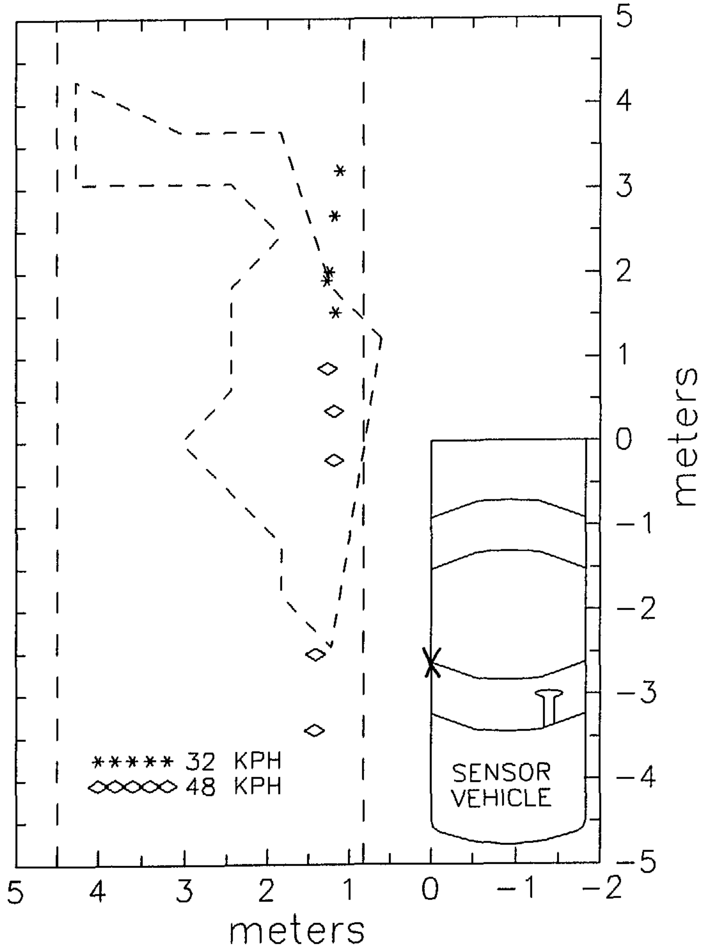

(a) 0° Angle of Approach

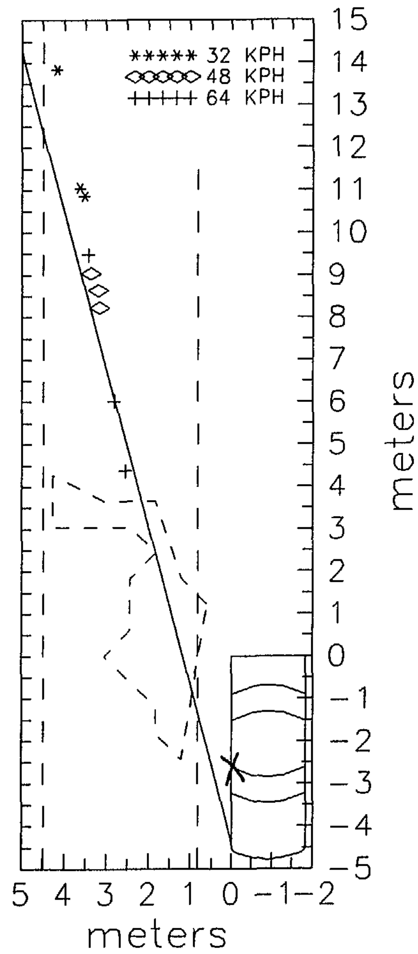

(a) 15° Angle of Approach

The results for the 15^{o} merge tests are presented in Figure 6.7-11 (b). A solid line indicating the angle of approach has been added to illustrate the path of the target vehicle's approach. As the angle of approach is increased from O^{0}, it is apparent that most of the detections occur well beyond the extent of the measured static detection zone. In fact the apparent detection zone extends over twice the range expected from the static measurements. This may be explained in part by the aiming angle of the dual horn configuration of this sensor. This particular trajectory may represent an area in which the antenna patterns overlap, causing a greater probability of detection. However, on the average, each data cluster is separated by about 3 to 4m as suggested by the measured system latency.

Road Test

This system was evaluated under realistic road conditions involving freeway, city, two-lane highway, and parking lot driving. The total exposure time was 31.2 minutes which is about half the average trial time due to an inadvertent data collection error. Statistics were compiled on the number and types of targets detected. The results are summarized in Figure 6.7-12.

Figure 6.7-12: Summary of Road Test Statistics - System 'G"

System: 'G"
Total number of detects: 93

Classification	Freeway	Two-lane	City	Parking Lot	TOTAL
TP	10	0	0	0	10
I	0	4	53	21	78
FP	0	3	1	1	5
TOTAL	10	7	54	22	93
FN	0	0	0	0	0
TN					97.7 %

General Comments:

This system was exposed on the open road for less time than the average system (only 31.23 min) due to an inadvertent data collection error

Five false alarms were triggered

78 inappropriate alarms - most were obstacles (parked vehicles, signs, posts, etc.) which were being passed at low relative speeds

System showed evidence of clutter rejection during city driving in which parked vehicles were passed without a detect

6.8 System "H”

6.8.1 System Description

This system uses microwave radar technology at 10.5GHz to sense objects in the blind spot of the host vehicle. It is a proximity detector that makes no attempt at discriminating between general ground ‘clutter and objects which represent potential collision hazards. The unit includes a display which uses a red indicator light when an object is detected. This blind spot detector was mounted on the right side of the host vehicle towards the rear bumper. The sensor was positioned 34” above the ground.

6.8.2 Overview of System Performance

The unit tested performed was characterized by very short range and narrow static detection zones. In addition, the measured system latency was greater than 1 sec. As a result, the sensor failed to detect targets with closing speeds in excess of 16.1 KPH. Consequently, sensor performance could be classified as poor during the controlled dynamic tests.

During the road test, the long system latency combined with the small static detection zone resulted in a fairly large percentage of missed detects (FN). Most of these, however, occurred during the city and parking lot portions of the road test. Thus, most of the false negatives were parked vehicles which do not pose a collisional threat to the host vehicle. There were two incidents on the freeway in which a missed detection could have resulted in a collision had a lane change been attempted. These misses must be considered serious and will thus limit the utility of the sensor as a lane change aid.

6.8.3 Test Results

Static Tests

Static patterns were measured for the following types of targets:

1) 0.3m x 0.3m foil covered Styrofoam
2) human
3) motorcycle
4) Ford Taurus

The small cross section targets were located at the vertical height of the system.

Figure 6.8-1 summarizes the results of the static tests for this sensor. The static detection zones measured with the 0.3m x 0.3m is compared to a human target in figures (a) and (b). Both targets are characterized by small detection zones which barely extend beyond the rear of the vehicle. The foil target has less than a 2m x 2m detection zone and that of a human target'is barely 1m x 1m.

The static detection zone of both a motorcycle and car are shown in figures (c) and (d). The motorcycle target has been referenced to the front wheel and the Taurus has been referenced to post Pl. Both of these larger, more distributed, targets show an increased detection zone over the "point source" targets. However, the zone of detection tends to be relatively narrow (2 to 2.5m) and does not extend much beyond the rear of the host vehicle.

Vertical Extent

The vertical extent of the static pattern was determined by placing a target at a distance, D, from the sensor and measuring the system response as a function of vertical position. Figure 6.8-2 summarizes the angular extent of this sensor. The sensor has a total vertical FQV of 11.5^{o} and is angled slightly upward.

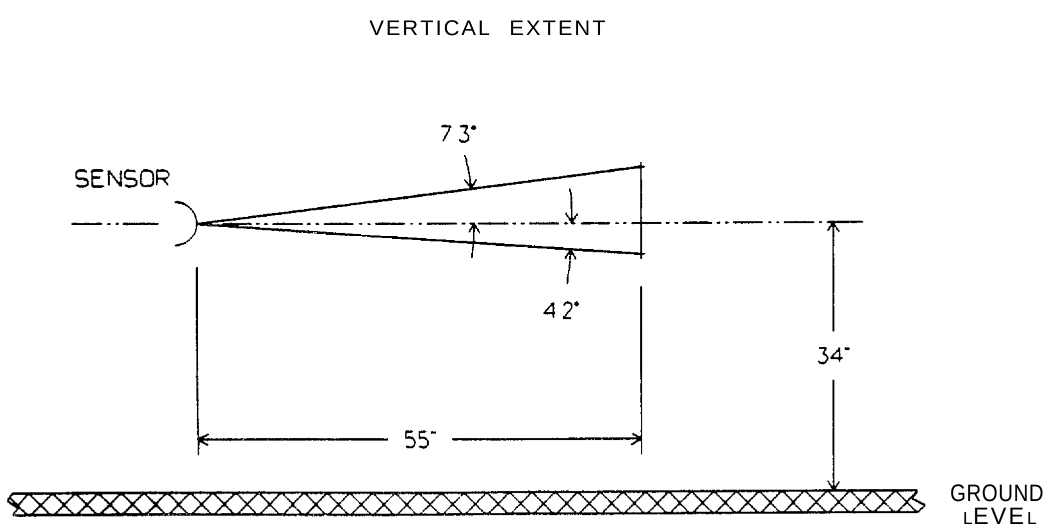

Figure 6.8-2: System 'H" - Vertical Extent

Figure 6.8-1: System "H" Static Test Results

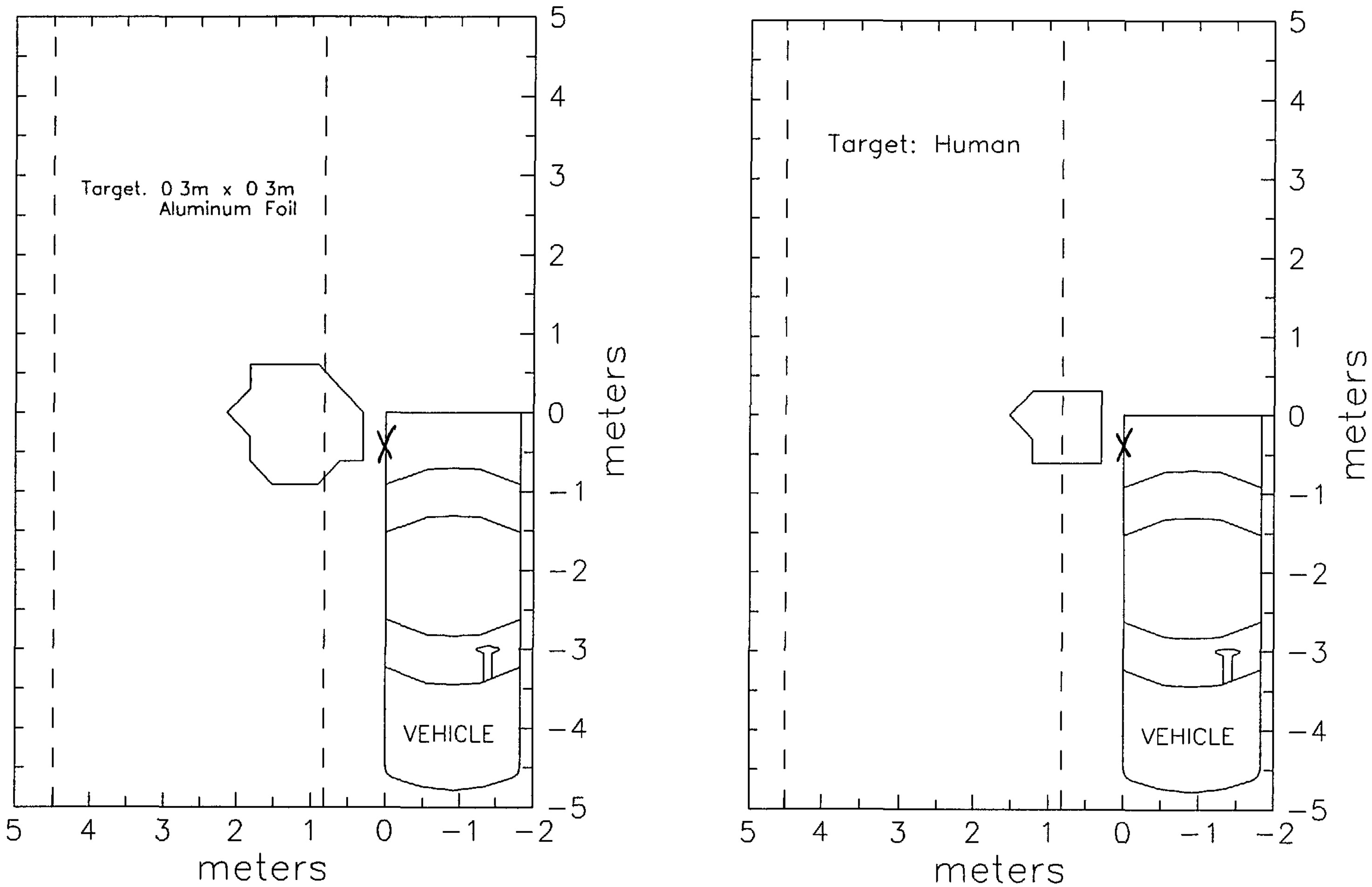

(a) 0.3m x 0.3m Aluminum Foil Target

(b) Human Target

Figure 6.8-1: System "H" Static Test Results (con'd

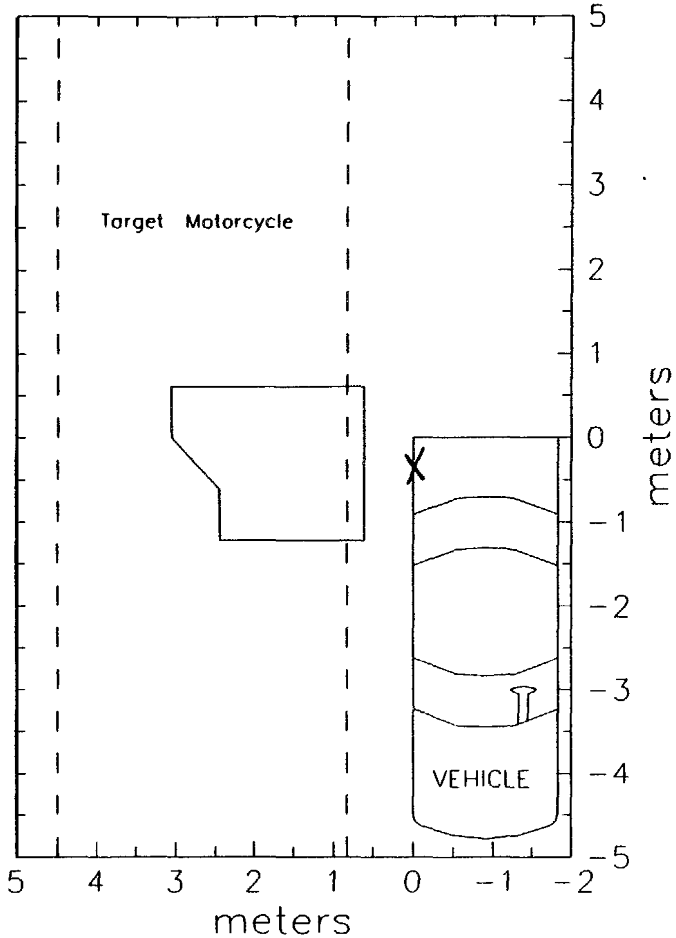

(c) Motorcycle Target

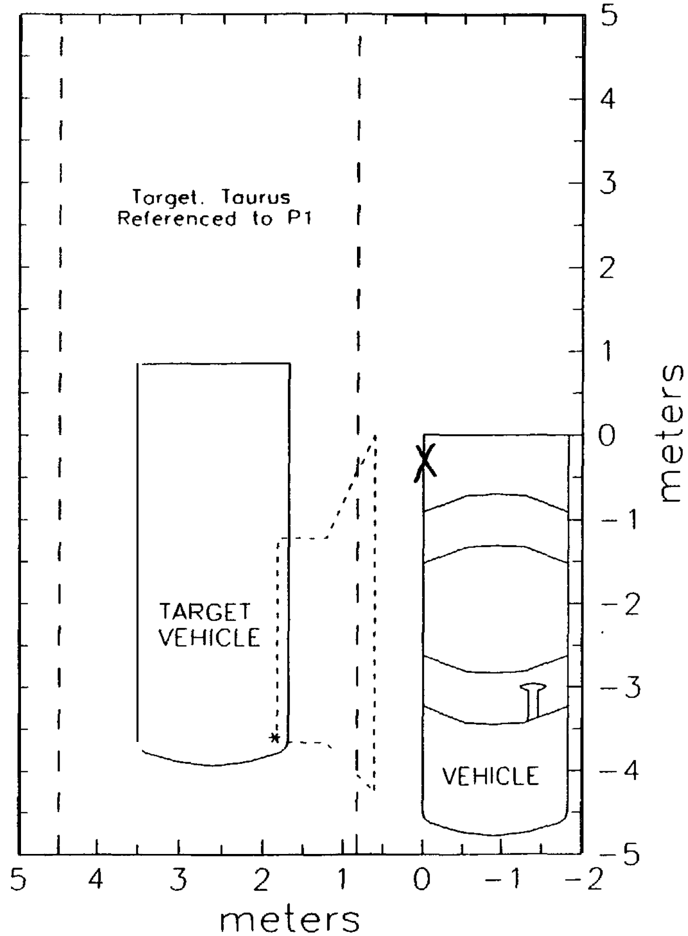

(d) Ford Taurus Target

Dynamic Tests

Perpendicular Delay Time

Perpendicular delay time tests were attempted for this system at vehicle speeds of 1.6, 8, 16.1, 24.1, 32.2, and 40.2 KPH. However, because of the fact that the static detection zone does not extend appreciably behind the rear of the host vehicle, not a single positive response was observed.

Parallel Delay Time

The results of the parallel delay time tests are presented in Figure 6.8-3. The speed of the approaching target vehicle was varied between 1.6 and 24.1 KPH.

Figure 6.8-3: Parallel Latency Time
System "H"

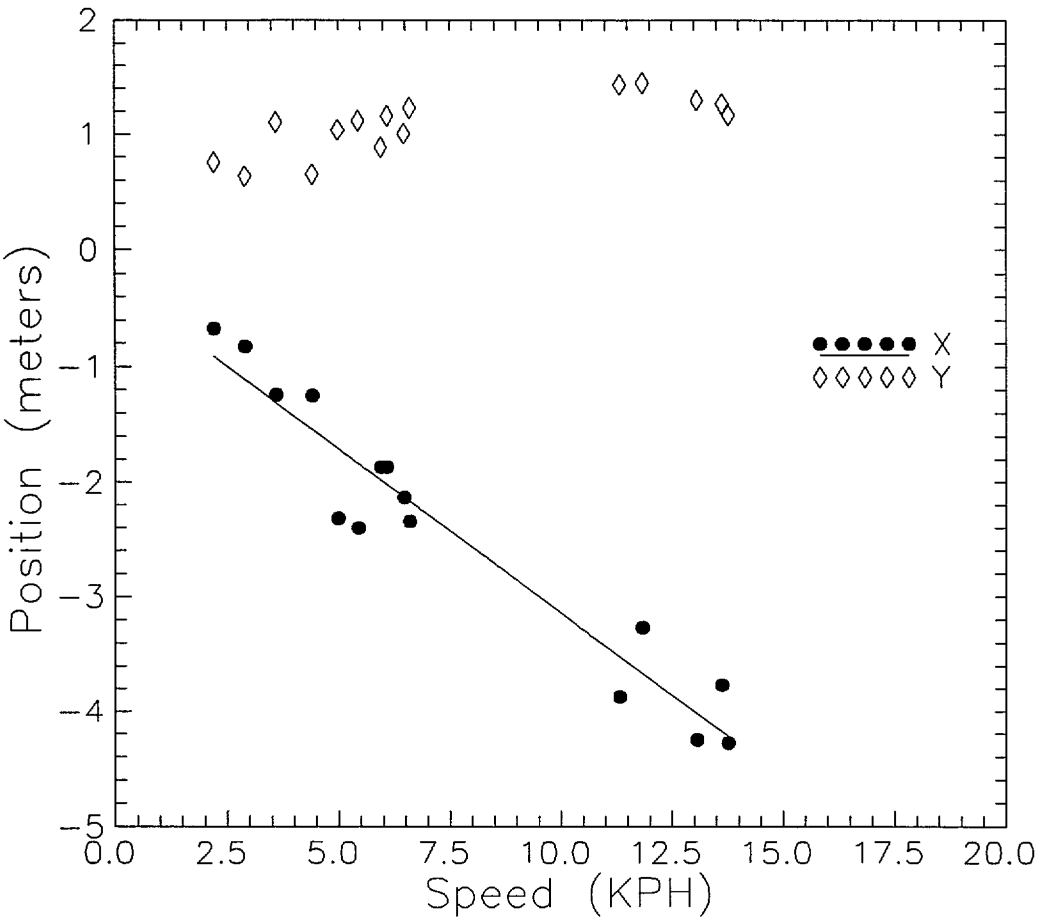

The system, however, failed to react to the approaching target at speeds in excess of 16 KPH.

The lateral separation is shown by the open triangles. The scatter in this parameter is less than 0.5m. The parallel coordinate of the approaching vehicle at the instant the system responds is shown by the filled circles. At these low speeds the scatter is small, less than 0.5m. The parallel latency time computed from this data, however, is quite long at 1.03 sec +/- 20 msec.

Persistence Time

Information on the system persistence has been extracted from the parallel delay time test results. The position of the target vehicle at the instant the system display turns off is' plotted in Figure 6.8-4. This data has been computed from a projection of the car's position based on the trajectory and speed calculated from two earlier reference video frames. All data has been referenced to post P1 on the driver's side of the target vehicle. Typical scatter in the parallel delay time data was +/-0.5m whereas the scatter in this data is as much as flm. Since the position of the target vehicle when the system turns off is far out of the field of view of the video cameras, the errors associated with projecting the data forward will be greater. This suggests that the increased scatter in the data is probably due to inaccuracies in the projection caused by variations in the trajectory and speed of the target vehicle. The latency time associated with system turn-off is 1.8 sec +/- 0.3 sec.

Controlled Passing Tests - Target Vehicle Passing Sensor Vehicle

A series of controlled passing tests was performed on the High Speed Track in which the sensor vehicle was driven at a constant speed and passed on the right by the target vehicle. The vehicle speeds for this test were:

Sensor Vehicle Speed (KPH)	Target Vehicle Speed (KPH)	Closing Velocity (KPH)	Number of Passes
56.3	64.4	8	4(4)
64.4	72.4	8	6(6)
80.4	88.5	8	6(6)
80.4	96.5	16.1	1(6)
96.5	104.6	8	5(6)

The numbers in parenthesis indicate the total number of passes made. For instance, the notation 5(6) means that five out of six passes resulted in a detection.

Figure 6.8-4: System Persistence Time
System "H"

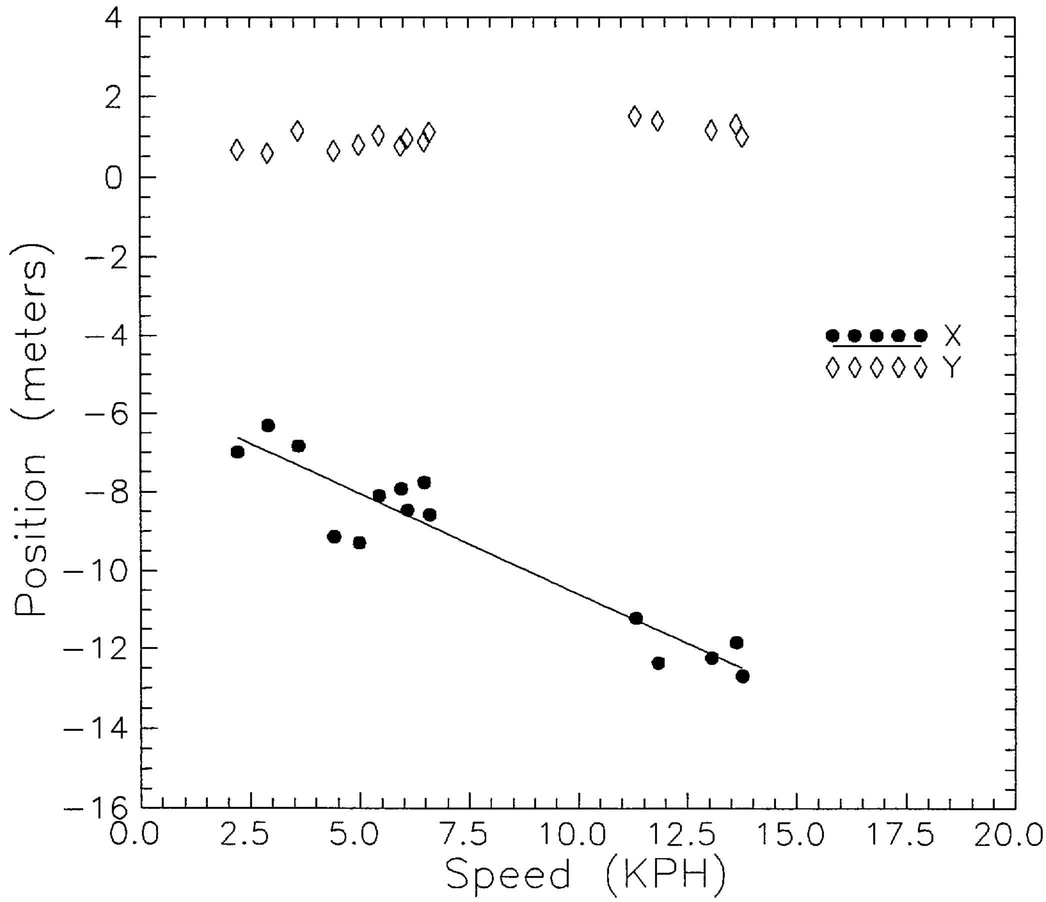

Roughly 30% of these tests were conducted on the curved portion of the High Speed Track. The intent of these tests was twofold: 1) to investigate the system performance as a function of relative speed and correlate the results with the measured system latency and 2) to investigate the effect on system performance when passing occurs on a curved path.

Figure 6.8-5(a) summarizes the target vehicle range at which the system first reacts to the passing vehicle. All results have been referenced to post P1 on the front driver side of the passing vehicle and have been segregated according to the closing velocity of the test. The static detection zone measured with the Ford Taurus target is denoted by the dashed line. Lane markers are identified by the vertical dashed lines. Note that only one data point was collected at a relative vehicle speed of 16.1 KPH. It is also interesting to note that a large fraction of the data lies outside the front boundary of the detection zone. Because this system

Figure 6.8-5: System "H" Controlled Passing Test Results
Target Vehicle Passing Sensor Vehicle

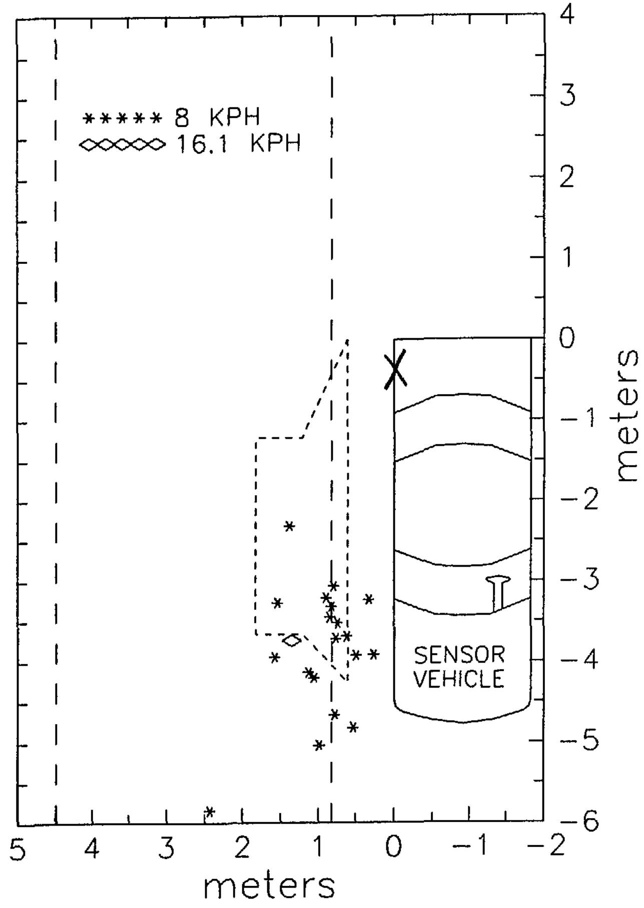

(a) System Performance vs. Relative Speed

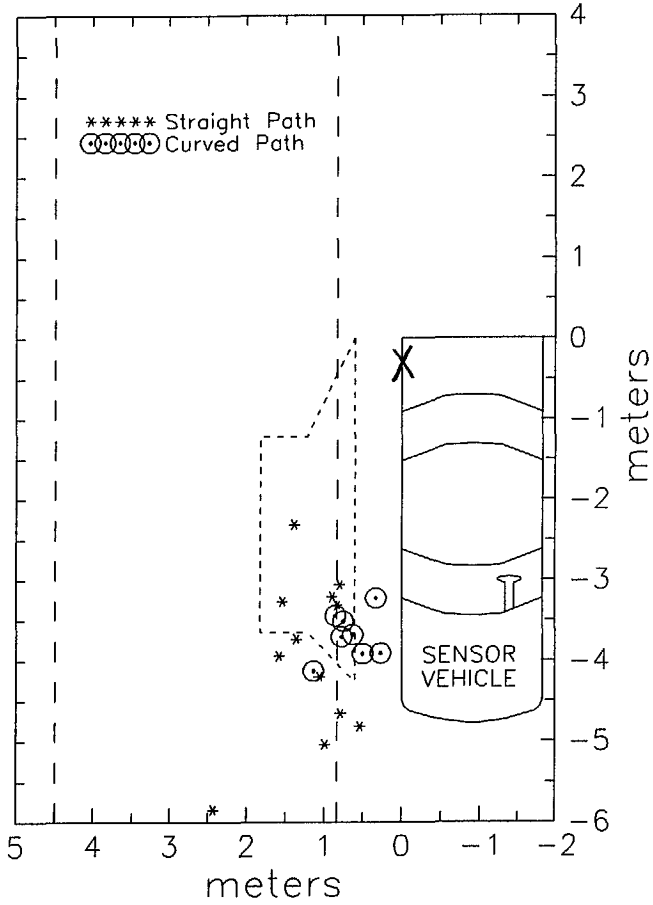

(b) Curved vs. Straight Path

has a latency of about 1 sec the delay can be as much as 2.7 m at 8 KPH and 5.3 m at 16.1 KPH. Thus delays of one half to a full car length can be expected. Several of the data points lie within 0.5 m laterally of the sensor vehicle. These close approach passes were made deliberately in an attempt to cause a positive response from the system.

The effects of a curved path is shown in Figure 6.8-5(b). The data has now been plotted as a function of straight and curved path. The results indicate that the system performance is not affected by the curvature of the host vehicle's trajectory due to the short range nature of the sensor system.

Based on the results of the above tests and the fact that the sensor looks to the side of the host vehicle and not backwards, there was no reason to repeat these passing tests with a clutter vehicle that would be located far behind the static detection zone.

Controlled Passing Tests - Sensor Vehicle Passing Target Vehicle

A series of tests was performed in which the sensor vehicle passes the target vehicle in order to evaluate the system's ability to distinguish between positive and negative closing speeds. A summary of the tests performed is as follows:

Sensor Vehicle Speed (KPH)	Target Vehicle Speed (KPH)	Closing Velocity (KPH)	Number of Passes
72.4	64.4	-8	6
80.4	64.4	-16.1	4(5)
88.5	80.4	-8	6
96.5	80.4	-16.1	5(7)

Once again, the number in parenthesis indicates the total number of passes made. The results are presented in Figure 6.8-6. Consistently, the data collected at the higher closing speed was characterized by a longer delay. System latency can explain delays of up to 5.3 m. This data exhibits a great degree of scatter which represents a real variation in the system performance.

Approach and Pass Tests

A short series of tests was performed to investigate the system's utility in a typical highway passing scenario in which an approaching car in the same lane as the sensor vehicle swerves into an adjacent lane to pass. Six separate maneuvers were made with the sensor vehicle driving at a fixed speed of 64.4 KPH. The

Figure 6.8-6: System "H" Controlled Passing Test Results
Sensor Vehicle Passing Target Vehicle

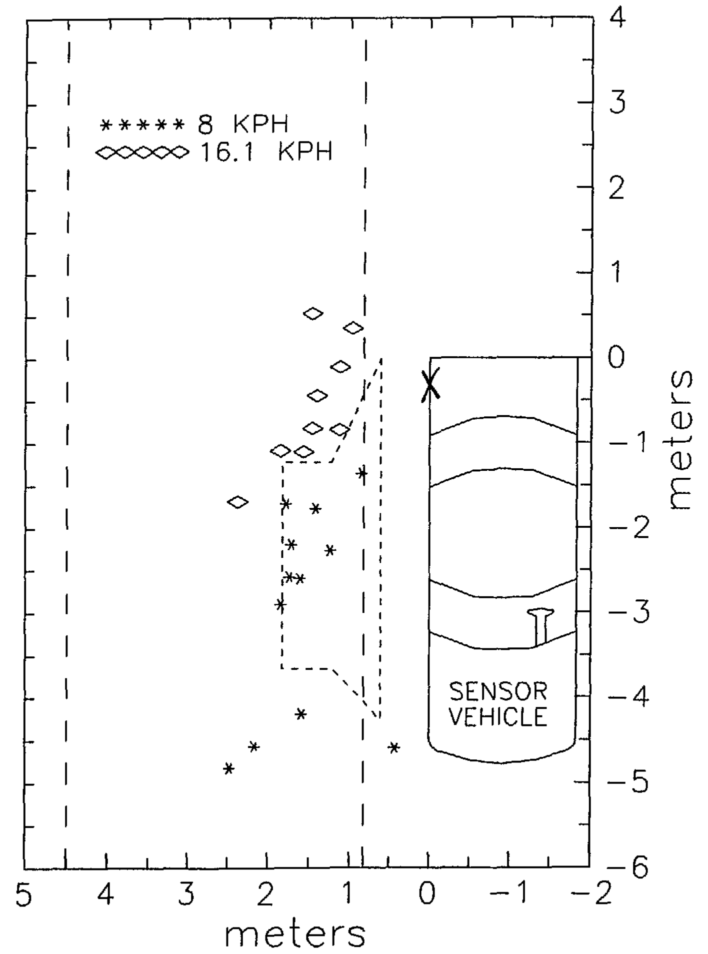

results are summarized in Figure 6.8-7. All data has been referenced to post P1 on the target vehicle. An attempt to pass the sensor vehicle at relative speeds of 8 and 16 KPH was made. No positive system reactions were observed at 16 KPH. In addition, one of the six passes made at a relative speed of 8 KPH failed to set off the system. Similar to the controlled passing tests, the system does not detect the approaching vehicle until that vehicle has almost completely passed through the static detection zone. Once again, system latency can account for a roughly 2.7m delay in the data.

Three Lane Tests

A series of 21 three lane maneuvers was performed to understand the potential for vehicles in a non-interfering lane to trigger a false alarm. These tests were done with the nose-to-nose separation between vehicles varying from 0 to one car length. The number of passes that were made at the various separation distances are as follows:

Number of Passes	Separation Distance, s	System Reaction
7	0 (nose-to-nose)	YES
5	1/2 car length	YES
4	3/4 car length	YES
5	1 car length	YES, 2 of 5

Three of the passes made with the separation distance equal to one car length failed to get a system response. Of the 18 passes remaining, a total of nine (six at s=0, two at s =3/4, and one at s = 1 car length) had only two reference points visible in a single video camera. This is insufficient to get an accurate computation of the range. Therefore, only the nine cases in which sufficient video data (either three points in a single camera or the same point in view in two cameras) have been analyzed. The results are summarized in Figure 6.8-8. Three data points, one with s = 0 and two with s= 1/2 car length, are characterized by a very early turn-on. The target is detected just as the vehicle is initiating its lane change. These data points are real and reflect actual system performance. A probable explanation for this data is that since the antenna pattern essentially points straight out from the sensor vehicle, a car presenting a broadside view to the sensor has a much higher cross section and may therefore be detected at longer range as it move laterally towards the sensor vehicle. Otherwise, the data seems to be fairly consistent with the static patterns measured.

Figure 6.8-7: System "H" Approach and Pass Test Results

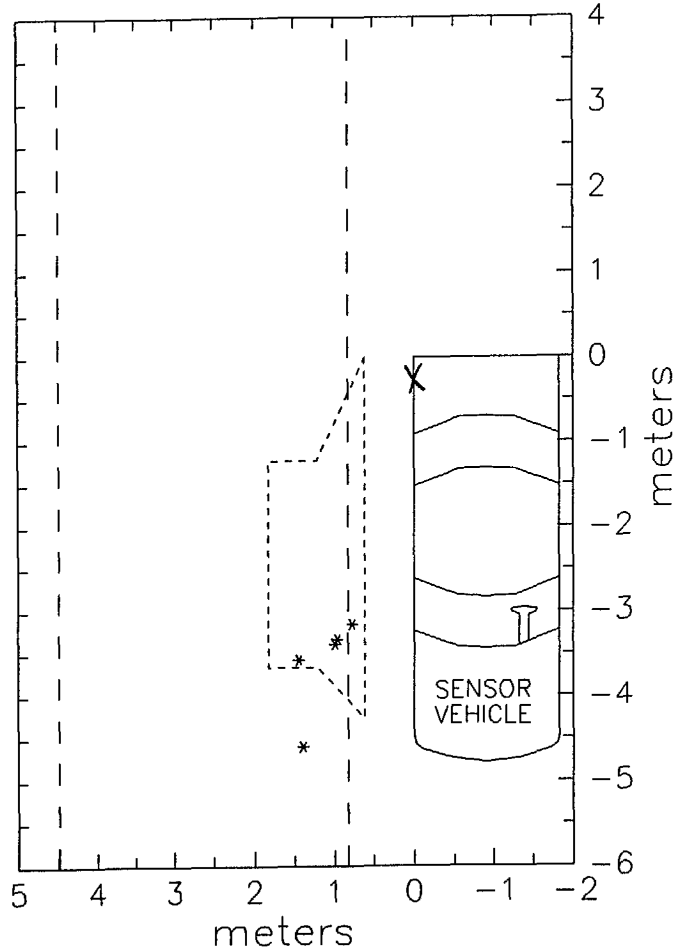

Figure 6.8-8: System "H" Three Lane Test Results

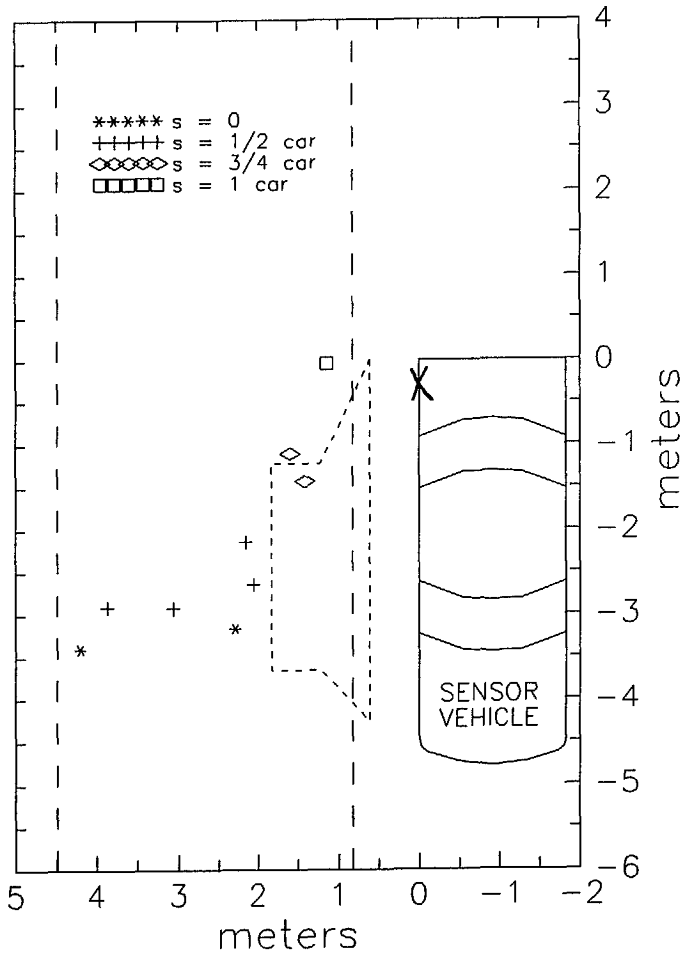

Merge Tests

Since the merge tests are typically performed at relative vehicle speeds in excess of 32.2 KPH and this system has been shown to miss approaching targets with relative speeds of more than 16.1 KPH, the merge tests were not completed for this system.

Road Test

This system was evaluated under realistic road conditions involving freeway, city, two-lane highway, and parking lot driving. The total exposure time was 82.15 minutes. Statistics were compiled on the number and types of targets detected. Figure 6.8-9 summarizes the results.

This system performed poorly during the road tests. There was a total of 6 false alarms and 27 missed detects. Most of these misses occurred at relative velocities exceeding 16 KPH. As demonstrated in the controlled dynamic tests, this system did not respond to any targets with relative speeds greater than 16 KPH. Two of these misses occurred during the freeway driving in which a false negative could increase the potential for a collision if a lane change is attempted.

Figure 6.8-9: Summary of Road Test Statistics - System 'H"

System: 'H" .
Total number of detects: 162

Classification	Freeway	Two-lane	City	Parking Lot	TOTAL
TP	11	3	88	54	156
FP	0	1	0	5	6
TOTAL	11	4	88	59	162
FN	2	0	17	8	27
TN					96.1%

General Comments:

Six false alarms (FP)

27 missed detects (FN)

Most FN occurred at relative velocities exceeding 16 KPH

Blind spot system with no clutter rejection

6.9 System “P”

6.9.1 Overview

System “P” is a solid state video camera, originally designed for use on refuse haulers. The camera is to be mounted at the rear of the vehicle, near the roof. The monitor display is mounted within view of the driver, usually on the dash. The monitor comes with adjustable support that allows it to be tilted and rotated.

For purposes of these tests, the camera was mounted on the roof of the Legend while the monitor was situated on the front dash. The video signal was split in two after the camera with one going to the monitor and the other going to a video cassette recorder. All of the test data was recorded on tape for post test analysis.

6.9.2 Comments

Although cameras with such wide field of views inevitably introduce distortion at the edges, and the contrast compression was severe, in practice during daylight hours the picture was quite good and gave a useful view toward the rear of the car.

6.9.3 Testing

Field of View/Distortion

A 60 cm by 60 cm grid of 2.54 cm squares was held normal to the axis of the camera at a distance of 11 .4 cm. The resulting pattern can be seen in Figure 6.9-1. The recorded video picture shows the expected barrel distortion that comes with a wide angle lens. From this figure we can calculate the field of view by essentially counting the squares vertically and horizontally and by knowing the distance from the camera to the grid. The calculated field of view is 115 degrees horizontally and 87 degrees vertically. This is to be compared to the vendor’s stated values of 123 degrees horizontal and 97 degrees vertical.

Figure 6.9-2 is a plot of the apparent square width (in pixels) versus the pixel number across the screen. Given that a camera with no distortion would yield a horizontal straight line, we can see that the apparent width at the edge shrinks to about 1/3 that at the center for a horizontal line, and 60 % for a vertical line. However if one realizes that the pixels across the screen really measure angular width, then a square in the plane normal to the camera axis but displaced from that axis will subtend a smaller angular width. Thus the apparent width is exactly what one would expect from the cameras perspective.

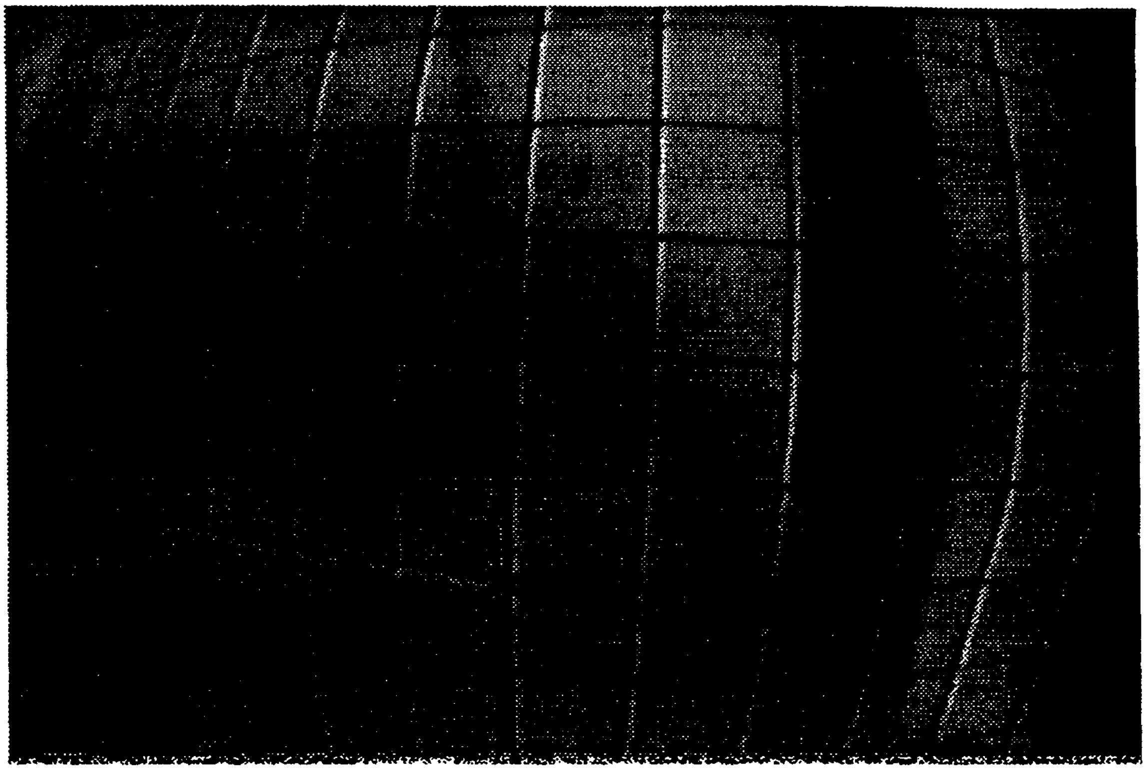

Figure 6.9-1 System P View of Grid at 11.4 cm

<u>Resolution</u>

The data collected using the NBS chart was not viable by itself because it was positioned too far away to be useful, so another set of lines were hand drawn with a spatial frequency of .16 line pairs/mm. These were held at a distance from the camera of 15 cm and at 30 cm. The resulting data is plotted in Figure 6.9-3 referenced to 15 cm, where the hand drawn lines are equivalent to .31 line pairs/mm. This data was gathered from the video record of the chart. The video frame was digitized, formed into a bit map, and the intensity is plotted as a function of pixel number. Given the limited amount of data for this camera, we have plotted in Fig. 6.9-4 the change in intensity from black line to white line as a function of spatial frequency. Defining the resolution as the spatial frequency at which the change in intensity drops to one-half its maximum value is equivalent to saying that the camera can resolve two points whose intensity profiles overlap at the one-half point. In this case, the best estimate of angular resolution is .02 radians or 1.2 degrees. Given the sparcity of data, this is a crude estimate.

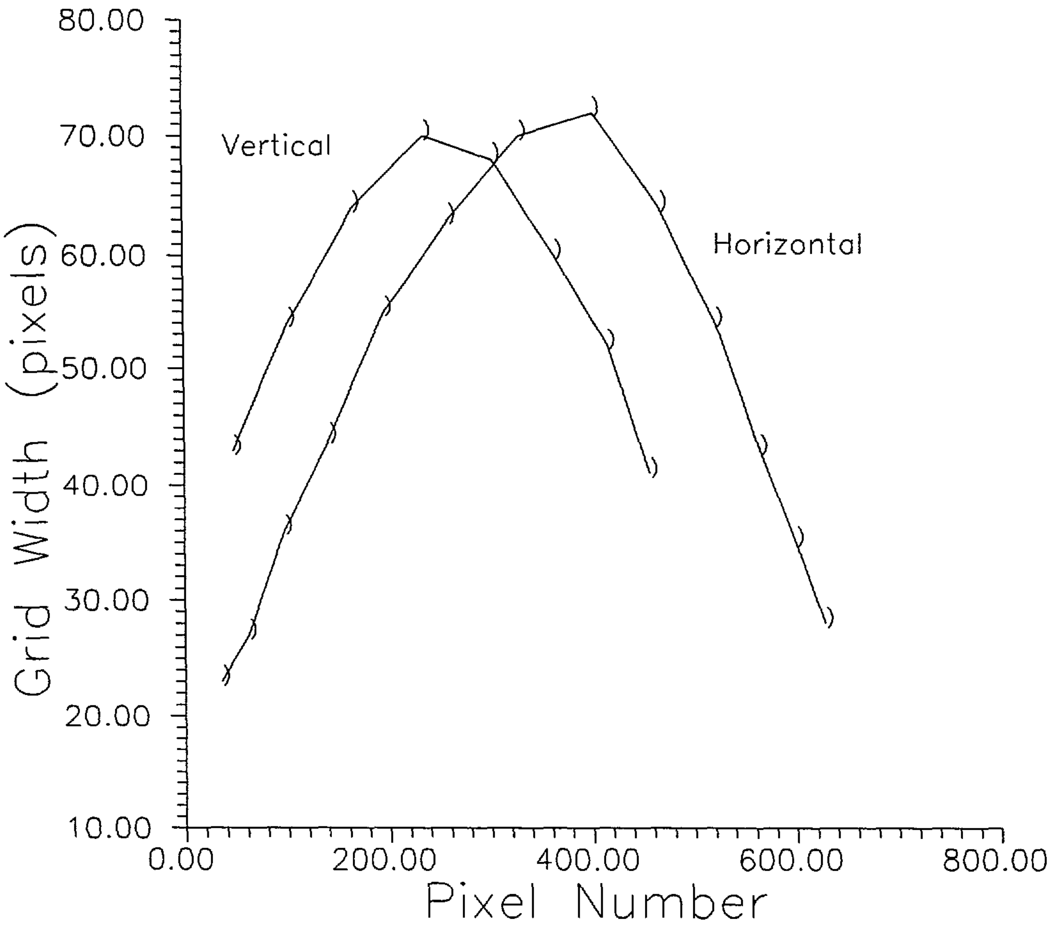

Figure 6.9-2 Apparent Unit Width as a Function of Screen Position

Contrast

The three constructed targets of varying shades of gray turned out to be of insufficient contrast for making quantitative measurements. However the Macbeth color chart contained six shades of gray varying from white to black. Furthermore they were supplied with the manufacturer's reflectance specification. From the reflectance of each color patch a contrast ratio can be calculated between any two shades. These calculated values could be compared to that measured by using a spot meter to get the luminance in candelas / m^2. Doing this in varying light levels, from direct sun to a darkened indoor room yields consistent results for all values of illumination. For the purposes of this report we have defined the contrast ratio as

$$R = (L_W - L_G) / L_G$$

where L_W is the luminance of the white square and L_G is the luminance of any of the other gray squares. The results are summarized in Table 6.9-1.

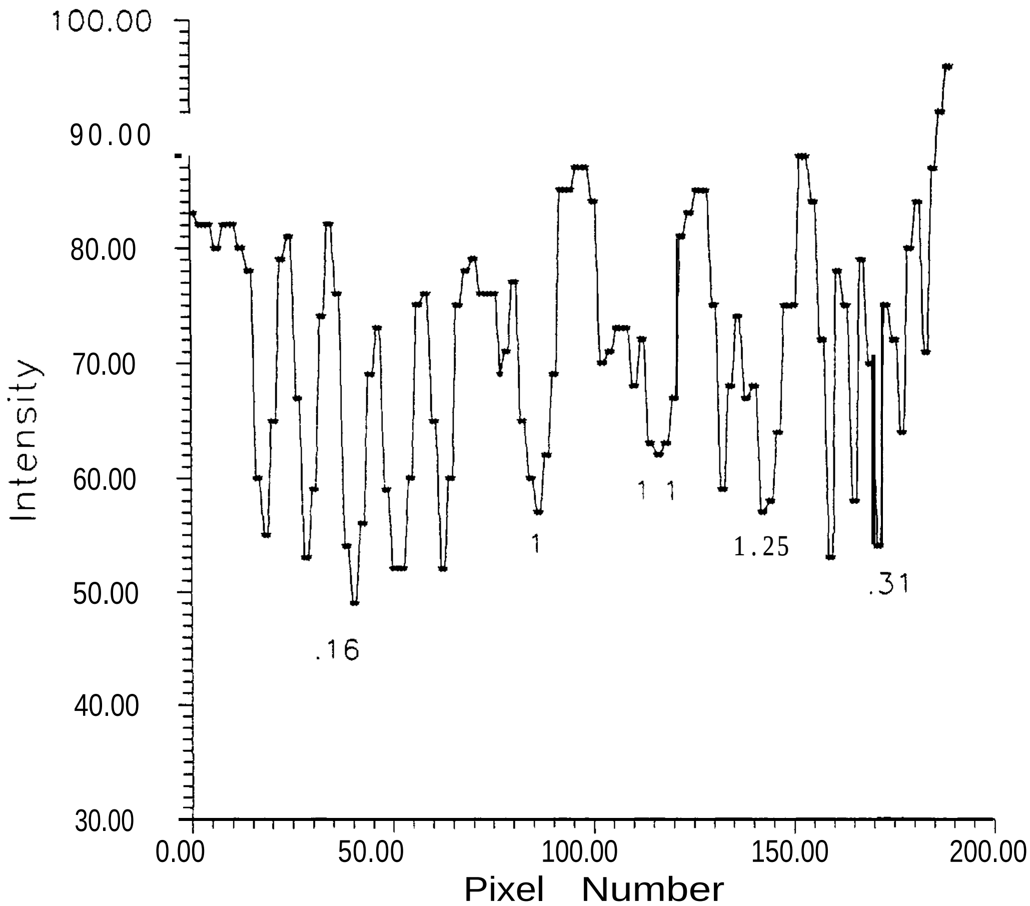

Figure 6.9-3 NBS Chart intensity Profile

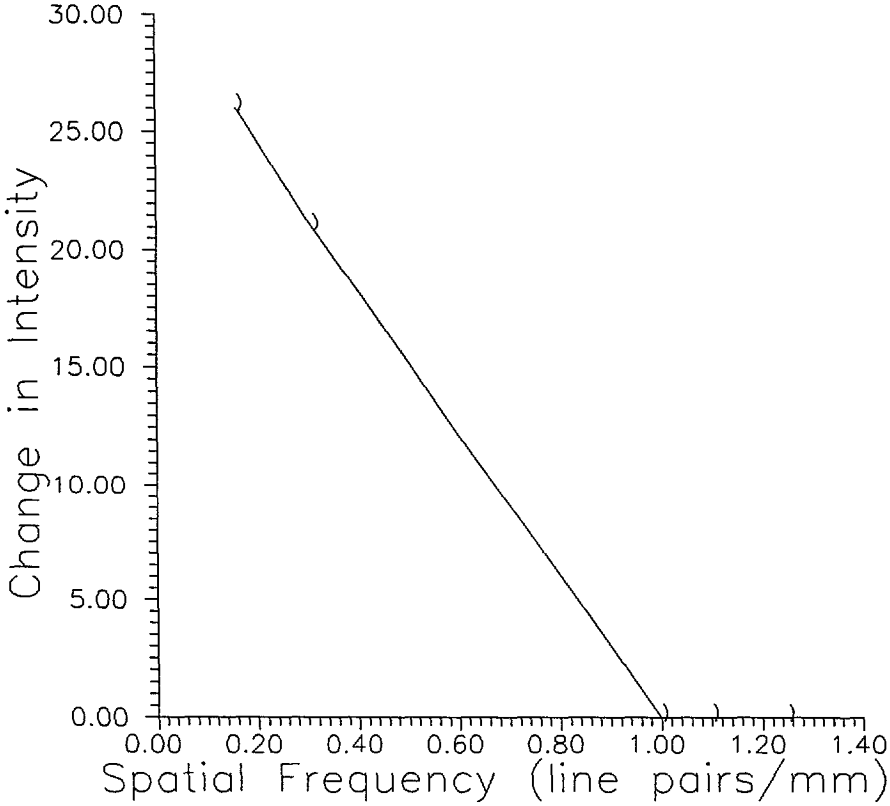

Figure 6.9-4 Resolution Capability as a Function of Spatial Frequency

Shade	Calc. Value	Measure Value	Measured from Monitor		Measured from Tape	
			w/ filter	w/o filter	w/ filter	w/o filter
White						
Neutral 8	.52	.53	.06	.03	.08	.12
Neut. 6.5	1.49	1.46	.09	.11	.32	.32
Neut. 5	3.55	3.33	.45	.31	.73	.74
Neut. 3.5	9.0	7.29	1.11	.89	1.71	1.61
Black	28	21	1.82	1.19	2.8	2.48

Table 6.9-1: Contrast Values for System "P"

This table contains much information. First the calculated and measured values of the direct target contrast are relatively close, with the slight exception of the two largest values. Second, and most important, the contrast values as measured on the monitor are much lower than that measured on the target itself. Reductions are on the order of a factor of 10. Calculating the contrast ratios from the intensity values stored on the video tape, we see that most of the contrast compression occurred at the camera. There is perhaps a factor of two difference between the value after the camera and the value measured on the monitor. The difference between these two values is not unreasonable when one considers that the luminance as measured by the spotmeter has two sources - the fluorescence of the CRT screen and the reflected background light. The presence of background light serves as a pedestal on top of which is added the screen fluorescence. ,The net effect is a reduction in the contrast ratio. Finally, the presence of the IR filter makes little difference. This also is not surprising since there is bound to be very little reflected IR radiation from a matte target. The only place where the filter might have an effect is in filtering out the IR component from headlights.

A significant finding in the testing of this video system has been the reduction of contrast. However, the driver was able to steer in reverse quite well during daylight hours using this system. Video systems such as this have value as a rear vision enhancement system, although its collision avoidance potential cannot be measured in the same way as the warning type systems.

6.10 System "Q”

6.10.1 Overview

System ‘Q” is a solid state video camera and monitor. The camera is to be mounted at the rear of the vehicle, near the roof. The monitor display should be mounted within view of the driver, usually on the dash. A feature of this system is an acoustic microphone provided for the purpose allowing the driver to be aware of sounds coming from the rear of the vehicle.

For purposes of these tests, the camera was mounted on the roof of the Legend while the monitor was situated on the front dash. The video signal was split in two after the camera with one going to the monitor and the other going to a video cassette recorder. All of the test data was recorded on tape for post test analysis.

6.10.2 Comments

Although cameras with such wide field of views inevitably introduce distortion at the edges, and the contrast compression was severe, in practice during daylight hours the picture was quite good and gave a useful view toward the rear of the car. The human factors experts also found it to be quite useful at night.

6.10.3 Testing

Field of View/Distortion

A 60 cm by 60 cm grid of 2.54 cm squares was held normal to the axis of the camera at a distance of 16.5 cm. The resulting pattern can be seen in Figure 6-10-1. The recorded video picture shows the expected barrel distortion that comes with a wide angle lens. From this figure we can calculate the field of view by essentially counting the squares vertically and horizontally and by knowing the distance from the camera to the grid. The calculated field of view is 103 degrees horizontally and 52 degrees vertically. There was no vendor literature with which to compare these values

Figure 6.10-2 is a plot of the apparent square width (in pixels) versus the pixel number across the screen. Given that a camera with no distortion would yield a horizontal straight line, we can see that the apparent width at the edge shrinks to about 1/2 that at the center for a horizontal line, and 75 % for a vertical line. However if one realizes that the pixels across the screen really measure angular width, then a square in the plane normal to the camera axis but displaced from that axis will subtend a smaller angular width. Thus the apparent width is exactly what one would expect from the cameras perspective.

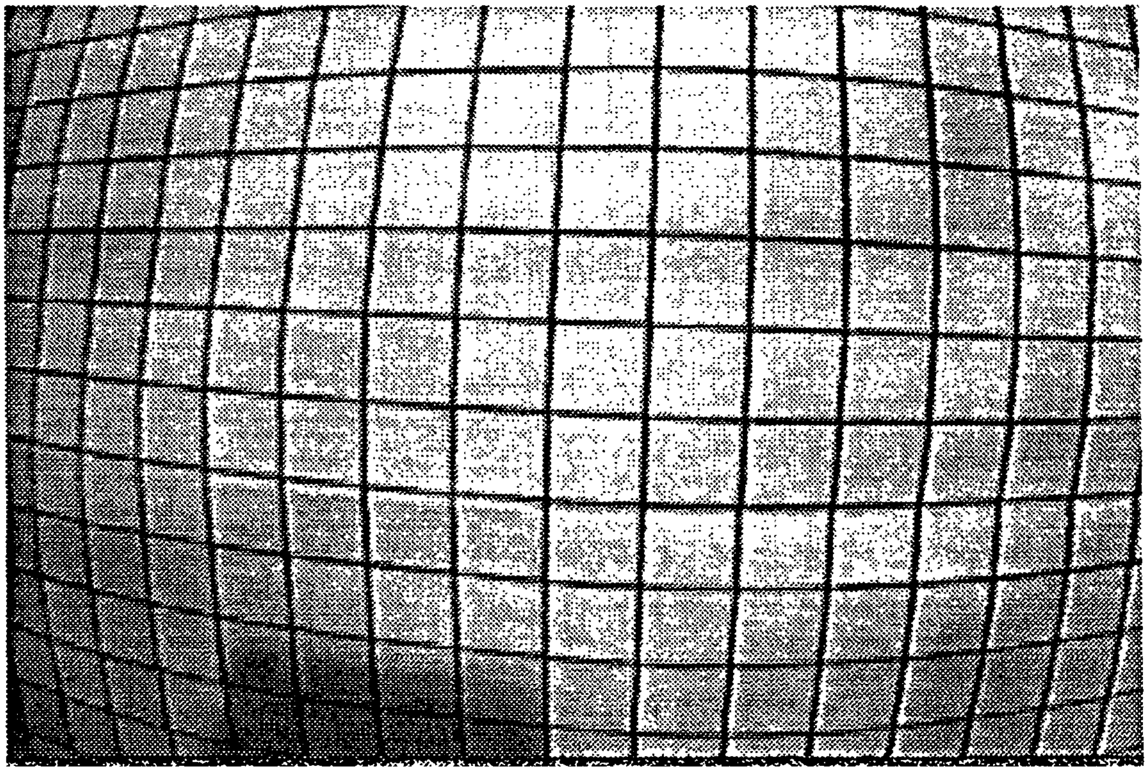

Figure 6.10-1 System Q View of Grid at 16.5 cm

Resolution

Data was collected using the NBS chart. Six groups of lines ranging from 1.0 to 1.6 line pairs/mm were tested. The chart was held at a distance from the camera of 7.5 cm. The resulting data is plotted in Figure 6.10-3. This data was gathered from the video record of the chart. The video frame was digitized, formed into a bit map, and the intensity is plotted as a function of pixel number. Plotted in Figure 6.10-4 is the change in intensity from black line to white line as a function of spatial frequency. Defining the resolution as the spatial frequency at which the change in intensity drops to one-half its maximum value is equivalent to saying that the camera can resolve two points whose intensity profiles overlap at the one-half point. In this case, the best estimate of angular resolution is .0054 radians or .31 degrees.

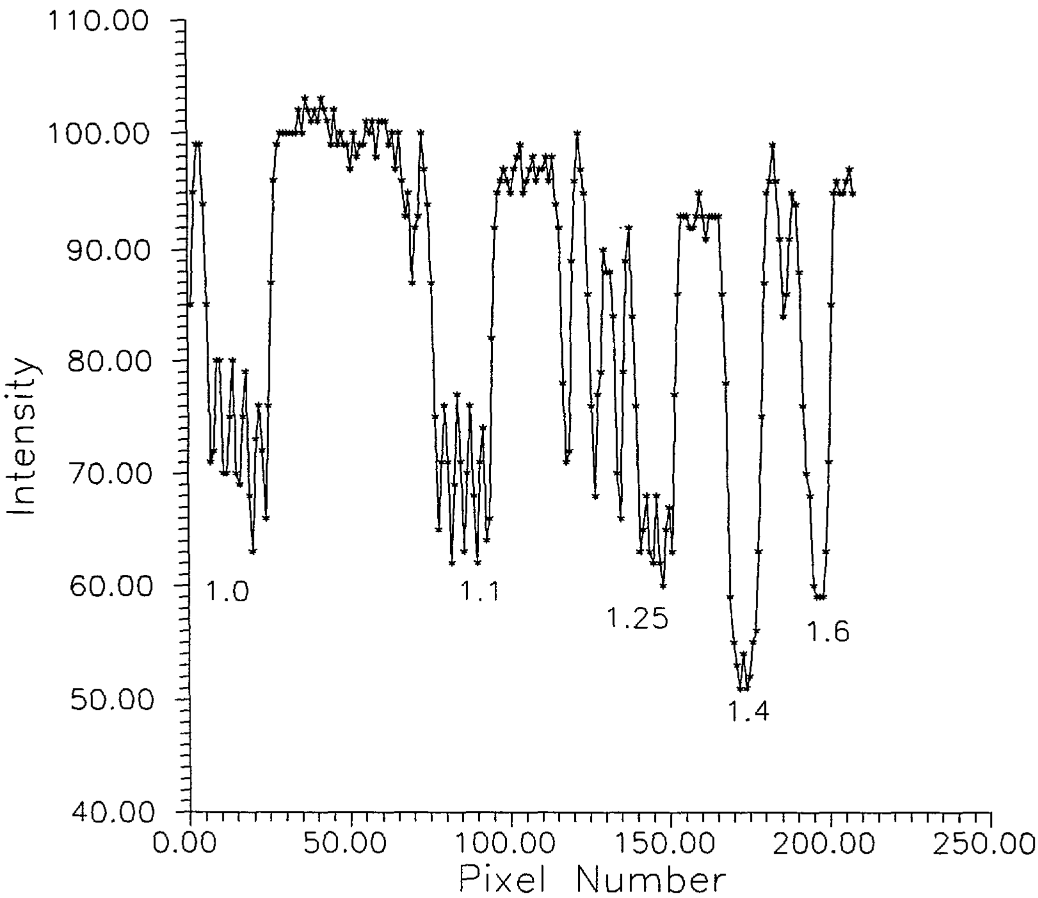

Figure 6.10-2: Apparent Unit Width as a Function of Screen Position

Contrast

The three constructed targets of varying shades of gray turned out to be of insufficient contrast for making quantitative measurements. However the Macbeth color chart contained six shades of gray varying from white to black. Furthermore they were supplied with the manufacturer's reflectance specification. From the reflectance of each color patch a contrast ratio can be calculated between any two shades. These calculated values could be compared to that measured by using a spot meter to get the luminance in candelas / m^2. Doing this in varying light levels, from direct sun to a darkened indoor room yields consistent results for all values of illumination. For the purposes of this report we have defined the contrast ratio as

$$R = (L_W - L_G) / L_G$$

where L_W is the luminance of the white square and L_G is the luminance of any of the other gray squares. The results are summarized in Table 6.10-1.

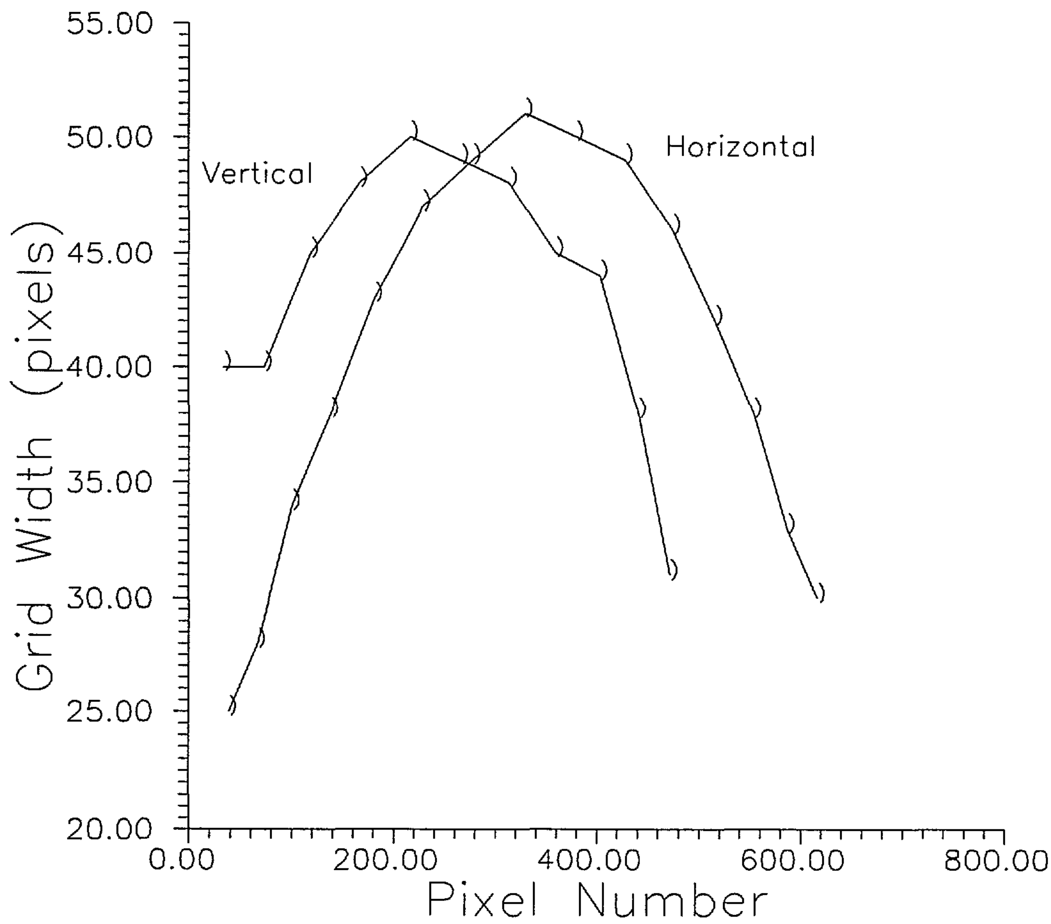

Figure 6.10-3: NBS Chart Intensity Profile

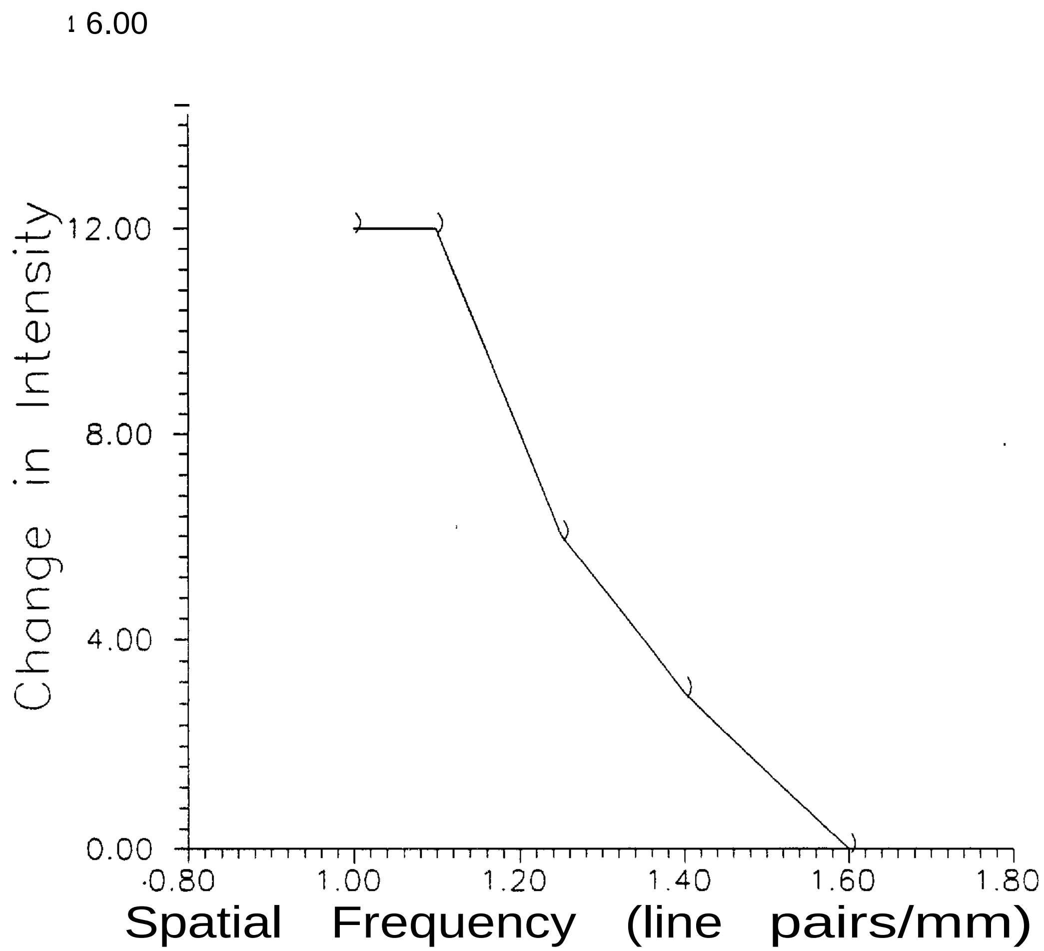

Figure 6.1 O-4: Resolution Capability as a Function of Spatial Frequency

Shade	Calc. Value	Measure Value	Measured from Monitor		Measured from Tape	
			w/ filter	w/o filter	w/ filter	w/o filter
White						
Neutral 8	.52	.53	.04	.04	.13	.11
Neut. 6.5	1.49	1.46	.07	.14	.36	.34
Neut. 5	3.55	3.33	.43	.45	.89	.77
Neut. 3.5	9.0	7.29	1.08	1.15	1.43	1.44
Black	28	21	1.5	1.42	1.96	2.12

Table 6.10-1 : Contrast Values for System Q

This table contains much information. First the calculated and measured values of the direct target contrast are relatively close, with the slight exception of the two largest values. Second, and most important, the contrast values as measured on the monitor are much lower than that measured on the target itself. Reductions are on the order of a factor of 10. Calculating the contrast ratios from the intensity values stored on the video tape, we see that most of the contrast compression occurred at the camera. There is perhaps a factor of two difference between the value after the camera and the value measured on the monitor. The difference between these two values is not unreasonable when one considers that the luminance as measured by the spotmeter has two sources - the fluorescence of the CRT screen and the reflected background light. The presence of background light serves as a pedestal on top of which is added the screen fluorescence. The net effect is to reduce the contrast ratio. Finally the presence of the IR filter makes little difference. This also is not surprising since there is bound to be very little reflected IR radiation from a matte target. The only place where the filter might have an effect is in filtering out the IR component from headlights.

A significant finding of the testing of this video system has been the reduction in contrast. In practice, under a variety of lighting conditions, this system performed well. The driver was able to steer in reverse quite well during daylight hours using this system. Also, testing performed under the human factors part of this program by VRTC was able to determine that illumination by taillights was sufficient for using this system at night. Video systems such as this have value as a-rear vision enhancement system, although its collision avoidance potential cannot by measured in the same way as the warning type systems.

6.11 System 'R"

6.11.1 System Description

This system is a backing system that uses ultrasonic ranging to warn the driver of obstacles located within the rear blind spot of the vehicle. Normally, the system is activated when the vehicle is placed in reverse. The system consists of two sensors mounted just above the rear bumper at a height of lm and placed symmetrically about the longitudinal axis of the car separated by lm. The system will warn the driver with a sequence of audio tones, depending on the distance from the object to the sensors. At the furthest distance the warning is an interrupted series of low frequency tones. At the middle range the pitch is raised. Finally, at the closest ranges, the warning becomes a continuous high pitched tone. It was found that the furthest range was, in fact, split in two as evidenced by an observed change in the repetition frequency of the low pitch tones.

.6.11.2 Overview of System Performance

In most cases, this system performed adequately during both the controlled static and dynamic tests. Operation during cold weather conditions, however, caused a measurable degradation in system performance. During one testing interval in which the outside temperature was between 15^{o} and 20^{o}F, the system required several "warm-up" periods in which the system was brought inside to warm up to temperatures approaching 60-70°F. Otherwise, the system sounded an alarm continuously. In addition, this system was observed to give a false positive indication when triggered by the sound of a truck's air brakes. This system exhibited a large day to day variability. Specifically, it was found that the fourth (farthest) zone would, on occasion, disappear.

During the road test, the unit tested was characterized by a very high rate of false alarms. In fact, the rate of false alarms was so high that the system was rendered practically useless.

6.11.3 Test Results

Static Tests

Static patterns were measured for the following types of targets:

1) 0.3m x 0.3m foil covered Styrofoam
2) human
3) motorcycle
4) Ford Taurus

The foil target was located at the vertical height of the sensor approximately lm above the ground.

The static detection zone measured with the 0.3m x 0.3m target is shown in Figure 6-11-1. The detection zone has been subdivided into four zones according to the range of the target. These are 1) close range, 2) mid range, 3) mid-far range, and 4) far range. The boundary of the detection zone extends backwards from the car a little over 3m and sideways about 0.5m. There is a noticeable blind spot in the center of the vehicle adjacent to the rear bumper. This is due to the fact that two sensors located about 0.6m equidistant from the car centerline are used. When the field of view of both of these sensors are combined, there is an area in the center which may not always be covered, depending on the size, shape, and height of the target.

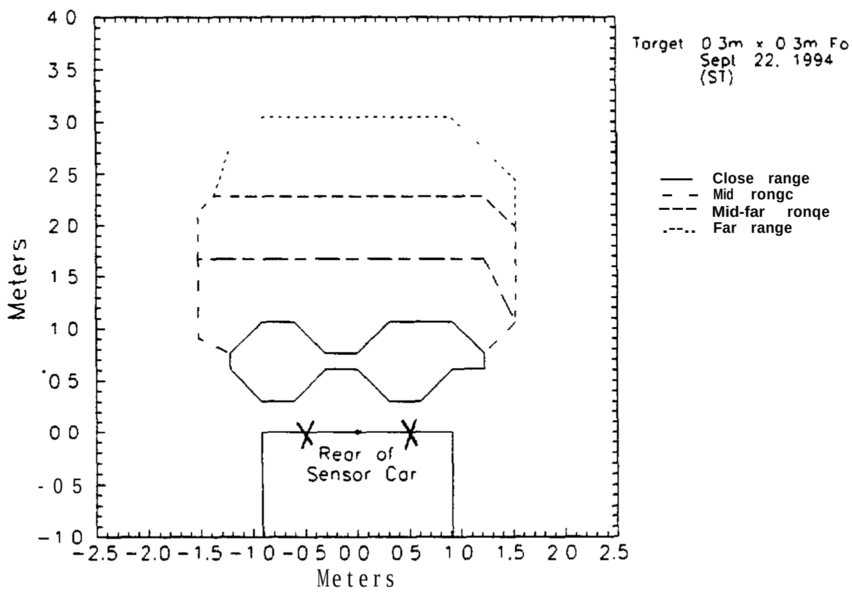

Figure 6.11-1 : Static Test Results - System 'R"
0.3m x 0.3m Foil Target

Figure 6.11-2 shows the static detection zone for a human target. The extent of the pattern is slightly smaller than that seen for the foil target extending less than 2m to the back of the car and about 0.25m to the side.

The measured static detection zone for a motorcycle target is shown in Figure 6.11-3 in which the data has been referenced to the front wheel of the target. This pattern extends approximately 3m behind the host vehicle and shows very little spill-over across the edge of the host vehicle. Because of the larger cross section of the target, the blind spot that was seen with the earlier targets has disappeared.

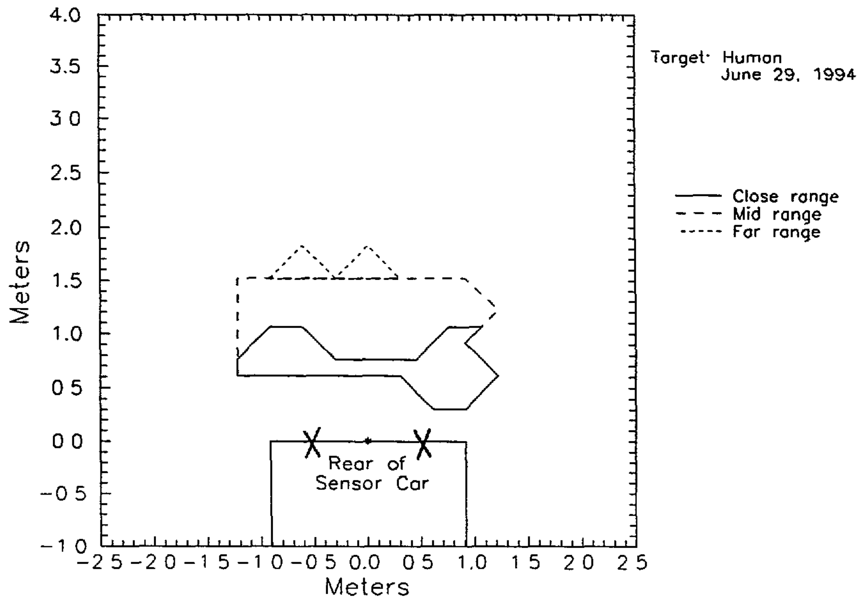

Figure 6.11-2: Static Test Results - System "R"
Human Target

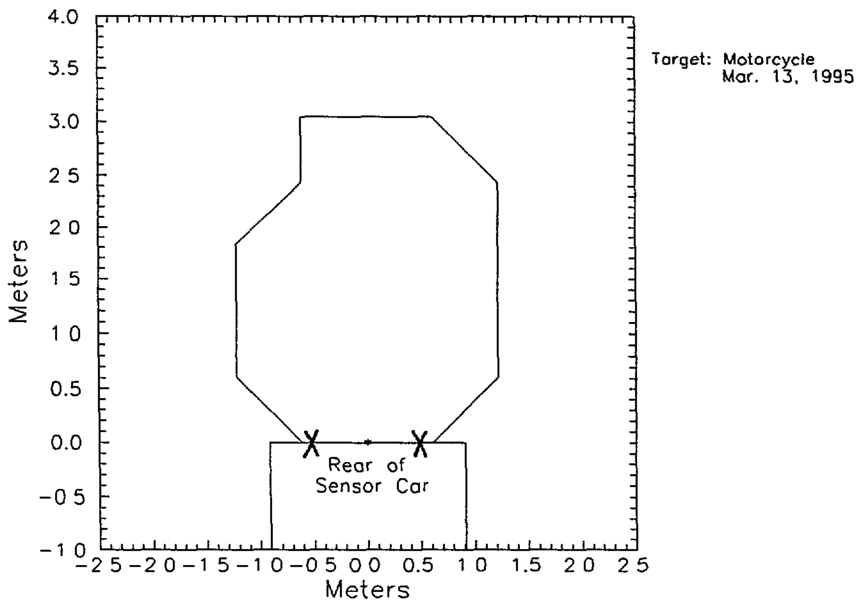

Figure 6.11-3: Static Tests Results - System "R"
Motorcycle Target

The system static response to a Ford Taurus target is shown in Figure 6.11-4. The point of reference on the target vehicle is the center front grill of the car. It appears also that the pattern extends farther off to the side than the other patterns. This is understandable since the target now has a 2m width. This means that the real edges of the zone lie along the edge of the target vehicle which is approximately 1m inside the plotted edge. Another interesting point is that the sensor has a view forward on the passenger side of the sensor vehicle. Again, it must be kept in mind that this edge is referenced from the front and center of the target vehicle. Thus, the system is actually responding to the rear of the target vehicle which is located about five meters up from the edge of this plot.

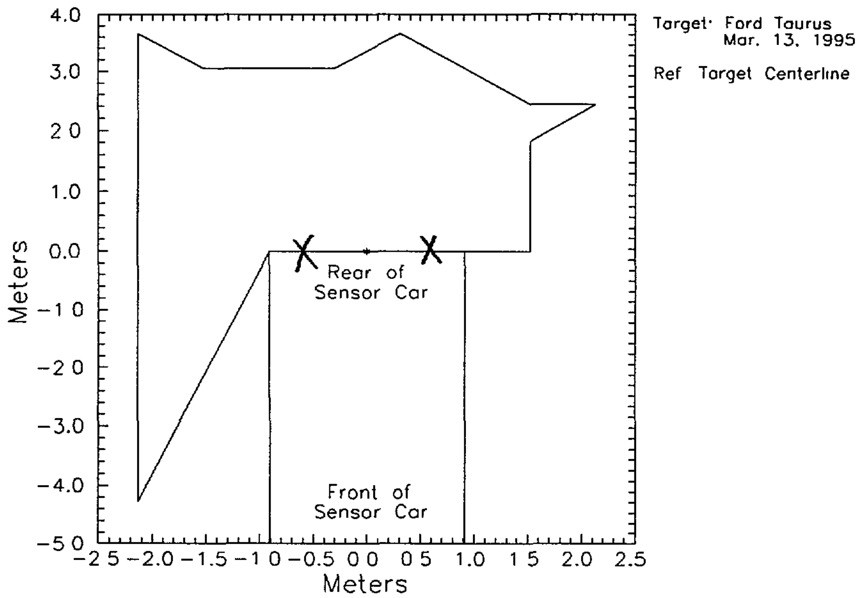

Figure 6.11-4: Static Test Results - System "R"
Ford Taurus Target

Vertical Extent

The vertical extent of the static pattern was determined by placing a target at a distance, D, from the sensor and measuring the system response as a function of vertical position. Figure 6.11-5 summarizes the angular extent of this sensor. The sensor has a total vertical FOV of 46.5° and is angled upward.

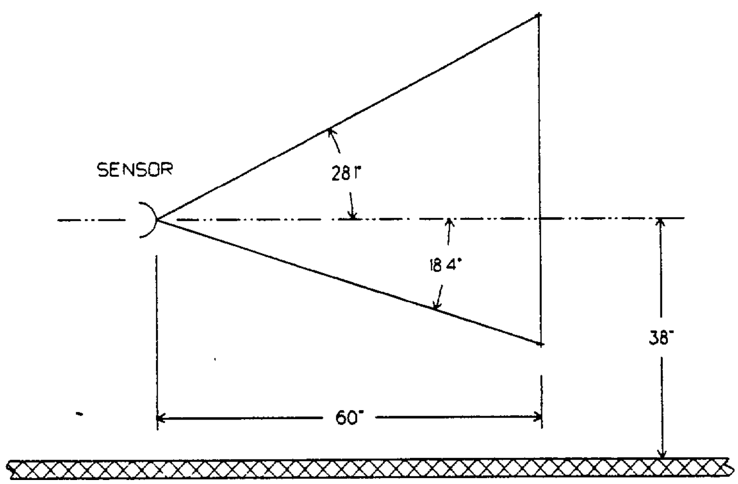

Figure 6.11-5: System “R” - Vertical Extent

Dynamic Tests

Perpendicular Delay Time

Figure 6.11-6 summarizes the results of the perpendicular delay time tests for this system. The target vehicle was driven past the sensor vehicle at speeds of 1.6, 8,16.1, 24.1, 32.2, and 40.2 KPH. Actual speeds, however, have been calculated directly from two reference frames in the video data. All data has been referenced to post P2 on the front passenger side of the target vehicle.

The lateral separation (x) between the two vehicles is denoted by the open triangles. This distance is held to roughly 1.5m +/- 0.5m.

The Y position of the target vehicle at the instant of system reaction is shown by the filled circles. The slope of a linear best fit to the data yields the perpendicular latency time. Understandably, data taken at the higher vehicle speeds shows increased scatter. The perpendicular latency calculated from this data is 0.36 sec +/- 0.15 sec.

Parallel Delay Time

Because this system is a backing system, no data was collected on parallel delay time. Since the field of view extends only to the rear of the host vehicle and not to the sides, the system will not be able to detect a vehicle traveling parallel and to the side of the host vehicle.

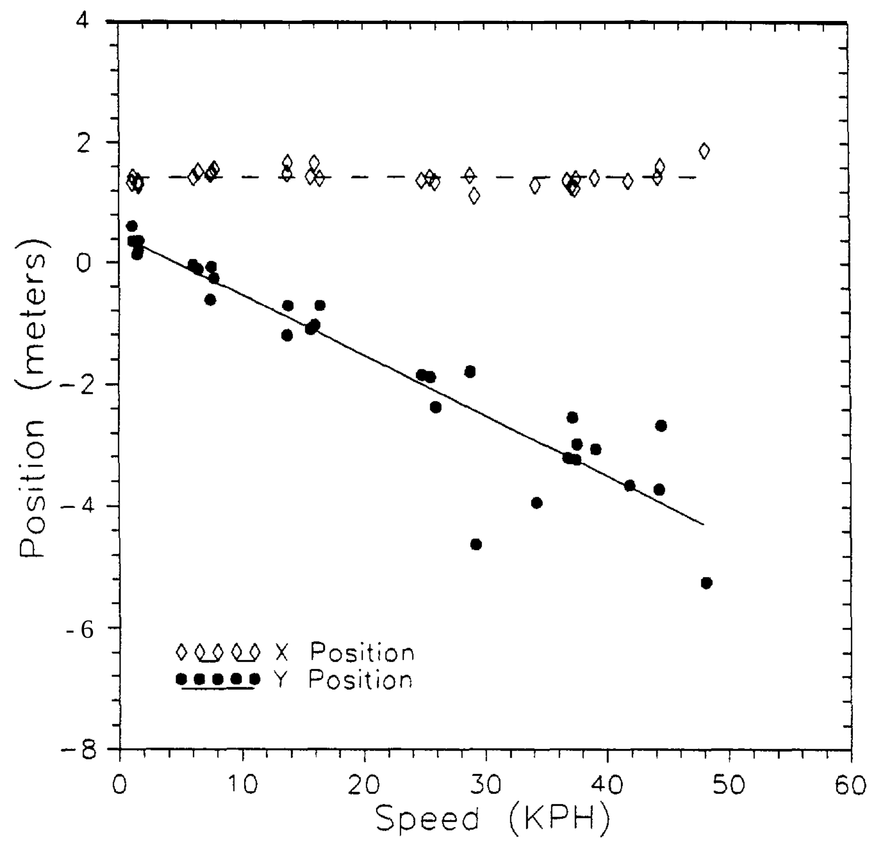

Figure 6.11-6: Perpendicular Latency Time
System 'R"

Persistence Time

Since this is a backing system, information on the system persistence has been extracted from the perpendicular delay time test results. The position of the target vehicle at the instant the system display turns off is plotted in Figure 6.11-7. This data has been computed from a projection of the car's position based on the trajectory and speed calculated from two earlier reference video frames. As before, all data has been referenced to post P2 on the passenger side of the target vehicle.

The system response can be bounded within two distinct slopes as shown. A linear best fit to the entire set of data yields a latency time of 0.52 sec. This value can be bounded by a minimum delay time of 0.17 sec and a maximum delay time of 0.78 sec.

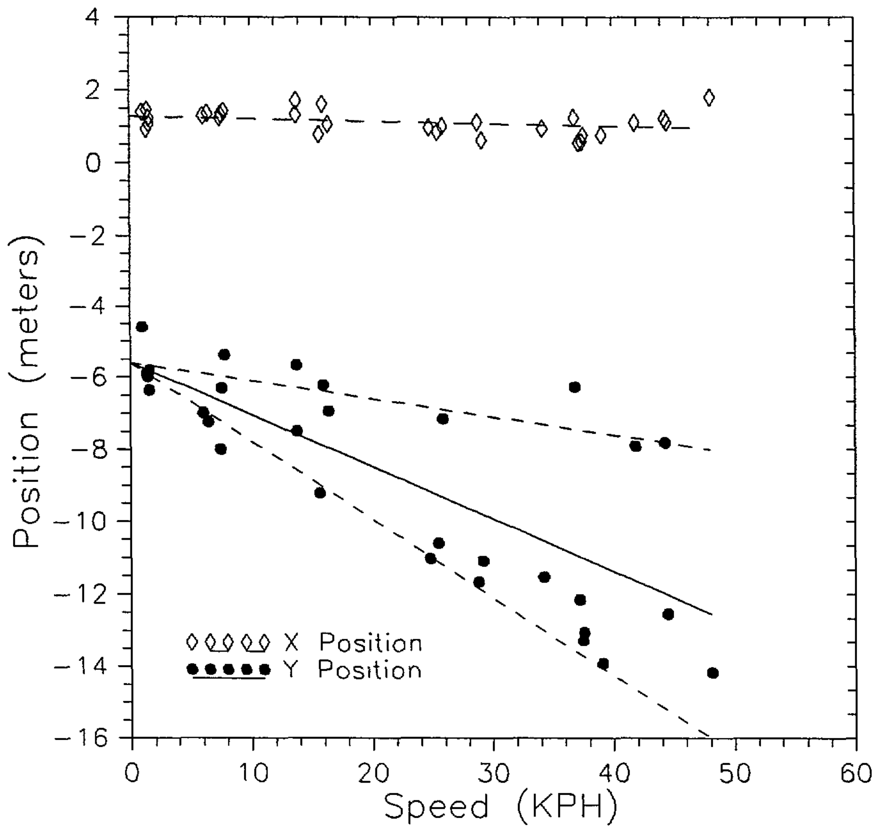

Figure 6.11-7: Persistence Time

Backing Tests - Straight Path

The first test performed with this system involved backing the sensor vehicle straight into various targets. This was done with and without the presence of a clutter vehicle. Three types of targets were evaluated: a 0.3m x 0.3m foil target, a human, and a vehicle. Figure 6.11-8 shows the system response to the foil target in the absence of clutter. System response fell within the farthest zone of the system. The vehicle speed for this backing maneuver was approximately 8 KPH or less. From the measured system latency, this corresponds to a system delay of between 0.47m and 1.13m. Since no data falls more than 0.8m within the outer zone boundary, the data collected is consistent with the static detection pattern and system latency measured.

System response to the human target is shown in Figure 6.11-9. Notice that the system reacts to the target about 0.5m outside the measured static boundary. In fact, the data is more consistent with the static pattern measured with the 0.3m x

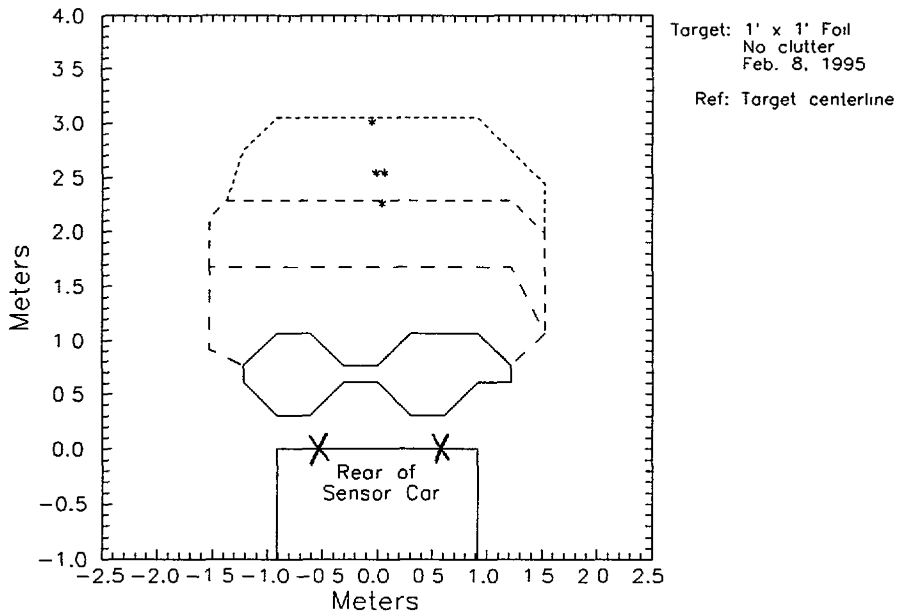

Figure 6-11-8: Backing Tests - Straight Path
0.3m x 0.3m Foil Target

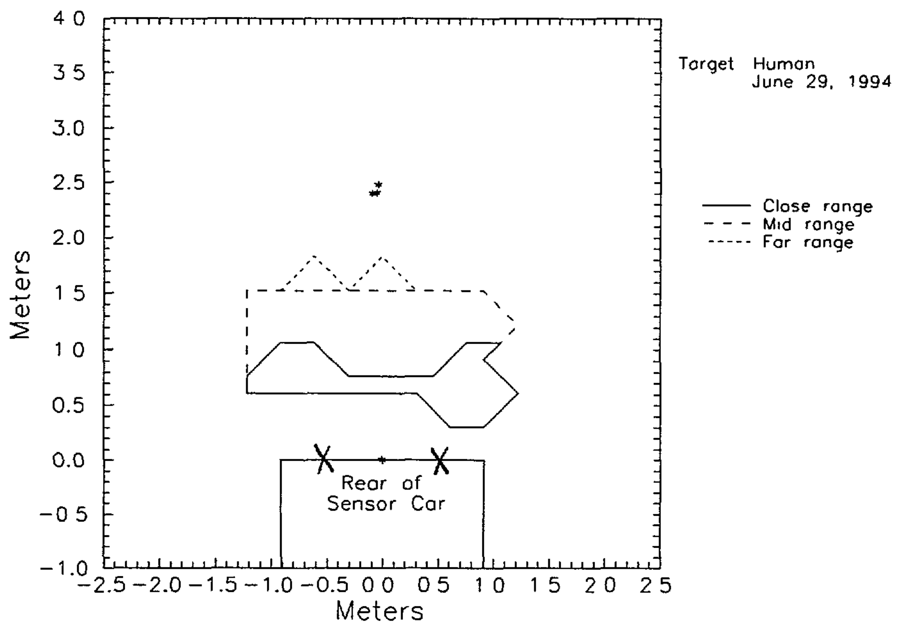

Figure 6.11-9: Backing Tests - Straight Path
Human Target

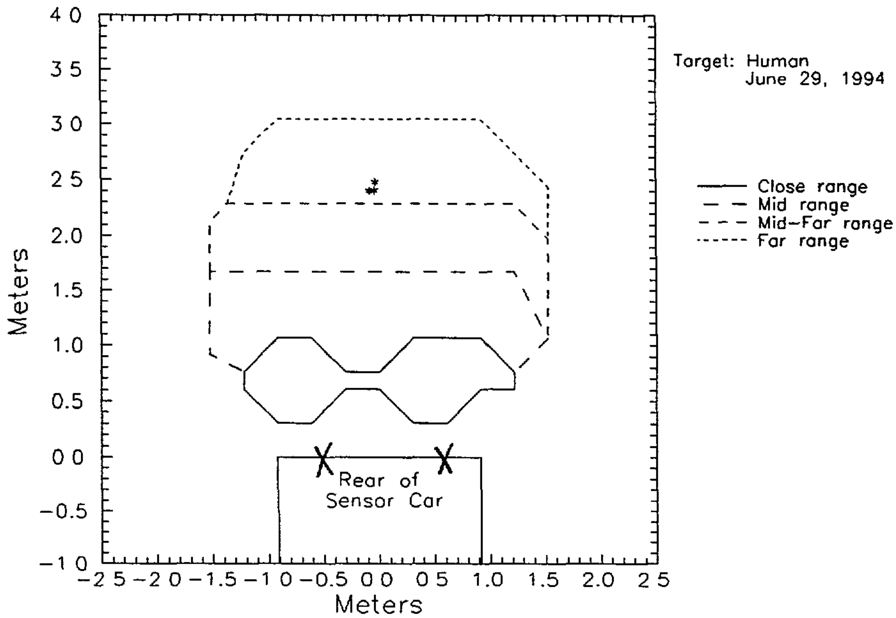

Figure 6.11-10: Backing Tests - Straight Path
Human Target (0.3m x 0.3m Foil Static Pattern)

0.3m foil as shown in Figure 6.11-10. Static patterns for this system were measured by different operators on different days. The static pattern with the human target was measured in June of 1994 and that of the 0.3m x 0.3m foil target in September. The static data collected with the 0.3m x 0.3m foil target is, in general, more consistent with the dynamic measurements. Therefore, the dynamic results have been compared to this static pattern.

This test was repeated a third time with a Ford Taurus. The results are displayed in Figure 6.11-11. The results have been compared to the static pattern measured with the 0.3m x 0.3m target. The results lie on the outer edge of the static detection zone.

For the human and vehicle targets, these straight backing tests were repeated in the presence of a clutter vehicle. Figure 6.12-12 displays the results measured with the human target. The lateral spacing between the human target and the clutter vehicle was fixed at 1.5m while the "nose-to-nose" distance was varied between s =0 (i.e., nose of clutter vehicle is even with the human target) to s = 4.6m (human target standing near rear of clutter vehicle).

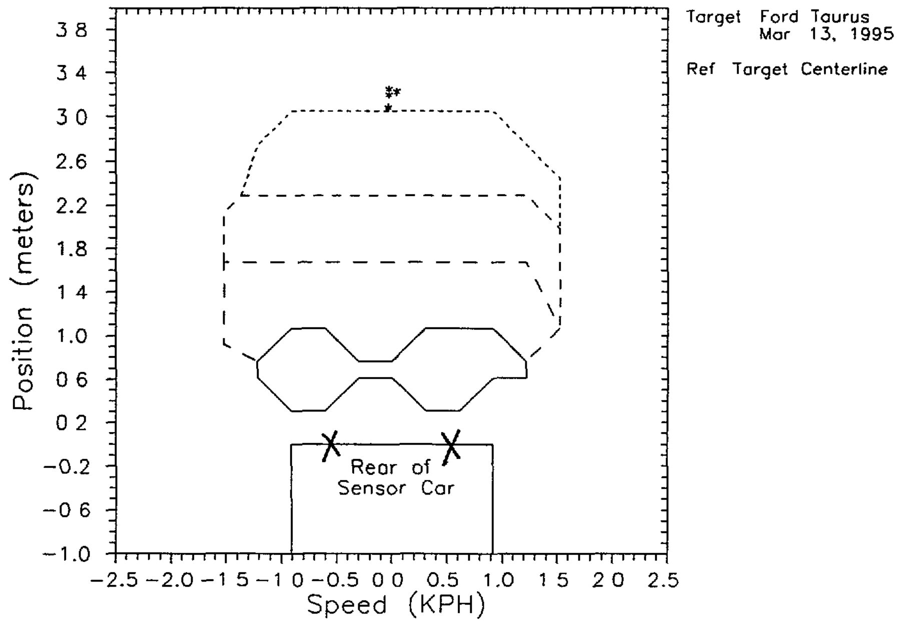

Figure 6.11-11: Backing Tests - Straight Path
Ford Taurus Target (0.3m x 0.3m Foil Static Pattern)

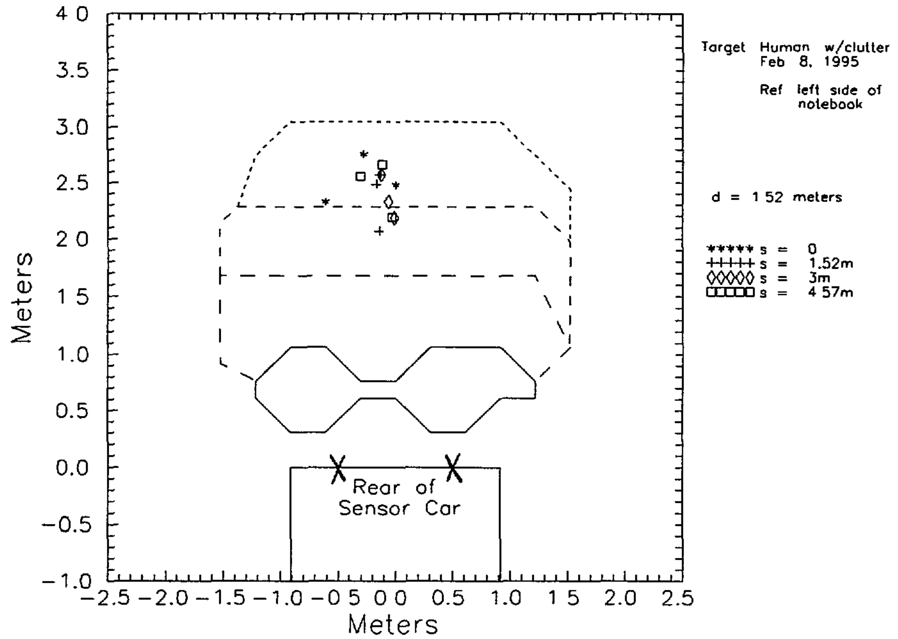

Figure 6.11-12: Backing Tests With Clutter - Straight Path
Human Target

The data has been compared to the static pattern measured with the 0.3m x 0.3m foil target for reasons discussed earlier. Note that the presence of the clutter vehicle does not trigger an early system response. Although there is scatter in the data, overall it is consistent with the measured system latency.

The measurements made with the Ford Taurus target in the presence of a clutter vehicle are shown in Figure 6.11-13. The reference point is once again the center of the front grill of the target vehicle. As with the earlier data, the static pattern shown is that of the 0.3m x 0.3m foil target. Without exception, the repeatability of the data is excellent showing very little scatter. Thus, it is apparent that system performance is not adversely affected by the presence of a clutter vehicle.

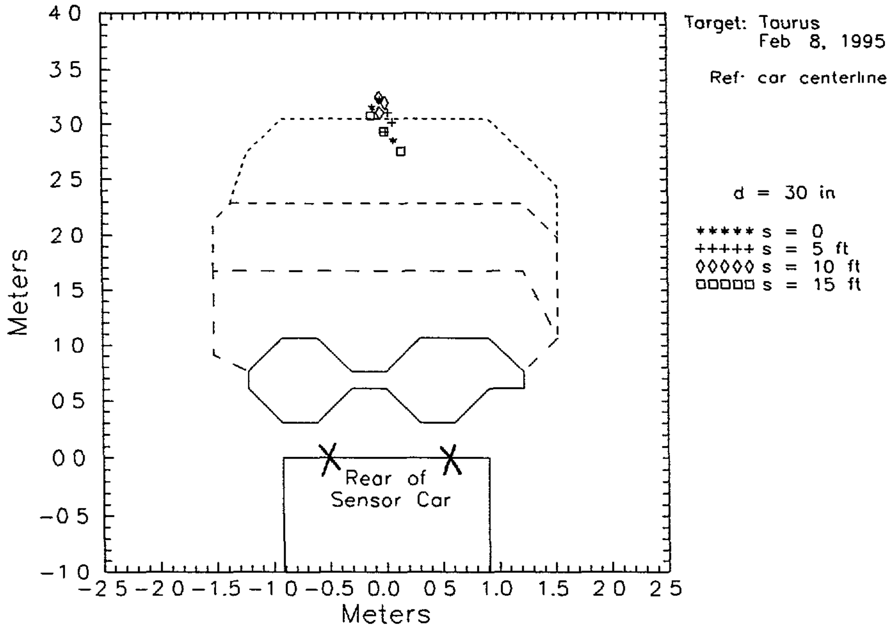

Figure 6.11-13: Backing Tests With Clutter - Straight Path
Ford Taurus Target

Backing Tests - Curved Path

A common backing scenario involves maneuvering along a curved trajectory. The utility of this backing system was tested using two different radius of curvatures, t = 3m and t = 6m. Figure 6.11-14 shows the resulted of backing along a curved path into a human target. The shorter radius of curvature data is represented by the circles and the longer radius of curvature data by the asterisks. With a short turning radius, the detects appear more towards the edge of the static detection zone. All of the data collected is consistent with the 0.3m x 0.3m static pattern measured and the system latency.

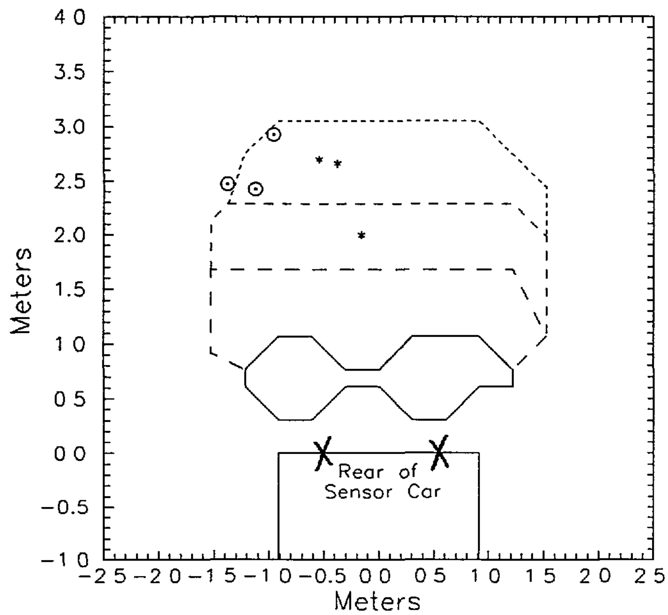

Figure 6.11-14: Backing Tests - Curved Path
Human Target

The system response to a vehicle target is shown in Figure 6.11-15 as a function of the radius of curvature of the sensor car's trajectory. In this case, the reference point on the target vehicle is post P2 on the front passenger side of the car. On a curved trajectory, this point represents the closest point to the sensor vehicle. All of the data collected appears outside the left edge of the static boundary.

These tests were repeated for the tightest radius of curvature with a clutter vehicle positioned next to the target in an attempt to trigger an early response from the system. For the human target, this clutter vehicle was positioned 2m laterally from the target. For these tests the "nose-to-nose" separation was varied between s = -1.5m and s = 6m. The results are presented in Figure 6.11-16. The data has been referenced to the left side of an 8.5" x 11" notebook held in the hands of the human subject. The data collected shows the same magnitude of scatter seen in the previous data. There were no early alarms triggered by the presence of the clutter vehicle.

The data collected with a Ford Taurus target is presented in Figure 6.11-17. Two series of tests were conducted in which the clutter vehicle was placed 1.2m and 2.8m laterally from the target vehicle. Once again, the data has been referenced to post P2 on the target vehicle. The data is characterized by more scatter than is typical of the previous results (t = 3m). Generally, all the data falls outside the left edge of the measured static detection zone. This was true, however, of the

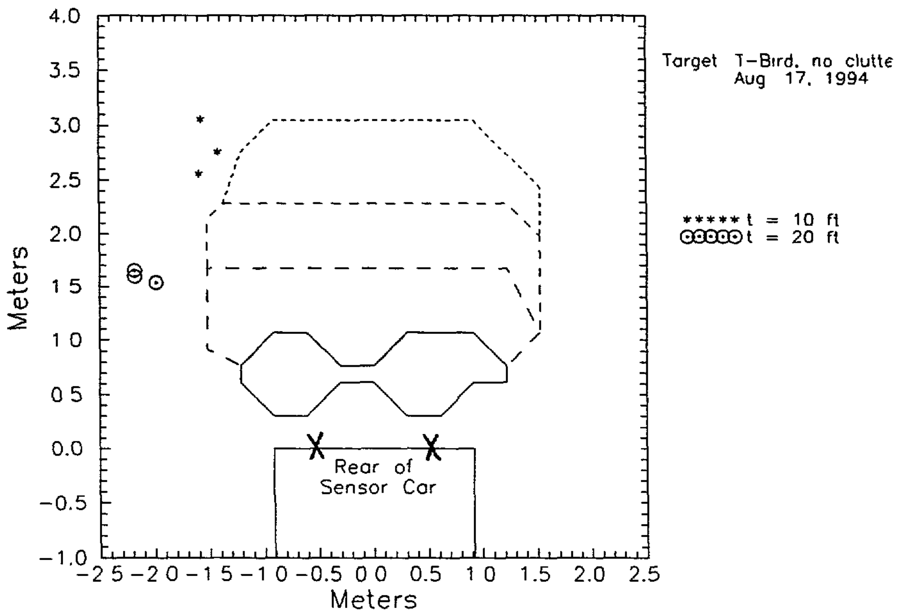

Figure 6.11-15: Backing Tests - Curved Path
Ford Taurus Target

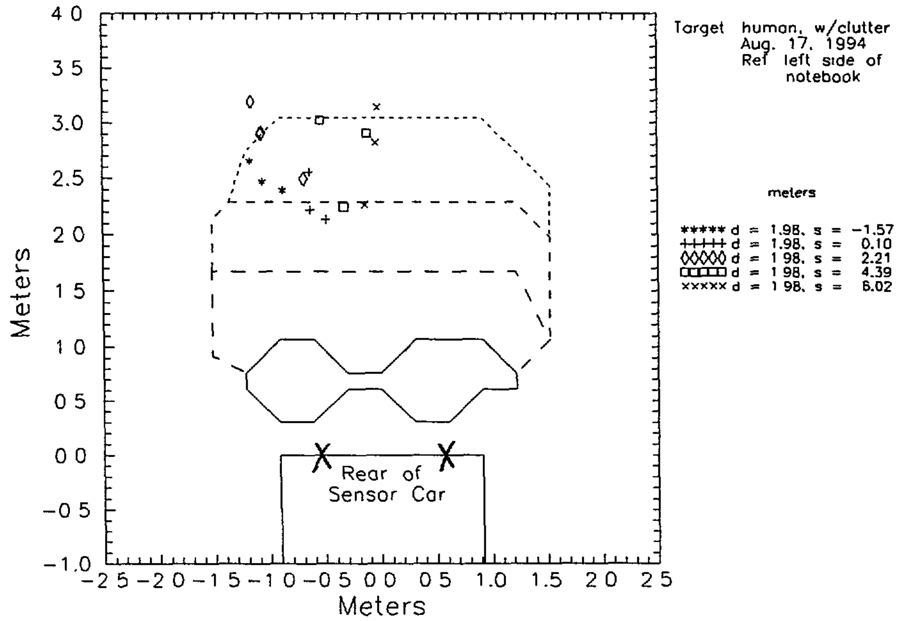

Figure 6.11-16: Backing Tests With Clutter - Curved path
Human Target

data collected in the absence of a clutter vehicle. Therefore, it is difficult to conclude that the clutter vehicle degrades the system performance in any way.

Figure 6.11-17: Backing Tests With Clutter - Curved Path
Ford Taurus Target

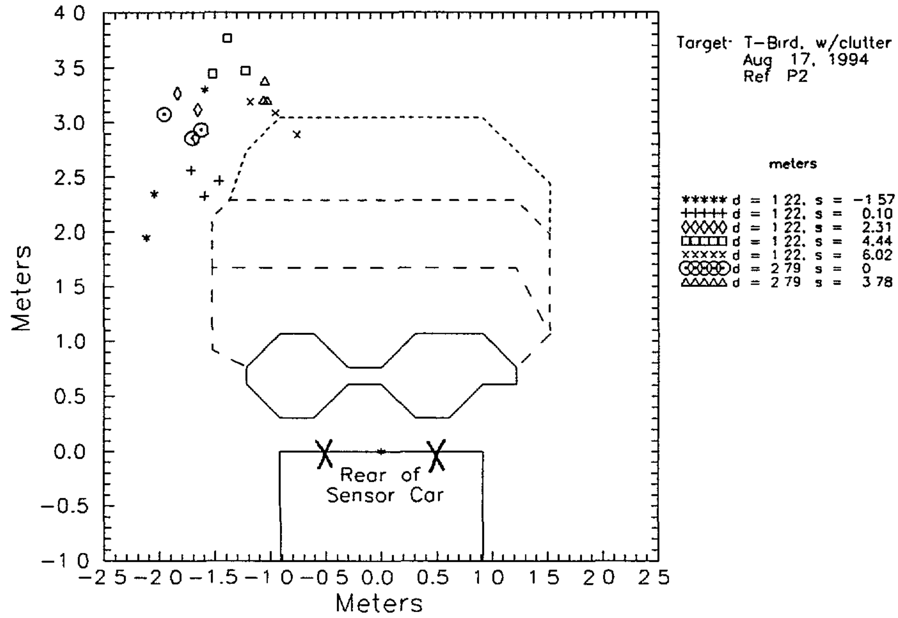

Road Test

As with side systems, this backing system was evaluated under realistic road conditions involving freeway, city, two-lane highway, and parking lot driving. Even though this system was meant to be activated only when the vehicle is placed in reverse, it was left on during the entire duration of the road test to generate sufficient statistics relevant to its performance. The total exposure time was 74.47 minutes. Statistics were compiled on the number and types of targets detected. Figure 6.11-18 summarizes the results.

Figure 6.11-18: Summary of Road Test Statistics - System 'R"

System: 'R"
Total number of detects: 280

Classification	Freeway	Two-lane	City	Parking Lot	TOTAL
TP	0	3	11	6	20
FP	111	72	37	40	260
TOTAL	111	75	48	46	280
FN	0	0	0	0	0
TN					97.7 %

General Comments: This system generated a significant number of false alarms even during parking lot maneuvers

Overall, this system performed very poorly during the road test demonstrating a high rate of false alarms (3.5/min) These false alarms appeared to be random in nature. A significant fraction of these false alarms occurred in parking lots under circumstances for which the system was designed as an aid.

6.12 System "S"

6.12.1 System Description

This system is a backing system that uses ultrasonic ranging technology along with a voice messaging system to warn the driver of obstacles located behind the vehicle. The system has a total of eight detection zones whose size can be individually adjusted from 0.05m to 0.1m. When an object enters the detection zone, the system alerts the driver with a voice message indicating the distance of the target. The system consisted of two units which were placed on the rear bumper 0.43m equidistant from the centerline of the car and 0.58m off the ground.

6.12.2 Overview of System Performance

This system performed adequately during both the controlled static and dynamic tests. Weather conditions for this particular set of tests were clear and cold (≈ 15 - 20° F). Cold weather did not appear to have an adverse effect on system performance. However, it became apparent that proper aiming of the sensor was critical. If the sensor was pointed too far down, reflections from the asphalt would trigger false alarms. When this occurred, the sensor was simply reaimed until the unwanted alarms ceased. Eliminating sensitivity to reflections from the pavement while at the same time maintaining the capability of detecting a small child will be a challenge for this particular system.

Correlation between the verbal indication of the distance of the target and the actual distance was very good as measured during the static testing. At no time was the error greater than 0.3m.

The unit tested proved to be a useful aid during typical backing maneuvers such as parallel parking and backing into parking spaces. However, there were many incidents in which the system was triggered for no apparent reason. During the course of the test, the sensor was repeatedly reaimed in an attempt to reduce the frequency of these false alarms. All in all, the system's performance could be classified as fair.

6.12.3 Test Results

<u>Static Tests</u>

Static patterns were measured for the following types of targets:

1) 0.3m x 0.3m foil covered styrofoam

2) human
3) Ford Taurus

The foil target was located at the vertical height of the sensor.

The static detection zone measured with the 0.3m x 0.3m target is shown in Figure 6-12-1. The boundary of the detection zone extends backwards from the car for 2.8m and sideways about 2m. There is a noticeable blind spot in the center of the vehicle adjacent to the rear bumper. This is due to the fact that two

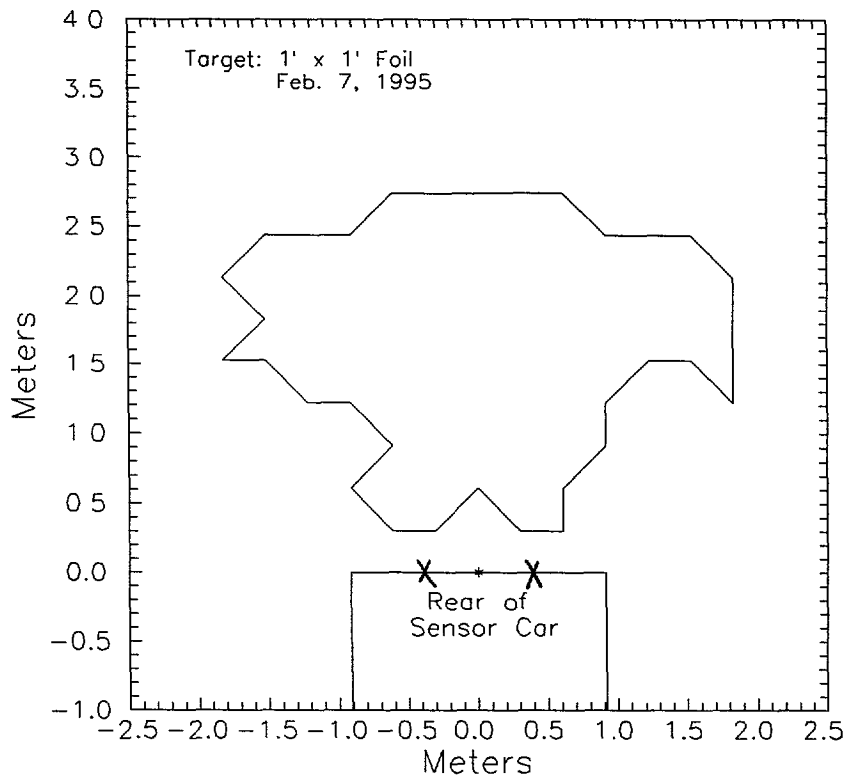

Figure 6.12-1: Static Test Results - System "S"
0.3m x 0.3m Foil Target

sensors located near the tail lights are used. When the field of view of both of these sensors are combined, there is an area in the center which may not always be covered, depending on the size, shape, and height of the target.

Figure 6.12-2 shows the static detection zone for a human target. The extent of the pattern is slightly smaller than that seen for the foil target extending 2.5m to the back of the car and 0.5m - 1m to the side. This pattern also shows a similar blind spot located in the center of the host vehicle near the rear bumper.

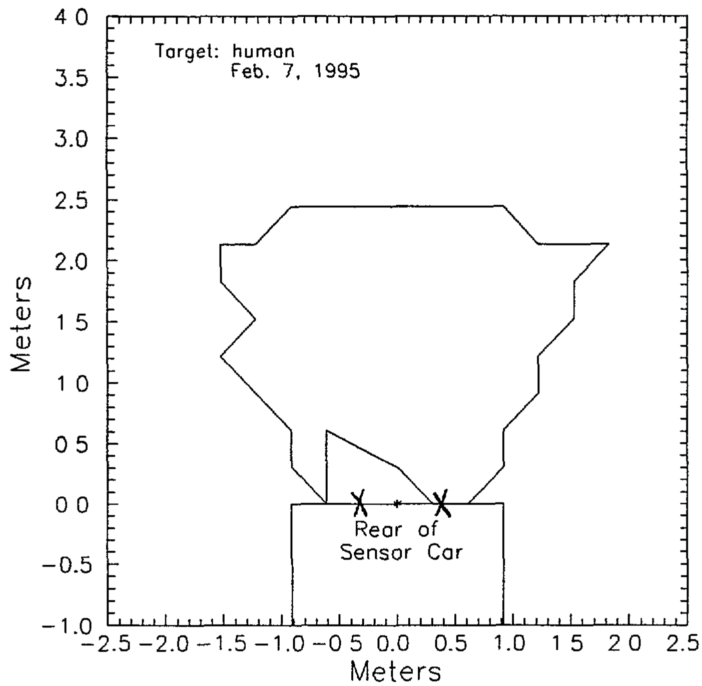

**Figure 6.12-2: Static Test Results - System "S"
Human Target**

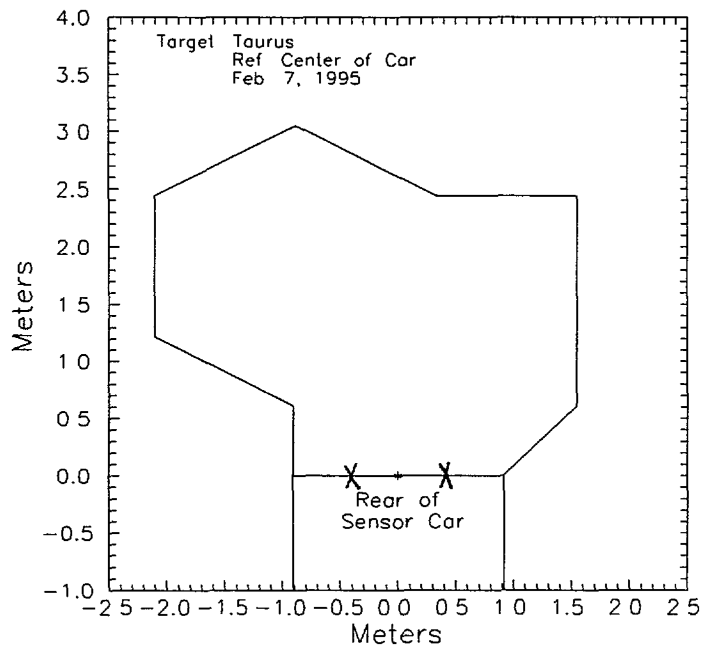

**Figure 6.12-3: Static Tests Results - System "S"
Ford Taurus Target**

The system static response to a Ford Taurus target is shown in Figure 6.12-3. The point of reference on the target vehicle is the center of the front grill of the car. Because of the larger cross section of the target, the blind spot that was seen with the earlier targets has disappeared.

Vertical Extent

The vertical extent of the static pattern was determined by placing a target at a distance, D, from the sensor and measuring the system response as a function of vertical position. Figure 6.12-4 summarizes the angular extent of this sensor. The sensor has a total vertical FOV of 32.3" and is angled downward.

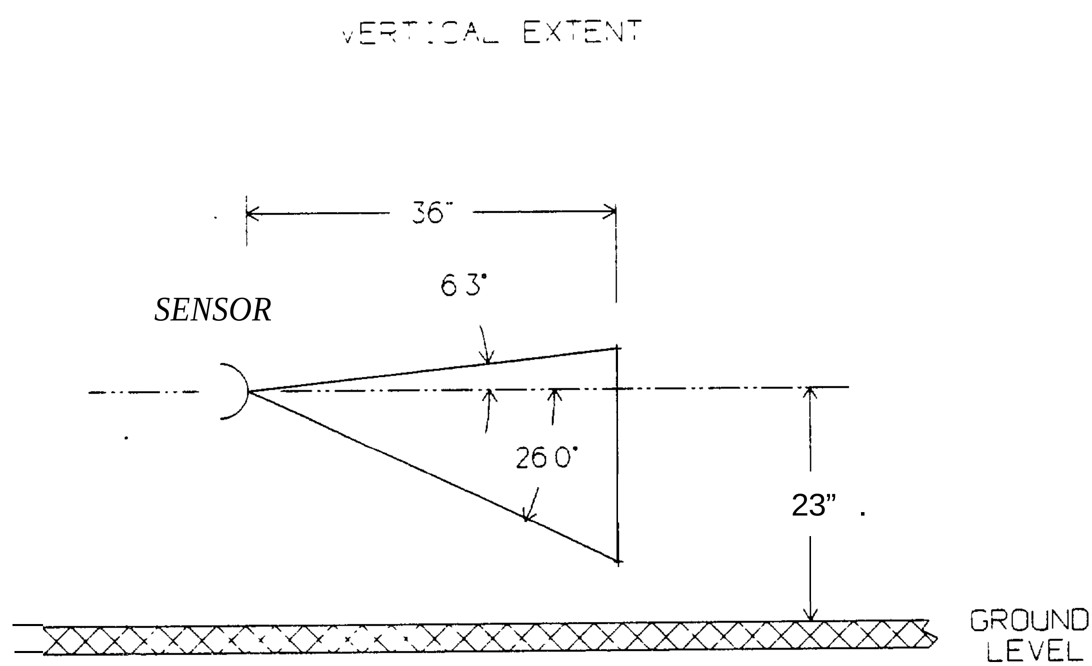

Figure 6.12-4: System "S" - Vertical Extent

<u>Dvnamic Tests</u>

perpendicular Delay Time

Figure 6.12-5 summarizes the results of the perpendicular delay time tests for this system. The target vehicle was driven past the sensor vehicle at speeds of 1.6, 8,16,1, 24.1, 32.2, and 40.2 KPH. All data has been referenced to post P2 on the front passenger side of the target vehicle.

The lateral separation (X) between the two vehicles is denoted by the open triangles. This distance is held to 1m ± 0.5m, increasing slightly at higher vehicle speeds.

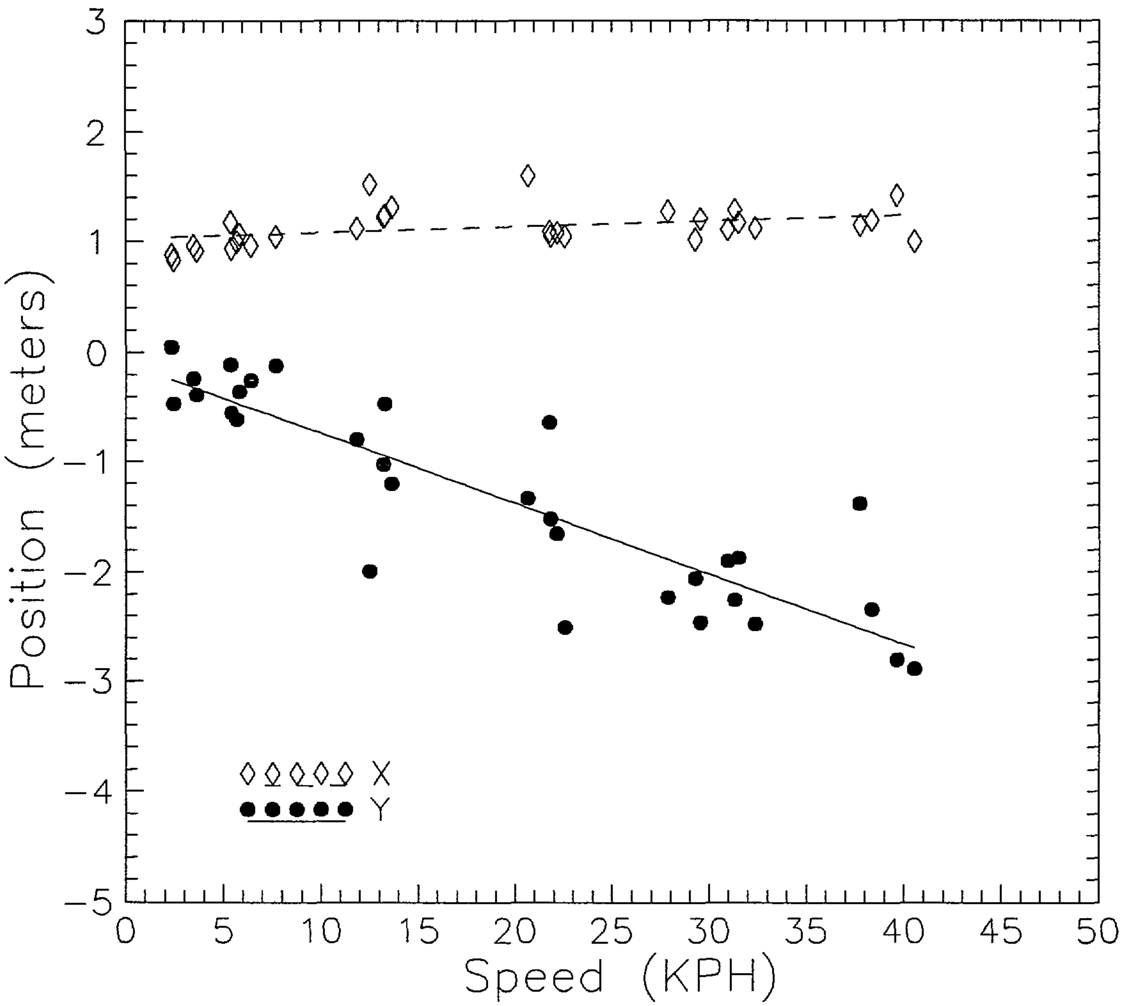

Figure 6.12-5: Perpendicular Latency Time

The Y position of the target vehicle at the instant of system reaction is shown by the filled circles. The slope of a linear best fit to the data yields the perpendicular latency time. With a characteristic scatter of roughly ±1m, the latency is calculated to be 0.23 sec ± 0.13 sec.

Because this system is a backing system, no data was collected on parallel delay time. Since the field of view extends only to the rear of the host vehicle and not to the sides, the system will not be able to detect a vehicle traveling parallel and to the side of the host vehicle.

Persistence Time

Since this is a backing system, information on the system persistence has been extracted from the perpendicular delay time test results. The position of the target vehicle at the instant the system display turns off is plotted in Figure 6.12-6. This data has been computed from a projection of the car's position based on the trajectory and speed calculated from two earlier reference video frames. All data has been referenced to post P2 on the passenger side of the target vehicle.

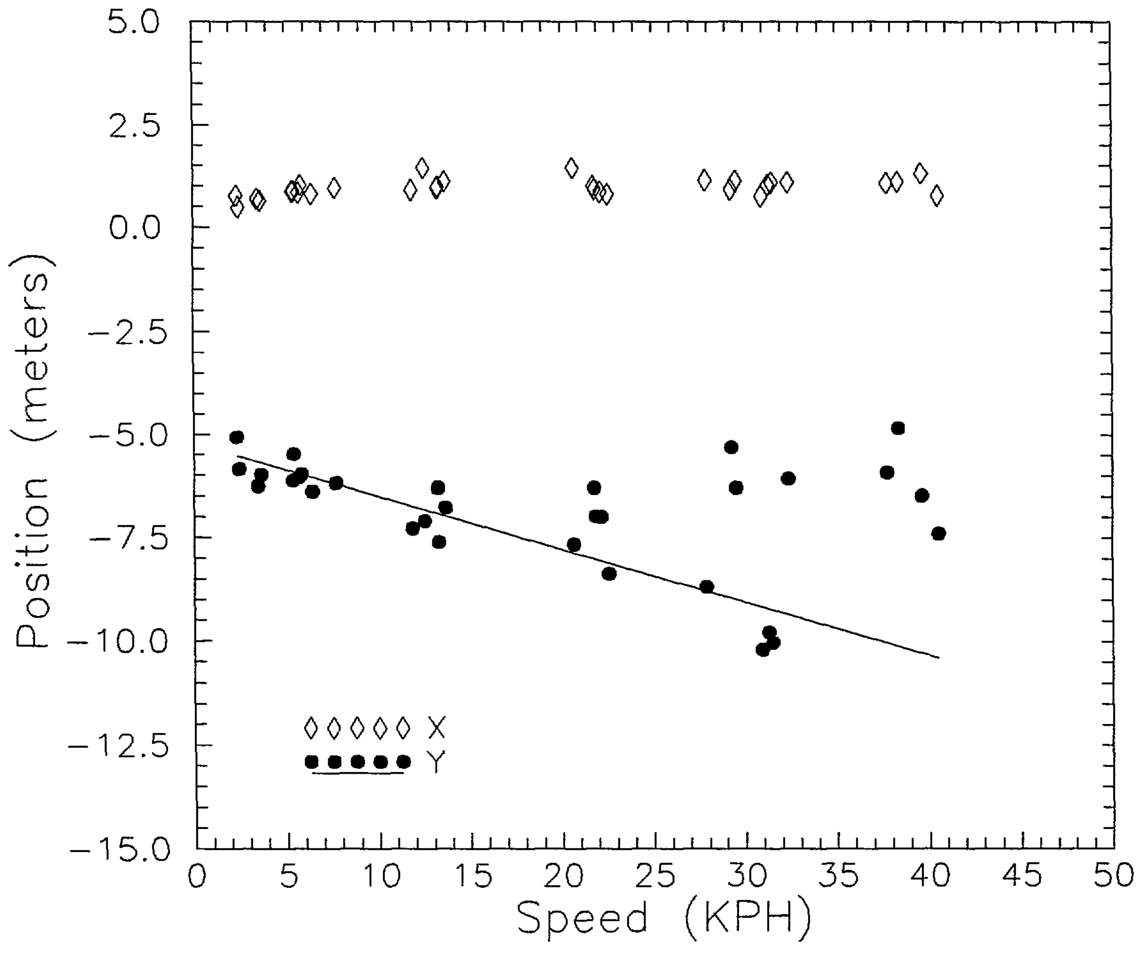

Figure 6.12-6: Persistence Time

At the higher vehicle speeds, the system response shows a tendency to flatten out indicating that the persistence may be dependent on velocity. If the seven points (three at 30 KPH and 4 at 40 KPH) are filtered from the computation of the slope, the calculated persistence is 0.46 sec ± 0.22 sec.

Backing Tests - Straight Path

Evaluation of this system was initiated by backing the sensor vehicle straight into various targets. This was done with and without the presence of a clutter vehicle. Figure 6.12-7 shows the system response to a 0.3m x 0.3m foil covered target. Notice that the system reacts to the target about 0.3m to 0.6m inside the measured static boundary. This vehicle speed for this backing maneuver was

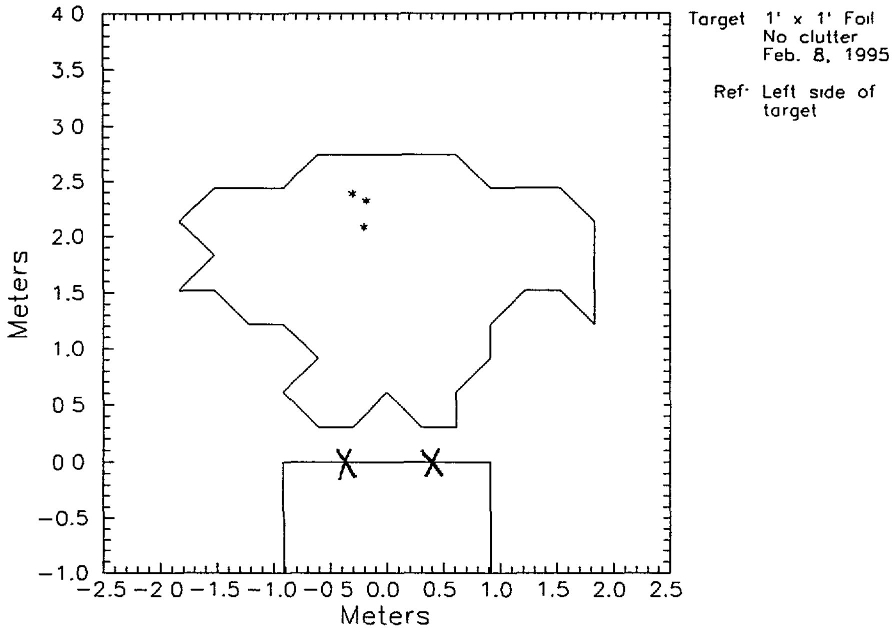

Figure 6-12-7: Backing Tests - Straight Path
0.3m x 0.3m Foil Target

approximately 8 KPH or less. From the measured system latency, this corresponds to a system delay of between 0.22m and 0.8m. Thus, the data collected is consistent with the static detection pattern measured.

This test was repeated with both a human target and the Ford Taurus. The results are displayed in Figures 6.12-8 and 9, respectively. In the case of the human target, one point in particular falls well within the interior of the measured detection zone. However, the detect occurs within 0.8m of the boundary which can still be explained by the system latency. The data taken with the Ford Taurus target appears at first glance to anticipate the static boundary. However, the reference taken here is the center of the Taurus meaning that the edge of the Taurus is crossing the "peak" of the static detection pattern at X ≈ -1m and Y ≈ 3m. It is this edge of the target vehicle that triggers the system response.

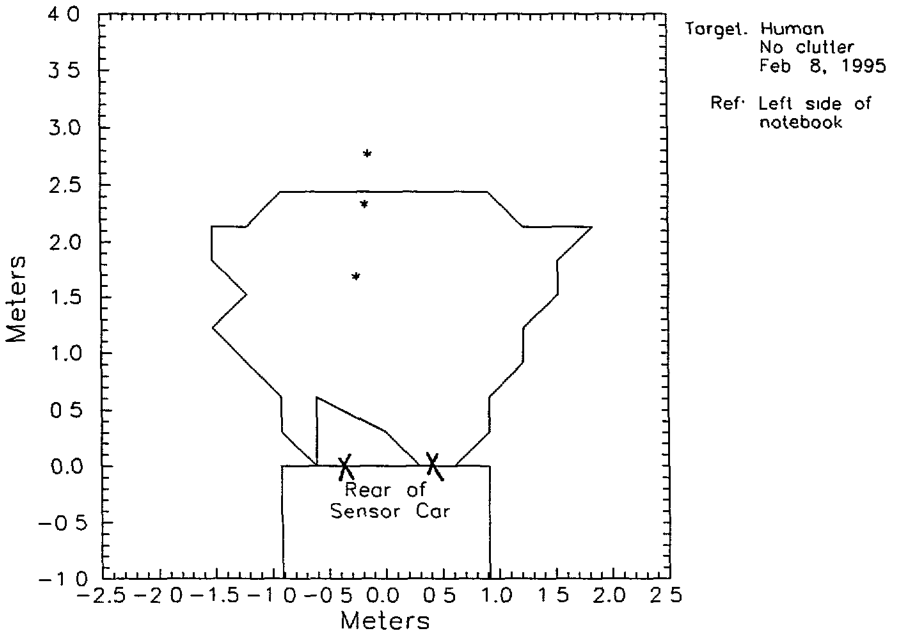

Figure 6.12-8: Backing Tests - Straight Path
Target: Human

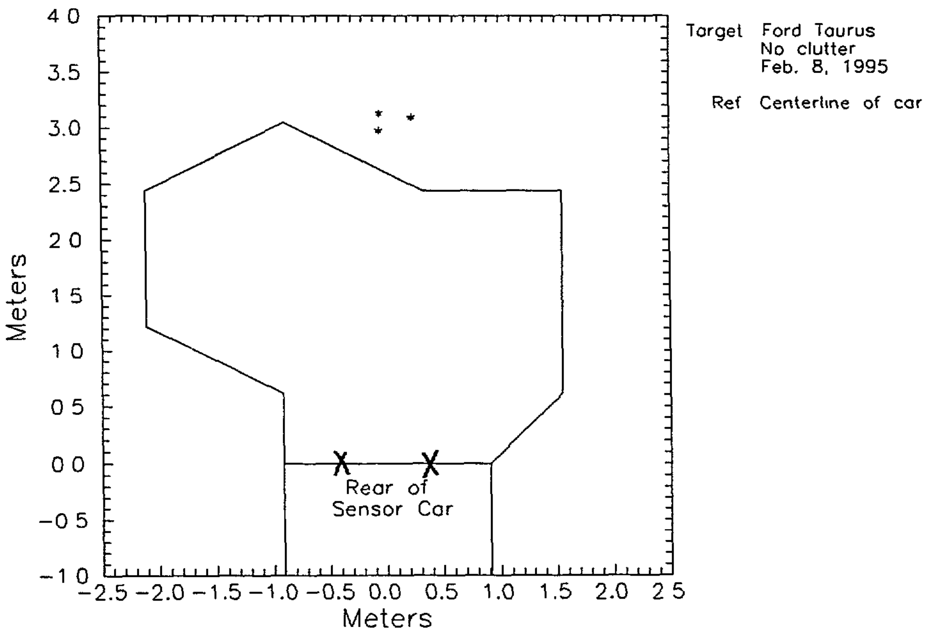

Figure 6.12-9: Backing Tests - Straight Path
Target: Taurus

For the human and vehicle targets, these straight backing tests were repeated in the presence of a clutter vehicle. Figure 6.12-10 displays the results measured with the human target. The lateral spacing between the human target and the clutter vehicle was fixed at 1.5m while the "nose-to-nose" distance was varied between s =0 (i.e., nose of clutter vehicle is even with the human target) to s = 4.6m (human target standing near rear of clutter vehicle).

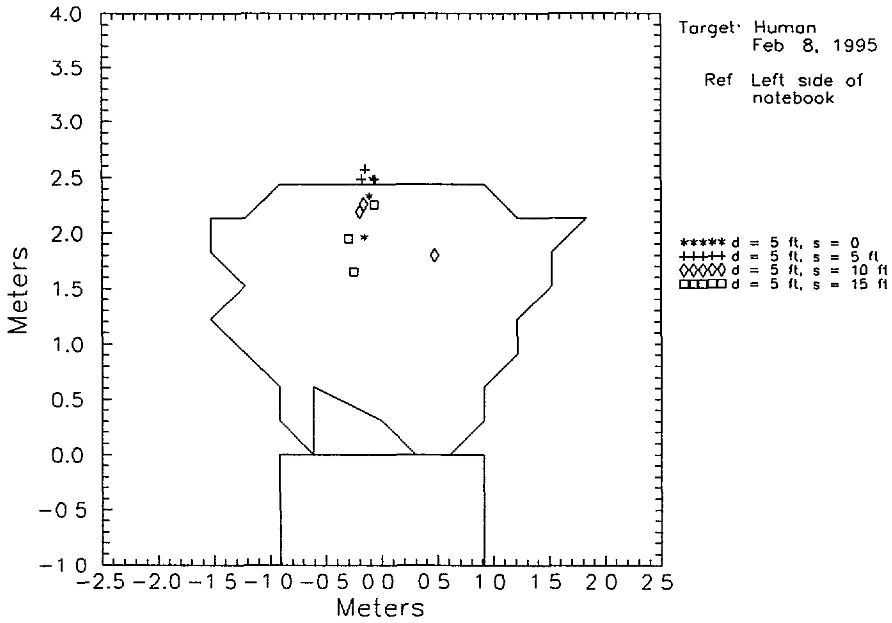

Figure 6.12-10: Backing Tests With Clutter - Straight Path
Human Target

The presence of the clutter vehicle does not trigger an early system response. Although there is scatter in the data, overall it is consistent with the measured system latency.

The measurements made with the Ford Taurus target in the presence of a clutter vehicle are shown in Figure 6.12-11. The reference point is once again the centerline of the target vehicle. With the exception of a single data point at s = 3m, the repeatability of the data is excellent showing no dependence on the position of the clutter vehicle.

Backing Tests - Curved Path

A common backing scenario involves maneuvering along a curved trajectory. The utility of this backing system was tested using two different radius of curvatures, t = 4.6m and t = 6.1m. Figure 6.12-12 shows the result of backing along a

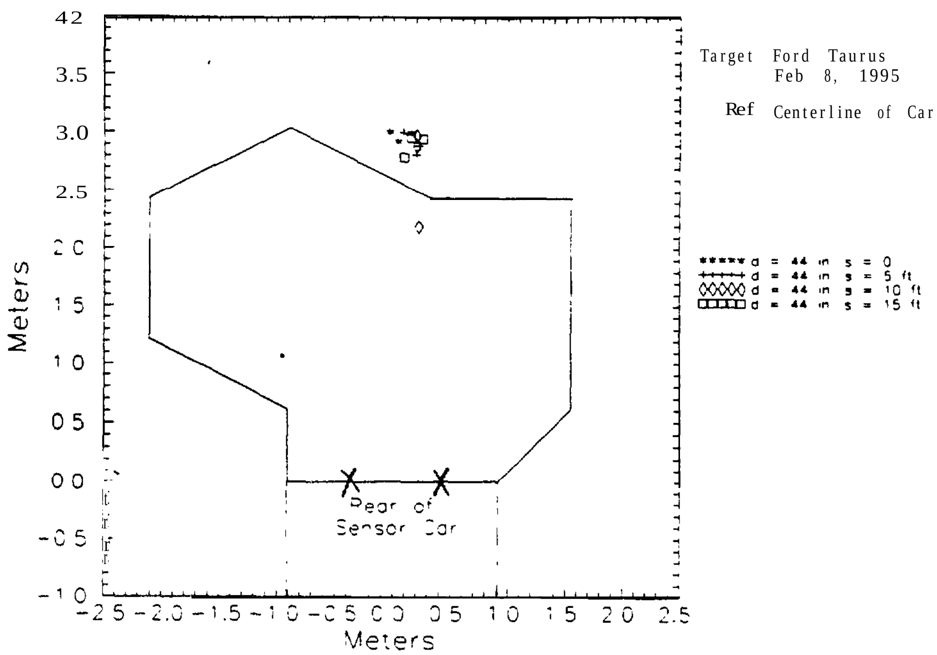

Figure 6.12-l 1: Backing Tests With Clutter - Straight Path
Ford Taurus Target

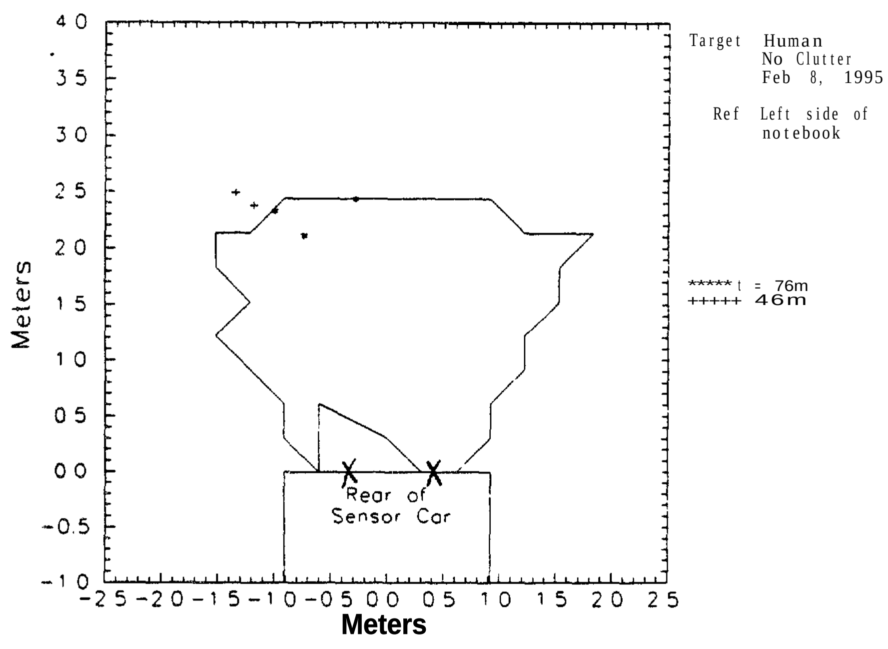

Figure 6.12-12: Backing Tests - Curved Path
Human Target

curved path into a human target. Since the sensor car trajectory is now curved, the detects appear more towards the edge of the static detection zone. All of the data collected is consistent with the static pattern measured and the system latency.

The system response to a vehicle target is shown in Figure 6.12-13 as a function of the radius of curvature of the sensor car's trajectory. In this case, the reference point on the target vehicle is post P2 on the front passenger side of the car. On a curved trajectory, this point represents the closest point to the sensor vehicle. The data collected along the tighter radius of curvature tends to cross the static boundary along the edge.

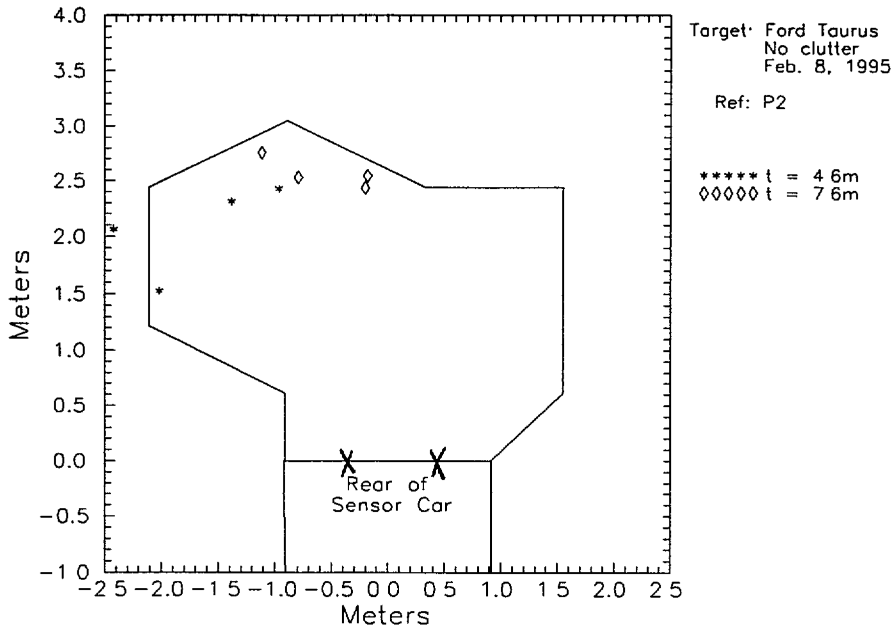

Figure 6.12-13: Backing Tests - Curved Path
Ford Taurus Target

These tests were repeated with a clutter vehicle positioned next to the target in an attempt to trigger an early response from the system. For the human target, this clutter vehicle was positioned 1.5m laterally from the target. Once again the "nose-to-nose" separation was varied between s = 0 and s = 4.6m. The results are presented in Figure 6.12-14. Most of the data has been referenced to the left side of an 8.5" x 11" notebook held in the hands of the human subject. Occasionally, this point was not in the view of enough of the video cameras for analysis. In these cases, the reference point chosen was the right side of the notebook and is denoted by the circles. The data collected shows the representative scatter seen in the previous data. There were no early alarms triggered by the presence of the clutter vehicle.

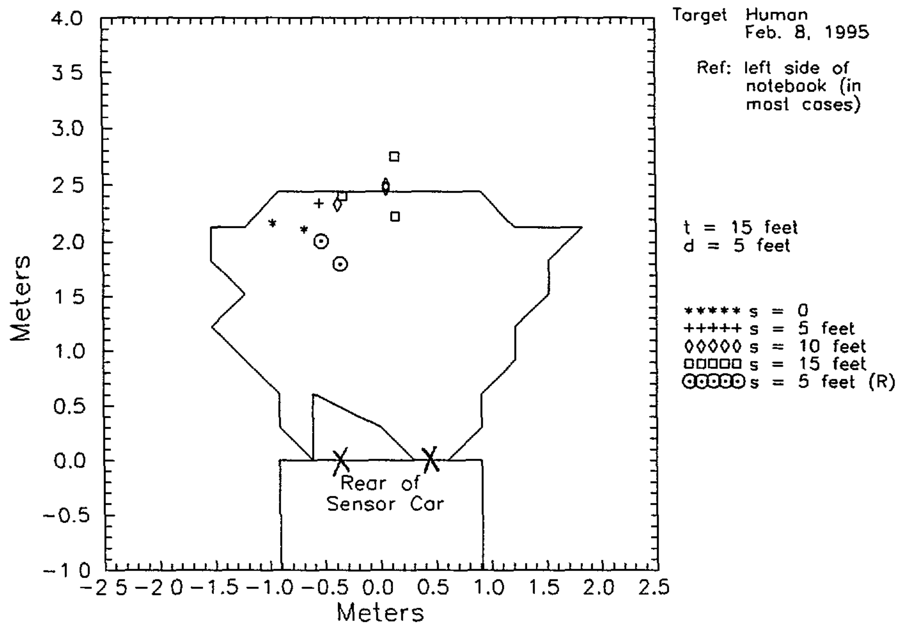

Figure 6.12-14: Backing Tests With Clutter - Curved path
Human Target

The data collected with a Ford Taurus target is presented in Figure 6.12-15. In this case the clutter vehicle was placed 1m laterally from the target vehicle. Most of the data has been referenced to post P2 on the target vehicle with the

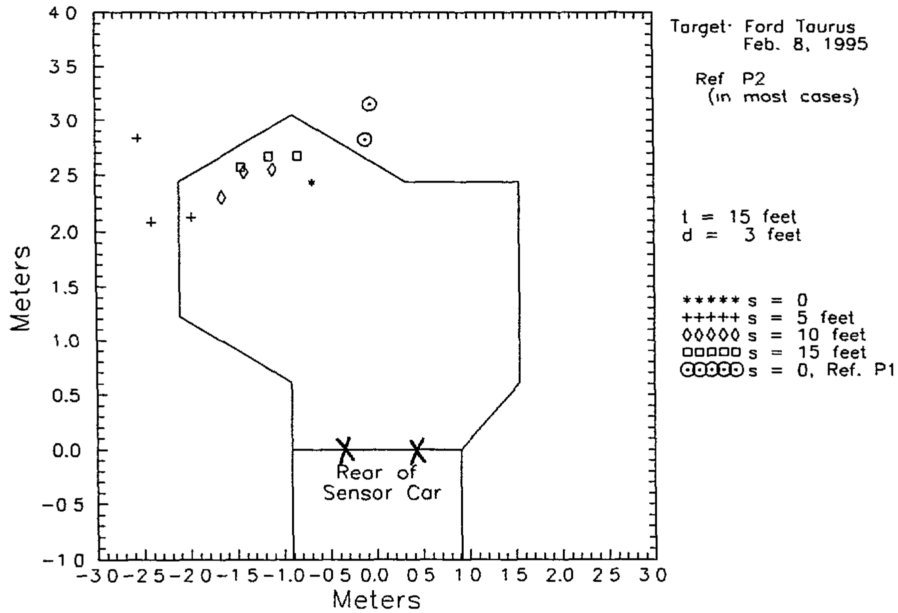

Figure 6.12-15: Backing Tests With Clutter - Curved Path
Ford Taurus Target

exceptions denoted by the circles. Once again, the data is characterized by scatter that is typical of the previous results indicating that the performance of this system is not adversely affected by the presence of a clutter vehicle.

Road Test

As with side systems, this backing system was evaluated under realistic road conditions involving freeway, city, two-lane highway, and parking lot driving. The total exposure time was 82.15 minutes. Statistics were compiled on the number and types of targets detected. Figure 6.12-l 6 summarizes the results.

Figure 6.12-l 6: Summary of Road Test Statistics - System 'S"

System: "S"
Total number of detects: 37

Classification	Freeway	Two-lane	City	Parking Lot	TOTAL
TP	0	1	6	7	14
FP	0	13	5	5	23
TOTAL	0	14	11	12	37
FN	0	0	0	0	0
TN					99.83 %

General Comments: No false alarms during freeway driving

False alarms triggered generally required reaiming of the sensor to clear

This system proved to be useful for standard backing maneuvers including parallel parking and backing into parking spaces

Overall, this system performed fairly during the road test. Most of the false alarms generated occurred in the parking lot and required reaiming of the sensor to clear. It should be noted that the number of false alarms would be much higher if the system was not cleared everytime it malfunctioned due most probably to reflections from the asphalt.